Comparison of the Cytochrome *c* Oxidase inherent Catalase Side-Reaction from *Paracoccus denitrificans* in the wild type and recombinant form

Dissertation
zur Erlangung des Doktorgrades
der Naturwissenschaften

vorgelegt beim Fachbereich 14
Biochemie, Chemie und Pharmazie
der Johann Wolfgang Goethe-Universität
in Frankfurt am Main

von
Florian Hilbers
aus Twistringen

Frankfurt (2012)
(D30)

vom Fachbereich 14 Biochemie, Chemie und Pharmazie der Johann Wolfgang Goethe-Universität als Dissertation angenommen.

Dekan: Prof. Dr. Thomas Prisner

1. Gutachter: Prof. Dr. Bernd Ludwig
2. Gutachter: Prof. Dr. Dr. h. c. Hartmut Michel

Datum der Disputation: 20. Dezember 2012

Diese Doktorarbeit wurde vom 01. Januar 2009 bis zum 20. Oktober 2012 unter Leitung von Prof. Dr. Dr. h.c. Hartmut Michel in der Abteilung Molekulare Membranbiologie am Max-Planck-Institut für Biophysik in Frankfurt am Main durchgeführt.

Eidesstattliche Erklärung

Hiermit versichere ich, dass ich die vorliegende Arbeit selbstständig angefertig habe und keine anderen, als die angegebenen Hilfsmittel und Quellen verwendet habe.

(Florian Hilbers)

Frankfurt am Main, den 20. Dezember 2012

Abstract:

The four subunit (SU) aa_3 cytochrome *c* oxidase (CcO) from *Paracoccus denitrificans* is one of the terminal enzymes of the respiratory chain. It uses electrons from cytochrome *c* to reduce molecular oxygen to water. Its binuclear active center, residing in SU I, contains heme a_3 and Cu_B, the latter being liganded by three histidine residues. Apart from its oxygen reductase activity, the protein possesses a peroxidase and a catalase activity.

To compare variants and the wild type (WT) protein in a more stringent way, a recombinant (rec.) WT CcO was constructed, carrying the gene for SU I on a low copy number plasmid. This rec. WT showed, as expected, no difference in oxygen reductase activity compared to the American Type Culture Collection (ATCC) WT CcO but surprisingly its catalase activity was increased by a factor of 20. The potential overproduction of SU I due to plasmid coding and the resulting deficiency in metal inserting chaperones might impair the correct insertion of heme a_3 and Cu_B because of a deficiency in metal inserting chaperones. This in turn might lead to differences in side chain orientation and to changes in the water network. However, slight changes might cause an increased accessibility of the active center for hydrogen peroxide, resulting in an increased catalase activity. The availability of chaperones and therefore the proposed structural reasons for the difference was improved by cloning the genes for the two metal inserting chaperones *ctaG* and *surf1c* on the same plasmid together with SU I. This new rec. WT CcO showed in fact a reduced catalase activity. Another WT with a deletion in the chromosomal second, non expressing gene of SU I was analysed to prove plasmid coding as the reason for the difference of the ATCC WT and the rec. WT. This strain showed an increased k_{cat} of the catalase activity as well, additionally pointing to a regulatory effect of the non expressed gene for SU I in the chromosome. To fathom the structural difference of the increased catalase activity, differential scanning calorimetry was used, but no significant difference in thermal stability between the ATCC WT CcO and the rec. WT CcO was detected. However, upon aging, the thermal stability of the rec. WT CcO declined faster than that of the ATCC WT CcO pointing to a decreased structural stability of the rec. WT CcO.

To characterize the catalase reaction, several known inhibitors were used to probe the contribution of the different metal cofactors in the catalase reaction. In addition

variants in aromatic amino acids near the active center were constructed to conclude on a possible reaction mechanism of the catalase activity of C*c*O. These variants in combination with the wild type forms were analysed for radical signals by EPR-spectroscopy. A radical relevant for the catalase reaction of C*c*O was found in the F-intermediate of all variants and all wild type forms. This narrow 12 G radical signal was assigned to a porphyrine radical probably involved in the catalase reaction of C*c*O. Moreover, gas chromatography-mass spectrometry measurements were used to analyse isotopically labelled oxygen produced in the catalase reaction.
As a result of these experiments, a reaction cycle of the catalase activity of C*c*O is postulated and the structural difference between the ATCC and rec. WT C*c*O is outlined. The catalase activity appears to be a true catalase activity and not a "pseudocatalase" activity.

Table of Contents

List of Figures

List of Tables

Abbreviations

Amino acids were abbreviated using the standard three or one letter code. Positions in subunits were denoted for example as W272, mutations were denoted for example as W272F.

Å	Ångström (0.1 nm)
ADP	Adenosine-5-diphosphate
Amp	Ampicillin
asis	Protein as purified
AOX	Alternative oxidase
ATCC	American tissue culture collection
ATP	Adenosine-5-triphosphate
BCA	Bicinchinoninic acid
BSA	Bovine serum albumin
C*c*O	Cytochrome *c* oxidase
CIAP	Calf intestine alkaline phosphatase
Cyt *c*	Cytochrome *c*
DDM	n-Dodecyl-β-maltoside
DNA	Deoxyribonucleic acid
DSC	Differential scanning calorimetry
$\varepsilon_{xxx\ nm}$	Extinction coefficient at XXX nm
EDTA	Ethylenediaminetetraacetic acid
EPR	Electron paramagnetic resonance
G	Gauss (10^{-4} Tesla)
GC-MS	Gas chromatography-mass spectrometry
HCO	Heme copper oxidase
imf	Ion motive force
IPTG	Isopropyl β-D-1-thiogalactopyranoside
k_{cat}	Turnover number
K_M	Michaelis-menten-constant
Kan	Kanamycin
kDa	kilo dalton
KP_i	Potassiumphosphate buffer
LB	Lysogenic broth medium
LDAO	n-dodecyl-N,N-dimethylamine-N-oxide
MALDI-TOF	Matrix-assisted laser desorption/ionisation time of flight
MeV	Mega electronvolt
MOPS	3-morpholinopropane-1-sulfonic acid
mRNA	messenger ribonucleic acid
m/z	Mass over charge
NAD^+	Nicotinamide adenine dinucleotide
NADH	Hydrogen nicotinamide adenine dinucleotide
nm	Nanometer
ORF	Open reading frame
ox	Oxidized
PCR	Polymerase Chain Reaction
PEG	Polyethylene Glycol
pmf	Proton Motive Force

ppm	Parts per Million
PVDF	Polyvinylidene Fluoride
Rif	Rifampicin
ROS	Reactive Oxygen Species
rpm	Rounds per Minute
SDS-PAGE	Sodium Dodecylsulfate Polyacrylamide Gel-Electrophoresis
SOD	Superoxide Dismutase
SOTS-1	Superoxide Thermal Source-1
SU	Subunit
T_M	Melting Temperature
Tet	Tetracycline
TMPD	Tetramethylphenylene-Diamine
UV/vis	Ultraviolet/visible Light
V_{max}	Maximum Velocity in Protein Turnover Rate
v/v	Volume per Volume
w/v	Weight per Volume
WT CcO	Wild Type
x g	times force of gravity (9.81 m/s^2)

1. Introduction

Chemical energy is needed by every living being for catabolic and anabolic processes. One example is the transcription and translation of DNA for the production of proteins [1].

Regulated by signals, such as promoters, chromosomal or plasmid-DNA is transcribed into mRNA, which is then translated into a protein with an amino acid sequence specified by the DNA. This polypeptide folds either spontaneously or with the help of chaperones into a protein with three-dimensional structure. Proteins derived from plasmid DNA, used to artificially transform bacterial cells, are termed to be expressed recombinantly [1]. The recombinant expression of proteins could lead to minor differences in specific protein activity compared to the wild type, as shown by Kenakin *et al.* and Butenas *et al.* [2; 3]. One major problem in expressing proteins heterologously is post-translational modification which is species dependent. Another problem arises if a different promoter controls transcription of the gene of interest, located on a plasmid, which leads to overproduction of the respective mRNA and subsequently of the protein. Therefore, a shortage of important chaperones could be a major reason for obscured differences e.g. in specific protein activity, of the recombinantly expressed proteins [2; 3].

One of the main energy carriers of all organisms involved in many metabolic reactions, and therefore considered as one of the most important molecules in life, is adenosine-5'-triphosphate (ATP). As almost all metabolic processes depend on ATP, it is especially important to maintain a constant pool of ATP [4].

ATP can mainly be generated in two different ways. Firstly, by transfer of phosphate groups to adenosine-5'-diphosphate (ADP) resulting in ATP (substrate level phosphorylation), e.g. the transfer of the phosphate group from phosphoenolpyruvate to ADP in glycolysis.

Secondly, and much more importantly, by oxidative phosphorylation: During oxidative phosphorylation reduced substrates are oxidized and the electrons are transferred via different protein complexes to terminal oxidases. These protein complexes belong to the respiratory chain. The terminal oxidases finally reduce oxygen to water. The energy of these processes is stored in the form of an electrochemical gradient, generated by pumping protons or other ions across the

periplasmic membrane of prokaryotes or across the inner membrane of mitochondria, (proton / ion gradient). Protons from the cytoplasmic side / intermembrane space of mitochondria used by these protein complexes for chemical reactions further increases the gradient generated by pumping protons [1]. Mitchell first described this proton motive force (pmf) or ion motive force (imf) in 1961 [5]. This pmf / imf is used by the F_0F_1-ATP synthase to synthesize ATP from ADP and inorganic phosphate (P_i) [5-7].

1.1. The Respiratory Chain

The respiratory chain is an electron transport chain that generates an electrochemical ion gradient across the membrane and usually consists of four different protein complexes. The proteins of the mitochondrial respiratory chain are described here as an example.

1. The NADH:ubiquinone-oxidoreductase or complex I shows a characteristic L-shape, oxidizes NADH to NAD^+ and reduces ubiquinone to ubiquinol, pumping four protons during the oxidation of NADH. Four protons are pumped across the membrane, two protons are used for the oxidation of ubiquinone and one proton is released from NADH. Complex I can form reactive oxygen species (ROS) [8-12].
2. Complex II is the succinate:ubiquinone-oxidoreductase. This enzyme connects the citric acid cycle to the respiratory chain and catalyzes the oxidation of succinate to fumarate, therefore reducing ubiquinone to ubiquinol. This complex does not pump protons across the membrane [9].
3. The third complex is the ubiquinol:cytochrome *c*-oxidoreductase. This complex switches the electron-transport chain from a two-electron transport to a one-electron transport. Complex III oxidizes ubiquinol to ubiquinone, releasing two protons into the intermembrane space. The first electron is used to reduce cytochrome *c*. The second electron is transported back to a second ubiquinone binding site near the mitochondrial matrix, subsequently reducing ubiquinone to ubiquinol, using protons from the mitochondrial matrix. Complex III therefore plays an important role, increasing the proton

gradient further. This complex is also known for its ROS-production [9; 10; 13].

4. Complex IV of the respiratory chain is the cytochrome *c:*oxygen-oxidoreductase (C*c*O). This complex reduces molecular oxygen to water, oxidizing cytochrome *c*. During one reaction cycle of C*c*O four electrons of four cytochrome *c* molecules are used to fully reduce oxygen without generating any ROS. Four protons of the mitochondrial matrix are used for this reaction. Four additional protons are pumped from the mitochondrial matrix, across the inner membrane into the intermembrane space [14-21].

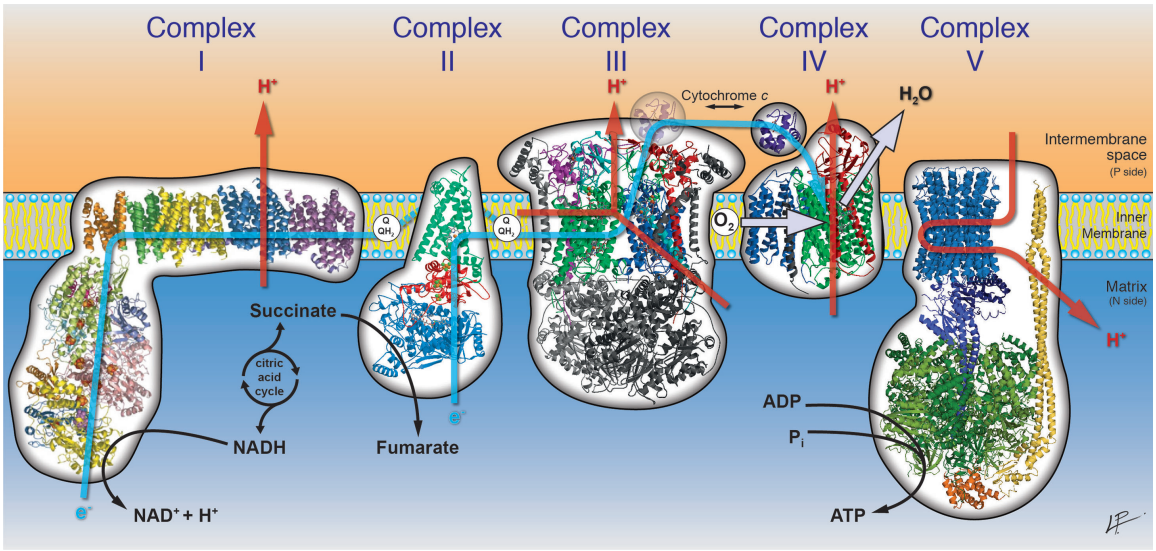

Figure 1.1: Schematic overview of the respiratory chain showing complexes I to IV with the F_oF_1-ATP synthase added as complex V.

The blue arrow depicts the electron pathway. Red arrows depict the transport of protons. This figure was kindly provided by Paolo Lastrico (MPI of Biophysics, Frankfurt, Germany).

Three of the protein complexes of the respiratory chain are actively contributing to the electrochemical gradient. At least two of the described complexes are capable of generating ROS as a common by-product [22]. For eukayotes, the pmf generated by these protein complexes is essential for survival under most growth conditions.

1.2. Heme-Copper Oxidases

Quinol and cytochrome *c* oxidases are terminal enzymes of the aerobic respiratory chains in all kingdoms of life. Cytochrome *c* oxidases use the full electron transport chain, whereas quinol oxidases bypass complex III [23].

These enzymes reduce molecular oxygen to water utilizing cytochrome *c* or quinol as electron donors. During this reaction, protons are pumped across the membrane and protons are used to generate water. This generates an electrochemical gradient, which is used to drive the synthesis of ATP by the F_0F_1-ATP synthase. Heme copper oxidases (HCO's) consist of at least three subunits, harboring the catalytic center in subunit (SU) I. The active center of all heme-copper oxidases consists of a high-spin heme and a Cu-ion, which is liganded by three highly conserved histidines. One of these histidines is covalently bound via the amino acid side chain to a tyrosine residue near the active center [18; 24-26]. This modification is believed to occur post-translationally [18; 27]. Protons pumped during the reaction cycle of HCOs pass the protein through either one or two proton channels [18].

Exceptions are alternative oxidases (AOX) and *bd* oxidases. AOXs are present mostly in plants and fungi, whereas *bd* oxidases are present in prokaryotes. Both oxidases use electrons and protons to reduce molecular oxygen to water without pumping any protons. AOX and *bd* oxidases are not discussed further [28-30].

Besides the possibility to characterize terminal oxidases by their electron donor, they can be divided into three groups that have different structural features in common (see figure 1.2).

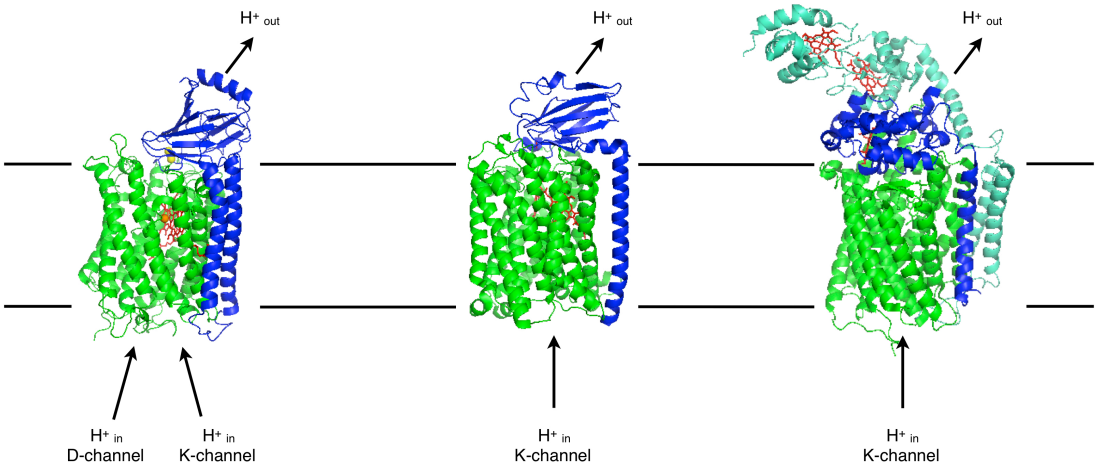

Figure 1.2: Structures of the catalytic subunits of all three major HCO-groups.
Arrows depict the proton flow into the enzyme through different channels and the release of protons. Heme molecules are shown in red, copper ions in orange. From left to right: aa_3 C*c*O of *Paracoccus denitrificans* (pdb: 3HB3), ba_3 C*c*O of *Thermus thermophilus* (pdb: 3S8G) and cbb_3 C*c*O of *Pseudomonas stutzeri* (pdb: 3MK7). Figure was prepared using Pymol.

A-type terminal oxidases have a so-called D- and K-proton-pathway (named after an essential amino acid contributing to the channel) formed by several highly conserved amino acids throughout all A-type C*c*Os. These pathways lead from the surface of the protein either to the active center for water generation, or across the membrane to pump protons, and directly contribute to the electrochemical proton gradient. Another feature is the side chain cross-link between a Cu-ion complexing histidine and a tyrosine near the active center. These two protein residues are located on the same helix in A-type HCOs. The functional core enzyme consists of two subunits. Two prominent examples for A-type (A1-type) oxidases are the mitochondrial HCO and the aa_3 cytochrome *c* oxidase of *Paracoccus denitrificans*. Both enzymes pump one proton per electron and therefore show a proton to electron ratio of 1.0.

A-type oxidases can be subdivided into A1- and A2-type HCOs. The difference between the A1-type and the A2-type HCOs is the last identified residue contributing to the D-pathway. In the A1-type this last residue is Glu 278 which has a distance of approximately 10 Å to the active center. Contrary to the A1-type, the D-channel of A2-type proteins ends with the second to last residue, Ser 193. A tyrosine residue followed by a serine residue is a common feature throughout the

A2-type proteins. This so-called YS-motif is thought to be functionally equivalent to the glutamate of the D-channel in A1-type HCOs.
B-type HCO's do not have a conserved D- or K-channel. Compensating for the lack of both channels, B-type HCOs show a K-channel analogue with three different residues at the entrance of the channel (K354T, T351S, S291Y). The cross-link of the Cu-complexing histidine to the tyrosine near the active center is conserved having both amino acids on the same helix. The core enzyme consists of two subunits. Another difference besides the altered K-channel is a reduced pump ratio of 0.5 to 0.75 protons to electrons.
The third type of HCOs is the C-type HCO. This type of terminal oxidase can have a prominent third subunit carrying a heme moiety, therefore contributing actively to the electron transfer. In these oxidases, Cu_A is substituted by a heme moiety. Another main difference is the K- or homologous K-channel. The tyrosine cross-linked to a copper complexing histidine at the end of the channel is not located on the same helix as the Cu-complexing histidine but rather on the helix opposite the cross-linked histidine. A D-channel analogue is not present in C-type HCOs. The proton to electron ratio of these proteins varies from smaller than 0.5 (measured in liposomes) to between 0.6 and 1, measured in whole cells of *Paracoccus denitrificans* and *Rhodobacter sphaeroides*, respectively (for reviews see [31; 32]).

1.3. Terminal Oxidases of *Paracoccus denitrificans*

The Gram-negative facultative anaerobic soil bacterium *Paracoccus denitrificans* (*P. denitrificans*) contains three terminal oxidases. The ba_3-type quinol oxidase, the cbb_3-type cytochrome *c* oxidase and the aa_3-type cytochrome *c* oxidase [23; 33; 34].
The studies in this work were performed on the aa_3 cytochrome *c* oxidase of *P. denitrificans* because of its high homology to the eukaryotic counterpart [34-37]

1.3.1. Genetic Situation of the aa_3 C*c*O of *P. denitrificans*

Structural genes coding either for subunits of C*c*O or for chaperones acting during the biogenesis of C*c*O are located on four different loci of the genome in the American Type Culture Collection (ATCC) strain of *P. denitrificans* [34; 38-40].

Contrary to that, all genes of the *cbb₃* C*c*O of *P. denitrificans* are located in one operon including the genes necessary for assembly [41]. The genetic organization of the *ba*$_3$ ubiquinol oxidase is similar to that of the *cbb*$_3$ C*c*O having all genes located on one operon, including the *surf1c* related heme inserting chaperone, *surfIq* [39]. To analyze the *aa*$_3$ C*c*O in a more detailed manner, variants had to be created. For this purpose, a strain with deletions in *ctaDII* (gene coding for SU I), *ctaDI* (non-expressed gene for SU I), *ccoN* (gene coding for the SU N of *cbb*$_3$ C*c*O), as well as *ORF4,* was used [42]. This deletion strain was complemented with the coding gene for SU I on a low copy number plasmid yielding a functional recombinant *aa*$_3$ C*c*O. The exact genetic situation of the ATCC WT and the rec. WT is depicted in figure 1.3. Different promoters control the expression of these four loci. Promoters are regions of DNA that facilitate the transcription initiation by assisting in formation of the RNA polymerase complex. Several genes controlled by one promoter are considered as one operon. Cloning one gene or a whole operon on a plasmid will typically result in overproduction of the desired protein simply because the number of plasmids is higher compared to the single copy found on the chromosome [1]. Complementing the deletion strain with the gene expressing SU I from a low copy-number plasmid increases the level of SU I in the rec. WT. The promoter used on the plasmid is the same as the promoter controlling the expression of chaperones and SU II [42]. This was done to ensure that the expression of chaperones, SU II and the plasmid encoded SU I is initiated similarly.

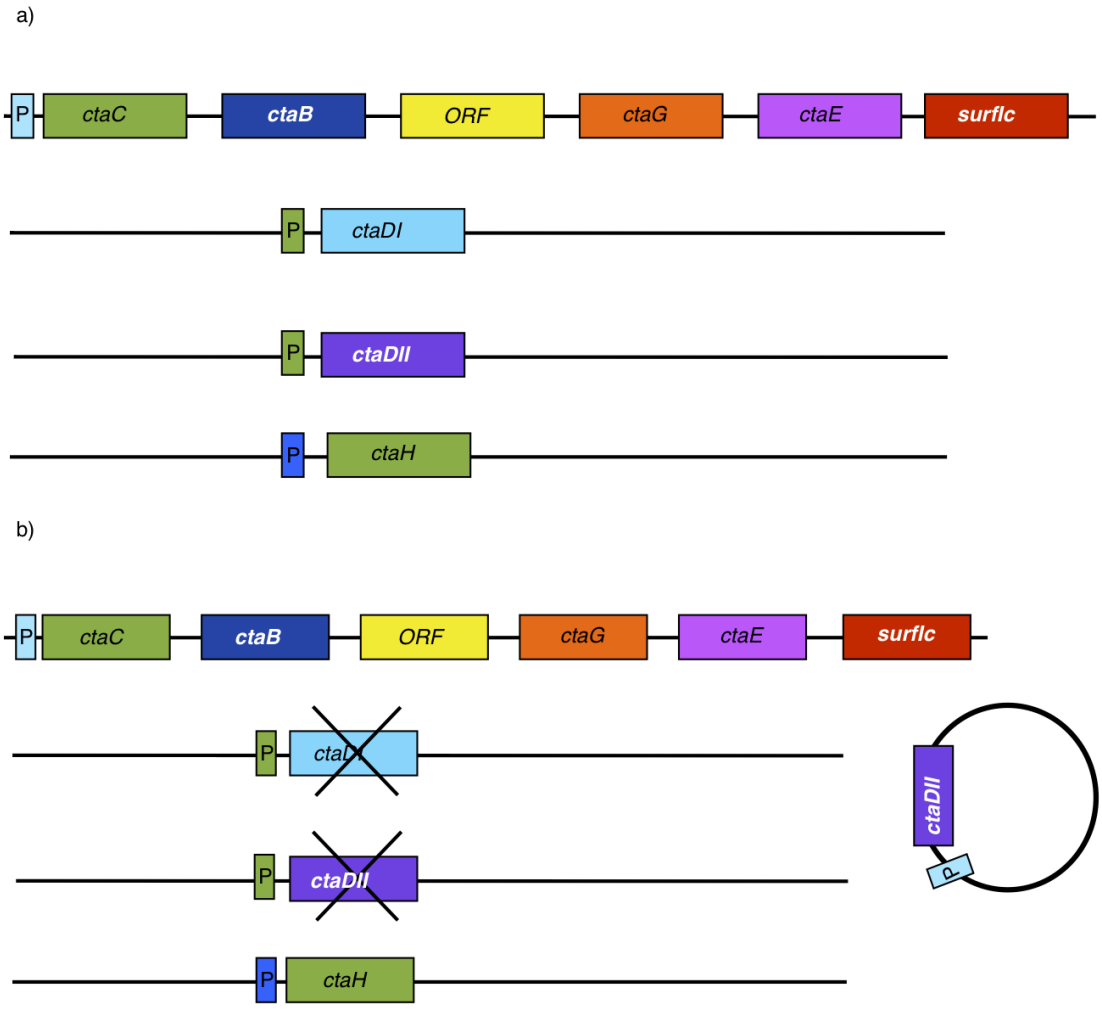

Figure 1.3: Genetic situation of both the ATCC WT (a)) and rec. WT (b)).

The rec. WT is a deletion mutant lacking both genes for SU I. The strain was complemented with a low copy-number plasmid carrying the coding gene for SU I (*ctaDII*) under the control of the same promoter, controlling the expression of SU II and III. Genes (not drawn to scale) are given in italics with their respective gene product in brackets: *ctaC* (SU II), *ctaB* (farnesyltransferase), *ctaG* (chaperone for copper insertion), *ctaE* (SU III), *surf1c* (chaperone for heme insertion), *ctaDI* (SU I, non-expressed), *ctaDII* (SU I, expressed), *ctaH* (SU IV).

1.3.2. Structure of the aa_3 Cytochrome *c* Oxidase

The aa_3 cytochrome *c* oxidase of *P. denitrificans* consists of four protein subunits (see figure 1.4) and has a theoretical molecular weight of 126.7 kDa [18]. Due to the purification method used in this work, an Fv-antibody-fragment is attached to SU II increasing the molecular weight to 154.2 kDa [43].

Table 1.1: Molecular weights of all subunits of *P. denitrificans* aa_3 C*c*O

subunit	**molecular weight / kDa**
I	62.4
II	28.0
III	30.8
IV	5.5
Fv-antibody fragment	27.5

The cytochrome *c* oxidase is a metallo-enyzme and contains four redox-active metal centers.

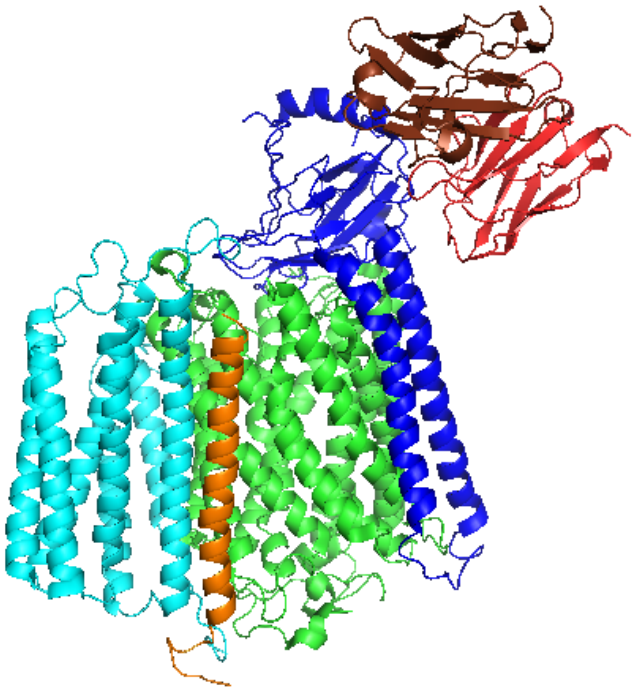

Figure 1.4: Crystal structure of the four-subunit aa_3 C*c*O of *P. denitrificans.*
SU I is shown in green, SU II in blue, SU III in turquoise, SU IV in orange and the Fv-antibody-fragment that is used for purification and crystallization attached to SU II in red and brown. Pdb code: 1QLE, figure was prepared using Pymol

The active center of the protein is located in SU I. Subunit I contains twelve hydrophobic transmembrane helices and harbors three of four redox-active metal centers, namely the low-spin heme *a*, as well as the binuclear center consisting of

the high-spin heme a_3 and Cu_B. In addition to the redox active metal centers, it contains two redox-inactive metal centers. The Mn^{2+} or Mg^{2+}-center is thought to contribute to the water exit channel, whereas the role of the Ca^{2+}-binding site remains unknown so far.

The high-spin heme *a* is liganded by two histidines at the axial position of the central iron atom and three arginines at the side chains [18; 21; 44].

Low-spin heme a_3 iron is five-fold coordinated with one histidine as axial ligand. The iron ion is approximately 0.7 Å out of plane towards Cu_B. The distance between heme a_3 and Cu_B is 5.2 Å to 4.5 Å for *Paracoccus denitrificans, Rhodobacter sphaeroides* and *Bos taurus* in the different published structures (pdb files: 1AR1, 3HB3, 1V54 and 1M56). Cu_B is liganded by three histidines, where one of those histidines (H276) is covalently linked to tyrosine 280 (*P. denitrificans* numbering) [18; 21; 27]. The shortest distance between both heme molecules is 4.7 Å, whereas the center to center distance is 13.2 Å. The overall fold of SU I shows at least two "pores" that might be accessible to solvent molecules. The aa_3 C*c*O from *P. denitrificans* belongs to the A-type HCOs and shows two proton channels, presumably located in these pores [31; 32]. The D-pathway starts at Asp124, leading, via one defined water molecule, to Asn131 and further via eleven defined water molecules, to Glu278. The entrance of the K-pathway is still under debate. Amino acids involved in the K-pathway are Thr351, Ser291, Lys354, Glu78 (in SU II) and there are at least two defined water molecules. Above the active center 13 water molecules could be modeled showing a water network around it [18; 44]. The presence of more water-filled cavities could not be ruled out so far. The cbb_3 oxidase of *Pseudomonas stutzeri* shows a water filled cavity around the active center as well [45], giving rise to the assumption that water filled cavities are necessary for the transport of product-water out of the protein.

SU II consists of three parts: A C-terminal globular, hydrophilic domain, two transmembrane helices and an N-terminal loop. SU II is in contact with SU I at the membrane level via the two transmembrane helices and at the periplasmic level via the C-terminal domain and the N-terminal loop. The C-terminal globular domain contains a ten-stranded β-barrel and interacts tightly with the N-terminal loop, closing one of the pores in SU I. Cu_A, the fourth redox active metal center, is a diatomic mixed valence cluster and is located in the C-terminal domain of SU II. The

fourth ligand of the second Cu-atom is the carbonyl oxygen of a glutamate. The distance between both Cu-atoms is 2.6 Å. This metal center forms the entrance point of electrons in the reaction cycle of C*c*O. Electrons needed for the reaction are delivered by cytochrome *c*, which binds to SU II mediated by electrostatic interactions [18; 44].

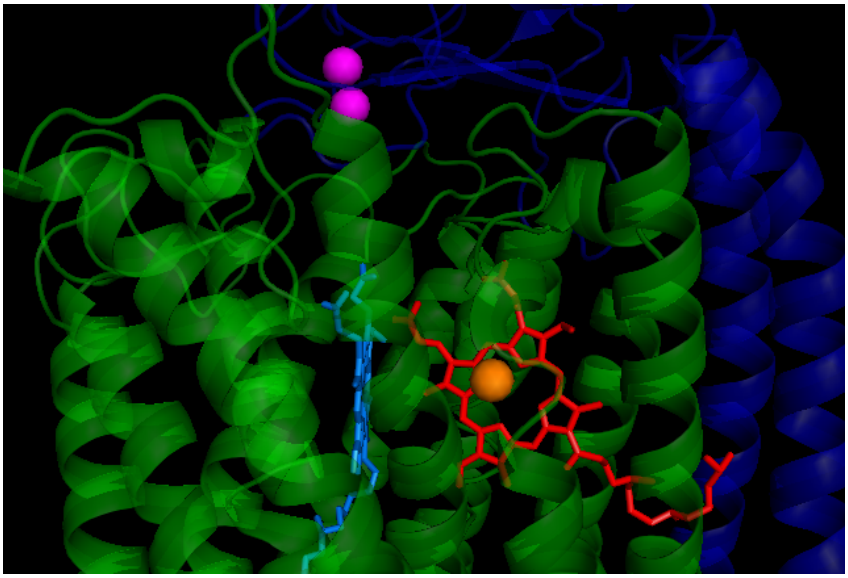

Figure 1.5: Close up of the redox active metal centers of *P. denitrificans* aa_3 C*c*O.
SU I is shown in translucent green, SU II in translucent blue, the diatomic Cu_A-center in pink, heme *a* in light blue and the binuclear center with Cu_B and heme a_3 in orange and red respectively. Pdb file: 3HB3. Figure was prepared using Pymol.

SU III consists of seven transmembrane helices that form two bundles with a V-shaped cleft in between. The function of SU III is unknown so far, as a core C*c*O formed by SU I and II only, is also fully functional as well. Lipid molecules were found in the described V-shaped cleft, raising the assumption that SU III could add to the stability of C*c*O. Another theory proposes the binding of the natural membrane-bound electron donor cytochrome c_{552} to this cleft [18].
SU IV is the smallest of all subunits with only one transmembrane helix. The function is unknown so far. Witt and Ludwig analyzed the importance of SU IV in 1997 [40] and found that SU IV did not act as an assembly factor and is not required for cofactor insertion. SU IV is in contact with all other subunits therefore it is thought that SU IV stabilizes the protein complex. Regulatory purposes as well as

adaptation to different conditions could not be ruled out as the function of SU IV [18].

1.3.3. Reaction Cycle of the *aa*$_3$ C*c*O of *P. denitrificans*

C*c*O catalyzes the four-electron reduction of molecular oxygen to water and couples this reaction to the pumping of protons from the negatively charged side of the membrane to the positively charged side of the membrane. The reaction is described by equation 1:

$$4\ \text{cyt}\ c^{+II} + O_2 + 8\ H^+_{(N)} \longrightarrow 4\ \text{cyt}\ c^{+III} + 2\ H_2O + 4\ H^+_{(P)} \qquad \text{(Equation 1)}$$

In 1981, Wikström observed natural intermediates for this reaction by partly reversing the reaction cycle of C*c*O in mitochondria. Reversing the F_OF_1-ATP synthase reaction, hydrolyzing ATP and actively pumping protons across the membrane, generated a high redox-potential which partly reversed C*c*O. Wikström discovered two intermediates and named them P and F with difference absorption maxima of the α-band at 607 and 580 nm respectively. The F-intermediate is an oxoferryl state at the heme *a*$_3$-iron, whereas the P-intermediate was proposed to bind a peroxide dianion between heme *a*$_3$ and Cu_B [46]. Ogura and Kitagawa were the first to show, by Resonance Raman-Spectroscopy, that the P-intermediate is also in an oxoferryl-state [47]. One of the first reaction mechanisms of C*c*O was published by Wikström in 1989, followed by a different reaction mechanism proposed by Michel, considering the electroneutrality principle proposed by Mitchell and Rich [48-50].

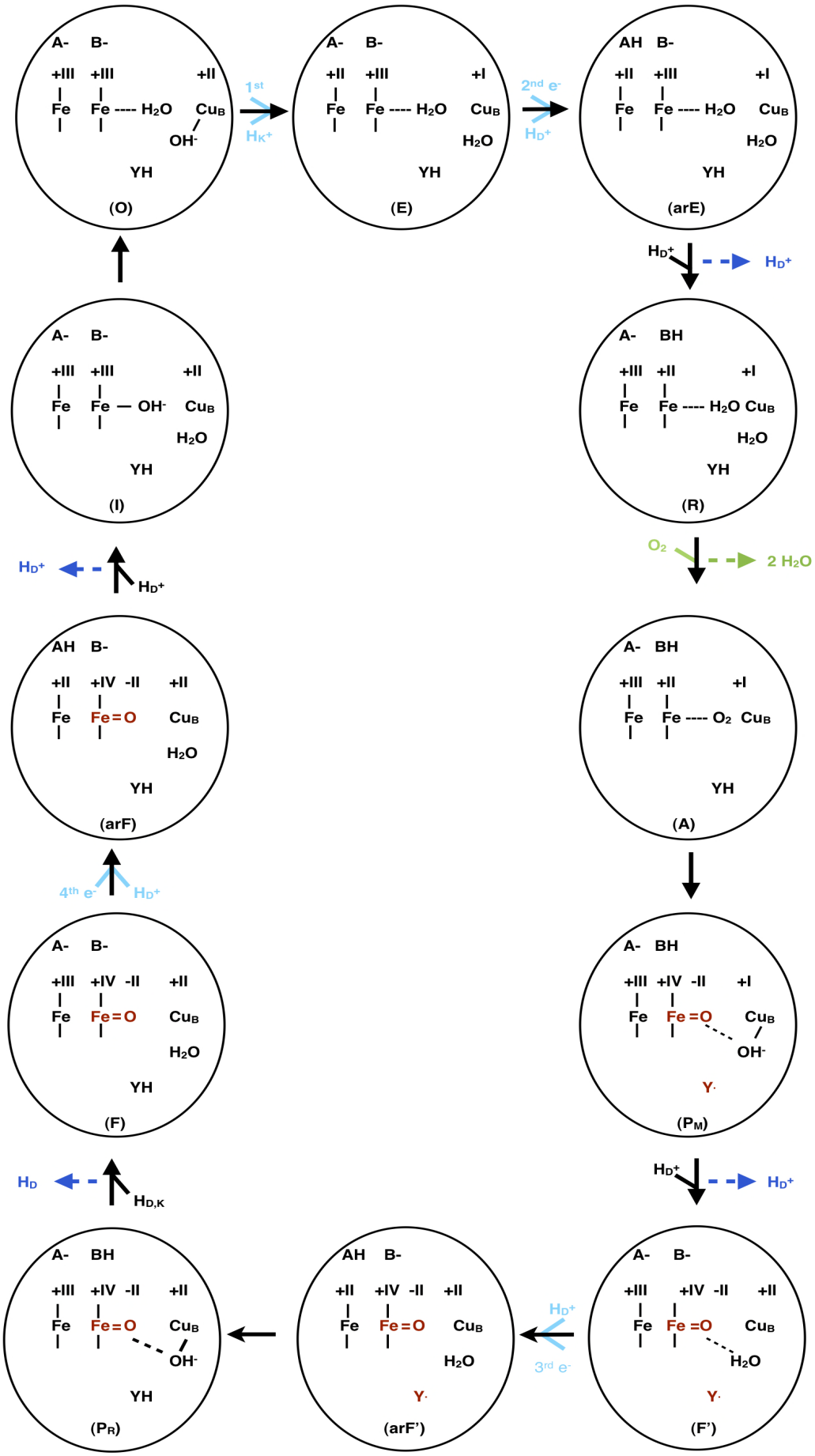
A- B-
+III +III +II
Fe Fe ---- H2O CuB
OH-
YH
(O)
1st
HK+
A- B-
+II +III +I
Fe Fe ---- H2O CuB
H2O
YH
(E)
2nd e-
HD+
AH B-
+II +III +I
Fe Fe ---- H2O CuB
H2O
YH
(arE)
HD+
HD+
A- BH
+III +II +I
Fe Fe ---- H2O CuB
H2O
YH
(R)
O2
2 H2O
A- BH
+III +II +I
Fe Fe ---- O2 CuB
YH
(A)
A- BH
+III +IV -II +I
Fe Fe=O CuB
OH-
Y·
(PM)
HD+
HD+
A- B-
+III +IV -II +II
Fe Fe=O CuB
H2O
Y·
(F')
HD+
3rd e-
AH B-
+II +IV -II +II
Fe Fe=O CuB
H2O
Y·
(arF')
A- BH
+III +IV -II +II
Fe Fe=O CuB
OH-
YH
(PR)
HD
HD,K
A- B-
+III +IV -II +II
Fe Fe=O CuB
H2O
YH
(F)
4th e-
HD+
AH B-
+II +IV -II +II
Fe Fe=O CuB
H2O
YH
(arF)
HD+
HD+
A- B-
+III +II +II
Fe Fe — OH- CuB
H2O
YH
(I)

Figure 1.6: Proposed reaction mechanism of C*c*O.
This reaction scheme is based on the electroneutrality principle. The figure shows the binuclear active center, as well as heme *a* and the corresponding propionate A. B depicts the heme a_3 propionate with at least aspartate 399. The Y stands for tyrosine 280. The four proton pumping steps (shown in blue) as well as electron and proton uptake, oxygen binding and water release are shown. The oxoferryl state and the tyrosine radical are shown in red. Proton pumping steps are shown in blue, proton and electron uptake in cyan, oxygen binding and water release in green. Figure modified from [49].

Michel proposed the oxidized state of the enzyme having a water molecule bound at heme a_3 and a hydroxyl ion at Cu_B. The first electron reduces Cu_B and one proton is taken up by the K-channel, forming water with the hydroxyl ion bound at Cu_B. The second proton enters the protein by the D-channel. The second electron reduces the iron atom of heme *a* and the proton binds near the propionate groups of heme *a*. Afterwards, another proton enters through the D-channel and binds near the heme propionates of heme a_3, whereas the proton near the heme *a* propionates gets pumped out of the protein. The resulting intermediate is called R-intermediate.
Following this step, two water molecules are released from the protein and a new oxygen molecule binds at heme a_3, forming the A-intermediate. This intermediate relaxes spontaneously to the P_M-intermediate. At this stage, an oxoferryl-state is formed at heme a_3 with the double bond of the dioxygen molecule already broken and the oxygen fully reduced in a single step.
A hydroxyl ion is now coordinated by Cu_B, having received the proton from a nearby tyrosine residue. Another proton enters the protein through the D-channel, forming water with the hydroxyl ion at Cu_B. During this step the proton near the heme a_3 propionate is pumped across the membrane. This intermediate is called F'.
The next intermediate is called arF' and is formed by the addition of the third electron and proton, while a proton enters the protein via the D-channel. The electron reduces heme *a* and the proton binds to the heme *a* propionates. The binding of the third electron and proton resulted in a change of the pK-value of the tyrosine, which is protonated by water bound to Cu_B. One electron rearranges from heme *a* to Cu_B forming a hydroxyl ion complexed by Cu_B synchronous to the rearrangement of one proton from the heme *a* propionate to the heme a_3 propionates. The entrance of another proton through the D- or K-channel triggers

the pumping of one proton out of the protein. The newly entered proton forms water by protonating the hydroxyl ion at Cu_B. This intermediate is called the F-intermediate. Binding of another proton to the heme *a* propionates simultaneously with the reduction of heme *a,* yields the arF-intermediate. The last proton enters the protein via the D-channel, resulting in pumping of the heme *a* propionate bound proton and in the formation of an iron hydroxyl complex at heme a_3.
In order to finish the cycle, one water-proton from Cu_B binds to the hydroxyl ion at heme a_3, forming water at heme a_3 and a hydroxyl ion at Cu_B reforming the O-intermediate. The electroneutrality principle is shown by the uptake of one electron together with a proton used for water generation [49].

The main events in this reaction cycle as shown in figure 1.6 are:

- Release of two water molecules and binding of molecular oxygen at the R-A transition (green arrows);
- Binding of four electrons and four protons at the O-E, E-arE, F'-arF' and F-arF transitions (turquoise arrows);
- Pumping of four protons at the arE-R, Pm-F', Pr-F and arF-I transition (blue arrows).

1.4. Side Reactions of Metalloproteins

Like C*c*O many proteins contain metal ions in their active center and are therefore named metallo-proteins. Many different reactions are catalyzed by these metal centers. Certain metals favor particular elements or functional groups to react with but the protein environment of the metal-center controls the specificity of these reactions. Iron ions, incorporated into heme molecules are, among others, present in C*c*O, catalases and peroxidases catalyzing the reduction of oxygen and the degradation of hydrogen peroxide, two completely different reactions [18; 51-54]. Side-reactions of metallo-proteins are feasible because the protein environment favors the main reaction but cannot completely abolish other possible reactions catalyzed by the corresponding metal. For example a catalase activity of met-hemoglobin was found, or an NO-reductase activity was reported for C-type C*c*Os [55-57].

As the specificity of a reaction catalyzed by a metal center is defined by the protein environment, the intensity of these side reactions is an indicator for changes of the polypeptide sequence or conformation.

Orii already described side reactions for A-type HCOs in 1963 showing a dismutation of hydrogen peroxide by C*c*O [58]. He also discovered a peroxidase activity of A-type C*c*O [59]. The dismutation of hydrogen peroxide, or the so called catalase activity of C*c*O was further described by Konstantinov and co-wokers, who also suggested a first reaction mechanism [60-62]. One reaction cycle of this mechanism included a conversion of the O to the P-intermediate upon reaction with the first hydrogen peroxide molecule and subsequently a conversion to the F-intermediate by a reaction with the second hydrogen peroxide molecule. A third hydrogen peroxide molecule is used to return to the O-intermediate. During this reaction, two superoxide molecules, as well as protons are produced. Without oxidation equivalents present, these superoxide molecules react with protons to give one water molecule and one oxygen molecule. However, an increase in pH was shown to be measurable if oxidizing equivalents were provided [60]. The catalase reaction seems to be a common side reaction throughout heme-containing metallo-proteins.

Orii described a turnover-number of 100 min^{-1} or 1.7 sec^{-1} for the catalase activity of bovine C*c*O [58]. Compared to the turnover number of genuine catalases, which is 40,000,000 sec^{-1}, this reaction is clearly considered to be a side reaction and was only poorly described [63]. The catalase activity of *P. denitrificans* aa_3 C*c*O has not been investigated at all so far.

This activity of C*c*O, analyzed from the right point of view, might become physiologically important as the enzymes of the respiratory chain of bacteria and mammalia were shown to form supercomplexes, whereas complex I and III were shown to generate reactive oxygen species (ROS) (see Introduction 1.1) [64; 65]. Therefore C*c*O could be an important member in the protection against ROS.

1.5. Catalases

ROS are a common threat to all cell types [66]. Hydrogen peroxide belongs to this group. Therefore it is highly necessary to break down hydrogen peroxide to avoid

damage of the cell, such as e.g. oxidation of lipids, oxidation of methionines and unwanted formation of cystines [67; 68]. This degradation of hydrogen peroxide is catalyzed by peroxidases that use external electron donors rather than hydrogen peroxide itself for this reaction, and catalases that disproportionate two molecules of H_2O_2 to two water molecules and one oxygen molecule [52; 69].

Catalases can be divided into three groups according to their structure and their active center. The first and smallest group contains a binuclear manganese center to catalyze the dismutation of hydrogen peroxide. The second and third group mostly contain heme *b* or heme *d* in their active centers. The main difference between the two groups is the catalyzed reaction. The second group acts as a catalase-peroxidase, not only catalyzing the dismutation of two molecules of hydrogen peroxide but also catalyzing the degradation of hydrogen peroxide using external electron donors.

The third group acts solely as a catalase, dismutating two molecules of hydrogen peroxide into one molecule of oxygen and two molecules of water [57].

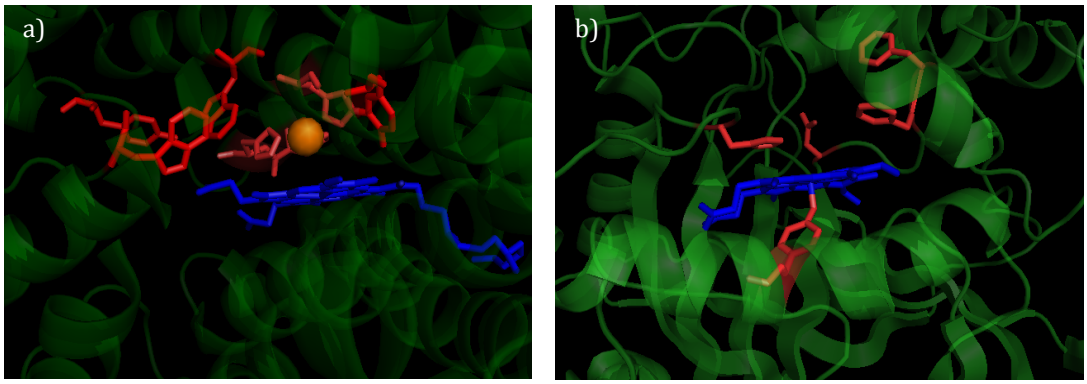

Figure 1.7: Active center of aa_3 C*c*O (a)) and human catalase (b)).
Both active centers contain a heme moiety and several aromatic amino acids in close proximity to the active site. Pdb Files: 1DGF and 3HB3. Figure was prepared using Pymol

We focus on the third group due to structural similarities to C*c*O. Catalases and C*c*Os both harbor a heme moiety in the active center and possess several aromatic amino acids near the active center.

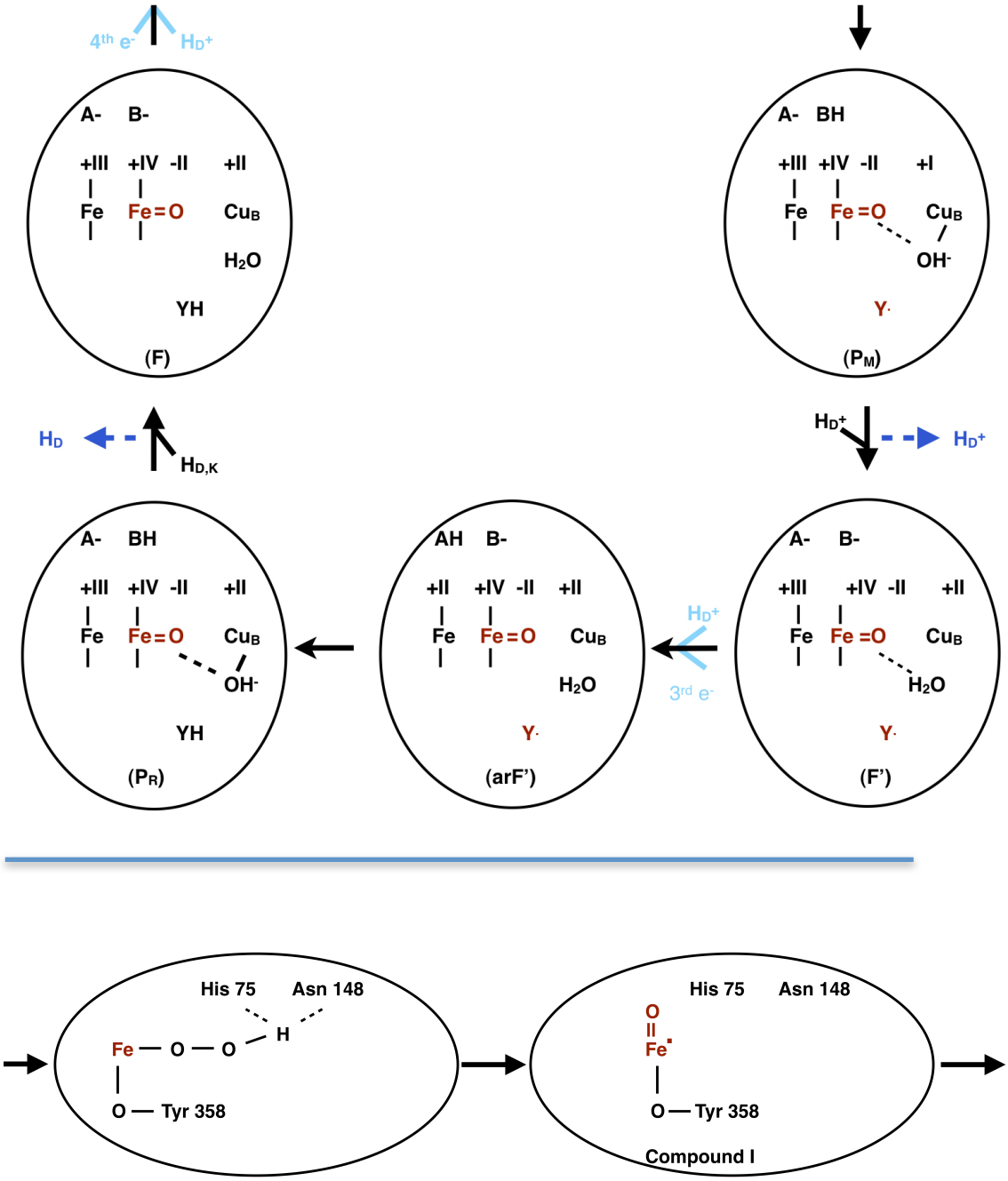

Figure 1.8: Steps of a proposed reaction cycle of C*c*O (top) and human catalase (bottom) showing similarities of both enzymes (red).
In both reaction cycles an oxoferryl intermediate is formed as well as a radical. The radical is located on an amino acid in case of C*c*O, and on the porphyrin ring in case of the catalase. Figures based on [49] and [53]

The second similarity is present in the reaction cycle of both enzymes. After the reaction of catalase with one hydrogen peroxide molecule, the enzyme forms an intermediate that is called compound I. This intermediate is very similar to the P- and F-intermediates of C*c*O, exhibiting an oxoferryl group at the heme-moiety.

Additionally, catalases show a porphyrin radical during their reaction cycle, especially at compound I [70]. C*c*O was reported to form an amino acid radical, located on tyrosine 167 (*P. denitrificans* numbering) upon reaction with hydrogen peroxide (in the P-intermediate) [71]. So C*c*O possesses all features necessary to show catalase activity.

1.6. Aim of this Work

This work focuses on the comparison of the native (ATCC WT C*c*O) and the homologously, recombinantly produced (rec. WT C*c*O) form of the aa_3 C*c*O from *P. denitrificans*. It was already shown before, that differences in recombinantly produced proteins do exist. Several proteins that are in everyday use, such as laundry detergent or more importantly insulin, are produced recombinantly. It is therefore crucial to understand possible reasons for distinctions and the nature of deviations in recombinant production of proteins.
Angerer described a difference of the native and recombinant aa_3 C*c*O from *P. denitrificans* in its catalase activity in 2009 [72]. In 1963, Orii and Okunuki first discovered the catalase activity of an A-type C*c*O [58] and Konstantinov and co-workers described the first full reaction cycle of the catalase reaction of an A-type CcO in 1993 [60]. Therefore, this work focuses on two main projects:

- The detailed structural comparison of all subunits and metal cofactors of the ATCC WT C*c*O and rec. WT C*c*O, by a wide spectrum of different biophysical methods, to explain the differences observed before.
  The rec. WT consists of a deletion strain (Δ*ctaDI*, Δ*ctaDII,* Δ*ORF4,* Δ*ccoN*) supplemented with a low copy-number plasmid carrying *ctaDII,* the gene coding for SU I of C*c*O. This might lead to an overproduction of SU I of C*c*O probably resulting in a lack of metal inserting chaperones. Therefore, the consequences of an elevated level of chaperones, responsible for the insertion of the redox-active metal centers, have to be considered. Newly constructed wild type versions with an increased chaperone level have to be analyzed kinetically and mechanistically.

Consequently another rec. WT C*c*O shall be constructed carrying a His_6-tag to provide copper near the apo-protein during assembly. A fifth wild type was kindly provided by the group of M. Wikström [34]. This wild type is an intermediate between the ATCC WT and rec. WT. It features a deletion in *ctaDI* and *ORF4* but the gene *ctaDII*, coding for SU I, is still located on the chromosome and not supplied on a plasmid. Kinetic and structural parameters of the catalase activity of these variations have to be compared to the rec. WT C*c*O and ATCC WT C*c*O.

- A second focus is on the detailed kinetic and mechanistic analysis of the catalase reaction of aa_3 C*c*O from *P. denitrificans.* Since a catalase reaction of a membrane protein seems very useful to break down hydrogen peroxide right in the membrane and prevent the oxidation of lipids, it is important to understand the mechanism of this reaction. The active site of the catalase reaction of C*c*O shall be probed using specific inhibitors. Amino acid residues of certain importance for the reaction mechanism have to be identified by site directed mutagenesis. The involvement of Cu_B in the catalase reaction will be clarified.

  Concluding, the catalase mechanism of aa_3 C*c*O has to be compared to heme containing catalases and the potential physiological relevance of this C*c*O side rection activity has to be discussed.

2. Materials and Methods

2.1. Materials

All chemicals and enzymes, if not stated otherwise, were obtained in highest purity from Carl Roth GmbH (Karlsruhe, Germany), Sigma-Aldrich (Taufkirchen, Germany), New England Biolabs (Ipswich, MA, USA), Thermo Scientific (Bonn, Germany), Invitrogen (Carlsbad, CA, USA) or Fermentas (St. Leon-Rot, Germany). Primers were obtained from MWG (Eurofins MWG Operon, Ebersberg, Germany), Invitrogen (Carlsbad, CA, USA), Biomers (Ulm, Germany).

Table 2.1: Plasmids

Plasmid	**Features**	**Reference**
pASK68	Amp^r, *lacI*, *f1IG*, $lac^{p/o}$, *ompA-(V_H)-strep, phoA-(V_L)-myc*	[73]
pUP39	pBBR1 MCS derivative Sm^r, Kn^r, *ctaC2*-Promoter *KpnI*/*XbaI*, *ctaDII XbaI*/*HindIII*	University of Frankfurt, Dr. Pfitzner
pAD1	pFH11 derivative, W164F	this work
pAD2	pFH11 derivative, Y167F	this work
pAD3	pFH11 derivative, W164F Y167F	this work
pFH11	pUP39 derivative, *ctaDII XbaI*/*SacI*	this work
pFH12	pFH11 derivative, *ctaDII* C-terminal end 2x Ala, 6x His	this work
pFH13	pFH11 derivative, *ctaG SacI*	this work
pFH17	pFH11 derivative, H276D	this work
pFH18	pFH11 derivative, H276E	this work
pFH19	pFH11 derivative, H276K	this work
pFH20	pFH11 derivative, H276R	this work
pFH21	pFH11 derivative, *ctaG SacI*/*ScaI*, *surf1c ScaI*	this work
pFH22	pFH11 derivative, W272F	this work
pFH23	pFH11 derivative, Y280F	this work
pFH24	pFH11 derivative, W272F Y280F	this work

Table 2.2: Oligonucleotides

Modifications	**Primer-Sequence 5' to 3'**
rec. WT C*c*O, his tagged rec. WT C*c*O, rec. WT C*c*O with chaperones	GATCGATCTAGAAACAGGCGAGTCCGTCGG

rec. WT C*c*O,	GATTCAGAGCTCTCAATGCGCGTGTGCGCG
his tagged rec. WT C*c*O	GATTCAGAGCTCTCAATGATGATGATGATG ATGCGCCGCATGCGCGTGTGCGCGATC
ctaG	ATCGAGCTCATCAGTACTTCAGTTTACGGTCGGTTC
ctaG	ATCTAGGAGCTCAGGAGGGGCGAACCAATGAGC
surf1c	TCAGAGCTCATTAGTACTAGGAGGGCCATTTCGATGCGCCGT
surf1c	ATTGAGCTCTAAAGTACTCTAGAATTGCCGCTG
surf1c	ATTAGTACTCTAATGATGATGATGATGATGTGCTGCGAATTGCCG
surf1c	GGCGAATTGGAGCTCTAAAGTACTCTAATGATGATGATGATGATGG CCGCCGAATTGCCGCTGCCTGATACGCCA
W164F	GGCGTCGGCTTTGTGCTC
W164F,	GAGCACAAAGCCGACGCC
Y167F	GTGCTCTTTCCGCCGCTC
Y167F	GAGCGGCGGAAAGAGCAC
W164F Y167F	GGCGTCGGCTTTGTGCTCTTTCCGCCGCTC
W164F Y167F	GAGCGGCGGAAAGAGCACAAACACGACGAC
W272F	TACCAGCACATCCTGTTTTTCTTCGGCCAT
W272F	ATGGCCGAAGAAAAACAGGATGTGCTGGTA
H276D	TATAGACCTCGGGATCGCCGAAGAACCACAG
H276D	CTGTGGTTCTTCGGCGATCCCGAGGTCTATA
H276E	TGATATAGACCTCGGGCTCGCCGAAGAACCACAGG
H276E	CCTGTGGTTCTTCGGCGAGCCCGAGGTCTATATCA
H276K	GATGATATAGACCTCGGGCTTGCCGAAGAACCACAGGAT
H276K	ATCCTGTGGTTCTTCGGCAAGCCCGAGGTCTATATCATC
H276R	GATATAGACCTCGGGACGGCCGAAGAACCACAG
H276R	CTGTGGTTCTTCGGCCGTCCCGAGGTCTATATC
Y280F	GCCCGGCAGGATGATGATAAAGACCTCGGGATG
Y280F	CATCCCGAGGTCTTTATCATCATCCTGCCGGGC
Seq-Primer 2	TTTTCCCAGTCACGACGT
Seq-Primer 3 *ctaG*	GACGAGCCGGTGACCGGC
Seq-Primer 4 *ctaG*	ACCGGCATCTCGACCCGC
Seq-Primer 5 *surf1c*	ACGGGCGCAGGATCCTGC
Seq-Primer 6 *surf1c*	TTCGTCGGGCCAGTGCAG

Table 2.3: Strains

Strain	**Genotype**	**Reference**
E. coli DH5α	*fhuA2 Δ(argF-lacZ)U169 phoA glnV44* Φ80 *Δ(lacZ)M15 gyrA96 recA1 relA1 endA1 thi-1 hsdR17*	[74]
E. coli GM2163	*F- dam-13*::Tn9 (Cam^r) *dcm-6 hsdR2* ($r_k^-m_k^+$) *leuB6 hisG4 thi-1 araC14 lacY1 galK2 galT22 xylA5 mtl-1 rpsL136* (Str^r) *fhuA31 tsx-78 glnV44*	[75]

	mcrA mcrB1	
E. coli JM83	F^- *ara* Δ(*lac-proAB*) *rpsL* (Str^r) *thi* Φ80dΔ*(lacZ)M15*	[76]
E. coli RP4-4	RP4-derivative in J53 with Amp^R, Tet^R, Km^R	Dr. Richter, University of Frankfurt, Frankfurt Main, Germany
P. denitrificans PD1222	wild type	American Tissue Culture Collection, LGC Promochem, Wesel, Germany
P. denitrificans MR3	Δ*ctaDI* Δ*ORF4* ::Km^r	[34]
P. denitrificans AO1	PD1222 derivative, Δ*ctaDI*::Km^r, Δ*ctaDII*::Tet^r, Δ*ccON*::Gm^r, Rif^r	[42]
P. denitrificans PUP206	Δ*ctaG*::Km^r	Ute Pfitzner, University of Frankfurt, Frankfurt Main, Germany

Table 2.4: Buffers and Solutions

Buffer/Solution	**Composition of buffers**
KP_i	Mix KH_2PO_4 and K_2HPO_4 with the same concentration till desired pH
RF1 Buffer	100 mM RbCl, 50 mM $MnCl_2$, 30 mM K-acetate, 10 mM $CaCl_2$, 15% (w/v) glycerol, pH 5.8/HCl
RF2 Buffer	10 mM MOPS, 10 mM RbCl, 75 mM $CaCl_2$, 15% (w/v) glycerol, pH 6.8/NaOH
Resuspension Buffer	200 mM KP_i, pH 8.0, 1 mM EDTA
Measuring Buffer O2	30 mM KP_i, pH 7.0, 0.05% (w/v) DDM
Measuring Buffer UV/vis	50 mM KP_i, pH 7.0, 0.05% (w/v) DDM
Washing Buffer 1	50 mM KP_i, pH 8.0, 1mM EDTA
Washing Buffer 2	50 mM KP_i, pH 8.0, 0.05% (w/v) DDM, 1mM EDTA
Washing Buffer 3	50 mM KP_i, pH 8.0, 0.08% (v/v) LDAO, 1mM EDTA
Elution Buffer 1	50 mM KP_i, pH 8.0, 0.05% (w/v) DDM, 1mM EDTA, 10 mM desthiobiotin
Elution Buffer 2	50 mM KP_i, pH 8.0, 0.08% (v/v) LDAO, 1mM EDTA, 10 mM desthiobiotin
Elution Buffer 3	600 mM KP_i, pH 8.0, 0.05% (w/v) DDM, 1 mM EDTA
Storage Buffer	10 mM KP_i, pH8.0, 0.01% (w/v) DDM, 0.2 mM EDTA
Periplasm Buffer	35 mM KP_i, pH 8.0, 1 mM EDTA,

	500 mM sucrose
MOPS Buffer (20x)	1 M 3-morpholinopropane-1-sulfonic acid, 1 M 2-amino-2-hydroxymethyl-propane-1,3-diol, 69.4 mM sodium lauryl sulfate, 20.5 mM EDTA
TBE Buffer	89 mM tris, 89 mM borate, 2 mM EDTA
AP Buffer	100 mM tris/HCl, pH 9.5, 100 mM NaCl, 5 mM $MgCl_2$
TBST Buffer	10 mM tris/HCl, pH 8.0, 150 mM NaCl, 0.05% (w/v) tween 20
Transfer Buffer	25 mM tris/HCl, pH 8.3, 150 mM glycine, 10% (v/v) methanol
Blocking Buffer	TBST Buffer + 20% (w/v) skim milk powder
Developing Buffer	AP Buffer + 250 µg/ml BCIP in DMF, 500 µg/ml NBT in 70% (v/v) DMF
6x PAP	0.25% (w/v) bromophenol blue, 0.25% (w/v) xylene cyanolFF, 15% (w/v) ficoll 400
S+G Solution	0.06% (w/v) coomassie G250, 2.2% (v/v) HCl
Ampicillin	10% (w/v), 50% glycerol (v/v)
Kanamycin	2.5% (w/v), 50% glycerol (v/v)
Streptomycin	2.5% (w/v), 50% glycerol (v/v)
Rifampicin	3% (w/v), 100% methanol
2x YTG-Medium	1% (w/v) trypton, 0.5% (w/v) yeast extract, 1% (w/v) NaCl, 15% (v/v) glycerol
LB-Medium	1% (w/v) trypton, 0.5% (w/v) yeast extract, 1% (w/v) NaCl (for plates 1.6% agar (w/v) was added.
Succinat-Medium	50 mM K_2HPO_4, 75 mM NH_4Cl, 11.5 mM Na_2SO_4, 1.25 mM $MgCl_2$, 1 mM citric acid, 1% (w/v) succinic acid, 100 µM $CaCl_2$, 90 µM $FeCl_3$, 50 µM $MnCl_2$, 25 µM $ZnCl_2$, 10 µM $CoCl_2$, 5 µM $CuCl_2$, 5 µM H_3BO_3, 10 µM Na_2MoO_4, adjust pH to 6.2 using KOH

2.2. Molecular Biological Methods

2.2.1. Construction of Plasmids

Biomolecular experiments were performed according to Sambrook and Russell [77].

The plasmid pFH11 (see figure 2.1) was constructed by introducing a new *SacI* restriction site at the end of *ctaDII*, therefore, slightly modifying the original vector pUP39.

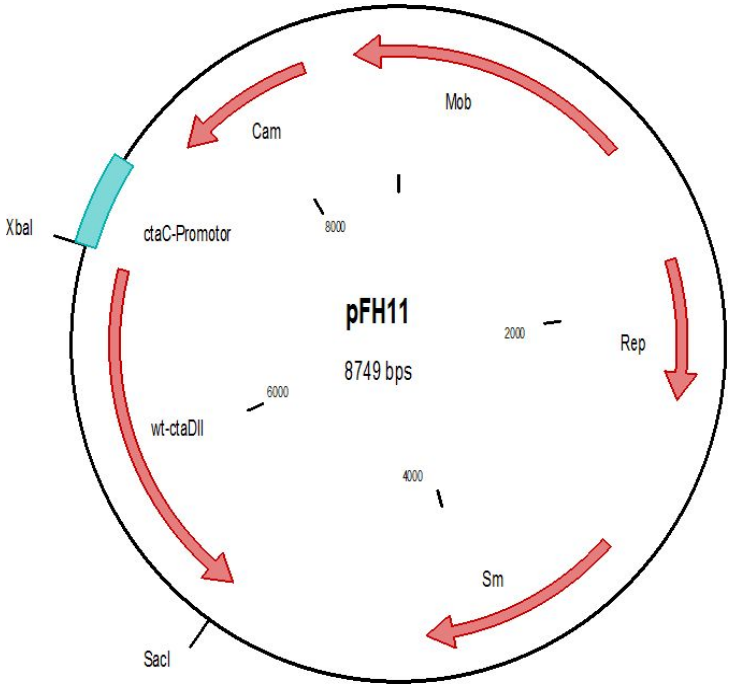

Figure 2.1: Plasmid-Map of pFH11

Genes given are *ctaDII* (coding for SU I of Cc*O*), *Sm* (coding for an streptomycin resistance), *Cam* (coding for an Chloramphenicol resistance), *Rep* (replication origin), *Mob* (giving the ability to transfer the plasmid into different organisms than *E. coli*.) and the *ctaC*-Promoter. *ctaDII* is flanked by an *XbaI* and a *SacI* restriction site.

To generate pFH12 the corresponding base pairs for a 2x alanine-spacer and a His_6-tag at the end of *ctaDII* were added additionally. The PCR-products for pFH11 and pFH12 were blunt-end-ligated into pJet1.2 (Fermentas, St. Leon Roth, Germany). The plasmid carrying *ctaDII* without the His_6-tag was used for mutagenesis-PCR. pJet1.2 carrying *ctaDII* with or without His_6-tag was cut using *XbaI* / *SacI*. The

desired gene fragment was re-ligated in the *XbaI* / *SacI* treated pUP39-backbone. The products were named pFH11 and pFH12 carrying no tag and a His_6-tag, respectively.

The plasmids pFH13 and pFH21 were constructed using pFH11. The genes *ctaG* and *surf1c* were amplified with genomic DNA from *P. denitrificans* PD1222 as a template, introducing a *SacI* restriction site on both ends of *ctaG* and a *ScaI* restriction site at the 3' end of *ctaG* and on both ends of *surf1c*. For the construction of pFH13, pFH11 as well as the *ctaG* PCR-Product were cut using *SacI* and subsequently ligated. The resulting plasmid was used for the generation of pFH21. pFH13 and the *surf1c* PCR-Fragment were both *ScaI* digested and subsequently ligated.

2.2.2. Plasmid Purification

E. coli strains DH5α [74] and GM2163 [75] were used for amplification of plasmid-DNA. Overnight cultures of single colonies were grown in either 5 ml or 100 ml LB-medium. Plasmid-DNA was purified with the Qiagen plasmid mini kit (5 ml) or midi kit (100 ml) (Qiagen, Hilden, Germany). The DNA was eluted with 30 µl or 500 µl ultra-pure water, respectively. DNA concentration was determined by measuring absorption at 260 nm with a NanoDrop ND-1000 spectrometer (NanoDrop Technologies, Inc., Wilmington, DE, USA). If the concentration was not satisfying, several 5 ml cultures were purified using the same Qiagen plasmid mini kit column. Plasmid-DNA was stored at -20°C.

2.2.3. Purification of Genomic DNA

Genomic DNA of 3 ml *Paracoccus denitrificans* PD1222 over night culture was purified with the help of the G-spin Genomic DNA extraction kit (Intron Biotechnology, Kyunggi-do, Korea). Genomic DNA bound to the column was eluted with 70 µl ultra pure water and stored at 4°C.

2.2.4. Agarose Gel Electrophoresis

Agarose gel electrophoresis was performed to separate DNA fragments according to their size. The range of separation is dependent on the agarose concentration. 1% (w/v) agarose gels were used exclusively. For this, 1% (w/v) agarose (Neo-Ultra, Roth, Karlsruhe, Germany) was melted in TBE-buffer, poured into the self-build gel chamber and left to gelatinize at room temperature. The DNA was mixed with the aquired amount of 6 x PAP and submitted to gel electrophoresis at 120 Volts for 1.5 hours. In this work, analytical as well as preparative gel electrophoresis were performed. The difference between an analytical gel electrophoresis (15 µl) and a preparative gel electrophoresis (65 µl) is the submitted volume. After finishing the gel electrophoresis run, the agarose gel was stained for 15 minutes using an ethidiumbromide solution (5 drops of 5 mg/ml stock solution diluted in 500 ml ultra-pure water) (Roth, Karlsruhe, Germany). The result was observed and documented at 302 nm using a BioRad gel documentation system (Universal Hood II, BioRad, Hercules, CA, USA). If the separated DNA was used for ligation afterwards, the corresponding bands were cut and stored at 4°C. The position of the cut bands was documented at 312 nm.

2.2.5. DNA-Elution from Agarose-Gels

DNA fragments purified by agarose gel electrophoresis were eluted from the agarose gel with the Qiagen QIAquick gel extraction kit (Qiagen, Hilden, Germany). DNA fragments bound to the supplied purification column were eluted with 30 µl of ultra-pure water. The DNA concentration of the eluates was determined using a NanoDrop ND-1000 spectrometer (NanoDrop Technologies, Inc., Wilmington, DE, USA).

2.2.6. Restriction Digest

Restriction digests were carried out either in a preparative scale, as a 50 µl batch setup, or in an analytical dimension, as a 10 µl batch setup. 10 x buffer, matching the suppliers description, and 1-2 µl of restriction enzyme were mixed in all cases. If the

treated DNA was to serve as a vector, 1 µl of CIAP was added to the batch setup. The missing volume was filled up with the desired DNA solution. All batch setups were incubated at 37°C for 1 hour or 3 hours for analytical scale and preparative scale, respectively, in an Eppendorf thermomixer (Thermomixer comfort, Eppendorf, Hamburg, Germany).

2.2.7. Ligation

DNA fragments obtained after restriction digest were covalently linked via ligation. 15 µl batch setups contained the recommended buffer, 1 mM ATP, T4-DNA ligase (Epicenter ligation kit, Promega and quick ligation kit, NEB), according to the supplier's recommendations, and either a 3:1 or 6:1 ratio of insert to vector. These batch setups were incubated at either 16°C overnight (Finnzymes, Espoo, Finnland) or at room temperature for 5 minutes (NEB Quick ligation kit, New England Biolabs, Ipswich, MA, USA). 2-5 µl of the ligation-mixture were used to transform the desired *E. coli* strain.

2.2.8. Generation of Competent Cells

Competent cells were obtained according to the method of Hanahan [74]. 5 ml over night culture of the desired strain were grown shaking at 37°C and 220 rpm. 1 ml of this over night culture was used to inoculate 200 ml LB-medium, which was then incubated at 180 rpm and 32°C until an optical density of 0.5 at 600 nm (Ultrospec 2100 pro, Amersham Biosciences, UK) was reached. Afterwards, cells were incubated on ice for 20 minutes and centrifuged for 20 minutes at 2500 x g (Sigma 4K15, Sigma centrifuges, Osterode, Germany). The cell pellet was resuspended in 70 ml RF1 buffer and incubated on ice for 20 minutes. The cell suspension was centrifuged at 1600 x g for 5 minutes (Sigma 4K15, Sigma centrifuges, Osterode, Germany). The supernatant was discarded. Pelleted cells were resuspended in 16 ml RF2 buffer and incubated on ice for 15 minutes prior to aliquoting, shock freezing in liquid nitrogen and storage at -80°C.

2.2.9. Transformation of Plasmid DNA

The desired chemocompetent *E. coli* strain was transformed with plasmid DNA via the heat shock method. For this purpose usually 150 ng DNA were added to 100 µl of *E. coli* and incubated on ice for 5 minutes prior to a 90 second heat shock at 42°C (Thermomixer comfort, Eppendorf, Hamburg, Germany). Cells were left on ice afterwards for 5 minutes and 800 µl of LB-medium was added. Cells were grown at 37°C for one hour before plating or inoculation of liquid medium.

2.2.10. Mutagenesis-PCR

To introduce mutations into SU I of C*c*O, mutagenesis-PCR was done with the Quickchange site-directed mutagenesis kit (Stratagene, La Jolla, CA, USA) according to the suppliers recommendations. Oligonucleotides used are listed in table 2.2. For this purpose pJET1.2 containing *ctaDII* without any tags served as a template. The PCR reaction (PCR T-Gradient, Biometra, Goettingen, Germany) followed the reaction scheme depicted in table 2.5.

Table 2.5: Mutagenesis-PCR reaction scheme

Temperature / °C	Time / seconds	Number of repeats
95	45	0
95	45	18
60	90	18
68	330	18
68	300	0
4	hold	0

The obtained PCR product was *DpnI* digested to remove the methylated parental DNA and transformed into either *E. coli* GM2163 or DH5α for plasmid amplification. Purified plasmid from these sources as well as original pFH11 was digested using *XbaI* / *SacI*, adding *CIAP* to the setup containing pFH11. Resulting fragments were purified by agarose gel electrophoresis. The pFH11 backbone was ligated with the

mutated *ctaDII* gene and transformed into *E. coli* DH5α. This culture was further used for triparental mating.
All mutations were verified in each plasmid via sequencing (Eurofins MWG Operon, Ebersberg, Germany / Seqlab, Goettingen, Germany) [78].

2.2.11. Triparental Mating

Paracoccus denitrificans is not transformable. Triparental mating had to be used to introduce plasmids into *P. denitrificans.* In this work the procedure published by Gerhus *et al.* [79] was used. 5 ml of the desired *Paracoccus denitrificans* strain [42] (Rif^r, Kan^r), 5 ml of the *E. coli* helper-strain RP4-4 (donating the plasmids via F-pili to *P. denitrificans*) (Amp^r) and 5 ml of *E. coli* DH5α carrying the desired plasmid ($Strep^r$) were grown at 37°C and 220 rpm overnight with the corresponding antibiotic in LB-medium. Cells were centrifuged at 3000 x g (Eppendorf Centrifuge 5424, Eppendorf, Hamburg, Germany) for 15 minutes. The cell pellets were resuspended in 500 µl LB-medium. All three strains were mixed in a ratio of 3:1:1 (300 µl *Paracoccus denitrificans*, 100 µl *E. coli* RP4-4, 100 µl *E. coli* DH5α containing the desired plasmid), centrifuged at 3000 x g for 10 minutes (Eppendorf Centrifuge 5424, Eppendorf, Hamburg, Germany) and resuspended in 100 µl LB-medium. These 100 µl aliquots were plated on an LB-agarplate as one drop and incubated over night at 32°C (Julabo Biotherm 37, Julabo, Seelbach, Germany). This cell drop was resuspended in 1 ml of LB-medium after incubation and diluted 1:1, 1:4, 1:8 and 1:16. 100 µl of each dilution were plated on a LB-agarplate containing rifampicin, kanamycin and streptomycin. Plates were incubated at 32°C (Julabo Biotherm 37, Julabo, Seelbach, Germany) for 2 days. Single colonies were transferred into liquid medium containing rifampicin, kanamycin and streptomycin and incubated shaking for 2 days at 32°C and 180 rpm (Lab Shaker, Adolf Kuehner AG, Basel, Switzerland). Plasmid DNA and glycerol-stocks were prepared from this liquid culture. Plasmid DNA was sent for sequencing to verify the mutation (Eurofins MWG Operon, Ebersberg, Germany / Seqlab, Goettingen, Germany).

2.2.12. Cultivation of Microorganisms

LB-Medium was prepared according to [80] and succinate-medium according to [81].

E. coli strains grown for the purification of plasmid DNA, were incubated shaking (Infors AG, Bottmingen, Switzerland) at 37°C and 180 to 220 rpm. LB-agarplates were incubated at 37°C for *E. coli* strains overnight and at 32°C for *P. denitrificans* strains (Julabo Biotherm 37, Julabo, Seelbach, Germany) for 2 days. *P. denitirifcans* cultures used for plasmid DNA preparation were grown at 32°C, shaking at 180 rpm (Infors AG, Bottmingen, Switzerland).

2.2.13. Cell Growth and Antibody-Fragment Purification from *E. coli* JM83 pASK68

The antibody-fragment Fv7E2 was produced in *E. coli* JM83 with the plasmid pASK68 (Amp^r) carrying the corresponding gene controlled by the lac-operator. This results in the ability to induce the expression of the gene of interest by the addition of IPTG. The antibody fragment is carrying a signal sequence, which leads to the secretion of the fragment into the periplasm. Fv-antibody fragments are able to bind to SU II of C*c*O and carry a C-terminal strep-tag [43]. For the production of the antibody fragment, 4 x 200 ml LB-medium containing 100 µg/ml ampicillin were inoculated with 50 µl of glycerol-stock and grown at 30°C shaking at 180 rpm (Infors AG, Bottmingen, Switzerland) overnight. The main culture, consisting of 24 l LB-medium with 100 µg/ml ampicillin, was divided in 2 x 12 l. The first half was inoculated with 80 ml overnight-culture, the second half was inoculated with 50 ml overnight-culture. Both halves were incubated at 23.5°C at 165 rpm (Infors AG, Bottmingen, Switzerland) measuring OD at 550 nm hourly. Production of the antibody fragment was induced with 0.5 mM IPTG as soon as the $OD_{550\,nm}$ reached 0.5 (Ultrospec 2100 pro, Amersham Biosciences, UK) and left growing for 3 hours. Cells were harvested at 3500 x g for 15 minutes at 4°C (Avanti J-26XP, Beckman Coulter, Brea, CA, USA). Pelleted cells were removed after every centrifugation step and stored on ice till further use. All cells were resuspended in periplasm buffer [43] and incubated on ice for 20 minutes prior to centrifugation at 24,000 x g, 4°C

for 60 minutes (Sorvall RC-5B, DuPont Instruments). Incubation in periplasm buffer led to the formation of spheroblasts due to osmotic shock. The supernatant (periplasm) contained the desired antibody-fragments. The purified periplasm was checked for hydrogen peroxide dependent oxygen production with an oxygen electrode (Unisense, Aarhus, Denmark) and stored in 30 ml aliquots at -20°C.

2.2.14. Cell Growth of *P. denitrificans*

P. denitrificans was grown aerobically in 4 x 50 ml Succinate-media (in 100 ml baffled flasks) shaking overnight at 180 rpm and 32°C, without antibiotics in case of the ATCC strain, and with 25 µg/ml streptomycin and 25 µg/ml kanamycin for all other variants. The medium was manganese depleted in all steps if the desired protein was to be used in EPR-measurements. The 50 ml cultures were used to inoculate 4 x 600 ml succinate-medium, with antibiotics for variants, in 2 or 3 l baffled flasks, which were incubated for 8 hours at 32°C and 180 rpm. The main culture consisted of 12 x 2 l succinate-medium in 5 l baffled flasks and was inoculated with 200 ml of the 600 ml cultures. The main-culture was incubated at 32°C and 170 rpm (Infors AG, Bottmingen, Switzerland) overnight. Cells were harvested at 10500 x g (Avanti J-26XP, Beckman Coulter, Brea, CA, USA) for 15 min and resuspended in 200 mM KP_i, pH 8.0, 1 mM EDTA. Cells were disrupted using a microfluidizer (Microfluidics, Newton, Massachusetts, USA) with a pressure of 1300 bar. Cell debris was removed with a 60 min centrifugation step at 6900 x g (Sorvall RC-5B, DuPont Instruments). Membranes were pelleted at 125,000 x g overnight and carefully resuspended in 50 mM KP_i, pH 8.0, 1 mM EDTA (L8-70M / L90K, Beckman Coulter, Brea, CA, USA). The volume was scaled down from 24 l total to 2 l in one 5 l baffled flask if cultures were to be used to check for expression of *ctaG* or *surf1c*. Cells were disrupted with a French Press (French Pressure Cell Press, SLM Aminco, Urbana, IL, USA) with a pressure of 1380 bar. The remaining steps were performed according to the already described protocol.

2.3. Biochemical Methods

2.3.1. Purification of C*c*O

Membranes (Protein concentration 15-25 mg/ml) were solubilised by stirring on ice for 12 minutes using 4.5% (w/v) β-dodecylmaltoside (DDM) (Glycon GmbH, Luckenwalde, Germany), 98.4 mM KP_i, pH 8.0, 1.7 mM EDTA, 90 µg/ml pefabloc, and 135 µg/ml avidine from hen egg (Gerbu Biotechnik GmbH, Heidelberg, Germany). After 12 minutes, 32.7% (v/v) *E. coli* periplasm preparation with the strep-tagged Fv-antibody fragment was added. To allow binding of the antibody fragment to SU II of CcO, stirring was continued for additional 12 minutes followed by a one hour centrifugation step at 235,000 x g and 4°C (L8-70M / L90K, Beckman Coulter, Brea, CA, USA). The supernatant was loaded on a strep-tactin superflow high capacity affinity chromatography column (IBA GmbH, Goettingen, Germany), equilibrated with washing buffer 1. Unbound material was removed by a washing step with 50 mM KP_i, pH 8.0, 1 mM EDTA, 0.05% (w/v) DDM (Washing Buffer 2). The bound protein was eluted with 50 mM KP_i, pH 8.0, 1 mM EDTA, 0.05% (w/v) DDM, 10 mM desthiobiotin (IBA GmbH, Goettingen, Germany) (Elution Buffer 1), concentrated using centriprep concentrators (Millipore, Billerica, MA, USA) and further concentrated using amicon concentrators (Millipore, Billerica, MA, USA), both with an exclusion volume of 50 kDa. If less detergent was needed in the protein samples, purification was performed with 0.01% (w/v) DDM and the eluted protein was concentrated with a 100 kDa-cut off concentrator. Protein concentration was determined spectrophotometrically wit a Cary 100 Scan (Varian, Darmstadt, Germany) using an extinction coefficient of $\varepsilon_{425\,nm} = 158\ mM^{-1}\ cm^{-1}$ [82].

If purified variants showed a shifted absorption spectrum and, therefore, a new extinction coefficient had to be determined or if the sample was needed for metal determination, a gel-filtration step was added to the described protocol. A Superdex 200 10/300 column (GE Healthcare, Buckinghamshire, UK) in combination with an Äkta-Purifier system (Amersham Biosciences, UK) was used to further purify C*c*O. Washing buffer 2 with a flow-rate of 0.5 ml/min was used to equilibrate the column with 2 column volumes. C*c*O was loaded and purified in the same buffer. Fractions

of 0.5 ml were collected and concentrated with an amicon concentrator (Millipore, Billerica, MA, USA) with an exclusion volume of 50 kDa.

Two subunit preparations were performed according to the protocol described for the four SU preparation of C*c*O but solubilisation was accomplished with additional 3% (v/v) of LDAO. Affinity chromatography was performed with 0.08% (v/v) of LDAO in all buffers instead of DDM. Elution was carried out using Elution Buffer 2. The eluted fraction was submitted to anion exchange chromatography for detergent exchange using Q-Sepharose column material (GE Healthcare, Buckinghamshire, UK). 50 mM KP_i, pH 8.0, 1 mM EDTA, 0.05% (w/v) DDM (Washing Buffer 2) were used to wash the column after binding. The protein was eluted with 600 mM KP_i pH 8.0, 1 mM EDTA, 0.05% (w/v) DDM (Elution Buffer 3). The following steps were performed according to the four subunit purification protocol.

2.3.2. Determination of Protein Concentration and Extinction Coefficients

Protein concentration of purified C*c*O was usually determined spectrophotometrically with either a Cary 100 Scan (Varian, Darmstadt, Germany) or a Lambda 35 (Perkin Elmer, Rodgau, Germany) spectrophotometer, calculating the protein concentration according to the Lambert-Beer-law using an extinction coefficient of $\varepsilon_{425\ nm} = 158\ mM^{-1}\ cm^{-1}$ [82].

If variants showed a shifted absorption spectrum, a new extinction coefficient had to be determined. If no differences in absorption spectra were visible, the previously described extinction coefficient was used. To determine a new extinction coefficient, excess Fv antibody-fragment had to be removed with a gel filtration step (Superdex 200 10/300 (GE Healthcare, Buckinghamshire, UK)). The further purified C*c*O was used for determination of protein concentration [83]. The assay is based on the binding of the negatively charged dye coomassie brilliant blue G250 to non-polar and positively charged amino acids (S+G assay). The ATCC WT C*c*O was used as a standard with a protein amount ranging from 1 µg to 40 µg. Samples were diluted 50-fold before using 5 and 10 µl for determining the protein concentration. Sample and standard volumes were adjusted to 500 µl with ultra-pure water, prior to adding 500 µl of S+G solution. Standards and samples were incubated 15 minutes at room temperature and chilled on ice afterwards. Absorption of samples and

standards were measured at 620 nm (Ultrospec 2100 pro, Amersham Biosciences, UK). Protein concentration of samples was calculated according to the standard curve.

Variants showing differences in absorption spectra in each purification were sodium-dithionite reduced prior to absorption spectra recording. If no changes were visible, the "as purified" spectra were used to calculate the extinction coefficient. With known protein concentration due to the S+G-assay and known absorption maxima, a specific extinction coefficient for each variant was calculated using the Lambert-Beer-Law. Extinction coefficients of various variants are displayed in table 2.6.

Table 2.6: Extinction coefficients of different variants

Variant	**Extinction coefficient**
H276D	$\varepsilon_{419\ nm}$ = 93.8 mM^{-1} cm^{-1}
H276E	$\varepsilon_{418.5\ nm}$ = 127.9 mM^{-1} cm^{-1}
H276K	$\varepsilon_{417\ nm}$ = 109.8 mM^{-1} cm^{-1}
H276R	$\varepsilon_{421.5\ nm}$ = 98.4 mM^{-1} cm^{-1}
W164F	$\varepsilon_{443\ nm}$ = 155.9 mM^{-1} cm^{-1}
W164F Y167F	$\varepsilon_{442.5\ nm}$ = 164.0 mM^{-1} cm^{-1}
W272F	$\varepsilon_{442.5\ nm}$ = 128.8 mM^{-1} cm^{-1}
Y280F	$\varepsilon_{443\ nm}$ = 146.4 mM^{-1} cm^{-1}
W272F Y280F	$\varepsilon_{442.5\ nm}$ = 168.2 mM^{-1} cm^{-1}

Protein concentration of solubilized membranes was determined using the BCA-assay (Pierce, Thermo Scientific, Ashville, NC, USA) [84]. This assay is based on the combination of reduction of Cu^{2+} to Cu^{1+} by protein in alkaline media and the colorimetric detection of Cu^{1+} by bicinchoninic acid. BSA served as standard in a concentration range of 0 to 1 mg/ml in 0.1 mg/ml steps. The samples were used non-diluted and in a 10-, 20- and 50-fold dilution. 10 µl of the standard solutions and sample solutions were mixed with 200 µl of a 50:1 mixture of solution A : solution B (BCA-Assay-Kit, Pierce, Thermo Scientific, Ashville, NC, USA) in a 96-well plate and incubated at 37°C for 30 minutes. Absorption was read with a Tri-Star LB 491 plate reader (Berthold Technologies, Bad Wildbad, Germany) at 562 nm.

2.3.3. SDS-PAGE

Sodium dodecylsulfate polyacrylamide-gel electrophoresis (SDS-PAGE) was performed to separate proteins and protein subunits according to their molecular weight. Pre-cast SDS-PA-gels were used (Invitrogen, Carlsbad, CA, USA) according to the supplier's instructions with the MOPS-system (1 x MOPS-buffer). Gel electrophoresis was performed at 200 V in an X-Cell sure lock gel-chamber (Power source: Power Pac Basic, Biorad, Hercules, CA, USA). Gels were either stained with coomassie brilliant blue (PAGE Blue protein staining solution, Fermentas, St. Leon-Rot, Germany) or silver stained (Silver Quest Staining Kit, Invitrogen, Carlsbad, CA, USA). Coomassie stained gels were destained with water.

The silver staining was performed according to the supplier's instructions containing the following steps.

1. Fixation of the protein with 40% (v/v) ethanol, 10% (v/v) acetic acid in H_2O (20 minutes)
2. Wash with 15% (v/v) ethanol (10 minutes)
3. Sensitize with 30% (v/v) ethanol, 1-3% (v/v) MES, 5-10% (v/v) N,N-dimethylformamide (10 minutes)
4. Wash with 30% (v/v) ethanol (10 minutes)
5. Wash with H_2O (10 minutes)
6. Stain with 1% (v/v) staining solution (15 minutes)
7. Wash with water (1 minute)
8. Develop with 10-30% (w/v) $AgNO_3$-Solution containing 1 drop of 30-60% (v/v) formaldehyde (4-8 minutes)
9. Stop the reaction with 10 ml stopping solution (10 minutes)
10. Wash with water (10 minutes)

Gels were dried for storage at 80°C for 2 hours.

2.3.4. Detection of Specific Proteins by Western-Blotting

Western-blotting was used to specifically detect CtaG and Surf1c using monoclonal antibodies to verify expression of both proteins. Prior to Western-blotting, proteins were separated according their size by SDS-PAGE. Proteins were transferred to a

polyvinylidene fluoride-membrane (PVDF-membrane) (Milipore, Billerica, MA, USA). For this purpose, the membrane was activated in methanol for 30 seconds, washed with water for 5 minutes and stored in transfer-buffer for 5-10 minutes. Western-blotting was performed in a compression cassette (Invitrogen, Carlsbad, CA, USA) using the semi-dry technique. The blotting setup contained the anode, 4 filter papers (Whatman, Kent, UK) soaked in transfer buffer, followed by the SDS-gel and the activated and washed PVDF-membrane. The membrane was covered with four more filter papers soaked in transfer-buffer and the lid of the compression cassette, containing the cathode. Blotting was performed at 4°C with a constant current of 15 Volts (Power Pac Basic, BioRad, Hercules, CA, USA) for one hour and 40 minutes. Parts of the membrane that were not covered by protein were blocked by incubation with 20% skim milk powder in TBST buffer tumbling for 1 hour at room temperature. If CtaG was to be detected, a 1:100 dilution of anti-CtaG serum (kindly provided by Achim Hannappel, University of Frankfurt, Frankfurt am Main, Germany) was used at room temperature for 1 hour. Excess antibody was washed away with ultra-pure water in three short washing steps. The membrane was equilibrated in TBST buffer at room temperature twice for 5 minutes prior to addition of the second antibody in a 1:3000 dilution (anti-rabbit, Sigma Aldrich, Taufkirchen, Germany), which was incubated tumbling for 1.5 hours. Excess antibody was washed away with three short washing steps with ultra-pure water. The membrane was incubated in TBST buffer three times for 5 minutes at room temperature, prior to equilibration in AP buffer three times for 5 minutes tumbling at room temperature. Bound antibody was detected with the developing-buffer.

Surf1c was detected by using a 1:2000 dilution of anti-His antibody (Sigma Aldrich, Taufkirchen, Germany), which was already linked to alkaline phosphatase. The membrane was incubated with the antibody for 2 hours at room temperature. Excess antibody was washed away with ultra-pure water in three short washing steps. Two washing steps with TBST buffer equilibrated the membrane again. The TBST buffer was washed away with ultra-pure water in three short washing steps. The membrane was equilibrated for 5 minutes at room temperature with AP buffer. A colour reaction with developing buffer showed the position of bound antibody. Membranes were air dried and stored.

2.4. Biophysical Methods

2.4.1. Determination of Metal Content

The construction of several mutations near the active center led to the need for metal determination, especially detection of Cu_B, to understand the changes in oxygen reductase activity. For this purpose samples were analyzed at the University of Surrey, U.K., using microPIXE [85; 86]. This technique uses a highly energized proton beam (1-4 MeV) rather than an X-ray or electron beam. Protons passing the electron shell either excite electrons or penetrate the electron shell, experiencing electrostatic repulsion and backscattering (Rutherford-Backscattering). The information of backscattered protons can be analyzed to yield sample thickness and mass of atoms.

Excited electrons relax back to their ground state by emitting photons in the X-Ray region of the spectrum. The energy of the emitted photons is characteristic for the atomic number of the corresponding atom. One of the advantages of this technique is the ability to internally calibrate the method by determining the number of sulfur atoms in the sample. With the known amount of sulfur atoms in the protein, the amount of determined metal ions per sample was calculated.

Samples used for this method were submitted to size exclusion chromatography to further purify C*c*O and to remove excess Fv-antibody fragment. The concentration was determined spectrophotometrically. Samples were sent on dry ice.

Analytical conditions were the following as stated by the operators:

The $_1H^+$-beam had an energy of 2.53 MeV, a current of ~120 pA and a beam size of ~ 3x3 µm. The detector scattering angle was 135° (IBM geometry) with a 120 µm Be-filter. The X-ray detector used was a Gresham (e2V) Si(Li) with the analogue output of a Titan pulse-processor. BCR126A lead glass CRM was used for energy calibration of detectors and filter thickness determination of the X-ray detector. Samples were pipetted onto 6 µm thin polypropylene foils (Prolene) and air-dried. Prolene foil is used because this foil itself yields only signals for carbon. Samples formed a drying ring of protein. Element maps were recorded to find points for analysis. Four points in sulfur rich regions were chosen for data collection. Absorption correction was determined using the film thickness and composition

determined from the particle spectrum. Data was processed by the OMDAQ- and GUPIXWIN-software.

2.4.2. Heme-Extraction and MALDI-MS

Heme extraction was done according to Luebben and Morand [87] to verify the correct heme composition of the ATCC and rec. WT C*c*Os. All steps were performed at room temperature. Both protein samples were used in a volume of 100 µl. 400 µl of methanol was added and both samples were mixed and centrifuged at 9000 x g for 10 seconds (Eppendorf Centrifuge 5424, Eppendorf, Hamburg, Germany). 100 µl of chloroform was added, samples were mixed and again centrifuged at 9000 x g for 10 seconds. 300 µl of ultra-pure water was added and samples were mixed and centrifuged at 9000 x g for 1 minute. The upper phase was removed after centrifugation and 300 µl of methanol was added to the lower and interphase. Phases were mixed and centrifuged at 9000 x g for 2 minutes to pellet the protein. The supernatant was submitted to matrix assisted-laser desorption ionisation-mass-spectrometry with the following parameters.

The combined organic phases were dried in a speed-vac at room temperature. The pellets were re-dissolved in 2,5-dihydroxy-benzoic acid (DHB, Bruker Daltonics, Bremen, Germany) matrix solution (30 mg DHB / 100 µl of a solution containing H_20 and acetonitrile (1:2) with 0.1% formic acid). Typically, 1 µl of resuspended sample was deposited on a ground steel MALDI target (dried droplet method). After crystallization of the matrix, MALDI-TOF mass spectra were recorded in a Bruker Autoflex III Smartbeam MALDI-TOF/TOF mass spectrometer (Bruker Daltonics, Bremen, Germany) in reflector mode. Typical settings for the detection of small molecules were applied, detecting in a mass range of m/z 300-3000. The mass spectrometer was calibrated on adjacent spots using a Bruker calibration standard (mass range: 1000-3000 Da, Bruker Daltonics, Bremen) and custom-made PEG 400 aqueous solution (1:100, mass range: 400-1000 Da) with resolutions <10ppm.

All solvents used in the MS section were HPLC-MS ultra-pure grade, purchased from Fluka (acetonitrile) or Roth (water).

2.4.3. UV/Vis-Spectroscopy

Apart from the described determination of protein concentration, UV/vis-measurements were performed using a Lambda 35 spectrophotometer (Perkin-Elmer Waltham, USA) and a quartz-cuvette (Hellma, Müllheim, Germany). Absorption of approximately 7 µM C*c*O in 50 mM KPi, pH 7.0, 0.05% (w/v) DDM was measured between 380 and 700 nm with a scan rate of 400 nm/min and a split bandwith of 2.0. P- and F-intermediates were induced by 5 and 500 molar equivalents of hydrogen peroxide, respectively. In case fully oxidized enzyme was needed, the protein solution was incubated with at least 100-fold excess potassium ferricyanide at 4°C overnight. The ferricyanide was removed by washing the protein several times in amicon concentrators (Millipore, Bellerica, USA) with the desired buffer. Data was processed using Origin 7 (Additive GmbH, Friedrichsdorf, Germany).

2.4.4. Amperometric Measurements

Oxygen consumption (oxygen reductase activity) as well as production (catalase activity) was measured using a Clark-type oxygen electrode (Ox-MR-Electrode) linked to a multimeter PA 2000 (Unisense A/S, Aarhus, Denmark) at 20°C. Signals were recorded using an A/D converter and the micro trace basic software (Unisense A/S, Aarhus, Denmark). Cytochrome *c* (Biomol, Hamburg, Germany), used for oxygen reductase activity measurements, was reduced with solid sodium dithionite. Excess dithionite was removed by gel filtration using a PD-10 column (Amersham Biosciences, UK). Cytochrome *c* concentration was determined spectrophotometrically via redox-spectra. Cytochrome *c* was oxidized by addition of 1 mM ferricyanide and spectra were recorded. The concentration of reduced cytochrome *c* was calculated using the Lambert-Beer law with an extinction coefficient of $\varepsilon_{\text{redox } 550\text{ nm}}$=18.7 mM^{-1} cm^{-1} [88]. Concentration of hydrogen peroxide (Merck, Darmstadt, Germany) solutions was determined every day, measuring absorption at 240 nm and using an extinction coefficient of $\varepsilon_{240\text{ nm}}$ = 40 M^{-1} cm^{-1} [88; 89]. Measurements were performed stirring the sample in 2 ml glass vessels with a sample volume of 600 µl. The glass vessels were not sealed and remained open

during measurements because measured oxygen consumption or production was fast enough (in the time scale of seconds) to neglect diffusion of oxygen in and out of the measuring buffer.

The electrode was polarized at least 24 hours prior to use at -0.8 V. A 0.1 M NaOH solution with 0.1 M sodium ascorbate was used to calibrate for zero oxygen. Air saturated measuring buffer at the corresponding temperature served as a second calibration point (100% saturation). Oxygen concentration was calculated according to [90] taking temperature and salinity into account.

Oxygen reductase activity was measured in 30 mM KP_i pH 7.0, 0.05% (w/v) DDM, 1 mg/ml phosphatidylcholine, 0.3 mM tetramethylphenylene-diamine (TMPD), 3 mM sodium ascorbate and 40 µM cytochrome *c*. 5 nM C*c*O were added to start the reaction.

Catalase activity of C*c*O was monitored in 30 mM KP_i pH 7.0, 0.05% (w/v) DDM, 1 mg/ml phosphatidylcholine and 50, 75, 125, 200, 250, 450, 500 and 600 µM hydrogen peroxide corresponding to 100 to 1200 equivalents hydrogen peroxide with regard to C*c*O concentration (2.4 mM H_2O_2 was added to test for a saturation behavior). After addition of hydrogen peroxide, slight oxygen production was visible due to spontaneous decomposition of H_2O_2. 500 nM C*c*O was added to start the reaction. After approximately 5 min the buffer was over-saturated with oxygen and started to outgas. Only the linear part of the initial slope after addition of C*c*O was used for data analysis (the first 20 to 40 seconds after C*c*O addition).

The pH dependence of the oxidase and catalase activity was measured in steps of 0.5 pH-units using 30 mM citrate (pH 4.5 - 6.5), 30 mM potassium phosphate (pH 6.5 – 8.0), 30 mM tris/phosphoric acid (pH 8.0 - 9.0) or 30 mM glycine (pH 9.0 – 10.0) as pH-buffers, each containing 0.05% (w/v) DDM. The pH dependence of the oxygen reductase activity was measured as described before. The pH dependence of the catalase activity was measured with 1 µM C*c*O and 1.2 mM H_2O_2.

The inhibitory effect of sodium azide (38 mM), potassium cyanide (1 mM), carbon monoxide (CO aerated buffer) and ammonia (20 mM, pH-adjusted to pH 7.0) on the catalase activity of C*c*O (1 µM C*c*O for measurements with N_3^-, CN^- and CO and 2 µM C*c*O for measurements with NH_3) was measured in 30 mM KP_i pH 7.0, 0.05% (w/v) DDM and 1 mg/ml phosphatidylcholine. Measurements using CO were performed in the dark in order to avoid flash dissociation of CO.

Temperature dependence of the catalase reaction was measured with the described setup, 500 nM C*c*O and 450 µM H_2O_2. C*c*O was heated to 40°C / 50°C / 60°C / 70°C and 80°C for 10 minutes prior to measurements.
Catalase activity of P and F'-intermediates was measured with 500 nM C*c*O at pH 6 (Citrate Buffer), pH 7 (KP_i Buffer) and pH 9 (Glycine/KOH). P and F'-intermediates were generated by adding 1, 5 or 10 equivalents of hydrogen peroxide. The only difference in generating the P- or F'-intermediates was the pH of the buffer used.
The influence of superoxide was probed with SOTS-1 (Superoxide Thermal Source) (Biomol, Hamburg, Germany) at pH 7.0 (30 mM KP_i, 0.05% (w/v) DDM). For control, measurements contained excess superoxide dismutase (SOD) (Sigma Aldrich, Taufkirchen, Germany) or excess catalase (Sigma Aldrich, Taufkirchen, Germany) or both. For control measurements, samples were incubated over night. The influence of 5 mM SOTS-1 on 500 nM C*c*O was observed for 2 hours.
Data analysis was performed with Origin 7 (Additive GmbH, Friedrichsdorf, Germany). The production of protons was measured in 150 mM KCl, containing 1 mM H_2O_2, 1 µM C*c*O and 10 mM $K_3Fe(CN)_6$. The measurement was calibrated by adding 166 µM HCl as well as 1.66 µM HCl. The pH-value was measured with a pH-Meter 766 (Knick, Berlin, Germany), a Heidolph MR 3000 (Heidolph, Schwabach, Germany) and an In lab Micro electrode (Mettler-Toledo GmbH, Gießen, Germany).

2.4.5. Gas Chromatography-Mass Spectrometry

Gas chromatography-mass spectrometry was performed in collaboration with AG Bode, University of Frankfurt, Germany.
Measurements were performed in 30 mM KPi, pH 7.0, 0.05% (w/v) DDM in ND18 vials sealed gas-tight (Neolab, Heidelberg, Germany). To remove aerial oxygen, buffers, vials and lids were pre-incubated in an anaerobic tent with a nitrogen atmosphere for at least one week. All solutions were added under anaerobic conditions and the vial was sealed before exposing it to aerial oxygen. The buffer was mixed with a hydrogen peroxide mixture containing $H_2{}^{16}O_2$ and $H_2{}^{18}O_2$ (Icon Isotopes, Summit, USA) in a defined ratio with a final concentration of 10 mM before adding 3 µM of C*c*O to start the reaction. The samples were then pre-incubated at 37°C for 120 minutes. After incubation all analyzes were conducted on a 7890A

model gas chromatograph (Agilent, Waldbronn, Germany) equipped with a CTC PAL Combi XT autosampler including headspace option (CTC Analytics AG, Zwingen, Switzerland) and coupled to Series 5975C mass selective detector (Agilent, Waldbronn, Germany). The system was equipped with a DB5ht column (Agilent, Waldbronn, Germany) with a length of 30 m, an inner diameter of 0.25 mm and a column film of 0.1 µm in strength. Helium was used as the carrier gas at a constant flow rate of 1 ml/min. For sample injection, a 2.5 ml headspace syringe was used (Hamilton Bonaduz AG, Bonaduz, Switzerland), kept at 35 °C and purged with nitrogen for two minutes after every injection.

Samples were incubated at 60 °C under agitation in the sample oven for ten minutes. After incubation 250 µl of the gas phase were aspirated and injected into the gas chromatograph. The method parameters were as follows: Inlet temperature: 250 °C; injection mode: Split, ratio 150:1; Oven temperature: 60 °C for 15 min, temperature transfer line: 280 °C., temperature ion source: 230 °C, temperature quadrupole: 150 °C. Mass data were recorded between 30-40 Da.

For data evaluation and quantification the data analysis tool from MSD ChemStation E.02.00.493 (Agilent, Waldbronn, Germany) was used. Areas underneath signals obtained from the extracted ion chromatograms of the oxygen species $^{16}O_2$ (m/z: 34), $^{16/18}O_2$ (m/z: 34), $^{18}O_2$ (m/z 36), were integrated for relative quantification.

The Software DataAnalysis Version 4.0 SP1 (Bruker Daltonics, Bremen, Germany) was used to create base peak (BP) and extracted ion chromatograms (EIC).

2.4.6. Capillary Differential Scanning Calorimetry

Thermal stability of both wild type C*c*Os (ATCC and rec. WT C*c*O) was determined using a VP-capillary differential scanning calorimeter (GE Healthcare, Buckinghamshire, UK) with a protein concentration of 5 mg/ml in 10 mM KP_i, pH 8.0, 0.2 mM EDTA, 0.01% (w/v) DDM. The sample was scanned from 10 to 120°C with a scanning rate of 90°C / hour with low feedback mode. Data analysis was performed using Origin 7 (Additive GmbH, Friedrichsdorf, Germany).

2.4.7. Electron Paramagnetic Resonance-Spectrometry

Electron paramagnetic resonance (EPR) measurements were performed in collaboration with the group of Fraser MacMillan, University of East Anglia, U.K. Protein concentrations of 100 µM (minimum) in 50 mM KPi, pH 7.0, 0.05% (w/v) DDM were used. P- and F-intermediates were induced by adding 5 or 500 equivalents of hydrogen peroxide, respectively. X-band measurements were performed with a Bruker ELEXSYS E500 (Bruker, Bremen, Germany) and a Bruker ER 4122 SHQ (Super High-Q) resonator (Bruker, Bremen, Germany) in combination with a Bruker ER 4112HV Helium temperature control system (Bruker, Bremen, Germany). Samples were measured at 20 K with 9.4 GHz, 100 kHz modulation frequency, 81.92 ms conversion time and 40.96 ms correlation time. Settings and number of scans are as follows:
Widescan (WS): 10 dB microwave power, 10 Gauss modulation amplitude, 2 scans
Nearscan (NS): 20 dB microwave power, 10 Gauss modulation amplitude, 10 scans
Radicalscan (Rad): 10 dB microwave power, 4 Gauss modulation amplitude, 5 scans
Radical Low Power scan (RadLP): 20dB microwave power, 4 Gauss modulation amplitude, 10 scans

Q-band measurements were performed with an ER 053 QRD microwave bridge and a Bruker ER 5106 QTW resonator (Bruker, Bremen, Germany) inside a Bruker ER 4118CF cryostat (Bruker, Bremen, Germany). Samples were measured at 85 K, ~ 33.9 GHz , 0.63 mW microwave power (25 dB power attenuation), 1000 Gauss sweep width, 50 scans, 15000 receiver gain, 1 G modulation amplitude, 100 kHz modulation frequency, 20.48 ms time constant.

3. Results

This work describes the differences in catalase activity between the ATCC WT C*c*O and the rec. WT C*c*O as a probe for variations in the structure of this C*c*O, recombinantly produced in the homologous host.

Different variants were constructed to elucidate the mechanism of the catalase activity of C*c*O analogous to heme containing catalases. EPR, UV/vis-spectroscopy as well as GC-MS and amperometric measurements with and without inhibitors were used to investigate the mechanism of hydrogen peroxide decomposition by C*c*O.

3.1. Comparison of the ATCC WT C*c*O and Recombinant WT C*c*O

Variants of *P. denitrificans* C*c*O have been used to analyze e.g. the role of the D- and K-pathway [42]. These variants, with SU I coded on a low copy number-plasmid, were compared to the ATCC WT C*c*O. To compare variants and the WT C*c*O in a more stringent way, a rec. WT was constructed. In 2008, Angerer compared the two WT C*c*Os and reported differences between the ATCC WT C*c*O and rec. WT C*c*O for the first time [72]. The origin of the differences was therefore investigated further.

Obvious reasons for occurring differences, such as subunit composition (see figure 3.1) and heme incorporation (see figure 3.2), were investigated first but no deviations of the rec. WT C*c*O from the ATCC WT C*c*O were detected.

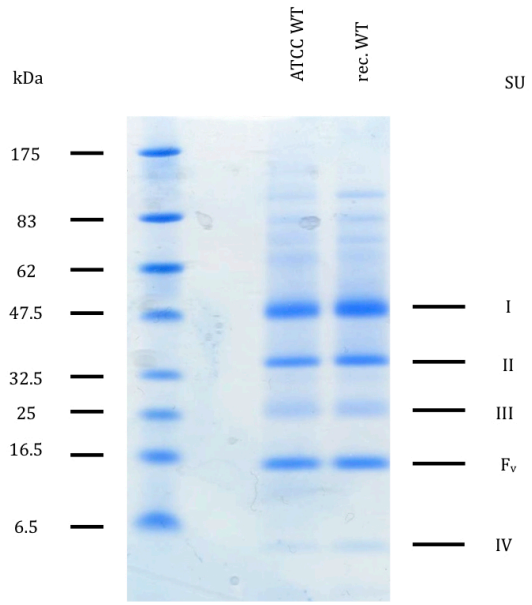

Figure 3.1: Coomassie stained SDS-PAGE of the ATCC WT C*c*O and rec. WT C*c*O.
Subunits I through IV and the F_v-antibody fragment are shown to be present in comparable amounts in both samples.

All SUs are present in both WT C*c*Os, as shown by SDS PAGE, as well as the Fv-antibody fragment with an apparent mass of 16 kDa. The faint band below the Fv-antibody fragment is subunit IV with an apparent molecular mass of approximately 4 kDa. The three prominent bands above are formed by SU I, II and III in descending order, with apparent molecular masses of 48 kDa, 34 kDa and 25 kDa respectively [18; 43; 81]. The amount of subunits as well as the overall yield of purified C*c*O is comparable in both wild types. Several faint bands were visible above SU I caused by aggregation and/or small amounts of impurities.
Metal determination via MicroPIXE [85; 86] (University of Surrey, IonBeam Center, Surrey, U.K.) showed no differences in iron and copper content.
MALDI-MS measurements were performed in collaboration with Dr. Julian Langer (MPI of Biophysics, Frankfurt Main, Germany) to investigate the incorporated heme species in both wild types.

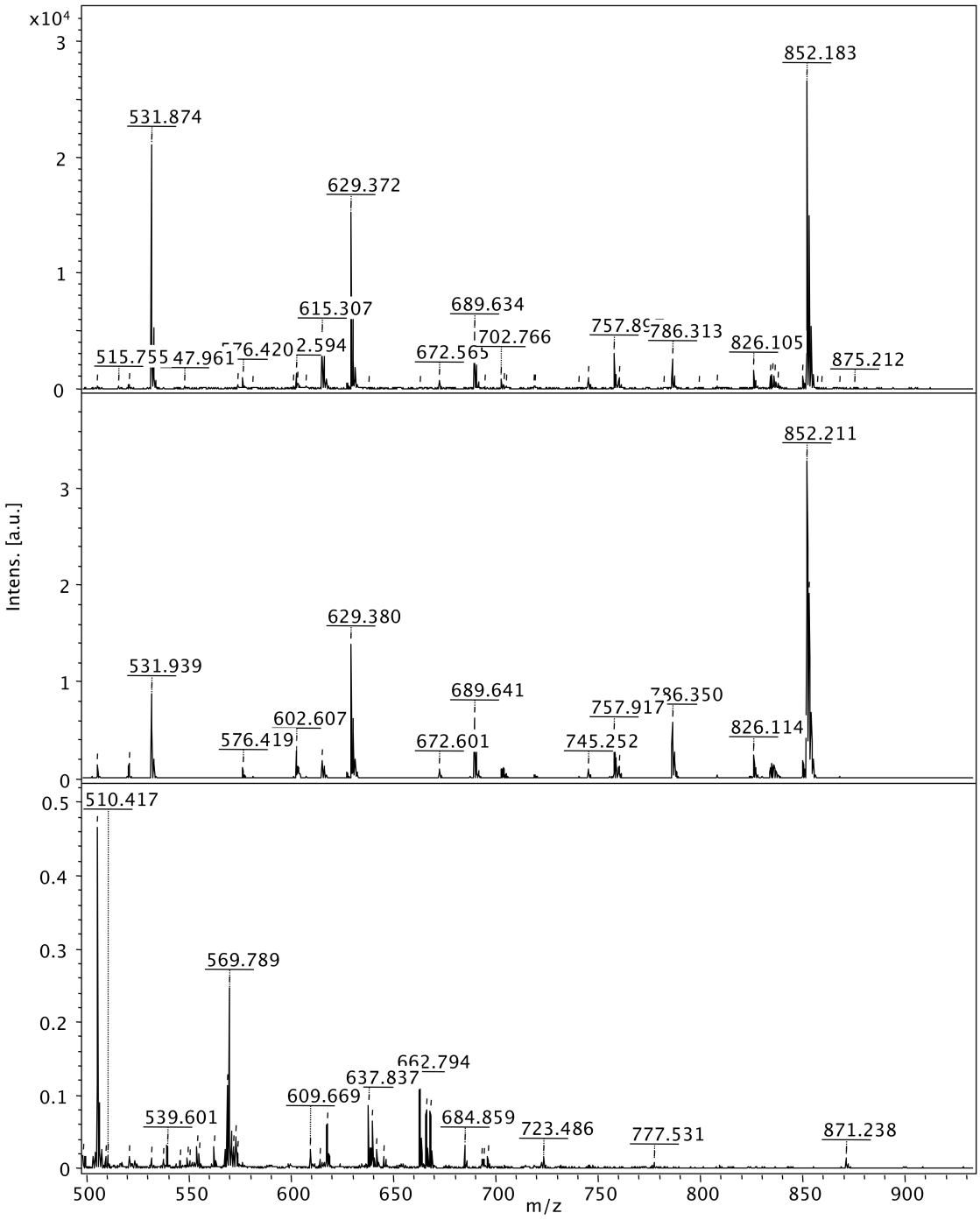

Figure 3.2: MALDI-MS-spectra of the heme extractions from the ATCC WT C*c*O (top), rec. WT C*c*O (middle) and buffer blank (bottom).

The buffer spectrum shows no significant signal, while both wild types show a strong signal at 852.2 Da.

Both MALDI-MS spectra show a significant signal at a molecular mass of 852.2 Da, most likely resulting from the heme *a* (852.8 Da, monoisotopic 852.4 Da) [91] present in both wild type C*c*Os. The control experiment with buffer only shows no significant signals.

Neither the subunit composition nor the hemes or copper ions incorporated show any indications of differences. To further characterize both proteins, oxygen reductase and catalase activity of both wild type C*c*Os were investigated at different pH values, ranging from 4.5 to 10 using different buffer systems (see figure 3.3)

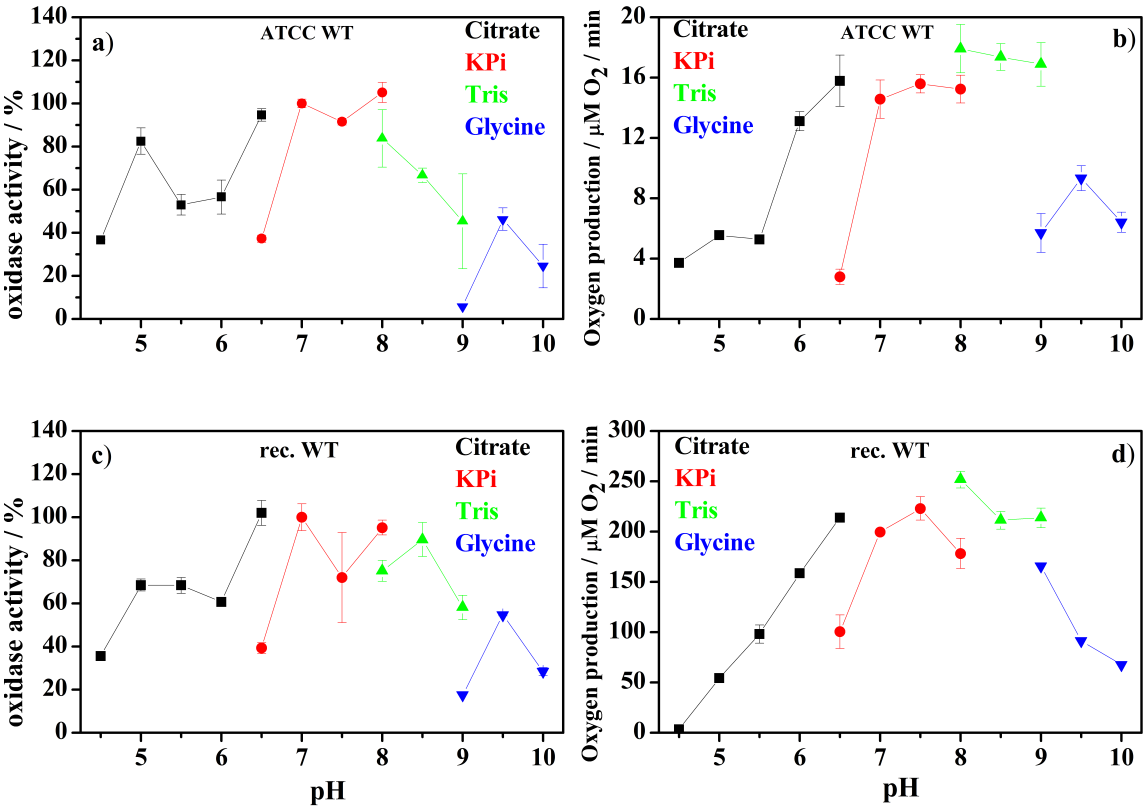

Figure 3.3: pH dependence of the oxygen reductase and catalase activity.

The ATCC WT C*c*O and rec. WT C*c*O were tested for their pH-dependence of the oxygen reductase activity (C*c*O concentration of 5 nM; 100% corresponds to approximately 450 e^- / s) (a) and c) respectively) and of the catalase activity (C*c*O concentration of 1 µM) (b) and d) respectively), exhibiting a mutual pH-optimum of both reactions at pH 7.0. Oxygen production was very high when Tris buffer was used.

The pH dependence measurements show a pH optimum around pH 7.0. Therefore, all further activity measurements were performed at pH 7.0. The catalase activity is

increased in tris buffer. The amount of oxygen produced comparing the same pH values of the ATCC WT C*c*O and rec. WT C*c*O in these measurements already suggested differences in the catalase activity but not in the oxygen reductase activity. The dimension of these differences was further examined by comprehensive measurements of the kinetics of the oxygen reductase and catalase reactions.

3.1.1. Oxygen Reductase and Catalase Activity

Differences were characterized by measuring the oxygen reductase and catalase activities of the rec. WT C*c*O and the ATCC WT C*c*O. Measurements were performed amperometrically using a Clark-type oxygen electrode. C*c*O catalyzes the reduction of molecular oxygen to water, decreasing the concentration of oxygen in the solution. The catalase activity leads to the decomposition of two molecules of hydrogen peroxide to two molecules of water and one molecule of dioxygen, which increases the oxygen concentration in the solution. The speed of those two reactions was high enough to ignore the influence of oxygen diffusing in and out of the buffer for at least 30 seconds.

Raw data of the catalase reactivity were recorded and analyzed according to Michaelis-Menten in a Lineweaver-Burk plot (see figure 3.4) yielding k_{cat} and K_M [92; 93]. Analysis of these data shows differences in catalase activity but no significant differences in oxygen reductase activity of the two WT proteins (compare figure 3.5).

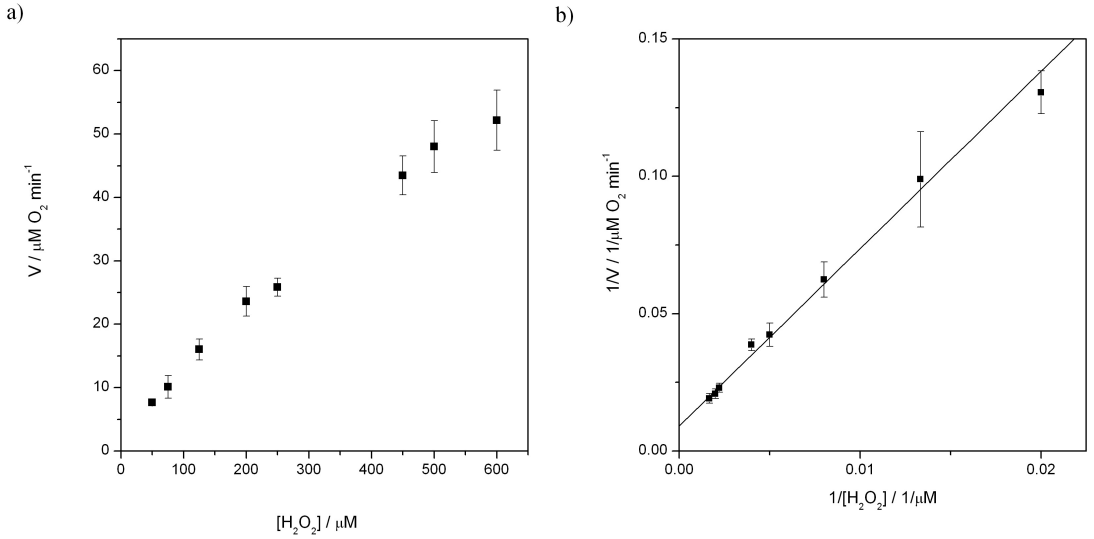

Figure 3.4: Data analysis.

Reaction velocity in µM oxygen per minute depending on the hydrogen peroxide concentration is shown in a) with its corresponding Lineweaver-Burk plot shown in b). A saturation behavior is not visible in this figure, however it is present using very high concentrations of hydrogen peroxide. Data using high hydrogen peroxide concentrations was not evaluated due to technical restrictions.

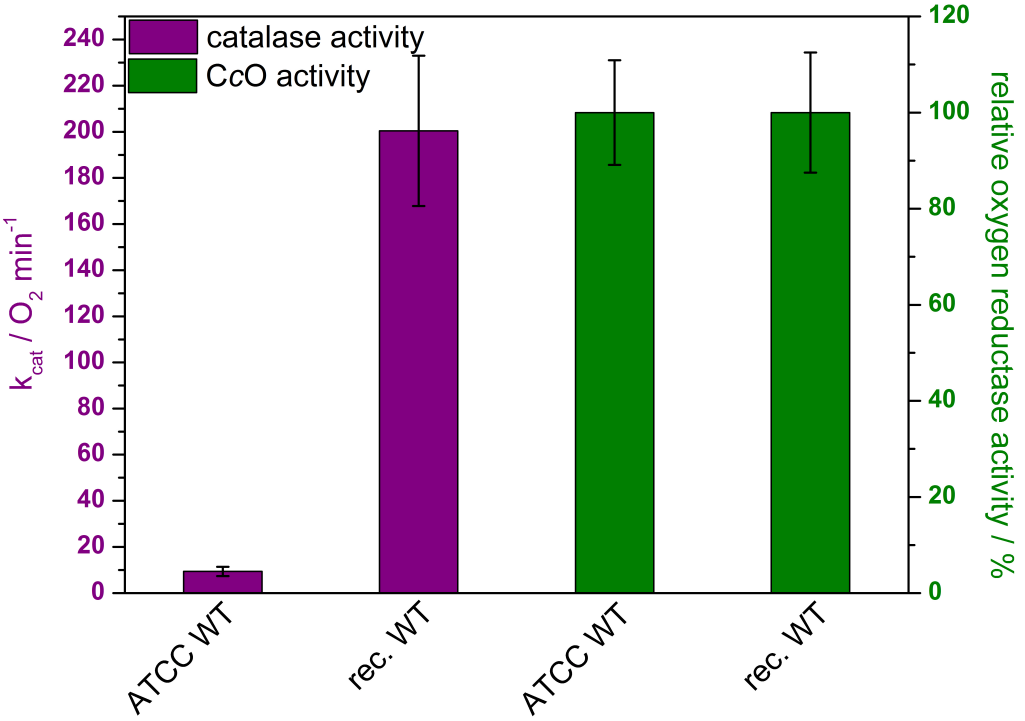

Figure 3.5: Comparison of the catalase and oxygen reductase activity (C*c*O activity) of the rec. WT C*c*O and ATCC WT C*c*O.

No significant differences in oxygen reductase activity were visible but a 20-fold increase in k_{cat} in catalase activity for the rec. WT C*c*O could be observed.

Oxygen reductase activity does not differ in either wild type C*c*O but the k_{cat} of the catalase reaction increases 20-fold for the rec. WT C*c*O. Kinetic parameters of the catalase reaction are shown in figure 3.6.

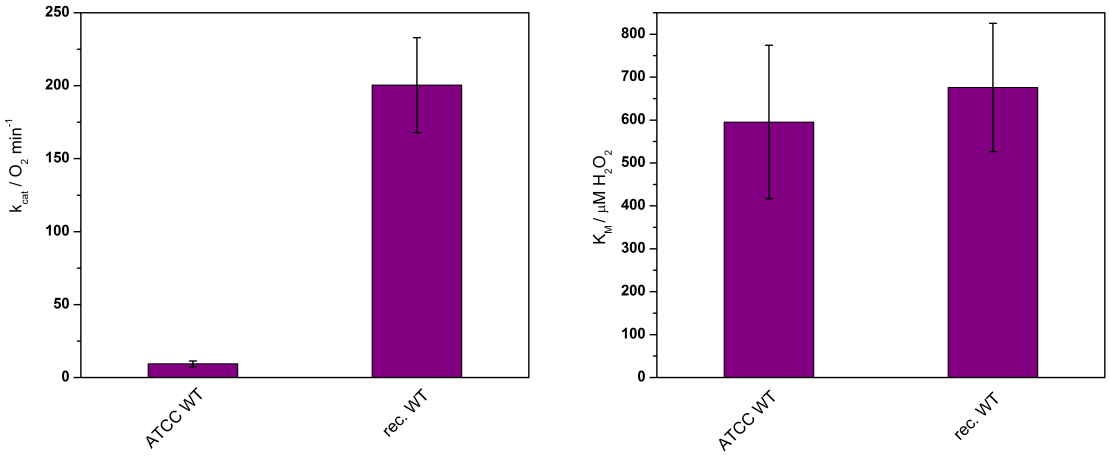

Figure 3.6: Kinetic parameters of the catalase reaction of the ATCC and rec. WT C*c*Os.
The k_{cat} (left hand side) of the rec. WT C*c*O increases 20-fold compared to the ATCC WT C*c*O. The K_M value (right hand side) did not show significant changes.

The analysis of the kinetic data from the catalase reaction adds up to a k_{cat} value of 9.4 ± 2 min^{-1} for the ATCC WT C*c*O and 200.4 ± 32.6 min^{-1} for the rec. WT C*c*O showing a 20-fold increase of k_{cat}. Contrary to that, the K_M value of 595.2 ± 178.9 µM H_2O_2 and 676.1 ± 149.5 µM H_2O_2, respectively does not differ significantly.

3.1.2. UV/vis-Spectroscopy

At least two of the intermediates of the catalytic cycle of C*c*O were already observed as natural intermediates, namely the P- and F-intermediates. Artificial P- and F-intermediates with a similar UV/vis-spectrum as their natural equivalents, [46] are generated in the presence of equimolar amounts or excess of hydrogen peroxide, respectively. Therefore, C*c*O catalyzing the dismutation of hydrogen peroxide shows a UV/vis-spectrum similar to the spectrum of the natural F-intermediate, with a difference absorption maximum at 580 nm. The P-intermediate shows a difference absorption maximum at 610 nm.

Since there are obvious differences in the catalase activity between the ATCC WT C*c*O and the rec. WT C*c*O, the differences in the UV/vis spectra of the hydrogen peroxide derived P- and F-intermediates were also investigated (see figure 3.8). Several groups described different O-intermediates of C*c*O, therefore two O-intermediates were used as starting point to generate the P- and F-intermediates of both wild types [94-97]. The first O-intermediate was called O_{asis}, representing the air-oxidized O-intermediate directly after purification. The second O-intermediate was generated by overnight oxidation with ferricyanide and was called O_{ox}. Difference spectra of the ATCC WT C*c*O and rec. WT C*c*O calculated by substracting O_{ox} from O_{asis} show two signals in the α-band. The first signal is present at around 580 nm, probably resulting from a certain amount of the F-intermediate in the O_{asis} state. The second signal is present at around 602 nm pointing to a small amount of the one electron reduced form present in the O_{asis} state. The difference spectra are shown exemplarily in figure 3.7. The intensity of the different signals varies with different purifications.

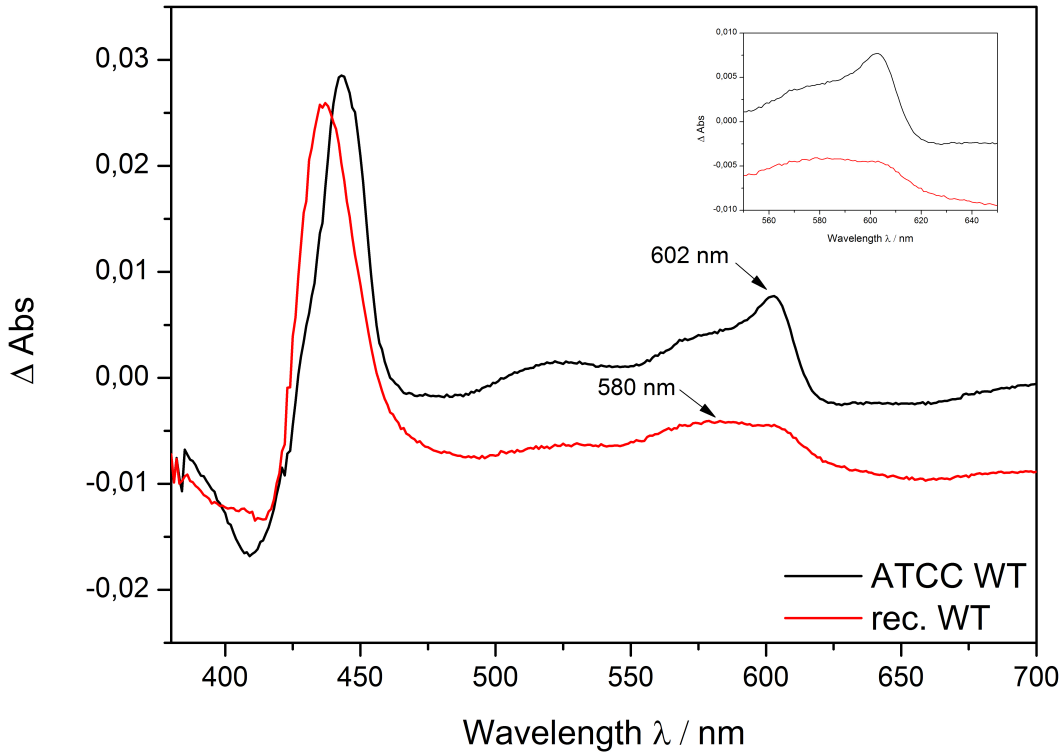

Figure 3.7: Difference aborption spectra of O_{asis} minus O_{ox}.
The inset shows a close up on the α-band. Both, the ATCC WT C*c*O and the rec. WT C*c*O exhibit maxima at 580 and 602 nm. The intensity of these maxima varies with different preparations.

Absorption spectra of the O-intermediates reveal only a slight broadening of the Soret-band as the difference between the ATCC WT C*c*O and rec. WT C*c*O. The maximum of the Soret-band shifts dependent on preparation from 427 to 428 nm to an absorption maximum at 425 nm in the oxidized form.

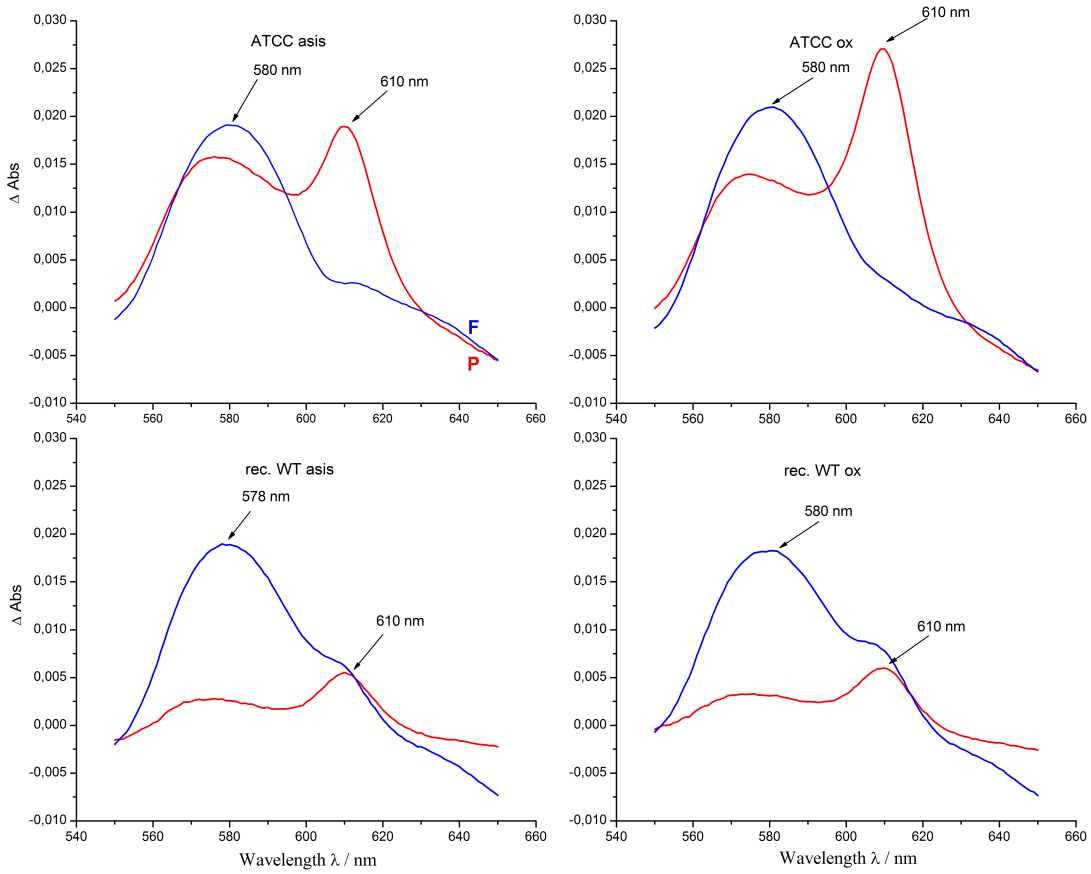

Figure 3.8: Difference absorption spectra from 550 to 650 nm of the ATCC WT C*c*O (top) and rec. WT C*c*O (bottom).

The P-intermediate induced by 5 equivalents of H_2O_2 is shown in red (P minus O), the F-intermediate induced by 500 equivalents H_2O_2 in blue (F minus O). Difference spectra were obtained by subtracting the spectra of the O-intermediate from spectra of the P- or F-intermediate. Two different O-intermediates were used, O_{asis} shown on the left and O_{ox} shown on the right. The left side shows P and F minus O_{asis} and the right side P and F minus O_{ox}.

Difference absorption spectra of the P- and F-intermediates show the successful formation of both intermediates independent of the O-intermediate used as starting point. The P-intermediate always shows a maximum in difference absorption spectra at 610 nm and the F-intermediate usually shows a maximum in difference absorption spectra at 580 nm, except in the rec. WT C*c*O F-intermediate originating from O_{asis}, where there is a difference absorption maximum of 578 nm.

The P-intermediate generated from the oxidized ATCC WT C*c*O shows a much higher absorption (~factor 1.5) at 610 nm compared to the P-intermediate originating from the O_{asis}-intermediate. Both spectra of the P-intermediate show shoulders at ~575 nm. Since the structural difference between the P- and F-

interemdiates is proposed to be solely the Cu_B ligand (see for example [97]), the shoulders suggest modifications of the ligand at Cu_B present in the P-intermediate. The difference absorption maximum of the F-intermediate increases slightly, nevertheless, no significant differences in both F-intermediate spectra of the ATCC WT C*c*O were visible, irrelevant of the O-intermediate used.

The P-intermediate spectra of the rec. WT C*c*O show a small shoulder at ~575 nm but there is no difference between originating from O_{asis} or O_{ox}. The absorption difference band of the F-intermediate at 578 nm or 580 nm starting with O_{asis} or O_{ox}, respectively, shows a small shoulder at 610 nm. This shoulder is more pronounced originating from O_{ox}. Consequently, the intensity of the main signal is slightly decreased.

In all four measurements, the same protein concentration was used, resulting in similar intensities of the absorption bands related to the F-intermediate. Contrary to that, the intensity of the P-intermediate absorption band is decreased 3-4-fold starting from O_{asis} and 5-6-fold starting from O_{ox} for the rec. WT C*c*O compared to the ATCC WT C*c*O.

3.1.3. EPR-Spectroscopy

EPR-Spectroscopy was used to investigate both O-intermediates and any differences in the resulting P- and F-intermediates after H_2O_2-treatment. The rec. WT C*c*O and ATCC WT C*c*O were compared in all six intermediate states (see figure 3.9).

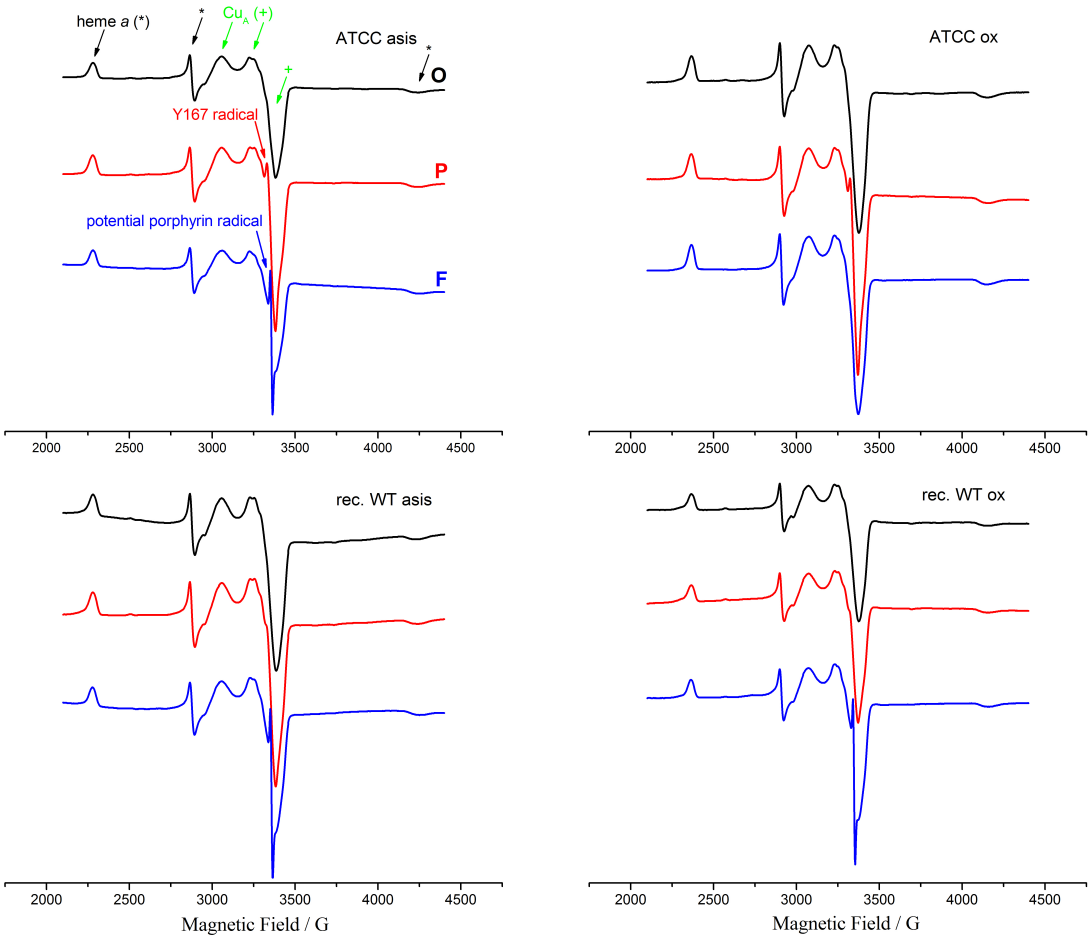

Figure 3.9: Near Scan EPR-spectra of the ATCC WT C*c*O (top) and rec. WT C*c*O (bottom) originating from O_{asis} (left) or O_{ox} (right).

The O-intermediate is shown in black, the P-intermediate in red and the F-intermediate in blue. Exemplarily for all spectra, the signals in the ATCC WT C*c*O spectra starting with O_{asis} are labeled with different arrows: The red arrow indicates the already known Y167 radical, whereas the blue arrow indicates a narrow signal with a width of ~ 12 G. Green arrows depict signals originating from Cu_A and black arrows identify signals originating from heme *a*. Cu_B and heme a_3 do not show any signal due to magnetic coupling [98]. Spectra are shown in arbitrary units of the first derivative. The parameters used are described in Materials and Methods (Section 2.4.7).

Comparing the EPR-spectra of the two different O-intermediates of both wild types, no significant differences were visible. In all four cases the P-intermediate, generated by adding 5 molar equivalents of hydrogen peroxide, resulted in an EPR-signal already described by Budiman *et al.* [71] as an amino acid radical located on tyrosine 167. The intensity of this signal is independent of the originating O-intermediate. The signal is less pronounced and only slightly visible in the EPR-spectra of the rec. WT C*c*O.

The EPR-spectra of the F-intermediate show a distinct and equally large 12 G wide signal for both wild type C*c*Os originating from O_{asis}. This signal is narrower than the Y167-signal. Upon oxidation of the ATCC WT C*c*O this signal disappears. Contrary to that, oxidation of the rec. WT C*c*O insignificantly changes the narrow signal.
The extent and width of these signals was further investigated by reducing the sweep width of the magnetic field, generating a "close up" of the area of interest (see figure 3.10).

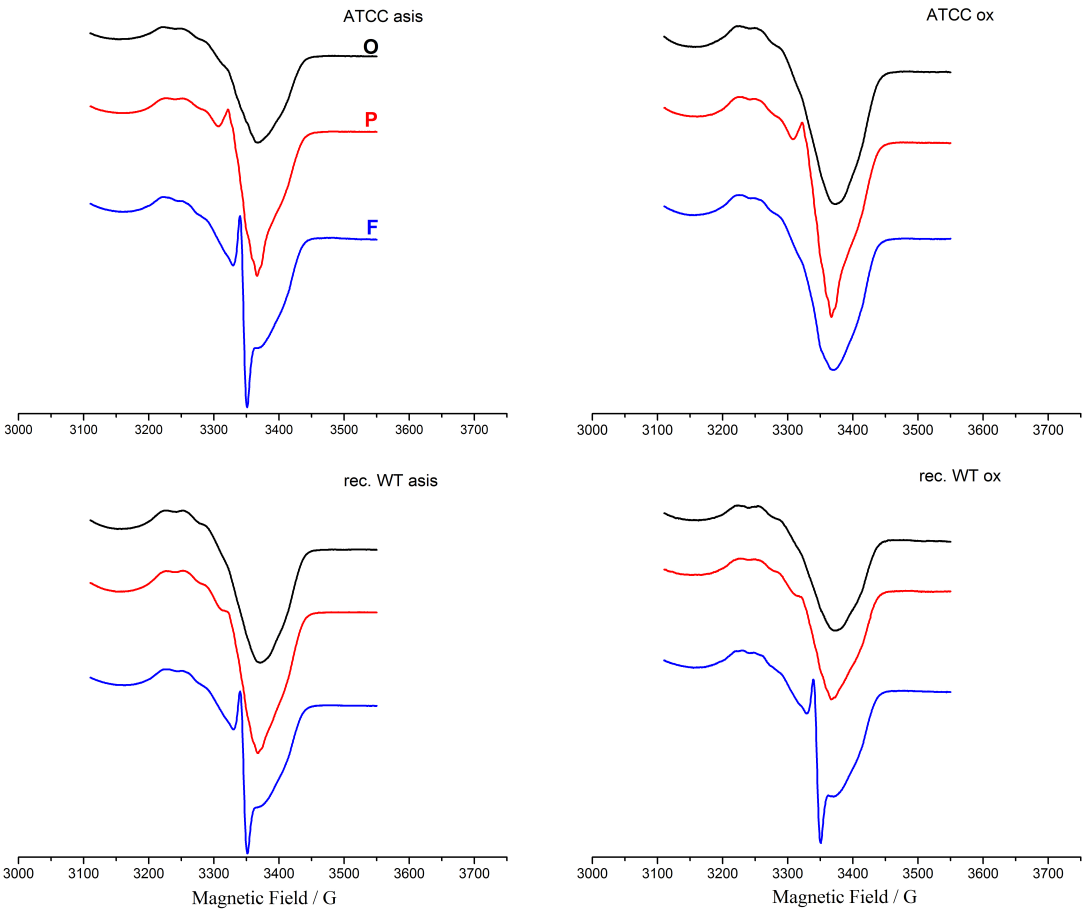

Figure 3.10: Radical low power scan of the ATCC WT C*c*O (top) and rec. WT C*c*O (bottom) originating from O_{asis} (left) and O_{ox} (right).
The spectra of the O-intermediate are shown in black, the P-intermediate induced by 5 molar equivalents H_2O_2 in red and the F-intermediate induced by 500 molar equivalents H_2O_2 in blue. Spectra are shown in arbitrary units of the first derivative. The parameters used are described in Materials and Methods (Section 2.4.7).

The magnetic field sweep width was reduced to 430 Gauss to analyze the Y167 radical related signal as well as the narrow signal in a more detailed way. The

modulation amplitude was also reduced to 4 Gauss to give a better resolution of the radical signal. The Y167 radical signal with a width of ~ 45 Gauss is present in the EPR-spectra of both P-intermediates of the ATCC WT C*c*O. The spectra of the rec. WT C*c*O show only a small amount of this radical signal in both P-intermediates. Both F-intermediates originating from O_{asis} show a very narrow signal of ~ 12 Gauss. This signal disappears upon oxidation of the ATCC WT C*c*O but does not change upon oxidation of the rec. WT C*c*O. The signal intensity originating from O_{asis} does not show significant differences comparing the ATCC WT C*c*O and the rec. WT C*c*O.

3.1.4. Introduction of Chaperones

The rec. WT C*c*O was constructed using a *P. denitrificans* strain carrying a deletion of both genes encoding for SU I (*ctaDI* and *ctaDII*) of aa_3 C*c*O. To obtain a functional aa_3 C*c*O, the strain was supplemented with a low-copy number plasmid carrying the expressing gene for SU I (*ctaDII*) under the control of the same promoter as the chromosomal coded SU II [42]. Despite the use of a low copy-number plasmid a potential overexpression of SU I due to plasmid coding could not be excluded.
SU I carries three of the four redox-active metal centers. These metal centers are inserted into SU I by chaperones. The potential overexpression of SU I could lead to a deficiency of metal inserting chaperones, if they are required in a specific stoichiometry. A His-tagged version of the rec. WT C*c*O was constructed to provide Cu, coordinated by the His-tag, in close proximity to the amino acid chain forming SU I. This was thought to potentially improve the insertion of Cu_B into SU I.
Two more wild types were created by inserting either the gene for the Cu-inserting chaperone, CtaG, alone or along with the gene for the heme inserting chaperone Surf1c on the same plasmid as *ctaDII* [39; 99]. These genes were added to the chaperone genes already present due to chromosomal coding. Expression of both added chaperone genes was verified via western blotting (see figure 3.11). Adding both genes coding for chaperones enhanced the overall chaperone level in the cell.

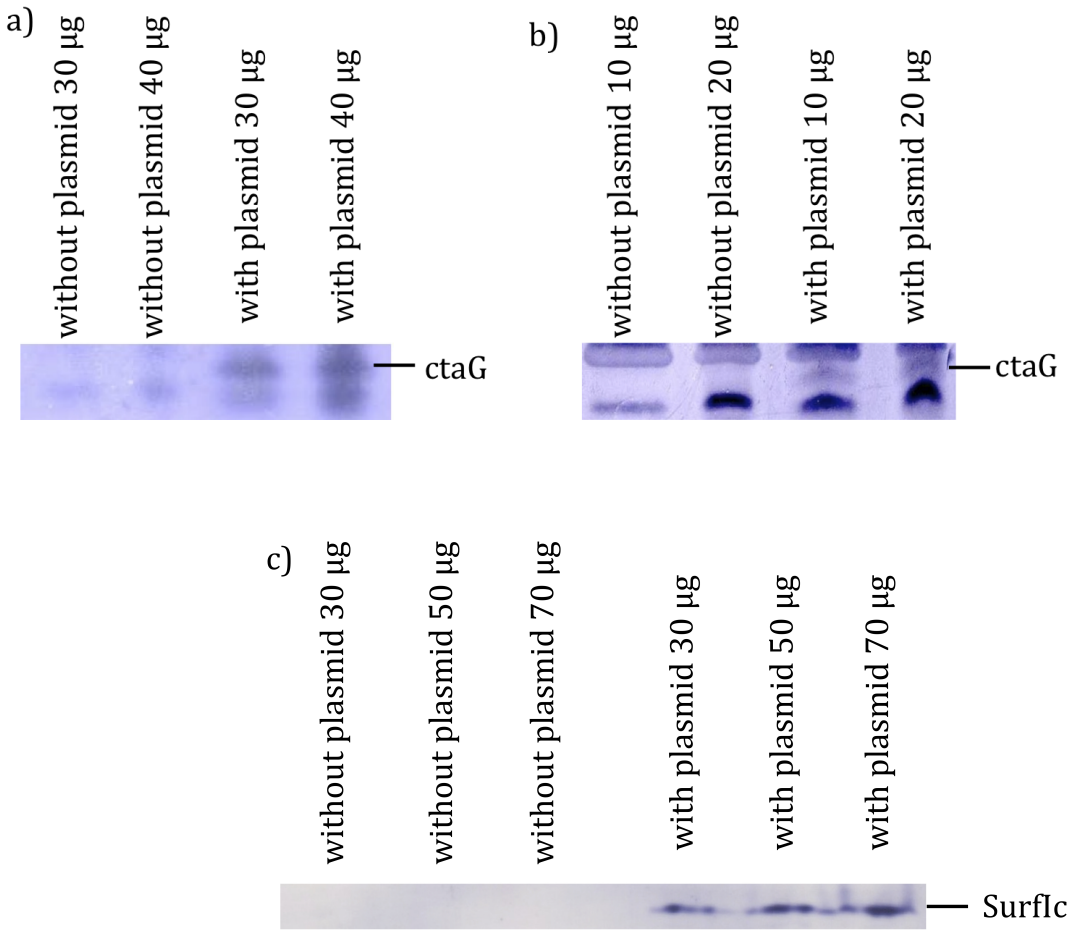

Figure 3.11: Expression of *surf1c* and *ctaG* in *P. denitrificans* AO1 and PUP206 membranes verified by Western blotting.

The rec. WT C*c*O supplemented with one chaperone was shown to express *ctaG* (a)), whereas the rec. WT C*c*O supplemented with both chaperones was shown to express *ctaG* (b)) and *surf1c* (c)). Western blotting was performed with plasmid containing strains as positives and the corresponding strains containing no plasmid as negatives. Antibodies directed against CtaG were applied as whole serum, therefore numerous unspecific reactions were visible. Surf1c was detected via its His_6-tag using poly-His-specific antibodies.

A change in metal composition, especially regarding the his-tagged rec. WT C*c*O, was ruled out by determination of the metal content via microPIXE. Metal analyses was carried out for the ATCC WT C*c*O, rec. WT C*c*O and his-tagged rec. WT C*c*O. Analyses showed two iron atoms and three copper atoms per C*c*O molecule, verifying the incorporation of all redox active metal centers in SU I. One discrepancy between the his-tagged rec. WT C*c*O and the other two wild types is the Zn content.

No significant amounts of zinc were detected in the ATCC and rec. WT C*c*O contrary to ~1.5 Zn atoms per his-tagged rec. WT C*c*O molecule.
After verifying the presence of all redox active metal centers, the oxygen reductase activity was monitored for all five described wild types (see figure 3.12).

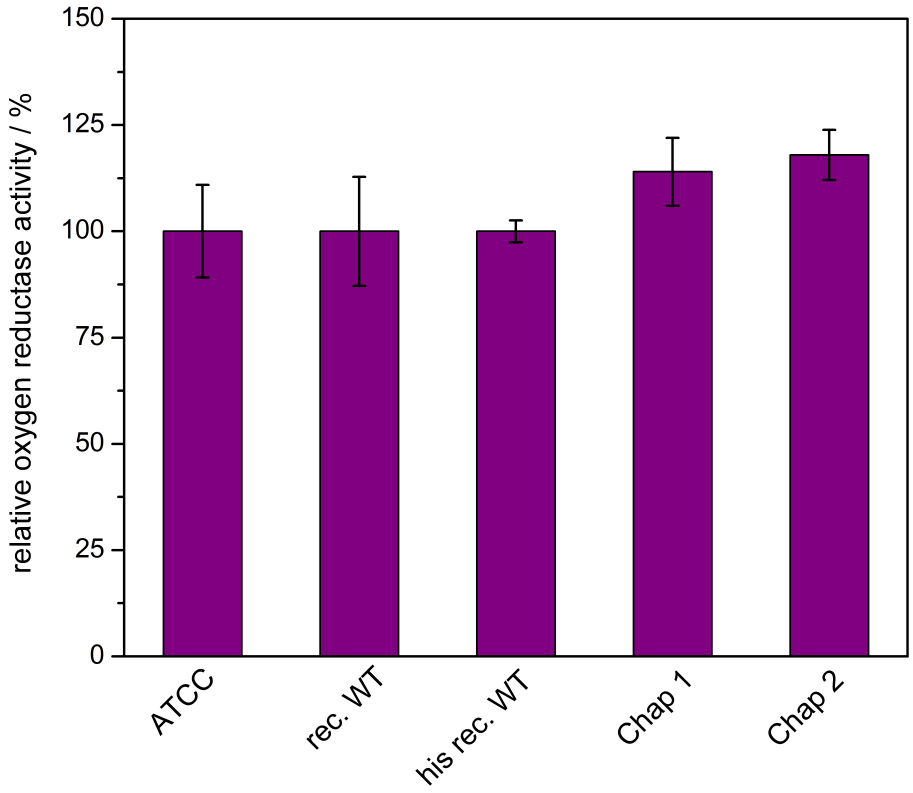

Figure 3.12: Relative oxygen reductase activity
The oxygen reductase activity of the ATCC WT C*c*O was used as standard (~450 e^-/s). Oxygen reductase activity, using cytochrome *c* as electron donor, was monitored for all five described wild types with the one-chaperone added WT C*c*O marked as Chap 1 and the two-chaperones added WT C*c*O marked as Chap 2. Relative activities were calculated.

Oxygen reductase activity was monitored for all five wild types and showed only a slight insignificant increase of ~10% for the chaperone added wild type C*c*Os. Therefore, all constructed wild type C*c*Os were considered to be fully functional. Apart from monitoring the oxygen reductase activity, the catalase activity dependent kinetic parameters were measured and analyzed (see figure 3.13).

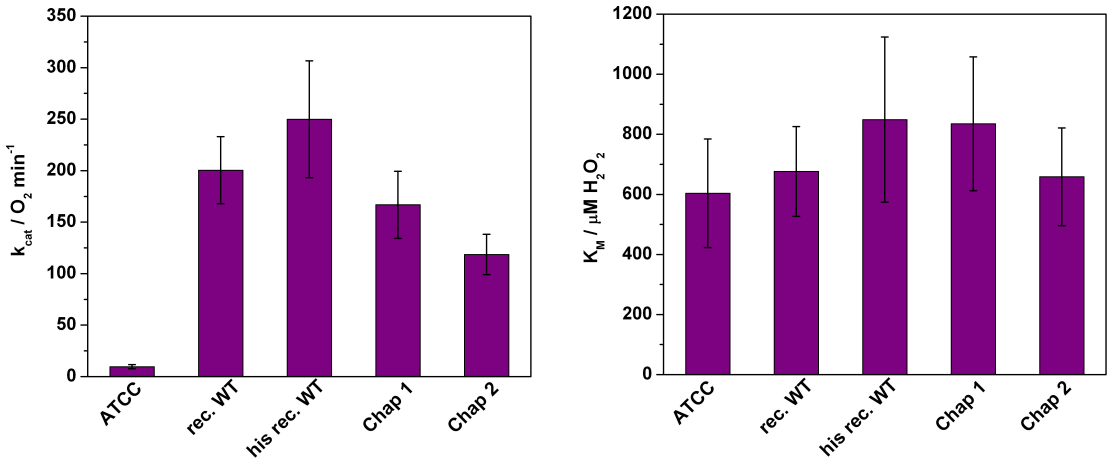

Figure 3.13: Kinetic parameters of the catalase reaction of the ATCC WT C*c*O, rec. WT C*c*O, his tagged rec. WT C*c*O (his rec. WT), one-chaperone added (Chap 1) and two-chaperones added (Chap 2) WT C*c*Os.

The left-hand side shows the k_{cat} values and the right-hand side the K_M values, depicting a small but insignificant increase in K_M for the his-tagged rec. WT CcO and the one-chaperone added WT CcOs.

Comparing the k_{cat} values of the catalase reaction of the rec. WT C*c*O and the his-tagged rec. WT C*c*O an insignificant increase by ~ 50 min^{-1} was observed. Adding the gene encoding the copper inserting chaperone CtaG to the same plasmid that *ctaDII* is located on, decreased the k_{cat} of the catalase reaction by 17%. The insertion of the genes encoding the copper and heme inserting chaperones CtaG and Surf1c resulted in a significant decrease of k_{cat} by 40%. Contrary to that, the K_M value merely shows a slight, insignificant increase for the his-tagged and one-chaperone added rec. WT C*c*O. Observing the decrease in k_{cat}, the influence of the increased level of chaperones on the UV/vis-spectra was analyzed originating from both ground states, O_{asis} and O_{ox} (see figure 3.14 and 3.15)

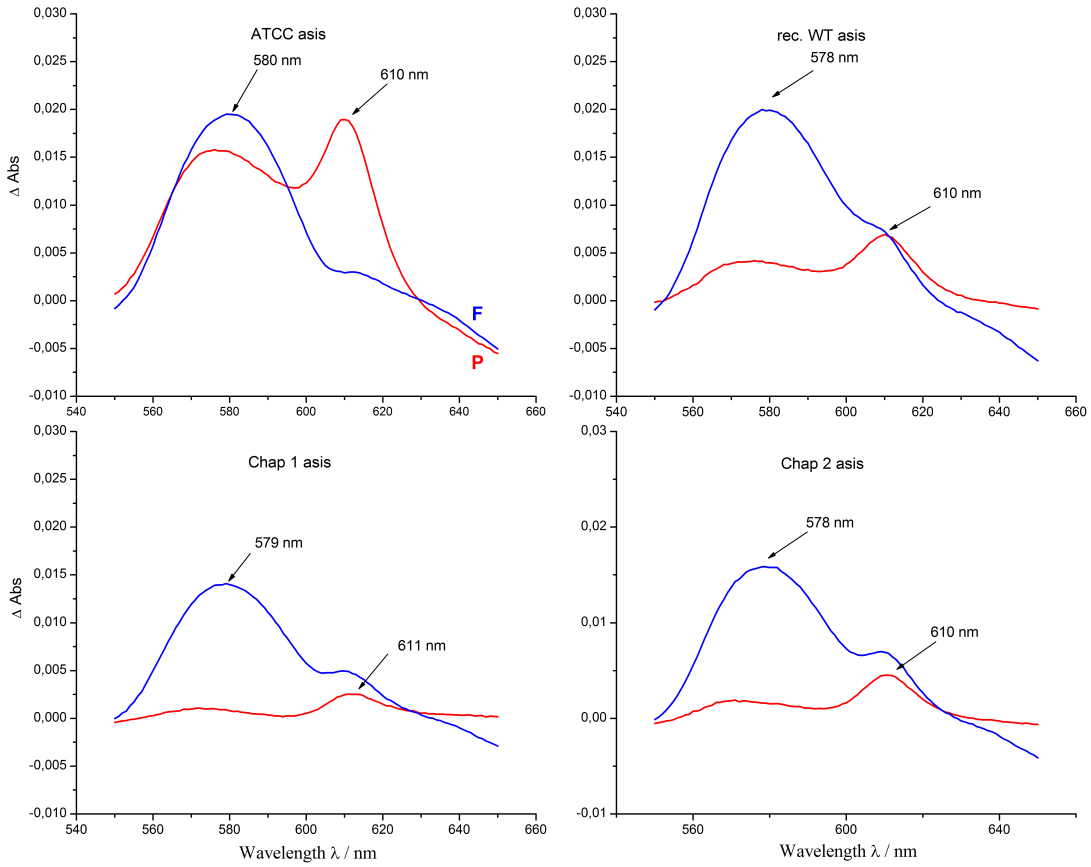

Figure 3.14: Difference absorption spectra originating from O_{asis}, of the P-intermediate (red (P minus O_{asis})) and the F-intermediate (blue (F minus O_{asis})).
The top left shows the ATCC WT C*c*O compared to the rec. WT C*c*O (top right), the one-chaperone added variant (bottom left) and the two-chaperones added variant (bottom right).

All characteristic difference absorption maxima, either showing the presence of the P- or F-intermediate, are present. Comparing both chaperone added wild type C*c*Os, a slight increase in P-intermediate yield is visible for the two-chaperones added wild type C*c*O compared to the one-chaperone added wild type C*c*O as well as a shift of the absorption maximum from 611 nm to 610 nm. The F-intermediate does not differ significantly from the rec. WT C*c*O without any extra chaperones. The absorption maxima of the F-intermediate related spectra for the one-chaperone added wild type C*c*O and the two-chaperones added wild type C*c*O are located at 579 nm and 578 nm, respectively. Comparing these wild type C*c*Os to the ATCC WT C*c*O and to the rec. WT C*c*O, an intensity decrease of the F- and P-intermediate signals is obvious. Both chaperone added wild type C*c*Os yield even less of both intermediates than the rec. WT C*c*O even though the catalase activities converge to the one of the ATCC WT C*c*O.

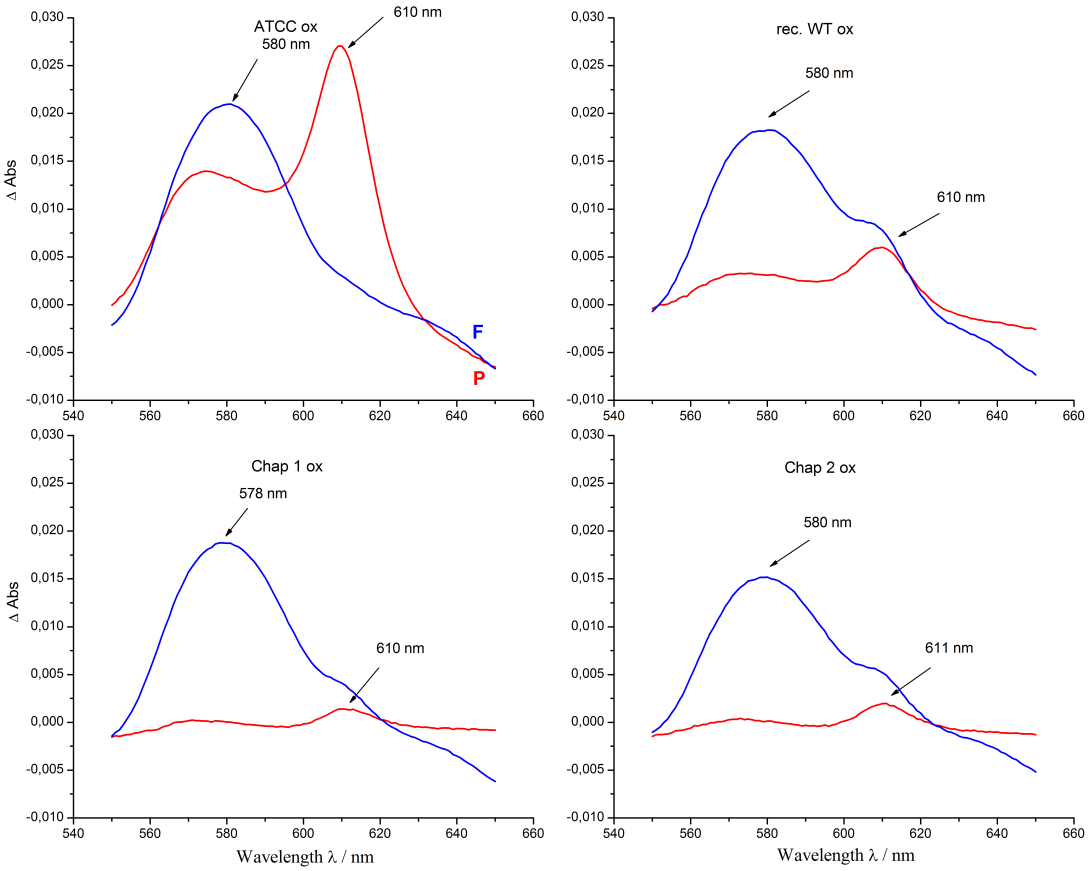

Figure 3.15: Difference absorption spectra of the ATCC WT C*c*O (top left), rec. WT C*c*O (top right), one-chaperone added rec. WT C*c*O (bottom left) and two-chaperones added rec. WT C*c*O (bottom right).

O_{ox} was used as starting state to induce the P-intermediate (red (Pminus O_{ox})) and F-intermediate (blue (F minus O_{ox})).

The difference absorption spectra of all described wild type C*c*Os shows a P-intermediate maximum around 610 nm and an F-intermediate maximum around 580 nm, suggesting the correct formation of the P- and F-intermediates.

Upon oxidation of the protein, the intensity of the P-intermediate related maximum of both chaperone added wild type C*c*Os decreased even more than originating from O_{asis}, compared to the difference between the ATCC WT C*c*O and rec. WT C*c*O. Additionally, a shift of the absorption maximum of the two-chaperones added rec. WT C*c*O to 611 nm was observed. Nevertheless, the difference between the one-chaperone added rec. WT C*c*O and the two-chaperones added rec. WT C*c*O is still present, showing a slightly higher yield of the P-intermediate for the two-

chaperones added rec. WT C*c*O. The intensity of this signal is decreased by a factor of two compared to the rec. WT C*c*O.

The F-intermediate related signal in the difference absorption spectrum of the two-chaperones added rec. wild type C*c*O is very similar to the rec. WT C*c*O. The F-intermediate of the one-chaperone added rec. wild type C*c*O is very similar to the ATCC WT C*c*O F-intermediate signal apart from the shift in maximum difference absorbance from 580 nm to 578 nm. The F-intermediate of the two-chaperones added rec. wild type C*c*O shows a slight shoulder at 610 nm and the lowest yield compared to all other wild type C*c*Os.

The properties observed in the optical spectra were investigated using EPR-spectroscopy. First measurements starting from O_{asis} and O_{ox} were done in the near scan range (see figure 3.16 and 3.17).

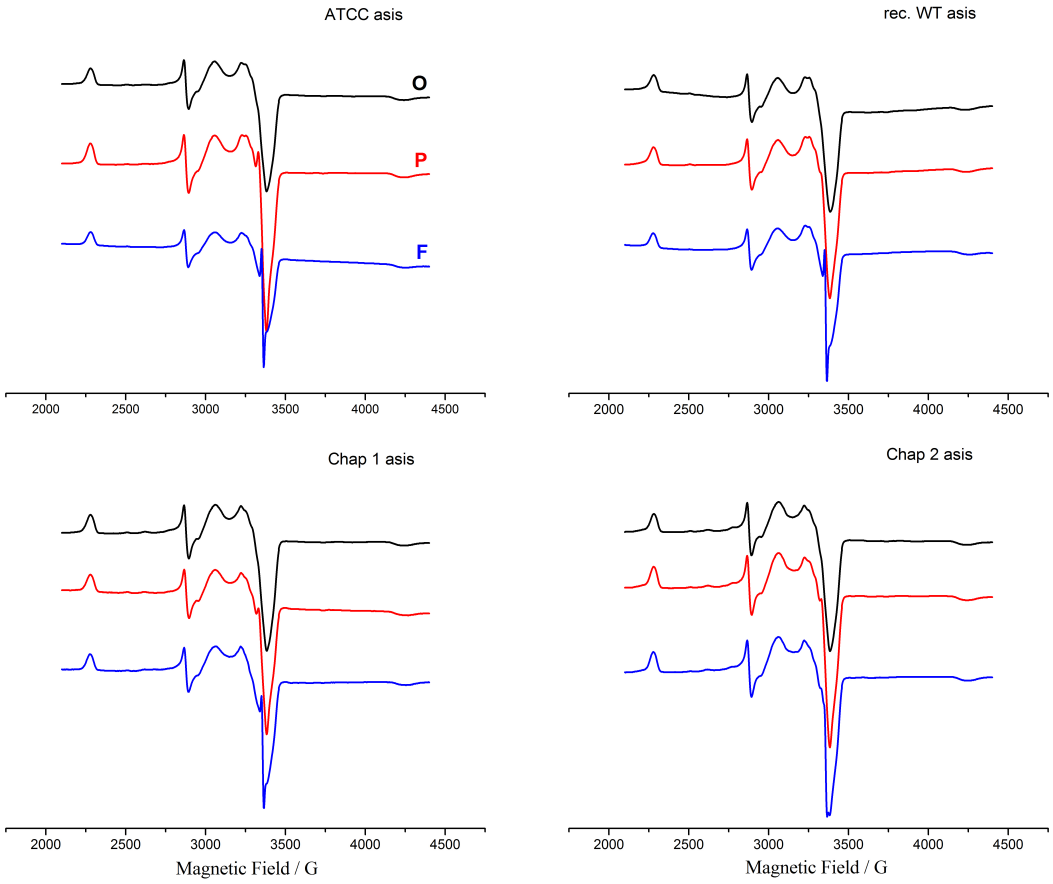

Figure 3.16: Near Scan EPR-spectra originating from O_{asis}

The O-intermediate (black), P-intermediate (red) and F-intermediate (blue) are shown for the ATCC WT C*c*O (top left), rec. WT C*c*O (top right), one-chaperone added rec. WT C*c*O (Chap 1, bottom left) and two-chaperones added rec. WT C*c*O (Chap 2, bottom right). EPR-spectra are shown in arbitrary units of the first derivative. The parameters used are described in Materials and Methods (Section 2.4.7).

The near scan EPR-spectra starting from O_{asis} of the one and two-chaperones added rec. WT C*c*Os did not show any new features compared to the rec. WT C*c*O and ATCC WT C*c*O. Nevertheless, in the P-intermediate of both chaperone added wild type C*c*Os the Y167 radical related signal is slightly visible, as well as the 12 G signal in the F-intermediate. Compared to the rec. WT C*c*O the one-chaperone added rec. wild type C*c*O shows a slight decrease in the 12 G signal intensity. The two-chaperones added rec. WT C*c*O shows an even further decrease of narrow signal intensity in the F-intermediate.

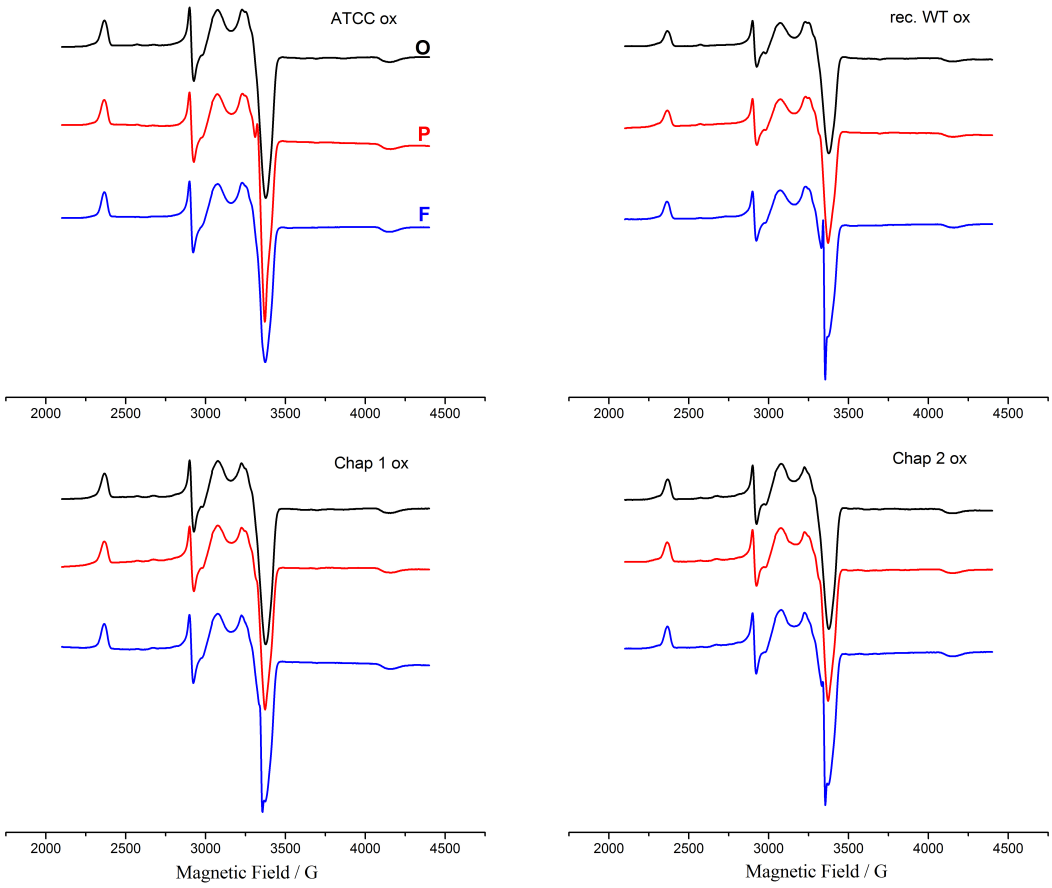

Figure 3.17: Near Scan EPR-spectra originating from O_{ox}.
The ATCC WT C*c*O is shown at the top left, the rec. WT C*c*O at the top right, the one-chaperone added rec. WT C*c*O in the bottom left and the two-chaperones added rec. WT C*c*O in the bottom right. The O-intermediate is shown in black, the P-intermediate in red and the F-intermediate in blue. Spectra are shown in arbitrary units of the first derivative. The parameters used are described in Materials and Methods (Section 2.4.7).

Similar to the spectra originating from O_{asis}, the near scan EPR-spectra starting from O_{ox} do not show any new features compared to the ATCC and the rec. WT C*c*O. In both chaperone added rec. WT C*c*Os, the spectrum of the P-intermediate shows a slight trace of the Y167 radical related signal. The narrow 12 G signal, visible in the F-intermediate is drastically reduced in both chaperone added rec. wild type C*c*Os compared to the rec. WT C*c*O.
The sweep width and modulation amplitude were reduced in order to analyze the Y167 related radical as well as the 12 G signal in the F-intermediate in a more resolved way.

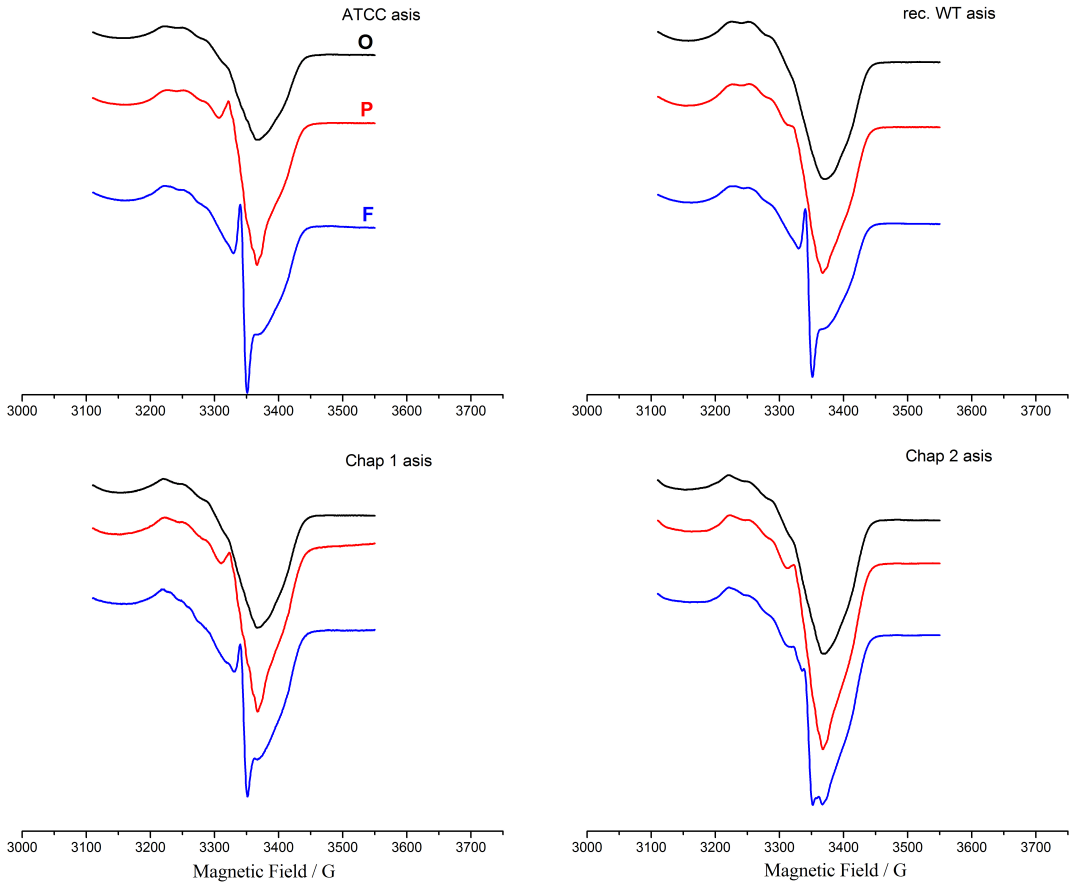

Figure 3.18: EPR radical spectra originating from O_{asis}.
Spectra of the O-intermediate (black), P-intermediate (red) and F-intermediate (blue) were recorded for the ATCC WT C*c*O (top left), rec. WT C*c*O (top right), one-chaperone added rec. WT C*c*O (bottom left) and two-chaperones added rec. WT C*c*O (bottom right). EPR spectra are shown in arbitrary units of the first derivative. The parameters used are described in Materials and Methods (Section 2.4.7).

Radical scans show no unexpected features for the chaperone added rec. WT C*c*Os. Compared to the ATCC WT C*c*O, the one-chaperone added rec. WT C*c*O shows a very similar spectrum for the P-intermediate. A prominent signal related to the Y167 radical is present.

This signal is also present in the spectrum of the P-intermediate of the two-chaperones added rec. WT C*c*O but not as prominent as in the one-chaperone added rec. WT C*c*O.

The two-chaperones added rec. WT C*c*O shows slight traces of the Y167 related signal in the F-intermediate. Comparing the spectra of the F-intermediates of the

chaperone added rec. WT C*c*Os, the narrow 12 G signal is visible in both spectra but the intensity decreases with increasing number of chaperones.

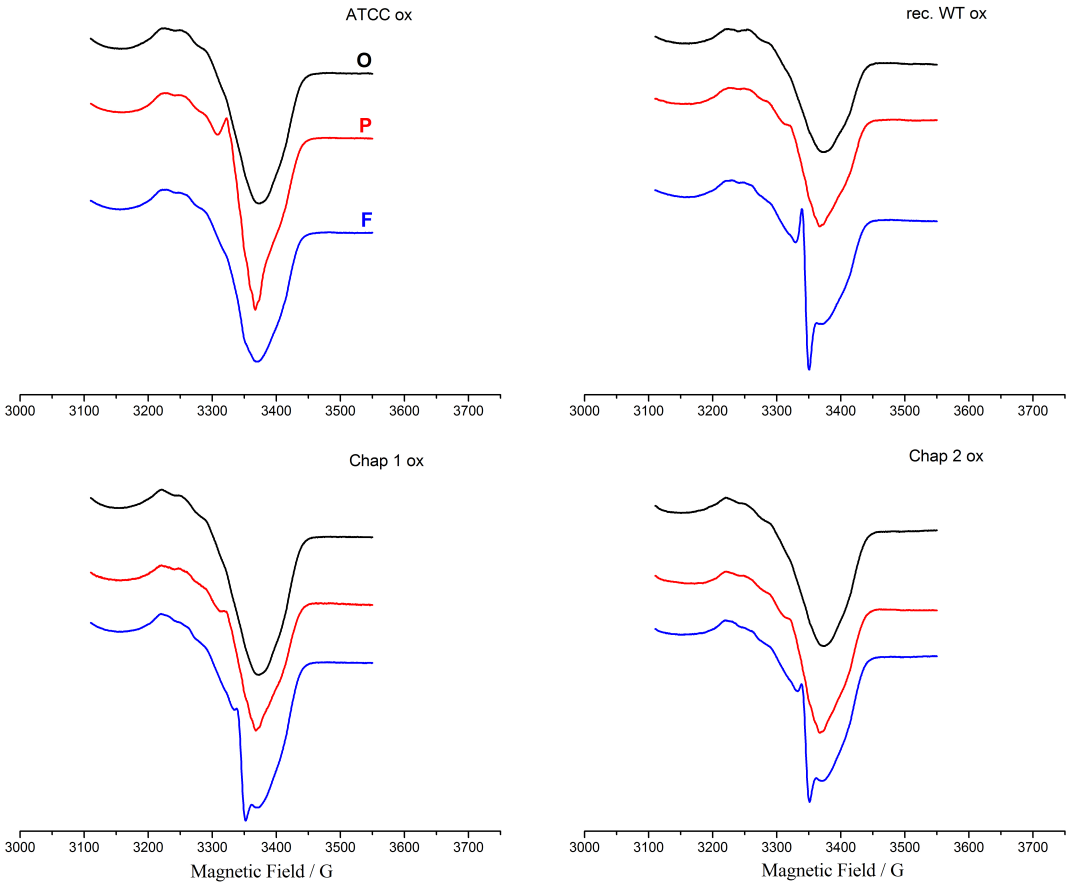

Figure 3.19: EPR radical spectra originating from O_{ox}.
Spectra of the ATCC WT C*c*O (top left), rec. WT C*c*O (top right), one-chaperone added rec. WT C*c*O (bottom left) and two-chaperones added rec. WT C*c*O (bottom right) were recorded in the O-intermediate (black), P-intermediate (red) and F-intermediate (blue). Spectra are shown in arbitrary units of the first derivative. The parameters used are described in Materials and Methods (Section 2.4.7).

Oxidizing the enzyme before treatment with hydrogen peroxide slightly decreases the Y167 radical related signal in the P-intermediate spectra in the case of the rec. WT C*c*O, the one-chaperone added rec. WT C*c*O and the two-chaperones added rec. WT C*c*O. Signal intensity does not change upon oxidation of the ATCC WT C*c*O. Contrary to that, the narrow 12 G signal nearly vanishes upon oxidation of the ATCC WT C*c*O and does not change upon oxidizing the rec. WT C*c*O. This signal decreases significantly in both chaperones added rec. WT C*c*Os. Signal intensity is only slightly but not significantly increased in the two-chaperones added rec. WT C*c*O compared

to the one-chaperone added rec. WT C*c*O. The Y167 related signal is not present in the F-intermediate of either of the chaperone added rec. wild type C*c*Os.

3.1.5. Differential Scanning Calorimetry

The addition of chaperones to the SU I encoding plasmid, results in a decrease of k_{cat} of the catalase reaction. In order to investigate the structural integrity and compare the structural stability of the rec. WT C*c*O and the ATCC WT C*c*O, differential scanning calorimetry (DSC) was used.

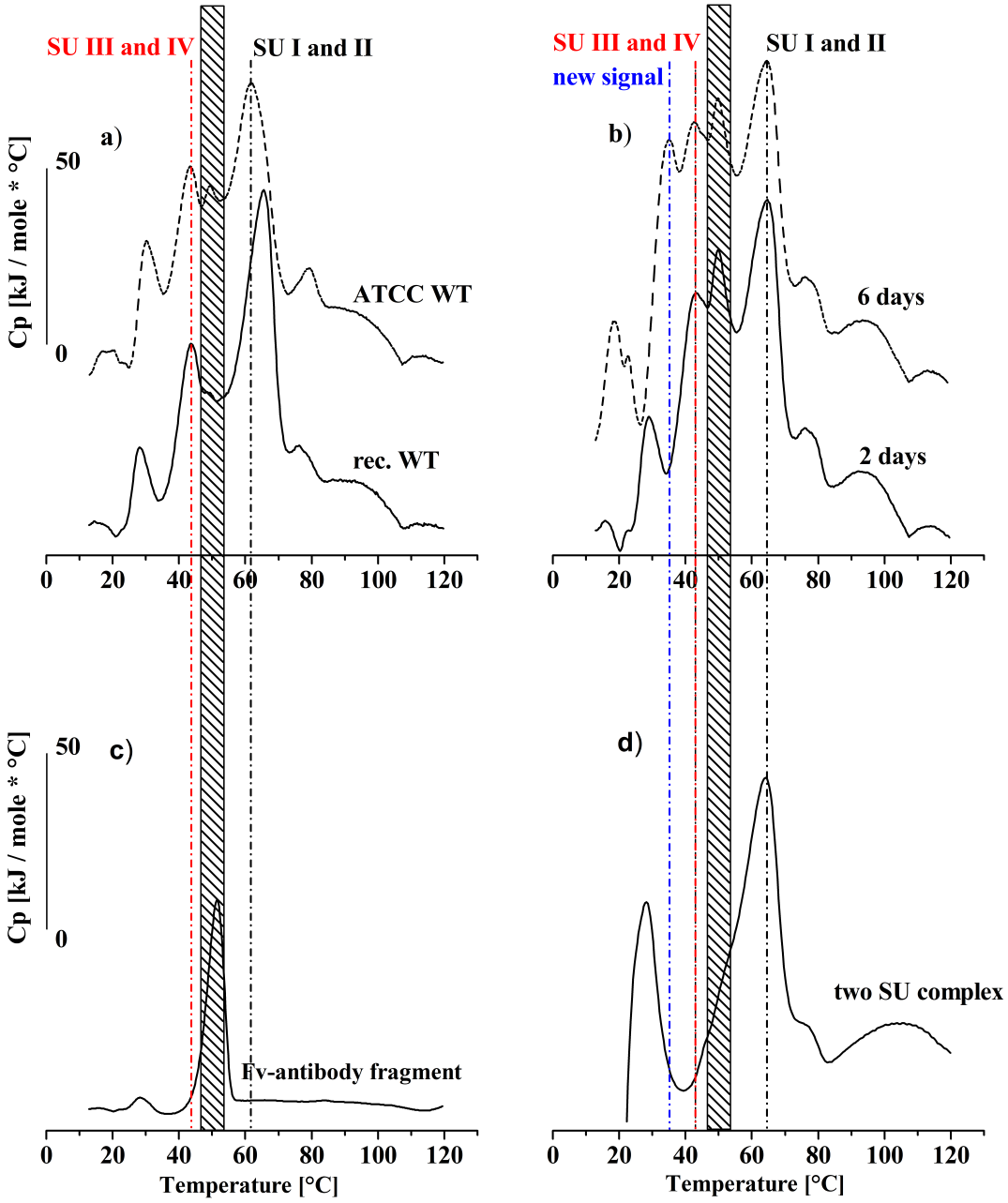

Figure 3.20: Differential scanning calorimetry curves of the ATCC WT C*c*O, the rec. WT C*c*O and the Fv-antibody fragment.

Differential scanning calorimetry data of the four SU ATCC WT C*c*O and rec. WT C*c*O are compared in a), whereas a time course of the rec. WT C*c*O after purification is shown in b). The 2 days old sample underwent two freeze-thaw cycles and the sample after 6 days, three freeze-thaw cycles. In c) the DSC data of the Fv-antibody fragment without any other protein is shown, whereas d) shows DSC curves of the two SU core enzymes, lacking SU III and IV but having the Fv-fragment attached to SU II. The shaded area depicts the signal obtained from free Fv-antibody fragment.

Capillary DSC was used to compare the stability of the rec. WT C*c*O and the ATCC WT C*c*O. Both four subunit preparations showed at least five different DSC signals

with transition midpoint temperature (T_m) ranges around 30°C, 43°C, 50°C, 65°C and 79°C (see figure 3.20 a)). Measuring additional denaturation of the core enzyme consisting of subunit I and II and denaturation of the Fv-antibody fragment used for purification alone, all signals could be assigned to different events (see figure 3.20 c) and d)). The signal with a T_m of 30°C is related to detergent effects visible in all samples with buffer containing DDM. The increase in heat capacity at 43°C is related to the melting or detachment of subunits III and IV. The signal at 50°C is the result of the denaturation of free Fv-antibody fragment, whereas the peak around 65°C shows the melting or detachment of subunits I and II [100]. The signal at 79°C is probably related to the detachment of the Fv-antibody fragment from subunit II.

DSC curves of both WT C*c*Os show a preparation dependent shift of the transition midpoint temperature of approximately 2°C at 65°C and 30°C. This shift presumably occurs because of different amounts of natural lipids and detergent still attached to the enzyme. Comparing both WT C*c*Os, a shift of the signal related to the melting or detachment of subunits I and II of approximately 5°C to higher temperatures is observed for the rec. WT C*c*O.

The ATCC WT C*c*O showed no significant dependence on storage time or freeze-thaw cycles. Contrary to that, the rec. WT C*c*O shows a significant decrease of thermal stability after storage at -80°C for six days and thawing the protein three times (see figure 3.20 b)). The signal at 43°C related to the melting of SU III and IV increases and an additional signal with a transition midpoint temperature of 35°C, appears. Another signal at approximately 18°C with a shoulder at 22°C, appears after six days of storage.

3.1.6. Structural Reasons for the Catalase Activity

Capillary DSC showed significant structural differences upon storage and freeze-thaw cycles for the rec. WT C*c*O. Therefore, it is assumed that the catalase activity is storage and/or freeze-thaw cycle dependent. Measurements resulting in the already described k_{cat} values included at least one freeze-thaw cycle. However, one could argue that the increased catalase activity is due to partial denaturation of the rec. WT C*c*O upon freezing the enzyme, resulting in a release of heme *a*. Therefore, the catalase activity and oxygen reductase activity of the rec. WT C*c*O were measured

directly after purification and after one freeze-thaw cycle and five days of storage at -80°C (see figure 3.21). Since the data shows that the catalase activity is only slightly dependent on freeze-thaw cycles, the ATCC WT C*c*O was not measured.

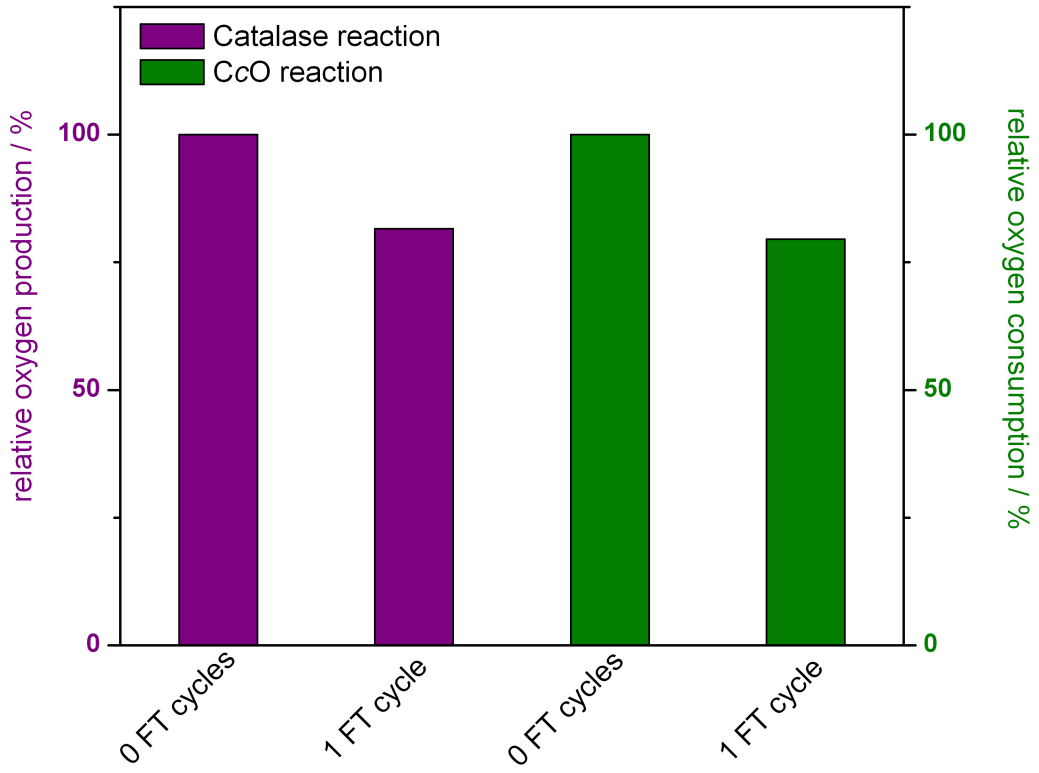

Figure 3.21: Relative catalase and oxygen reductase activity of the rec. WT C*c*O directly after purification and five days after purification with one freeze-thaw cycle.
"FT" abbreviates "freeze-thaw cycles".

The relative catalase and oxygen reductase activity is considered to be 100%, directly after purification. Storing the protein five days with one freeze-thaw cycle decreased both activities by approximately 20%.
In addition to that, the rec. WT C*c*O was heated to different temperatures to show that the catalase reaction is not due to a small population of denatured protein (see figure 3.22).

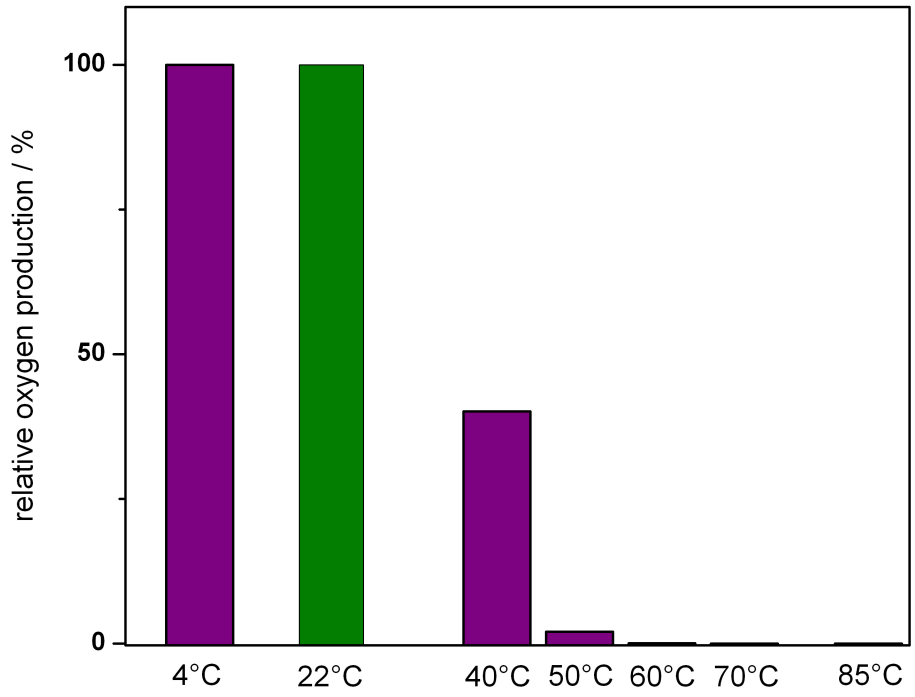

Figure 3.22: Relative oxygen production after incubation at different temperatures.
Purple bars denote the temperature C*c*O was incubated at for ten minutes; the green bar shows the catalase activity at the measuring temperature (22°C).

Measuring the catalase activity of the rec. WT C*c*O after incubation at the temperatures stated in the figure, showed that there was already a decrease in catalase activity after incubating the protein for ten minutes at 40°C. The measuring temperature of 22°C does not affect the protein. Incubating the protein at 50°C, reduced the catalase activity to almost zero, while any higher temperature lead to a complete loss of catalase activity.

A crude extract containing the cytoplasm and periplasm of *P. denitrificans,* and therefore the catalase and peroxidase, was also tested and showed a 34% increase in catalase activity after incubating the extract at 40°C. Incubating the extract at 50°C, resulted in a 97% loss of catalase activity. Nevertheless, the temperature dependence of this extract is completely different compared to the temperature dependence of the catalase activity of C*c*O.

3.1.7. The MR3 Wild Type

The MR3 wild type was first described by Raitio *et al*. [34]. This wild type features a deletion of the non-expressing gene for SU I of *aa*$_3$ C*c*O as well as a deletion of the neighboring *ORF4*. The remaining genes are solely located on the chromosome. Therefore, the MR3 wild type is an intermediate step between the ATCC WT and the rec. WT. This intermediate wild type shows a relative oxygen reductase activity of 100 ± 5.1%. The k_{cat} and the K_M of the catalase reaction were determined to be 188.8 ± 16.4 min^{-1} and 1094.4 ± 173.5 µM H_2O_2, respectively. The k_{cat} of the catalase reaction is therefore approximately 18-fold higher, compared to the ATCC WT C*c*O and nearly as high as the k_{cat} of the rec. WT C*c*O. The K_M value is slightly increased compared to the K_M values of the ATCC WT C*c*O and the rec. WT C*c*O.
The MR3 WT C*c*O was analyzed by UV/vis- and EPR-spectroscopy to correlate the findings with the data obtained for the already described wild type C*c*Os (see figure 3.23).

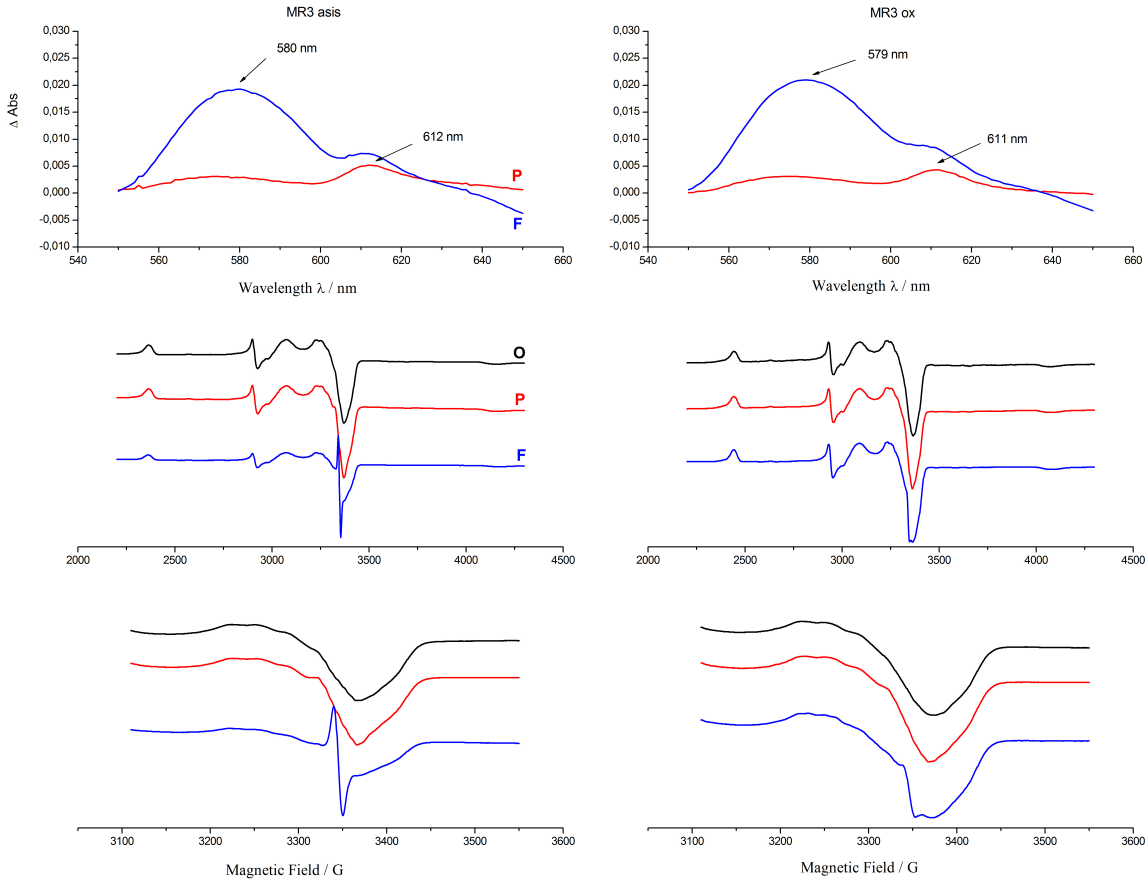

Figure 3.23: UV/vis-spectra (top), EPR near scan spectra (middle) and EPR low power radical spectra (bottom) of the MR3 WT C*c*O originating from O_{asis} (left) and O_{ox} (right)
The P-intermediate of the UV/vis-spectra is shown in red, the F-intermediate in blue (P or F minus O_{asis} on the left side and P or F minus O_{ox} on the right side), whereas the O-intermediate, the P-intermediate and the F-intermediate are shown in black, red and blue respectively in the EPR-spectra. EPR spectra are shown in arbitrary units of the first derivative. The parameters used are described in Materials and Methods (Section 2.4.7).

The optical difference spectra of the P- and F-intermediate originating from O_{asis} do not show significant changes upon oxidation. The maximum difference absorption of the F-intermediate shifts to 579 nm upon oxidation. It shows a slightly increased shoulder at 612 nm if starting from O_{asis}, which shifts from 612 nm to 611 nm upon oxidation. The difference absorption band of the P-intermediate also shifts from 612 nm to 611 nm upon oxidation of the protein prior to hydrogen peroxide treatment. The yield of both P-intermediates, originating from O_{asis} and O_{ox}, is reduced compared to the ATCC WT C*c*O but very similar to the rec. WT C*c*O. Signal

intensity of the difference absorption band of the F-intermediate is similar to the ATCC WT C*c*O and rec. WT C*c*O intensity.

The near scan EPR-spectra do not show any new features compared to the ATCC WT C*c*O and rec. WT C*c*O. The P-intermediate prepared from O_{asis} shows a slight trace of the radical signal associated with Y167. The F-intermediate shows a clear narrow signal starting from O_{asis}. Both signals seem not to be present when starting from the chemically oxidized enzyme. The disappearance of the narrow 12 G signal upon oxidation is similar to the behavior of the ATCC WT C*c*O.

Analyzing the radical scan reveals the Y167 radical related signal to be present in both P-intermediates but losing signal intensity upon oxidation.

The F-intermediate originating from O_{asis} shows the 12 G narrow signal with strong signal intensity. The signal nearly disappears when starting from the chemically oxidized MR3 WT C*c*O. The remaining signal intensity is very low but the signal is still present. Similar results were already observed for the ATCC WT C*c*O upon oxidation.

3.2. The Catalase Reaction Mechanism of *aa*$_3$ Cytochrome *c* Oxidase

Orii and Okunuki first described the catalase reaction of the cytochrome *c* oxidase in 1963 [58]. During their work with hydrogen peroxide and C*c*O, they discovered that C*c*O is able to degrade H_2O_2. Konstantinov further investigated these side reactions of C*c*O, suggesting the first catalase activity mechanism for CcO [60; 62; 101-103]. One main target of the present work was the investigation of the catalase reaction cycle of C*c*O. Various inhibitors as well as variants were used to obtain information about the reaction mechanism.

3.2.1. Probing the Active Site of the Catalase Reaction

Konstantinov suggested a catalase mechanism for C*c*O. This reaction cycle involves three hydrogen peroxide molecules. The first one leads to the O- to P-intermediate conversion, the second to the P- to F-intermediate conversion and the third restores the O-intermediate from the F-intermediate. The products of this reaction, as postulated by Konstantinov, are superoxide anions and protons. If there is no

oxidizing agent present, one superoxide anion reacts to form a hydrogen peroxide molecule using the produced protons and the other superoxide anion reacts to form molecular oxygen. However, using ferricyanide, an increase in pH was visible, suggesting that the proposed reaction mechanism might be true for the C*c*O used and naming this a "pseudocatalase" reaction [60]. Nevertheless, C*c*O from *P. denitrificans* showed no increase in pH during the catalase reaction if ferricyanide was present. Furthermore, the ability of C*c*O to generate oxygen from superoxide was tested using a superoxide thermal source (SOTS-1) [104]. The addition of SOTS-1 to buffer containing C*c*O showed only a very small effect. An increase of oxygen concentration was only visible for a short time. Additionally, the overall concentration of oxygen produced was 1000-fold lower than that of SOTS-1 used, therefore diminishing the influence of superoxide on the catalase activity of C*c*O.
Furthermore, different inhibitors were tested on their influence on catalase activity of C*c*O (see figure 3.24).

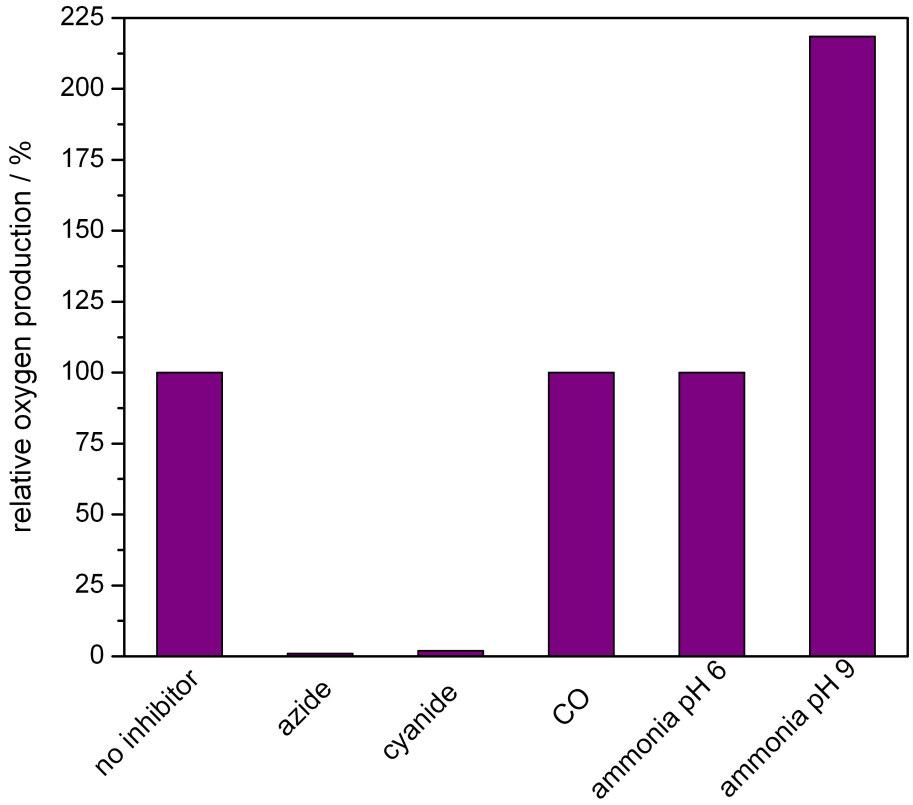

Figure 3.24: Effect of different inhibitors of C*c*O on the catalase activity.
Different well known inhibitors, such as cyanide, azide and CO were tested for their influence on catalase activity. In addition, ammonia was tested for its influence on catalase activity at different pH values.

Measurements using the known C*c*O inhibitors azide and cyanide resulted in a 98 - 99% loss of catalase activity. The addition of carbon monoxide and ammonia at pH 6 did not show any effect on the catalase activity. In the presence of ammonia at pH 9, catalase activity of C*c*O was more than doubled.
The F*-intermediate is spontaneously generated by equimolar amounts of hydrogen peroxide at pH 6 or lower [105; 106]. Knowing the effect of different inhibitors that bind to the active site of C*c*O, the P-intermediate and F*-intermediate were probed for catalase activity. The catalase activities of the P- and F*-intermediate were analyzed to check for their involvement in the catalase reaction cycle (see figure 3.25).

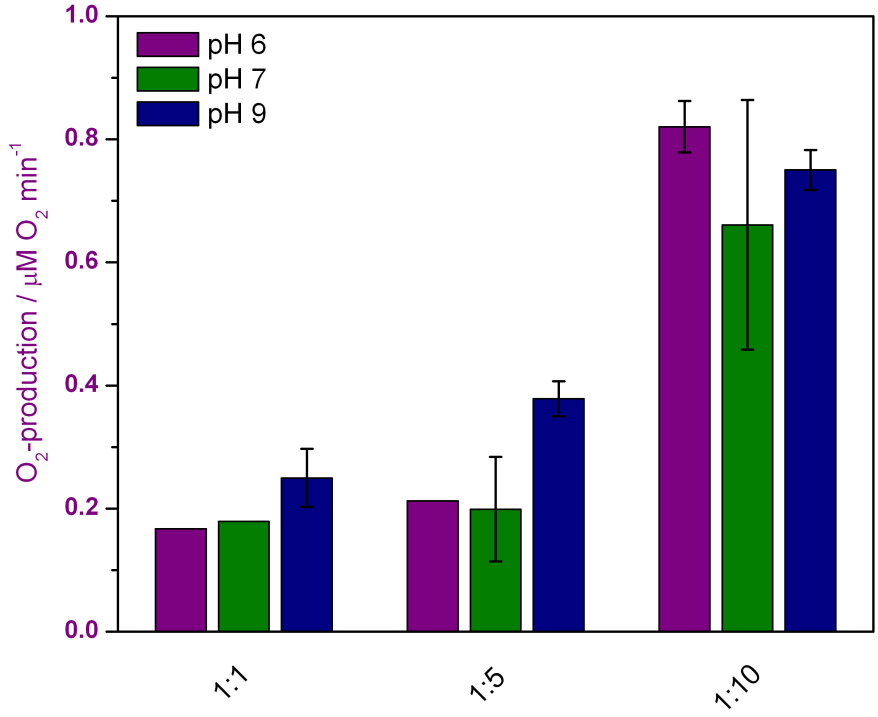

Figure 3.25: Catalase activity of C*c*O in the P- and F*-intermediates at different protein to hydrogen peroxide ratios.
The X-axis shows the molar protein to hydrogen peroxide ratios. The P-intermediate is formed at all three ratios from pH 7 to pH 9, whereas the use of all three ratios of hydrogen peroxide at pH 6 forms the F*-intermediate. C*c*O to hydrogen peroxide ratios are very low, the analysis time was restricted to no more than ten seconds.

Low catalase activity is present in the P- and F*-intermediates. The catalase activity increases with increasing amount of hydrogen peroxide only at pH 9. At pH 6 and 7 the catalase activity seems to start at a 1:10 ratio and higher. Nevertheless, the observed catalase activity is very slow and the standard deviation of different measurements is, therefore, very high. A 1:10 ratio seems to be the minimal ratio to record a catalase activity at pH values of 6, 7 and 9.

3.2.2. Analysis of the Oxygen Produced during the Catalase Reaction

During the decomposition of hydrogen peroxide, oxygen evolves. In catalases, the evolving oxygen originates from one single hydrogen peroxide molecule, whereas

the other hydrogen peroxide molecule involved in the same reaction cycle is used together with two protons to form two molecules of water [107; 108].

The origin of the oxygen molecule generated during the catalase reaction by C*c*O was investigated in cooperation with Wolfram Lorenzen (AK Bode, University of Frankfurt, Frankfurt Main, Germany). A mixture of hydrogen peroxide labeled with heavy oxygen isotopes ($H_2{}^{18}O_2$) and non-labeled hydrogen peroxide in an oxygen free medium containing C*c*O initiated the catalase reaction. The resulting oxygen should, therefore, either be a mixed molecule from labeled and non-labeled atoms or only labeled and non-labeled dioxygen. The mixture of oxygen molecules was separated by gas chromatography and analyzed by mass spectrometry (see figure 3.26)

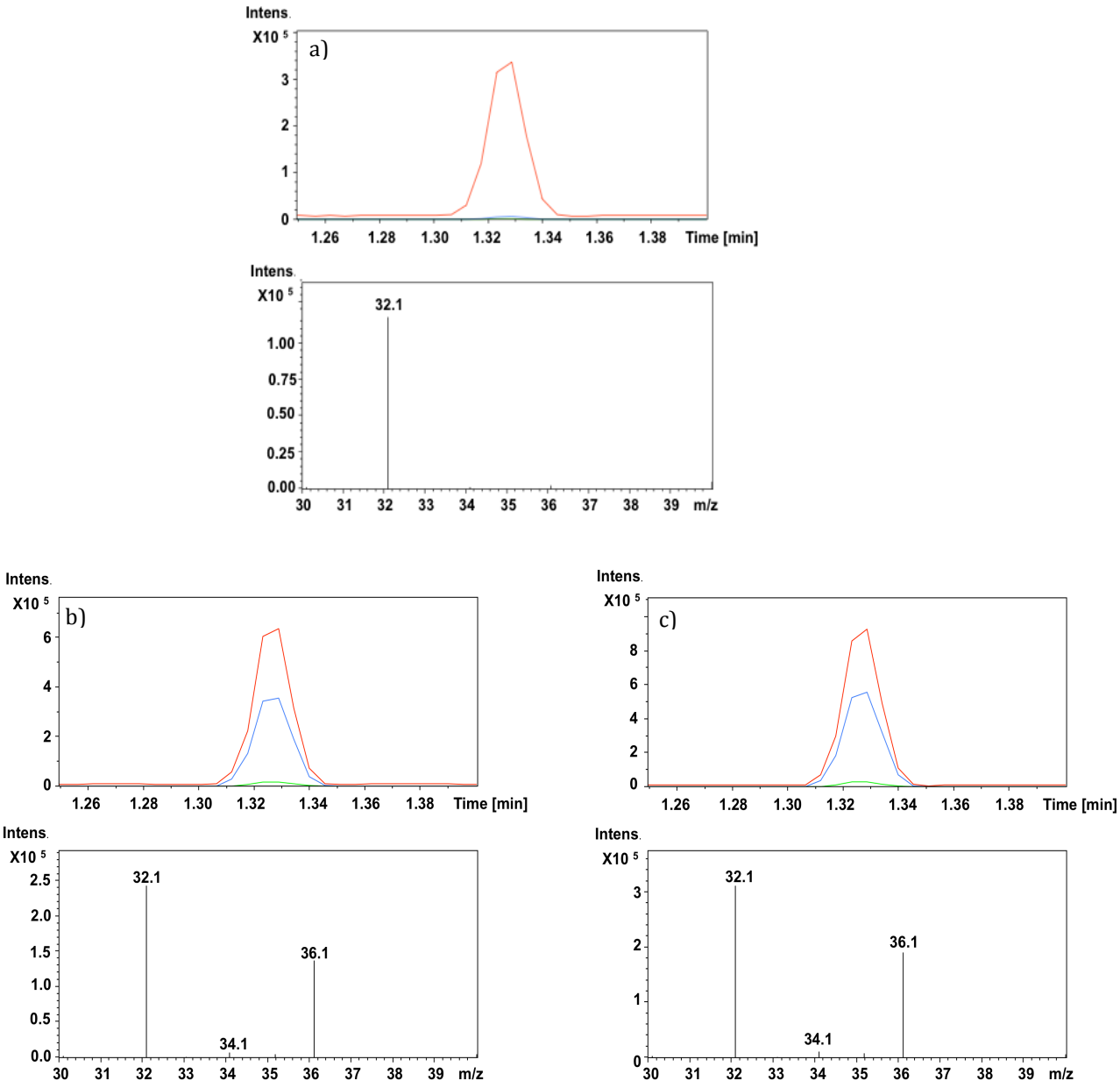

Figure 3.26: Gas chromatography-mass spectrometry (GCMS) chromatograms.
The chromatograms show a) buffer alone with a controlled ratio of labeled and non-labeled H_2O_2, b) ATCC WT C*c*O with a mixture of labeled and non-labeled H_2O_2 and c) rec. WT C*c*O with a mixture of labeled and non-labeled H_2O_2. The top part shows the extracted ion chromatogram and the lower part the mass spectrometry results. The red curve in the upper part shows mass according to non-labeled oxygen (^{16}O-^{16}O), the blue curve oxygen with both atoms labeled (^{18}O-^{18}O) and the green curve oxygen with only one atom labeled (^{18}O-^{16}O). Given the green curve, a very small population of ^{18}O-^{16}O could not be ruled out.

Measuring the reaction buffer showed only a $^{32}O_2$ related significant signal. Therefore, the system used was considered stable in terms of spontaneous

decomposition of the hydrogen peroxide mixture used. The ATCC WT C*c*O and rec. WT C*c*O show signals for both, non-labeled oxygen ($^{32}O_2$) and completely labeled dioxygen ($^{36}O_2$). Slight traces of molecular oxygen that seemed to be composed of labeled and non-labeled atoms were found as well ($^{34}O_2$). The relative amount of the completely labeled and non-labeled species was measured and compared to the calculated amount that was supposed to be present in the buffer (see table 3.1). There are two possible combinations of produced oxygen. The first combination would be an amount of $^{32}O_2$ and $^{36}O_2$ similar to the used mixture of both hydrogen peroxide species, whereas the second would be nearly none of the previously described oxygen populations but a high amount of oxygen being produced as $^{34}O_2$.

Table 3.1: Comparison of calculated and measured ratios of labeled and non-labeled oxygen.
Mean Ratios (in percentage) of two to three single measurements are displayed as $^{32}O_2$: $^{36}O_2$. 100% is reached via small amounts of $^{34}O_2$.

Measurement	ATCC WT C*c*O measured	rec. WT C*c*O measured
1	59.5 ± 3.2 : 38.7 ± 1.6	58.6 ± 4.0 : 39.5 ± 2.3
2	51.5 ± 4.4 : 46.3 ± 1.0	50.9 ± 1.2 : 46.9 ± 2.2
	ATCC WT C*c*O calculated	rec. WT C*c*O calculated
1	56:44	56:44
2	46:54	46:54

The comparison of the calculated and measured ratios of the two produced oxygen species of both wild type C*c*Os shows a positive deviation from non-labeled dioxygen by 4-6% and a negative deviation from labeled dioxygen of 5-7% for both mean values. Nevertheless, the magnitude is in the same range in all measurements. The second possibility, described previously, is a mixed oxygen molecule of labeled and non-labeled oxygen atoms ($^{34}O_2$). The calculated amount of this mixed species and the measured ratio is shown exemplarily in table 3.2.

Table 3.2: Calculated and measured amount of ^{16}O-^{18}O.
Mean ratios (in percentage) of two to three single measurements are shown.

Measurement	ATCC WT C*c*O calculated	ATCC WT C*c*O measured	rec. WT C*c*O calculated	rec. WT C*c*O measured
2	~ 92	3.98 ± 0.05	~ 92	4.04 ± 0.12

Table 3.2 shows exemplarily the calculated results of a mixed oxygen species of ^{16}O-^{18}O. The experimentally obtained results are lower by a factor of 20. Comparing both possibilities of the originating oxygen, the previously described first possibility ($^{32}O_2$ and $^{36}O_2$) seems more likely.

3.2.3. First Characterization of Different Variants

Different variants were constructed to probe the active site by removing Cu_B and introducing an acidic or basic amino acid instead; the Cu_B coordinating histidine 276 was exchanged for aspartate, glutamate, arginine or lysine (H276D/E/R/K). The surroundings of the active center were also probed for the influence of aromatic amino acids on the catalase reaction (W164F, Y167F, W164F Y167F, W272F, Y280F and W272F Y280F). All variants possess all four subunits as well as the Fv-antibody fragment present as verified by SDS PAGE (shown exemplarily for H276D and H276E in figure 3.27).

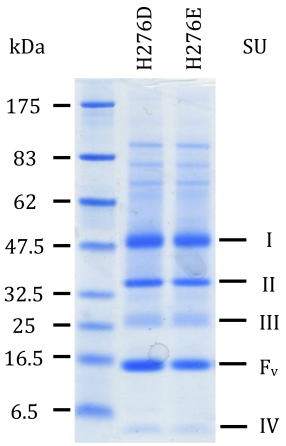

Figure 3.27: SDS PAGE of variants H276D and H276E.
The Coomassie stained SDS PAGE shows the presence of SU I through IV including the F_v-antibody fragment.

Each variant was checked for metal composition via microPIXE. The iron content of all variants did not show any deviations. The copper content of all variants is shown in figure 3.28 for H276D/E/R/K and in figure 3.29 for W164F, Y167F, W164F Y167F, W272F, Y280F and W272F Y280F.

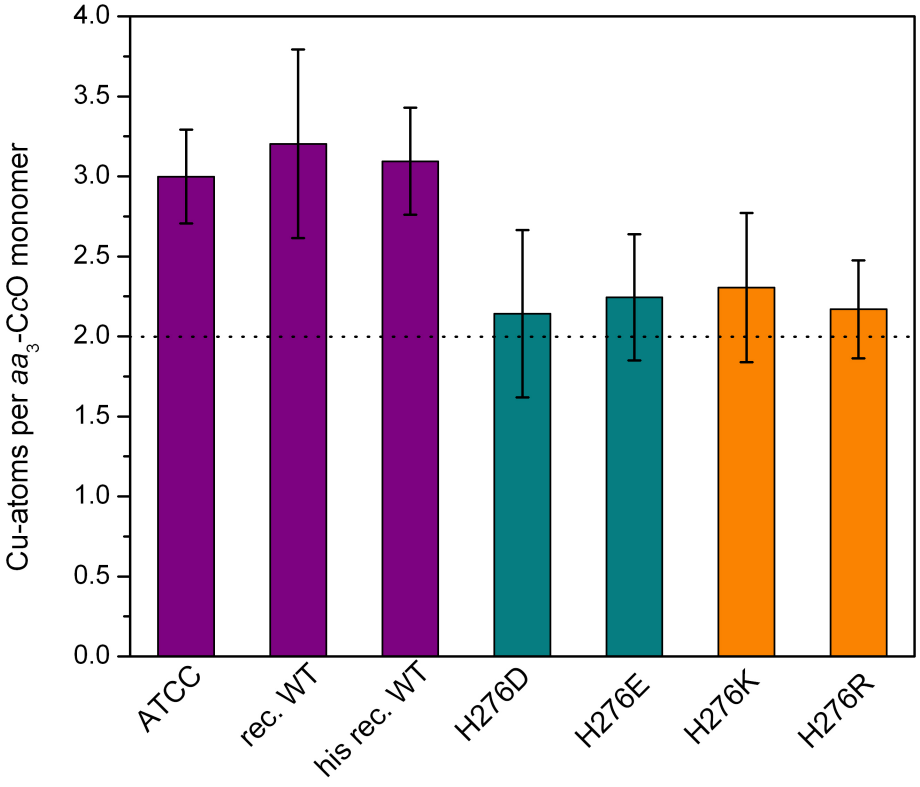

Figure 3.28: Results of copper determination of the purified ATCC WT C*c*O, rec. WT C*c*O and four variant C*c*Os determined by microPIXE.

The copper content determinations showed the absence of one copper atom per C*c*O molecule for all four variants (H276D/E/R/K, figure 3.28). Since Cu_A is a binuclear center [18] and the mutations concern one of the Cu_B complexing histidines, it is most likely that the missing copper atom is Cu_B. The active center is, therefore, not fully assembled in these variants. However, SDS PAGE did not show any differences compared to the ATCC WT C*c*O and rec. WT C*c*O.

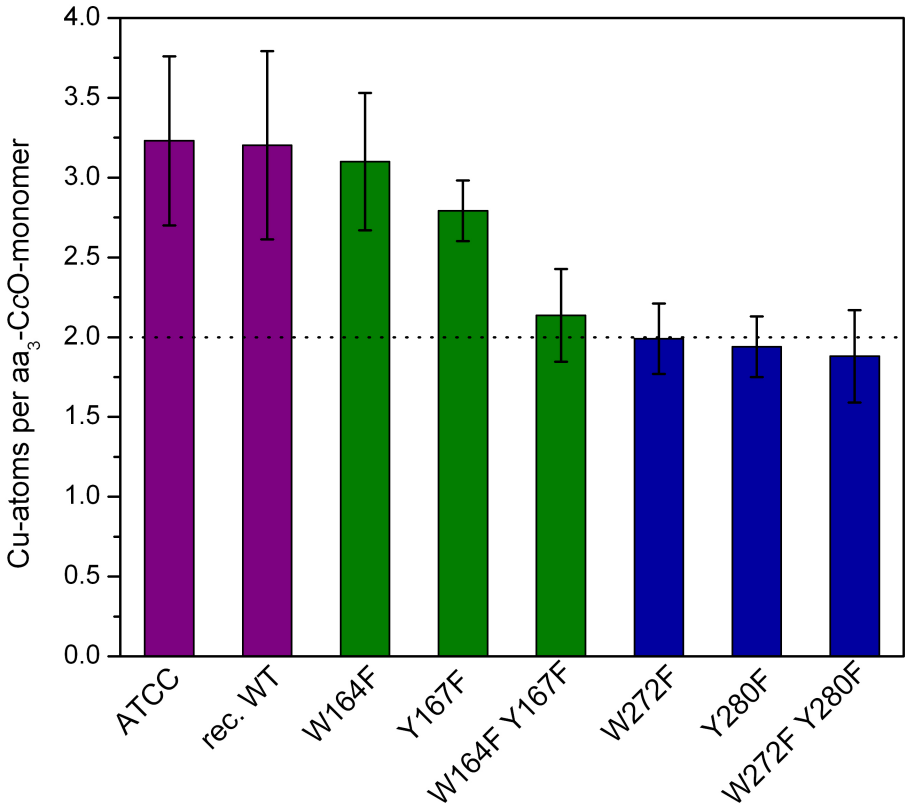

Figure 3.29: Results of the determination of copper contents for the purified ATCC WT C*c*O, rec. WT C*c*O and six different variant C*c*Os.

The ATCC WT C*c*O, rec. WT C*c*O, W164F and Y167F do not show any significant differences in metal content. The variants W164F Y167F, W272F, Y280F and consequently W272F Y280F show a loss of one copper atom per C*c*O molecule. Due to the mutations near the active center in SU I and Cu_A being a binuclear center in SU II, it is highly likely that the absent copper atom is Cu_B. The active center of these variants is therefore not fully assembled.

A loss of Cu_B would result in a loss of oxygen reductase activity, which was therefore measured to verify this assumption (see figure 3.30 and 3.31).

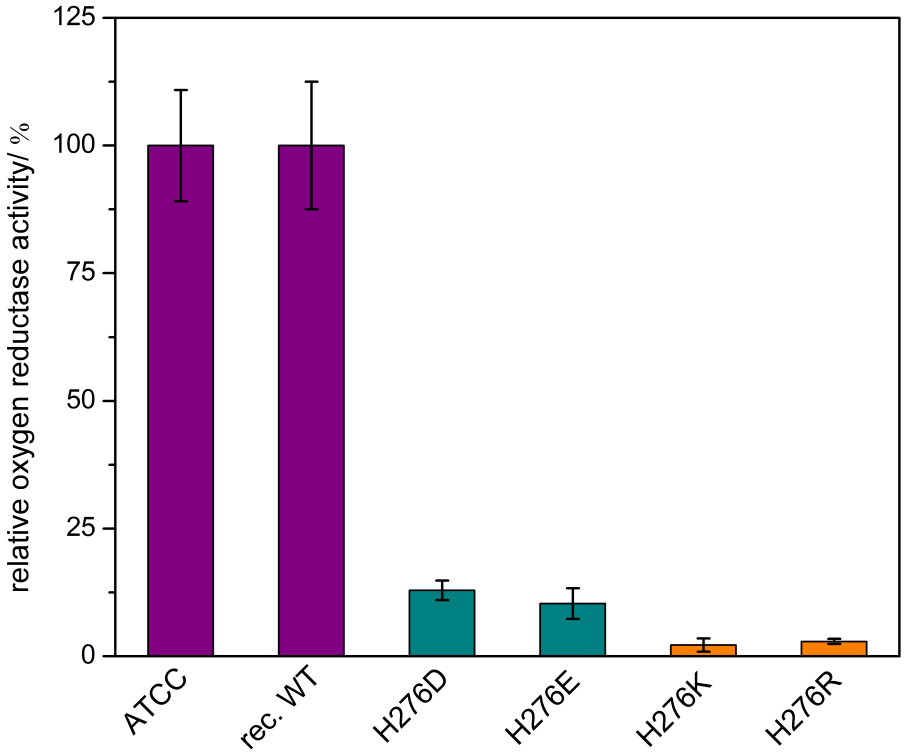

Figure 3.30: Oxygen reductase activity of the purified ATCC WT C*c*O, rec. WT C*c*O (purple) and four variant C*c*Os.
The two variants H276D and H276E are shown in turquoise and the two variants H276K and H276R in orange. 100% corresponds to ~450 e^-/s using horse heart cytochrome *c* as electron donor.

Oxygen reductase activity measurements of the variants H276D and H276E show a relative activity of 10% compared to the WT C*c*O. The variants H276K and H276R show a decrease of more than 95% compared to the WT C*c*O and are, therefore, considered as catalytically inactive. The oxygen reductase activity of the variants with H276 exchanged for an acidic amino acid is increased compared to the variants with basic amino acids.

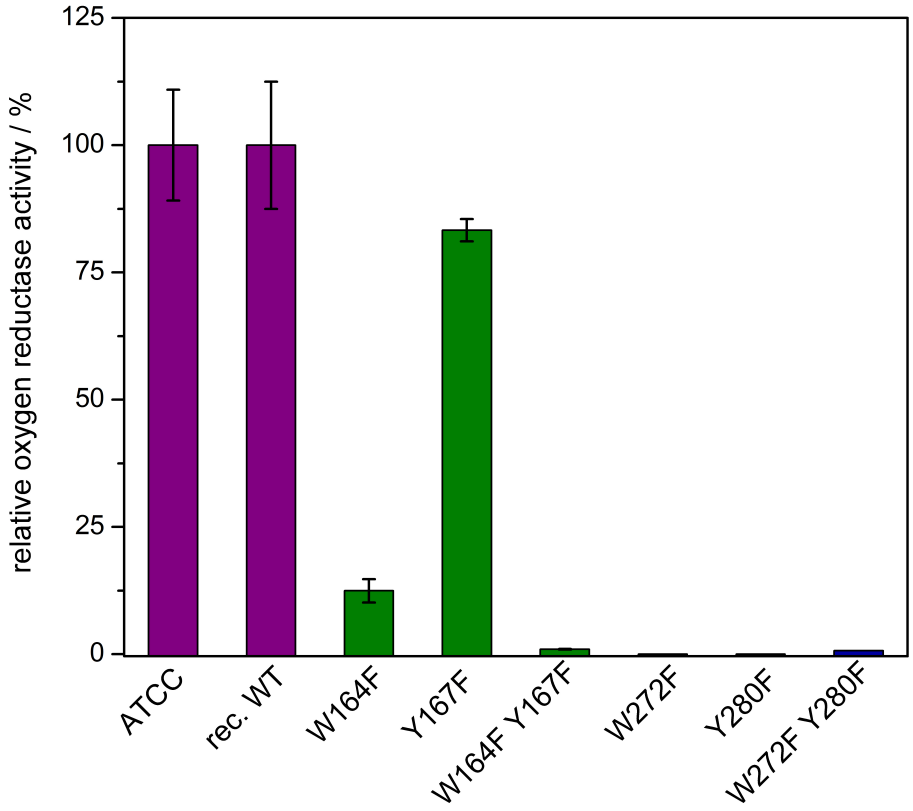

Figure 3.31: Oxygen reductase activity of the purified ATCC WT C*c*O and rec. WT C*c*O compared to the variants W164F, Y167F, W164F Y167F (green), W272F, Y280F and W272F Y280F (blue). 100% corresponds to ~450 e^-/s using horse heart cytochrome *c* as electron donor.

The oxygen reductase activities of the variants W164F Y167F, W272F, Y280F and W272F Y280F are less than 5% and therefore these variants are considered to be catalytically inactive. The variant W164F shows approximately 10% catalytic activity and the variant Y167F shows nearly wild type activity with approximately 80%.

Additionally to the oxygen reductase activity, the catalase activity of all ten variants was determined to rule out whether Cu_B is involved in catalase activity (figure 3.32 and 3.33).

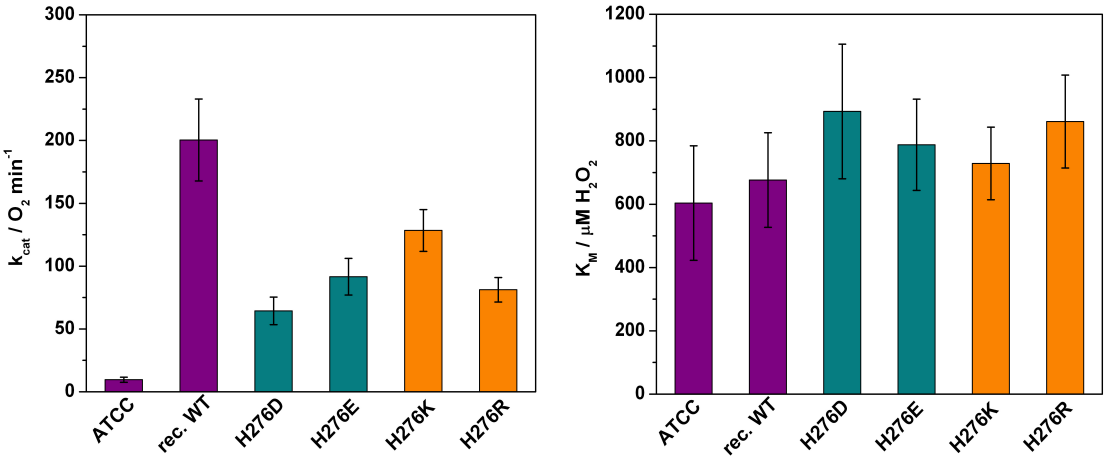

Figure 3.32: Catalase activity dependent kinetic parameters of the ATCC WT C*c*O and the rec. WT C*c*O (purple), H276D and H276E (turquoise), and H276K and H276R (orange).
The k_{cat}-values are shown on the left hand side, whereas the K_M-values are shown on the right hand side.

All variants show a considerably higher catalase activity compared to the ATCC WT C*c*O despite the loss of Cu_B. Cu_B is therefore negligible for the catalase activity of aa_3 C*c*O. The determination of kinetic parameters showed that none of the variants exhibited a catalase activity dependent k_{cat} similar to or higher than the rec. WT C*c*O. Nevertheless, none of the variants showed a k_{cat} lower than or equal to the ATCC WT C*c*O. The K_M values differ slightly but the variations are insignificant. The variant H276K shows a k_{cat} of about 3/4 of the rec. WT C*c*O, whereas the variants H276E and H276R show a k_{cat} of approximately half of the rec. WT C*c*O. H276D showed the largest decrease of k_{cat} to approximately 1/3 of the rec. WT C*c*O.

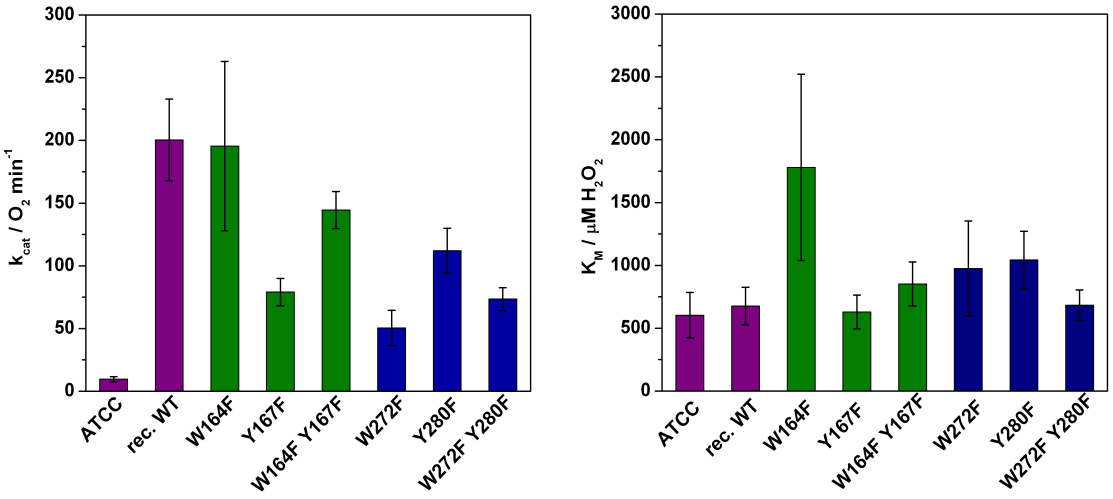

Figure 3.33: Kinetic parameters of the catalase activity of the ATCC WT C*c*O and rec. WT C*c*O (purple) as well as variants W164F, Y167F, W164F Y167F (green) and W272F, Y280F, W272F Y280F (blue). The k_{cat} values are shown on the left hand side and the K_M values on the right hand side.

The kinetic parameters of the catalase activity of the variants W164F Y167F, W272F and Y280F show a slight but non-significant increase in their K_M values. The K_M values of Y167F, and W272F Y280F do not increase compared to the ATCC WT C*c*O. The only variant showing a significant, approximately 2.5-fold, increase of K_M compared to the ATCC and the rec. WT C*c*O is W164F.

W164F shows a k_{cat} very similar to the rec. WT C*c*O value. Y167F and W272F show a similar decrease of k_{cat} by a factor of ~2.6 and 4, respectively, compared to the rec. WT C*c*O. Y280 is cross-linked to one of the Cu_B complexing histidines. The variant Y280F shows a 2-fold decrease in k_{cat} compared to the rec. WT C*c*O.

Both double variants exhibit a combination of the two corresponding single variant features, showing a decrease in k_{cat} by a factor of 1.3 and a decrease by a factor of 2.5 for W164F Y167F and W272F Y280F, respectively. The only exception of the proposed "rule" is the K_M-value of W272F Y280F, which is slightly lower than those of the corresponding single variants.

3.2.4. UV/vis-Spectroscopy of Variants

UV/vis spectra were recorded for variants carrying mutations in the aromatic amino acids near the active center, namely W164F, Y167F, W164F Y167F, W272F,

Y280F and W272F Y280F. These variants were chosen to prevent the formation of tryptophan and/or tyrosine radicals on one or two aromatic amino acids by introducing a phenylalanine on either or both these amino acids. Spectra were recorded originating from O_{asis} (see figure 3.34 and 3.35) and O_{ox} (see figure 3.36 and 3.37). Spectra of the O-intermediate and the hydrogen peroxide derived P- and F-intermediates were recorded and difference absorption spectra of the P-O and F-O state were calculated. However, if no clear P- or F-intermediates were visible, the according conditions were applied and the difference spectra were calculated nevertheless.

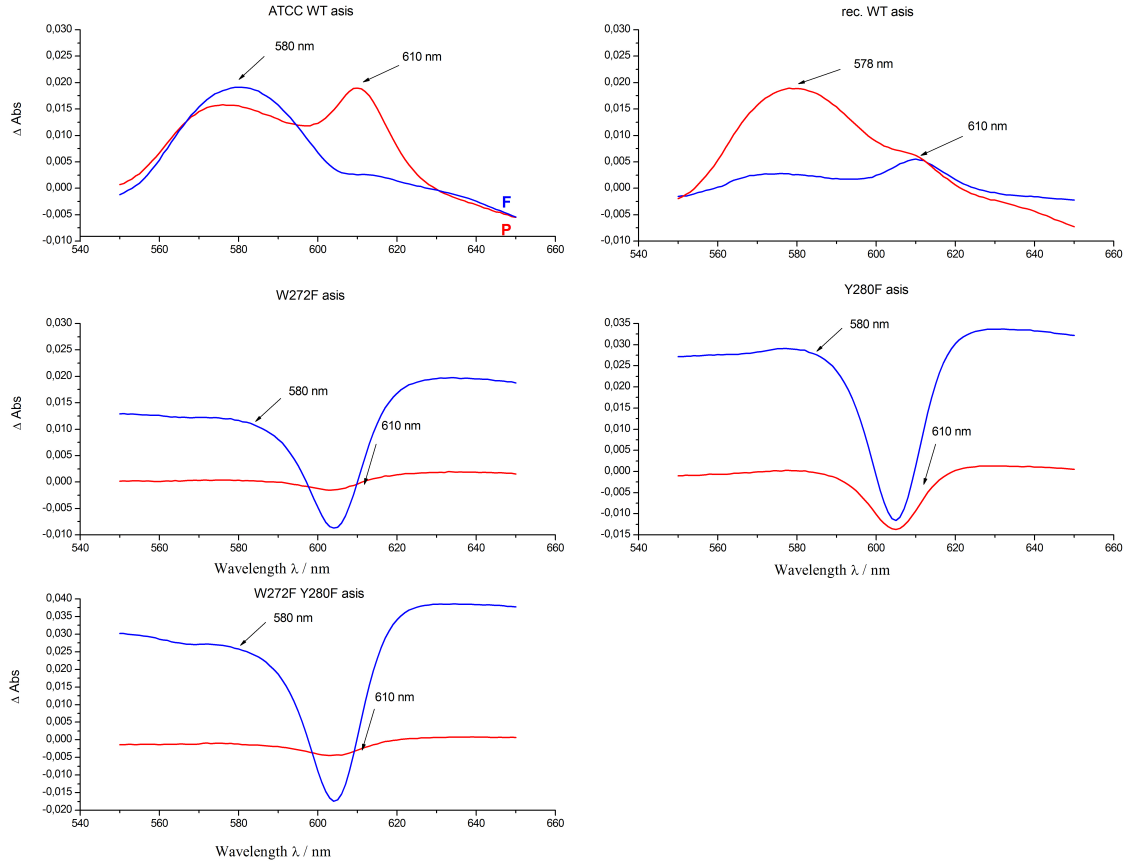

Figure 3.34: Difference absorption spectra of the P (red (P minus O_{asis})) and F (blue (F minus O_{asis})) intermediates originating from O_{asis}.
The top left shows the ATCC WT C*c*O, top right the rec. WT C*c*O, middle left W272F, middle right Y280F and bottom W272F Y280F.

The difference absorption spectra of the variants W272F, Y280F and W272F Y280F originating from O_{asis} show significant differences to the ATCC WT C*c*O and rec. WT C*c*O. The signal at about 610 nm, corresponding to the P-intermediate is missing in all three variants. Spectra of the variants W272F and W272F Y280F do not show any high intensity signals in the P-intermediate. A negative signal at 605 nm is present in both spectra of Y280F. The 580 nm signal, corresponding to the F-intermediate, is also missing in all three variants. A negative signal at 605 nm is present in all F-intermediate spectra of W272F, Y280F and W272F Y280F. This signal is significantly more intense than the negative signal in the P-intermediate spectra of Y280F. The difference absorption spectra of W272F and W272F Y280F are very similar.

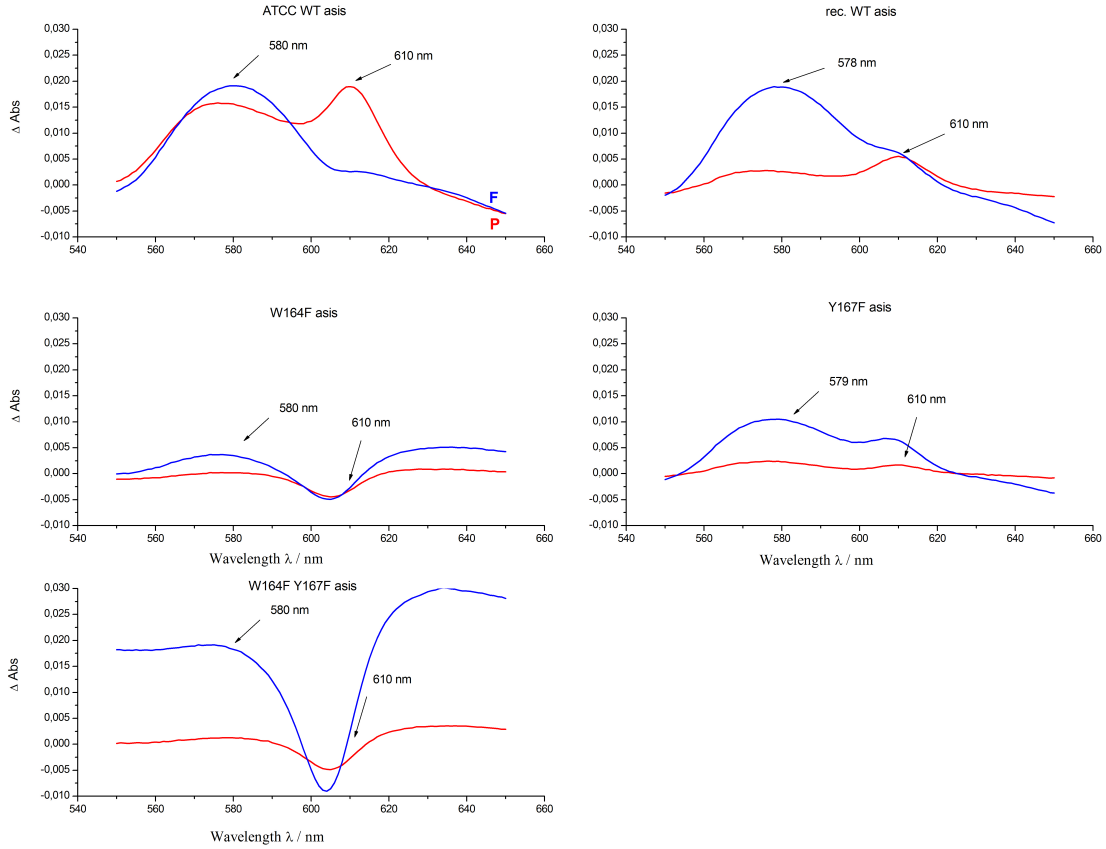

Figure 3.35: Difference absorption spectra of the P (red (P minus O_{asis})) and F (blue (F minus O_{asis})) intermediates of three variants.
The top left shows the ATCC WT C*c*O, top right the rec. WT C*c*O, middle left W164F, middle right Y167F and bottom W164F Y167F.

The variants W164F and W164F Y167F do not show any P-intermediate related signal in the UV/vis-spectra. Contrary to that, the single variant Y167F shows a very small signal at 610 nm, related to the P-intermediate. The F-intermediate related signal at 579 nm is again only present in Y167F at a very low intensity. The variants W164F and W164F Y167F show the previously described negative signal at 605 nm, whereas the signal intensity is increased in the double variant. W164F has a very low intensity signal at 580 nm, which could be due to the formation of the F-intermediate as well as to the overall structure of the difference absorption spectrum.

All six variants were oxidized to repeat the described experiments originating from O_{ox} (see figure 3.36 and 3.37).

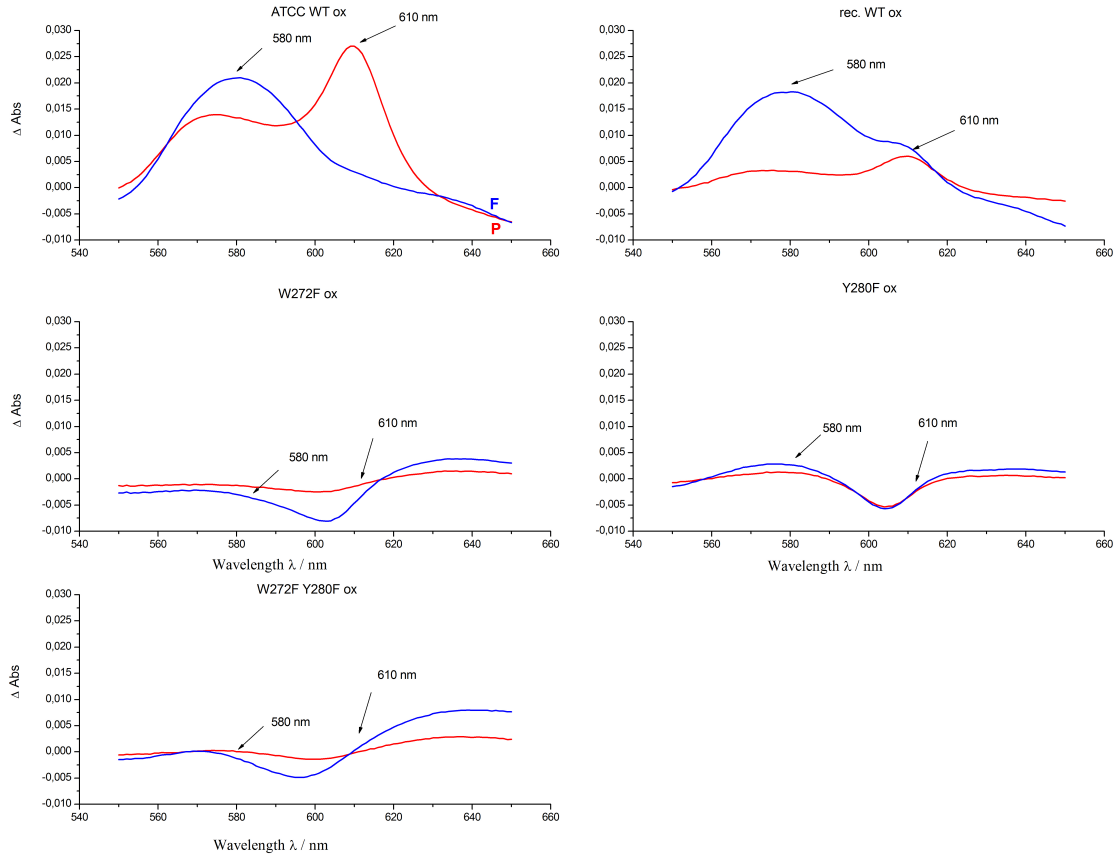

Figure 3.36: Difference absorption spectra of the P (red (P minus O_{ox})) and F (blue (F minus O_{ox})) intermediates originating from O_{ox}.

The alignment of the variants stayed the same as in fig. 3.34. The top left shows the ATCC WT C*c*O, top right the rec. WT C*c*O, middle left W272F, middle right Y280F and bottom W272F Y280F.

Only the Y280F variant showed a difference in the spectrum obtained by using P-intermediate analogous conditions upon oxidation. The intensity of the negative signal decreased by a factor of 2 in comparison to the O_{asis} state. The P-intermediate in variants W272F and W272F Y280F did not change upon oxidation. Contrary to that, the negative signal in the F-intermediates of all three variants decreased significantly. Nevertheless, a signal arising from a true F-intermediate was not visible in variants W272F and W272F Y280F. The variant Y280F showed a slight signal at 580 nm, which could not be clearly assigned to the F-intermediate.

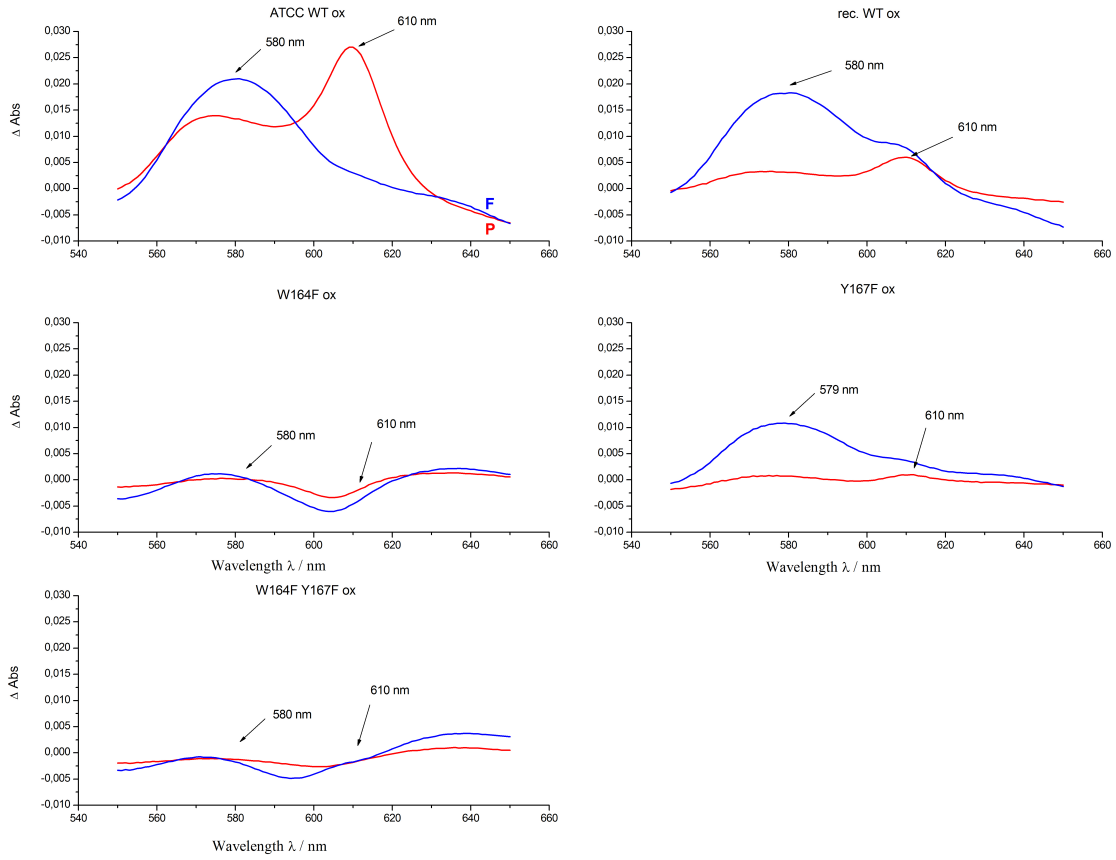

Figure 3.37: Difference absorption spectra originating from O_{ox} showing the P (red (P minus O_{ox})) and F (blue (F minus O_{ox})) intermediates.
The alignment of the variants stayed the same as shown above in fig. 3.35. The top left shows the ATCC WT C*c*O, top right the rec. WT C*c*O, middle left W164F, middle right Y167F and bottom W164F Y167F.

W164F and W164F Y167F show a comparable behavior for the P-intermediate: a decreased intensity of the negative signal at 605 nm and no P-intermediate related

signal present upon oxidation. Y167F shows no change in P-intermediate behavior upon oxidation, exhibiting only a low intensity signal at 610 nm. The F-intermediate of variants W164F and W164F Y167F is characterized by a decrease of the negative signal at 605 nm and a low intensity signal at 580 nm, which is not undoubtedly correlated to the real F-intermediate. The F-intermediate is clearly formed in Y167F as there is a slight increase in intensity of the 579 nm signal, corresponding to the F-intermediate.

The only variant clearly forming the P- and F-intermediate, characterized by their respective difference absorption maxima at 610 nm and 580 nm, is Y167F. All variants, except Y167F, are lacking true P- and F-intermediates. However, due to a lack of structural information of the active center, these intermediates are subsequently named “P-intermediate” and “F-intermediate”.

All variants were also checked for radical formation using EPR-Spectroscopy.

3.2.5. EPR-Spectroscopy of Variants

EPR-spectroscopy was performed in collaboration with the group of F. MacMillan (Henry Wellcome Unit for Biological EPR, University of East Anglia, Norwich, U.K.)

3.2.5.1. Initial EPR-Spectroscopy

The ability of variants to form radicals, such as the 12 G narrow signal, was measured by EPR-spectroscopy. Spectra of all six variants were recorded for the O_{asis} and O_{ox} states. Results were pooled in two groups either containing Cu_B or not. The narrow 12 G signal was analyzed in detail by Q-band EPR-spectroscopy.

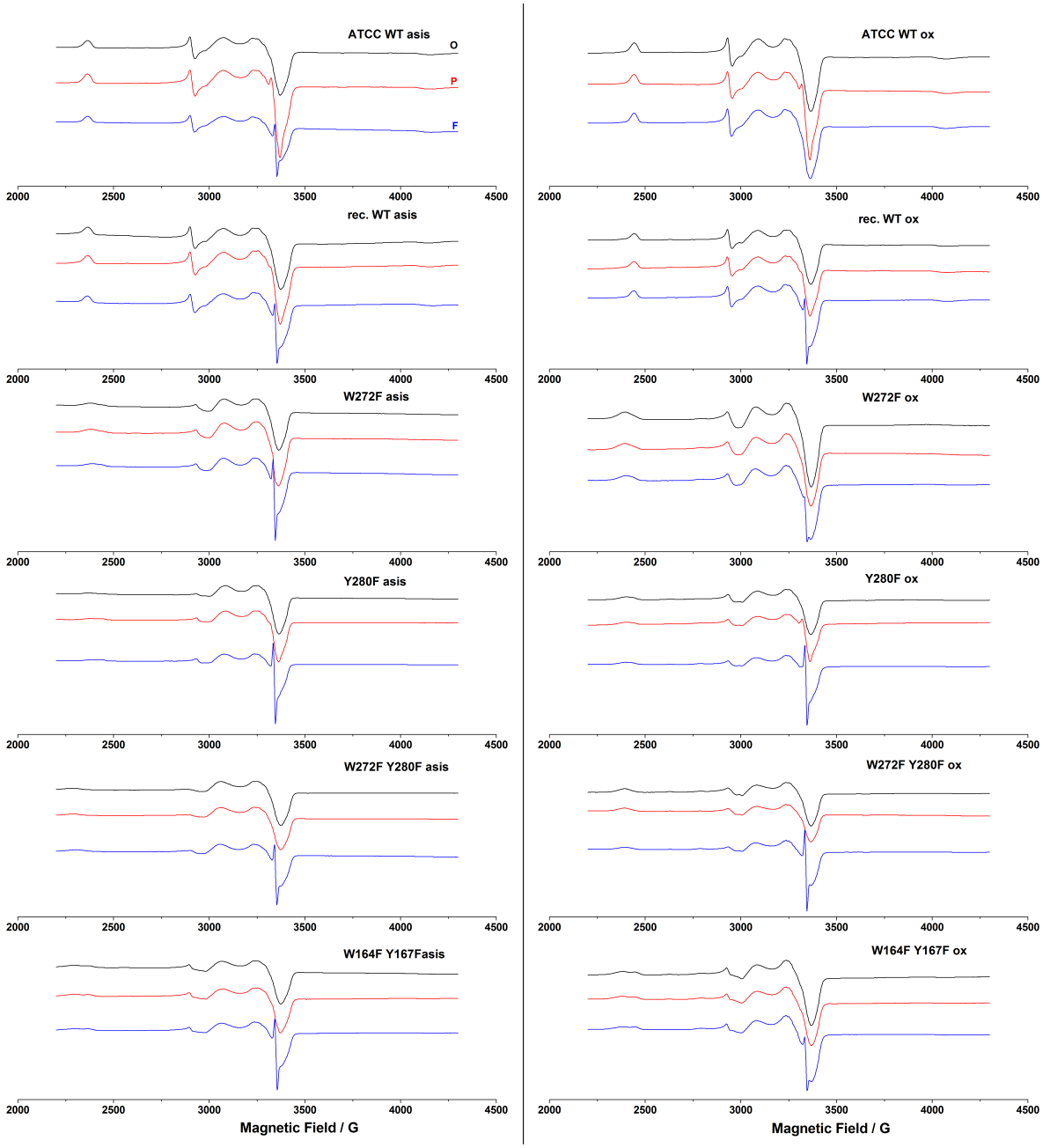

Figure 3.38: Near Scan EPR spectra of the O-intermediate (black), "P-intermediate" (red) and "F-intermediate" (blue) originating from O_{asis} (left) and O_{ox} (right).
The ATCC WT C*c*O is shown on top, followed by the rec. WT C*c*O, W272F, Y280F, W272F Y280F and W164F Y167F. All variants are lacking Cu_B. Spectra are shown in arbitrary units of the first derivative. The parameters used are described in Materials and Methods (Section 2.4.7).

All variants used for the spectra displayed in figure 3.38 are lacking Cu_B. The first striking difference of the WT C*c*O spectra compared to the variant spectra is the loss and/or change of the heme *a* related signal. The part of the heme *a* dependent signal

with a g-value (the g-value is independent of frequency and magnetic field strength and therefore intrinsic to the paramagnetic system) of approximately g~2.858 (2350 G) shifts and/or shows a splitting into two peaks in all variants. The intensity of this signal decreases drastically. The part of the signal with a g-value of approximately g~2.357 (2850 G), near the Cu_A related signal, shows lower signal intensity. The low intensity, negative dip with a g-value of approximately g~1.599 (4200 G) is not present/below the resolution limit in all described variants. The "P-intermediate" spectra of all variants, except Y280F, did not show a visible Y167 radical related signal in the near scan spectra originating from O_{asis}. The radical signal of Y167 increased upon oxidation of Y280F but remained below the resolution limit and was absent in the other variants. All variants showed a very high intensity 12 G signal in the "F-intermediate" spectra originating from O_{asis}. The signal intensity significantly decreased upon oxidation of W272F and W164F Y167F. Y280F did not show a significant change in signal intensity upon oxidation, whereas the signal intensity drastically increased upon oxidation of W272F Y280F. The intensity of the Cu_A related signal with a g-value of approximately g~2.202 (3050 G) increased slightly in all variants upon oxidation, compared to the second positive part of the Cu_A signal with a g-value of approximately g~2.066 (3250 G) The presence of possible radicals was further investigated by reducing the sweep width and modulation amplitude of the magnetic field (see figure 3.39).

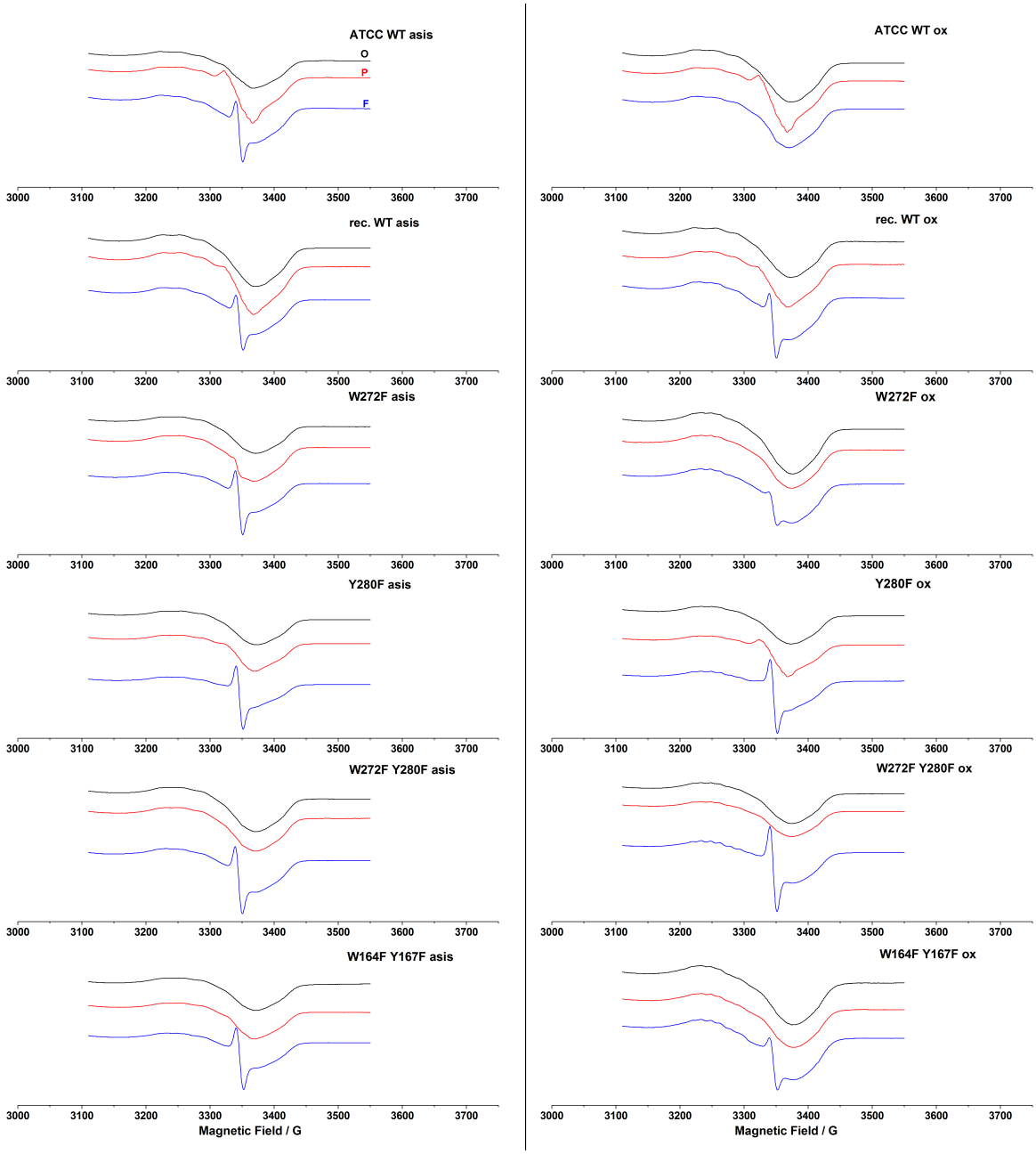

Figure 3.39: EPR low power radical spectra originating from O_{asis} and O_{ox} of the O-intermediate (black), "P-intermediate" (red) and "F-intermediate" (blue).
Arrangement of wild types and variants stayed the same as in figure 3.38. Spectra are shown in arbitrary units of the first derivative. The parameters used are described in Materials and Methods (Section 2.4.7).

The low power radical EPR spectrum shows that the narrow 12 G signal is already present in the "P-intermediate" spectrum of W272F originating from O_{asis} with a very low intensity. There are no new, undescribed features in the spectra.
Additionally to the variants lacking Cu_B, the variants with Cu_B present were analyzed by EPR-spectroscopy.

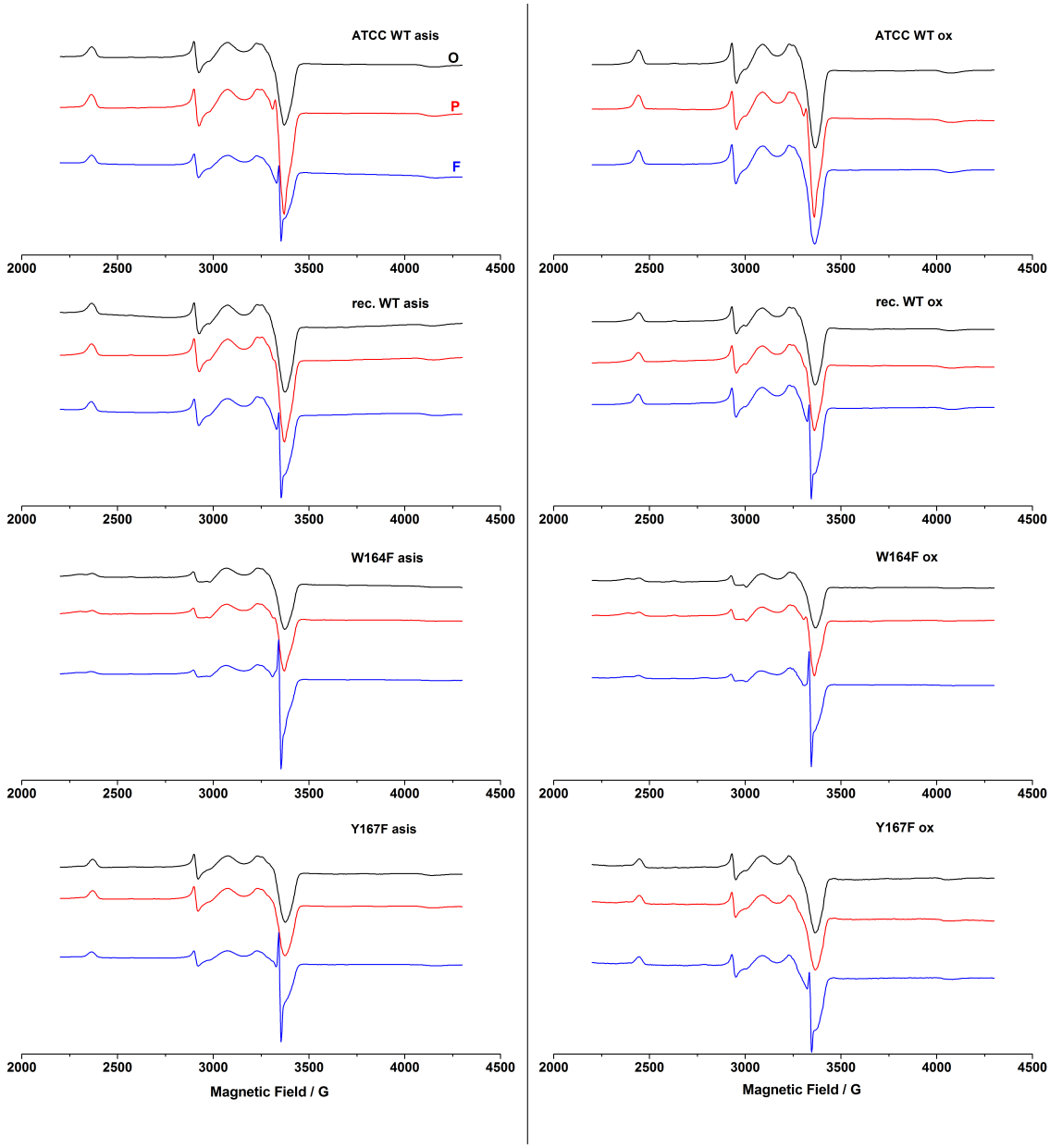

Figure 3.40: Near Scan EPR spectra of the O-intermediate (black), "P-intermediate" (red) and "F-intermediate" (blue) originating from O_{asis} (left) and O_{ox} (right).
The ATCC WT C*c*O is shown at the very top, followed by the rec. WT C*c*O, W164F and Y167F. EPR spectra are shown in arbitrary units of the first derivative. The parameters used are described in Materials and Methods (Section 2.4.7).

The W164F variant showed a splitting of the heme *a* related signal with a g-value of approximately g~2.858 (2350 G), whereas the signal intensity of the heme *a* related signal with a g-value of approximately g~2.357 (2850 G) decreased. The low intensity signal with g-value of approximately g~1.599 (4200 G) is absent. A slight trace of the Y167 radical related signal is visible in the "P-intermediate" spectrum of

W164F originating from O_{asis} and increases upon oxidation. The “F-intermediate” spectrum of W164F shows a significant, narrow 12 G wide signal that does not change significantly upon oxidation. The increase of the Cu_A related signal upon oxidation is also visible in the spectra of W164F.

The variant Y167F has EPR-spectra that are very similar to the rec. WT C*c*O. The only difference is the intensity of the narrow 12 G signal in the F-intermediate, originating from O_{asis}, showing a higher intensity for the Y167F variant. This signal decreases upon oxidation. The sweep width and the modulation amplitude were decreased to analyze the narrow 12 G signal at a better resolution.

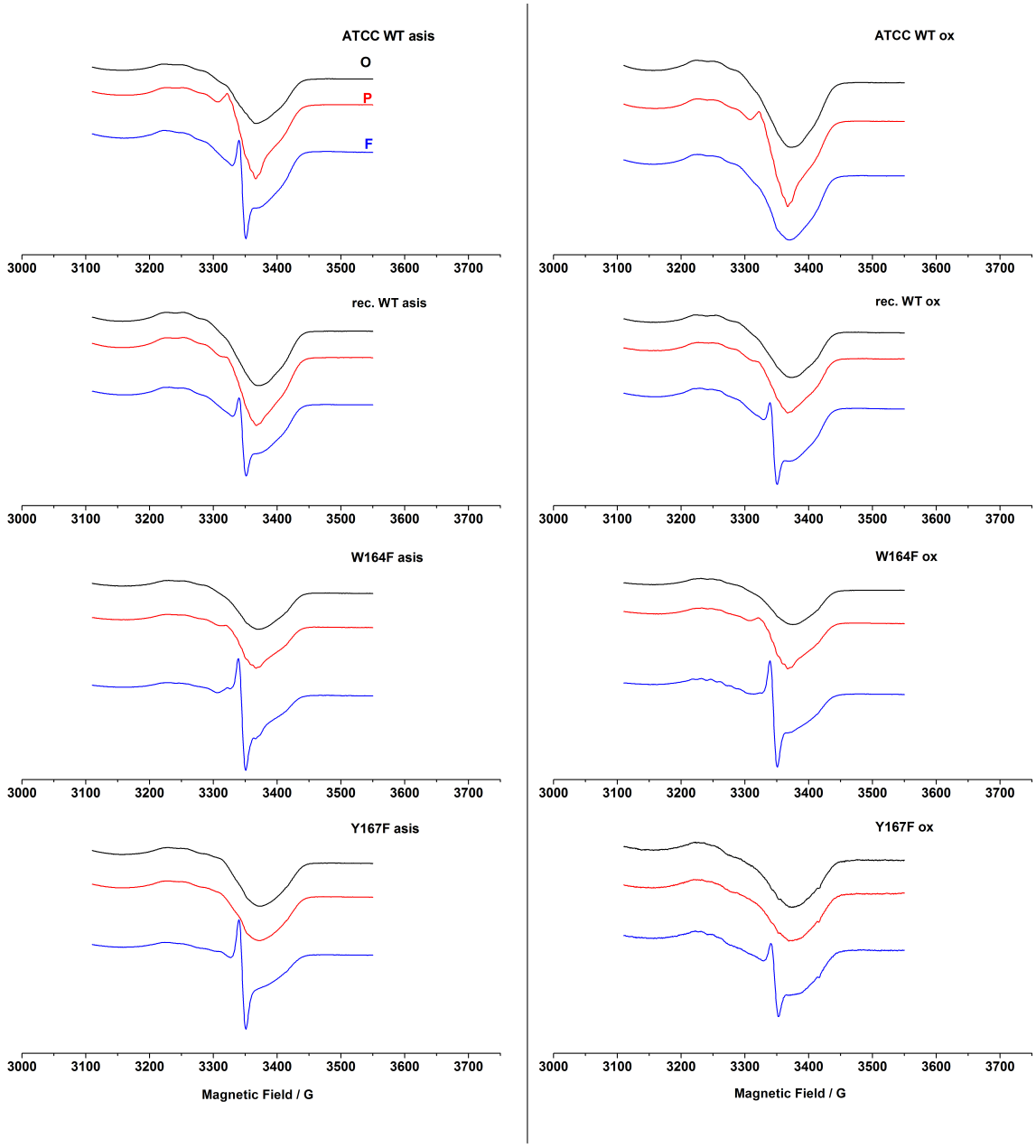

Figure 3.41: EPR low power radical spectra of the O-intermediate (black), "P-intermediate" (red) and "F-intermediate" (blue), originating from O_{asis} (left) and O_{ox} (right).
Arrangement of wild types and variants stayed the same as in fig. 3.40. Spectra are shown in arbitrary units of the first derivative. The parameters used are described in Materials and Methods (Section 2.4.7).

The EPR radical spectra showed the absence of a Y167 radical related signal in the Y167F variant. A low intensity signal related to a Y167 radical is present in the "P-intermediate" spectrum of W164F that slightly increases upon oxidation. Surprisingly, this variant also has the same signal in the "F-intermediate" spectrum originating from O_{asis} but with a very low intensity. Both variants show a high

intensity narrow 12 G signal in the "F-intermediate" spectrum originating from O_{asis} that significantly decreases upon oxidation in Y167F.
Except the very low intensity signal related to the Y167 radical in the "F-intermediate" originating from O_{asis} of W164F no new signals were resolvable.
The change in the heme *a* related signal was investigated further by increasing the sweep width of the magnetic field.

3.2.5.2. Wide Scan of Variants

In order to further investigate the changes in the heme *a* dependent signal, the magnetic field sweep width was increased to observe all metal-cofactor-related features.

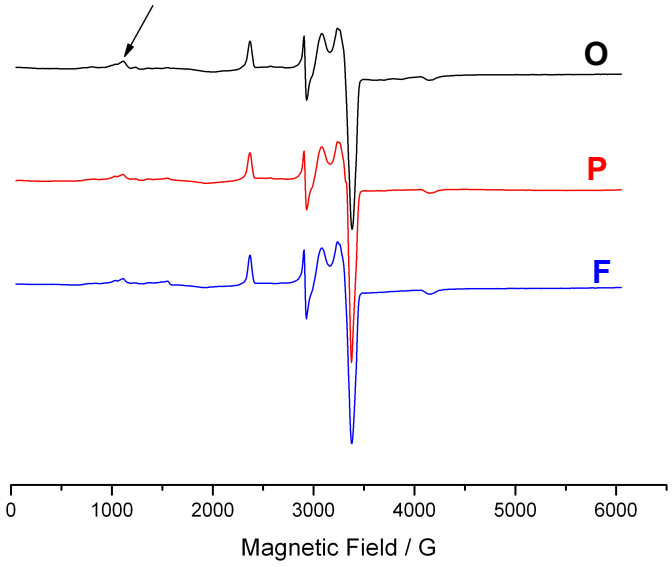

Figure 3.42: Wide scan EPR spectrum of the oxidized ATCC WT C*c*O showing the O-intermediate in black, the P-intermediate in red and the F-intermediate in blue.
The black arrow denotes the high-spin heme related signal. Spectra are shown in arbitrary units of the first derivative. The parameters used are described in Materials and Methods (Section 2.4.7).

The wide scan EPR spectrum of the ATCC WT C*c*O shows a small intensity signal with a g-value of approximately g~6.716 (1000 G), which is related to high-spin heme. All variants were checked for the intensity of this signal (see figure 3.43).

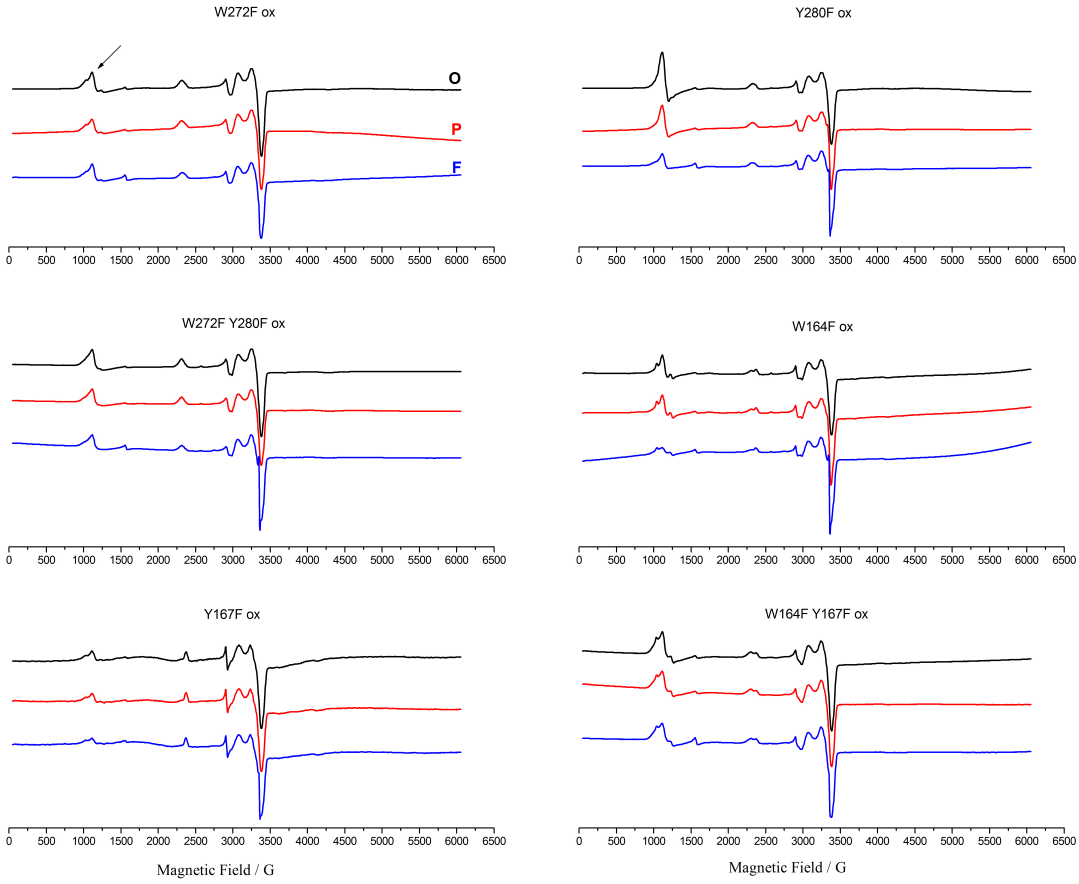

Figure 3.43: Wide scan EPR spectra originating from O_{ox} of variants W272 (top left), Y280F (top right), W272F Y280F (middle left), W164F (middle right), Y167F (bottom left) and W164F Y167F (bottom right).

The O-intermediate is shown in black, the "P-intermediate" in red and the "F-intermediate" in blue. The black arrow in the top left spectrum exemplarily denotes the high-spin heme related signal. Spectra are shown in arbitrary units of the first derivative. The parameters used are described in Materials and Methods (Section 2.4.7).

The high-spin heme related signal (black arrow) has significantly increased in all variants compared to the WT C*c*O. The variants W272F, W272F Y280F, W164F and W164F Y167F show a splitting of the denoted signal in all spectra, displaying a "double peak" compared to the ATCC WT C*c*O. The smallest increase in signal intensity is visible in the Y167F variant. Y280F shows a very intense signal, which changes intensity dependent on different intermediates. All variants show a decrease of intensity for this signal upon entering the "F-intermediate". All variants, except Y167F, show the appearance of another signal with a g-value of

approximately g~4.477 (1500 G) upon forming the "F-intermediate". This new signal is not visible in the ATCC WT C*c*O.
The 12 G radical signal is already apparent in the wide scan of W164F. For the W272F Y280F variant, this signal was further analyzed by Q-band EPR-spectroscopy.

3.2.5.3. Analysis of the narrow 12 G Signal

The previously described narrow 12 G radical signal that appears in the "F-intermediate" was analyzed by Q-band EPR-spectroscopy, with its improved resolution, to find its origin.

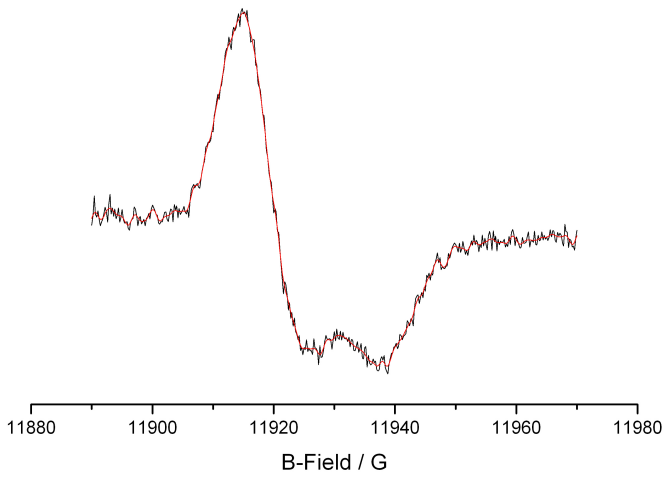

Figure 3.44: Q-band EPR spectrum of variant W272F Y280F originating from O_{ox} showing a close up on the narrow 12 G signal. The parameters used are described in Materials and Methods (Section 2.4.7).

The Q-band EPR-spectrum of variant W272F Y280F was recorded because this variant showed the highest intensity narrow 12 G radical signal originating from O_{ox}. The overall shape and position of the signal is very close to that of a free electron. Nevertheless, it suffers some restrictions in freedom. This signal shows similarities to previously described signals [109; 110] suggesting it being a porphyrin radical.

4. Discussion

This work focuses on the difference between the *Paracoccus denitrificans* aa_3 C*c*O of the naturally occurring ATCC WT strain and the partly plasmid encoded, homologously, recombinantly produced one (rec. WT) of the *Paracoccus denitrificans* deletion strain AO1. Both wild types of C*c*O were expressed in their natural host *Paracoccus denitrificans*. The strain AO1 possesses deletions in *ORF4,* in SU I of the cbb_3 C*c*O and in the two coding genes for SU I of the aa_3 C*c*O in the rec. WT. Therefore, this deletion strain was supplemented with a low copy-number plasmid carrying the expressing gene for SU I of aa_3 C*c*O [42]. This supplemented deletion leaves the aa_3 C*c*O as the only functional C*c*O. No differences were expected for the rec. WT C*c*O and the ATCC WT C*c*O since the amino acid sequence was not changed.
The two wild types were compared using techniques such as UV/vis-spectroscopy, EPR-spectroscopy, calorimetry and amperometric measurements. Moreover, the catalase activity of C*c*O was analyzed in detail to suggest a possible reaction cycle.

4.1. The Catalase Reaction of C*c*O

4.1.1. The ATCC WT C*c*O vs. the Rec. WT C*c*O

Variants of aa_3 C*c*O have previously been used for example to describe the D- and K-pathway present in A-type C*c*Os [42; 111]. These variants of *P. denitrificans* aa_3 C*c*O were constructed by expressing the mutated SU I homologously from a low copy-number plasmid in a deletion strain lacking both coding genes for SU I. This method led to difficulties in comparing the ATCC WT C*c*O with variants constructed in the described way, due to the different genetic situation (see figure 4.1). Therefore, variants were compared to the rec. WT C*c*O, which was constructed similarly to the variants but without introducing mutations.

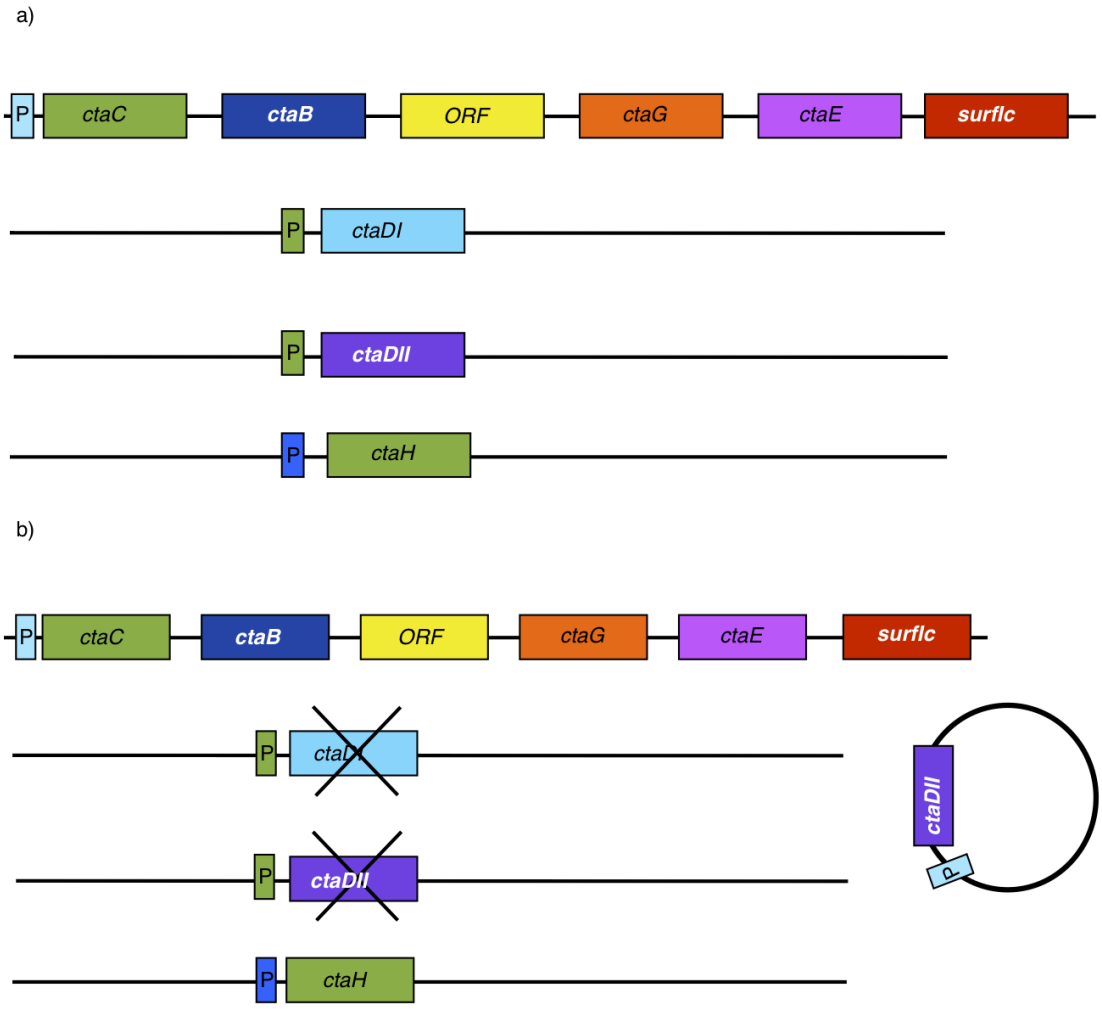

Figure 4.1: Gene arrangement in the ATCC WT C*c*O (a)) and the rec. WT C*c*O (b)).
Promoters are denoted with P. Genes are given in *italics* with their respective gene product in brackets: *ctaC* (SU II), *ctaB* (farnesyltransferase), *ctaG* (chaperone for copper insertion), *ctaE* (SU III), *surf1c* (chaperone for heme insertion), *ctaDI* (SU I, non-expressed), *ctaDII* (SU I, expressed), *ctaH* (SU IV).

4.1.1.1. Basic Structural Components

Prior to working with the rec. WT C*c*O, correct expression of the protein complex was checked, basic properties like oxygen reduction activity and UV/vis-spectra (see figure 4.2) were compared to the ATCC WT C*c*O to investigate if there were any unexpected differences.
UV/vis absorbance spectra did not show significant differences comparing the ATCC WT C*c*O and the rec. WT C*c*O.

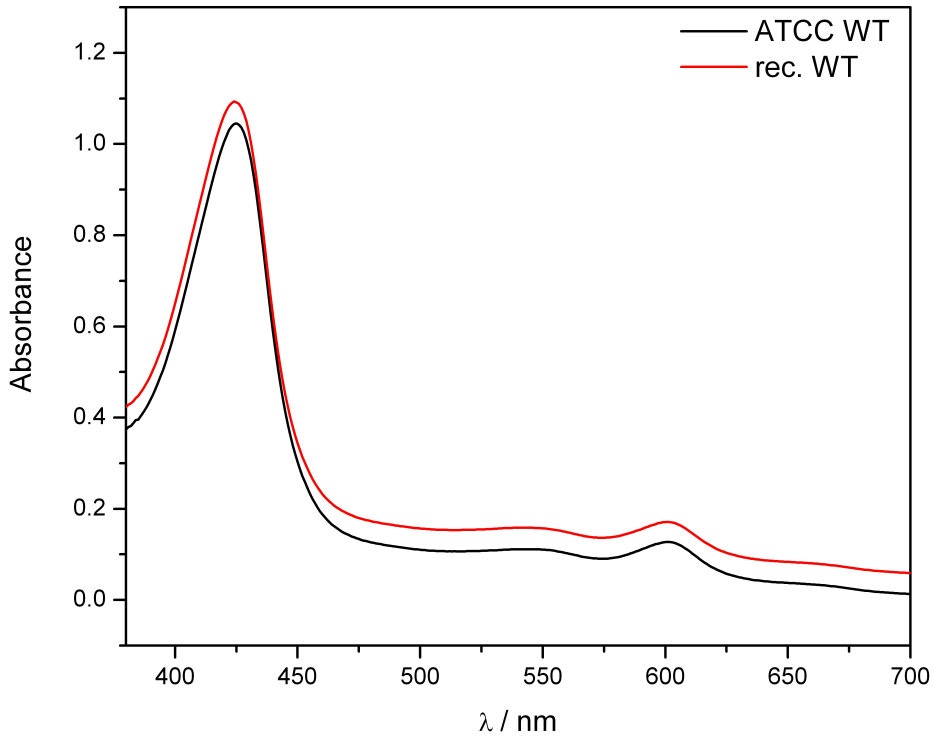

Figure 4.2: UV/vis absorption spectra of the ATCC WT C*c*O (black) and the rec. WT C*c*O (red).
The UV/vis spectra of these two wild types do not show significant differences, apart from a slight broadening of the Soret band of the rec. WT C*c*O.

However, both WT C*c*Os show two different O-states. The difference spectra of O_{asis}-O_{ox} show at least a one elctron reduced intermediate and an F-intermediate present in the O_{asis} state. The O_{asis} state is, therefore, clearly considered as a mixture of different natural intermediates. The intensity of the difference absorbance signals varied with different purifications, clearly pointing out that the amount of natural intermediates is different in every preparation.

SDS PAGE showed all subunits to be present in comparable amounts in both wild type C*c*Os. Metal determination revealed all redox active metal centers to be present and MALDI-MS of extracted heme species showed a single significant signal of 852.2 Da. The aa_3 C*c*O of *Paracoccus denitrificans* contains two heme *a* moieties with a molecular mass of 852.8 Da each [91]. Therefore, the MALDI-MS results show the presence of heme *a* in both, the ATCC and rec. WT C*c*O. The negligible deviation from the calculated mass is within the error range of this method (± 1 Da).

Comparing the catalytic oxygen reductase activity of both wild types, no differences were observed. This is also true for the pH-dependence of the oxygen reductase activity (see Results 3.1).

C*c*O showed only a low activity below pH 6.0. Approximately 100% activity was reached between pH 6.5 and 8.0, whereas the oxygen reductase activity decreased drastically above pH 8.0. The use of different buffer systems with different ionic strengths, showing different buffer capacities, could have led to small differences in the actual pH after addition of all compounds necessary. At pH values below 6.5 and above 8.0 C*c*O looses activity. As cytochrome *c* binding involves protonable residues such as aspartate, histidine and glutamate (see figure 4.3) [18; 112], this is probably due to protonation (below pH 6.5) and deprotonation (above pH 8.0) of amino acids in the binding site of cytochrome *c*. The correct pH range is crucial for binding cytochrome *c*. Another possibility could be the protonation and/or deprotonation of critical residues in the proton pathways.

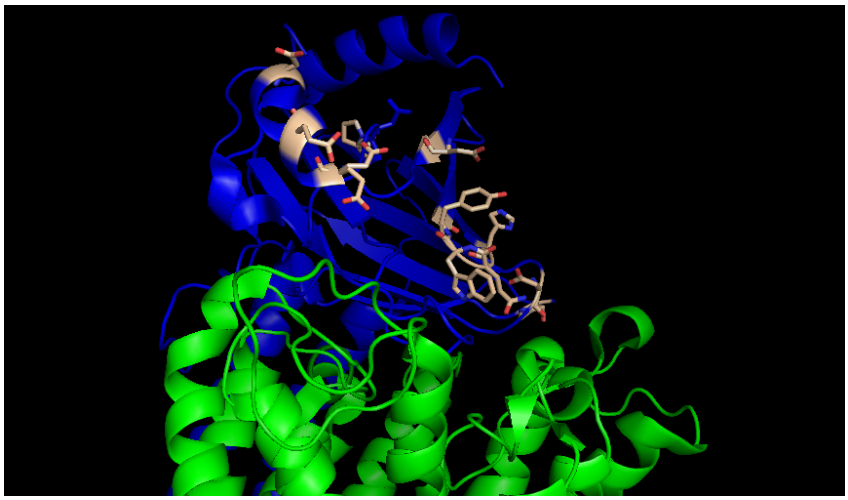

Figure 4.3: Binding site of cytochrome *c*.
Subunit I is shown in green and subunit II in blue. Critical residues for the binding of cytochrome *c* to C*c*O are shown as stick models. These critical residues involve aromatic amino acids as well as charged amino acids. Pdb file used: 3HB3, figure was created using pymol.

Additionally the binding site for cytochrome *c* is located on both SUs I and II. The correct contact between those two subunits might also play a crucial role for enzymatic activity. This contact is at least partly formed by pH-sensitive salt bridges and hydrogen bonds [18; 112; 113]. The correct pH-value is, therefore, crucial for the enzymatic activity in many terms.

Nevertheless, these measurements verified that no differences are present when the ATCC and rec. WT C*c*Os are compared.

4.1.1.2. Differences in Catalase Activity and Artificial Intermediates

After comparing the catalytic activities and basic structural components of the recombinant and native C*c*O, artificial intermediates generated by hydrogen peroxide and the related catalase reaction were compared. The catalase activity showed a saturation-like behavior using high H_2O_2 concentrations (2.4 mM hydrogen peroxide). We, therefore, determined k_{cat} and K_M. However, analysis of the data obtained at high hydrogen peroxide concentrations was not possible due to technical restrictions.

Orii and Okunuki described a catalase activity of C*c*O for the first time in 1963. This activity is discovered when a molar excess of hydrogen peroxide is added to C*c*O. An excess of hydrogen peroxide does not only result in a catalase reaction but also in changes in the UV/vis-spectrum characteristic for the F-intermediate [58; 114].

The catalase activity was investigated for both wild types, measuring k_{cat} and K_M. A 20-fold increase in k_{cat} was observed for the rec. WT C*c*O compared to the ATCC WT C*c*O, showing a first difference between both wild type C*c*Os. The K_M value of this reaction is similar in both wild types. The difference in k_{cat} seems puzzling at first. The catalase activity and the corresponding reaction were further investigated. The UV/vis-spectra of the artificial P- and F-intermediates (see figure 4.4) were also checked. Both intermediates are induced by hydrogen peroxide and might therefore be related to the catalase activity.

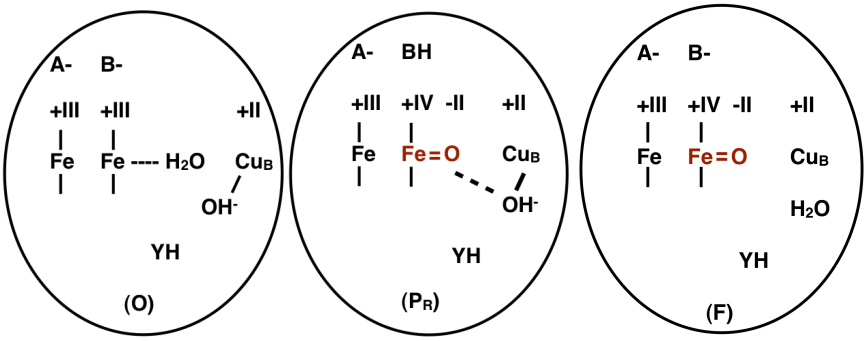

Figure 4.4: Proposed schematic structure of the O (left), P (middle) and F-intermediate (right) of the catalytic cycle of C*c*O [49].
The O-Intermediate shows a water molecule bound at heme a_3, whereas the P- and F-intermediate show an oxoferryl state. The most striking difference between the P- and F-intermediate is the fourth ligand of Cu_B, being an hydroxyl ion in the P-intermediate and water in the F-intermediate.

The UV/vis spectra of the O-intermediates (see figure 4.4) do not show significant differences between the ATCC WT C*c*O and rec. WT C*c*O (see figure 4.2 showing the ATCC WT C*c*O and rec. WT C*c*O in the O_{ox}-state exemplarily). Subsequently, the optical difference spectra of both wild type C*c*Os were compared, showing a slight shift in absorption maximum of the F-intermediate of the rec. WT C*c*O from 580 nm to 578 nm when starting from O_{asis}.
More prominent than the shift of the absorption maximum is the difference in yield of the P-intermediate. The maximum difference absorption of the P-intermediate was reduced by a factor of approximately 4 for the rec. WT C*c*O when starting from O_{asis} and by a factor of approximately 5 upon oxidation prior to measurements (O_{ox}). The yield comparing the P-intermediates originating from O_{asis} and O_{ox} did not change significantly upon oxidation of the rec. WT C*c*O. The O_{asis}-intermediate is thought to be a mixture of different natural intermediates present directly after purification, [115] which is probably one of the reasons for the observed results. Few C*c*O complexes actually possess a true O-intermediate, which leads to a lower yield of the P-intermediate and/or proteins reacting in a different way with H_2O_2 in the ATCC WT C*c*O. The decreased yield of the P-intermediate, and the fact that the intensity of the difference absorption band at 610 nm did not change upon oxidation in the rec. WT C*c*O, are due to the increased catalase reaction degrading the small amount (five molar equivalents) of hydrogen peroxide. The P-intermediate therefore degrades faster in the rec. WT C*c*O than in the ATCC WT C*c*O.

The slow catalase reaction of the ATCC WT C*c*O also explains the shoulder at 580 nm appearing in the ATCC WT C*c*O P-intermediate. This shoulder suggests that the F-intermediate is already partly formed at low hydrogen peroxide concentrations. This shoulder is not present in the rec. WT C*c*O because the excess hydrogen peroxide needed to generate this shoulder is degraded by the fast catalase reaction of the rec. WT C*c*O.

The F-intermediate of the ATCC WT C*c*O did not show differences when starting from O_{asis} and O_{ox}. Contrary to that, the rec. WT C*c*O shows a shift of maximum absorption from 578 nm to 580 nm. The absorption maximum at 578 nm suggest the formation of an F*-related intermediate [82; 106] which shifts to the F-intermediate upon oxidation meaning that the F*-intermediate is not only pH dependent but also oxidation state dependent. Nevertheless, EPR-data shows that the only radical signal present in the F-intermediate EPR-spectra is the narrow 12 G radical signal and not the Y167 radical as postulated for the F*-intermediate. The rec. WT C*c*O shows a shoulder at approximately 610 nm appearing in both spectra of the F-intermediates, suggesting the rapid degradation of hydrogen peroxide and, therefore, the beginning transition to the P-intermediate. Formation of the F*-intermediate only occurs at pHs below 8, as is the case in this work, as a small amount of protein forms the F*-intermediate [72; 106].

The UV/vis-spectroscopy data strengthen the amperometric data showing a drastically increased catalase activity of the rec. WT C*c*O compared to the ATCC WT C*c*O, implied by the low yield of the P-intermediate. The hydrogen peroxide dependent artificial intermediates of the rec. WT C*c*O show significant differences to the ATCC WT C*c*O intermediates, as there is increased catalase activity in the rec. WT C*c*O. The catalase activity of C*c*O was, therefore, investigated further.

4.2. The Catalase Reaction Mechanism of aa_3 Cytochrome *c* Oxidase

The catalase reaction of C*c*O was discovered by Orii and Okunuki in 1963 for the beef heart C*c*O and further investigated by Konstantinov and co-workers, suggesting a first reaction mechanism. The catalase reaction was monitored between 100 and 1200 molar equivalents of hydrogen peroxide in this work. Konstantinov previously reported that a biphasic behavior is observable for the

catalase reaction of beef heart C*c*O. The reported k_{cat} and K_M values are nevertheless correct for the described concentration range. The mechanism reported by Konstantinov involves the formation and degradation of superoxide [58; 60-62; 101-103; 116; 117].

4.2.1. Intermediate Steps of the Reaction Cycle

The chemical superoxide source (SOTS-1) was used to test whether C*c*O is able to act as a superoxide dismutase [104]. Using superoxide, oxygen production was only present in a short period of time. Nevertheless, a small amount of oxygen was measured but this was by a factor of 1000 lower than the amount of SOTS-1 used. The influence of superoxide could, therefore, not be ruled out completely yet the amount of oxygen produced was only measurable using very high concentrations of SOTS-1. ROS, including superoxide, are known to denature proteins [66]. Since C*c*O is not a Superoxide-Dismutase, it is very likely that the use of superoxide denatures C*c*O. Therefore, bound oxygen could be released and be the source of the low, positive signal. Anyhow, the concentration of oxygen produced is three orders of magnitude lower than expected for the complete turnover of SOTS-1. Therefore, the influence of superoxide on the catalase activity was considered to be negligible. Additionally, we were not able to reproduce the results presented in [60] and therefore rule the influence of superoxide out.

One could argue that the catalase activity of C*c*O, and therefore the oxygen production and the observed structural and spectroscopic changes, is the result of partly denatured enzyme due to freeze-thaw cycles and storing the enzyme. Partly denaturing the enzyme might result in a decomposition of hydrogen peroxide at the heme moiety showing a Fenton-like reaction [118]. Therefore, the catalase and oxidase activities of the rec. WT C*c*O were tested directly after purification without storing the enzyme and without freezing the enzyme. The results were compared to the activities after five days of storage at -80°C and one freeze-thaw cycle.

Storing the enzyme for five days with one freeze-thaw cycle resulted in a decrease in oxygen reductase and catalase activity of 20% suggesting some denaturation of the enzyme by freezing and thawing. Contrary to the point that the catalase activity might result from denatured enzyme, this denaturation did not lead to an increase

in catalase activity. Additional to the measurements directly after purification, the catalase activity of the rec. WT C*c*O was tested after incubation at different temperatures and it already showed a decrease in catalase activity at incubation times of 10 minutes at 40°C. Incubation at 50°C (and higher) led to a complete loss of catalase activity. This shows that the observed catalase activity is clearly protein dependent and not due to free divalent ions. The catalase activity of C*c*O is considered to be a true catalase activity and not a "pseudocatalase" activity because experiments shown in [60] were not reproducible in our case. Superoxide as product of the described reaction of C*c*O and a "pseudocatalase" activity was therefore ruled out.

The influence of different inhibitors on the catalase activity was also analyzed. The almost complete inhibitory effect of cyanide and azide points out that a heme moiety is the active site of the catalase reaction in C*c*O since these two inhibitors are known to bind to heme moieties. Thus the active site was already narrowed down to two different reaction sites, heme *a* and heme a_3.

Von der Hocht *et al.* already described the influence of ammonia on the catalase and CcO reaction in 2011, suggesting the binding of ammonia to Cu_B at high pH [97]. Ammonia at pH 6 did not influence the catalase reaction at all but raising the pH to 9 resulted in a strong activating effect, raising the catalase activity more than two-fold. This again supports the proposal by von der Hocht *et al.* that ammonia binds to Cu_B at high pH. A second reason for the increase in catalase activity caused by ammonia would be a complexing/polarization or at least an interaction of ammonia with hydrogen peroxide increasing the catalase activity, reducing the pH results in the protonation of ammonia. The ammonium ion formed does not bind to Cu_B and, therefore, no longer influences the catalase activity. The binding of ammonia to Cu_B probably changes the distance of the copper atom to the heme moiety and decreases the interaction of Cu_B and heme a_3 because otherwise it would be very difficult to fit a hydrogen peroxide molecule and an ammonium molecule in the active center, due to sterical reasons. The decreased interaction may lead to a more freely accessible and flexible heme a_3, which in turn increases the probability of the catalase reaction and, therefore, also the speed and amount of oxygen production. Orii and Okunuki showed previously in 1963 that hydrazine increases the catalase activity [58].

The last inhibitor used was carbon monoxide showing absolutely no effect. Since carbon monoxide binds to reduced heme moieties only, the presence of a reduced heme (an Fe^{2+}-atom in heme a_3) was ruled out [119]. The experiments containing carbon monoxide were performed in the dark to avoid flash photolysis of the CO.
Measurements using inhibitors therefore yielded the conclusion that a reduced heme a_3 is not present in the catalase reaction cycle of C*c*O and that heme a_3 is the active site of the catalase activity while Cu_B is dispensable for the catalase reaction of C*c*O. Complexing Cu_B even resulted in an increased catalase activity. SOTS-1 was used as a superoxide source showing that very little oxygen is produced during the reaction of superoxide with C*c*O. The origin of this oxygen could not be clearly shown. Nevertheless, these experiments showed that superoxide is neither an educt nor an intermediate of the catalase reaction of *P. denitrificans* aa_3 C*c*O.
One intermediate of the catalase reaction is the F-intermediate. The catalase activity of the P-intermediate, which is present at low hydrogen peroxide concentrations, was tested as well. Measurements at pH 9 showed a slight increase in oxygen production increasing the hydrogen peroxide concentration from 1:1 to 1:5 and 1:10 (molar ratios). Data obtained at pH 6 and pH 7 show no gradual increase but a jump to a comparable oxygen production at a 1:10 ratio. At pH 6 and 7 the P-intermediate gradually changes to the F*-intermediate because of the pH-value. Speculating about the F*-intermediate being protonated at crucial residues such as H325 or H326 and, therefore, presumably inhibiting either educt or product accessibility [120].
Despite the measurable oxygen production, data obtained during the determination of k_{cat} in some cases showed, even at a 1:100 ratio of C*c*O to hydrogen peroxide, a sigmoidal curve. This suggests that some kind of activation is necessary to achieve full catalase activity. Because of that, the P-intermediate is not included in the catalase reaction mechanism of C*c*O. So far, the reaction cycle only includes the O-intermediate and F-intermediate independent of the Cu_B-ligand as well as some unknown state with low catalase activity that needs to be activated. An activating process that changes the copper ligand and therefore expands the free space near the active center could be feasible.

4.2.2. Variants of H276

Cu_B was shown to be of low importance for the catalase activity of C*c*O, therefore, mutations on one of the copper complexing histidines were introduced to remove Cu_B. Cu_B was removed by replacing the copper complexing H276 (see figure 4.5) with either an acidic charged amino acid residue, such as aspartate or glutamate, or a basic charged amino acid residue, such as lysine or arginine.

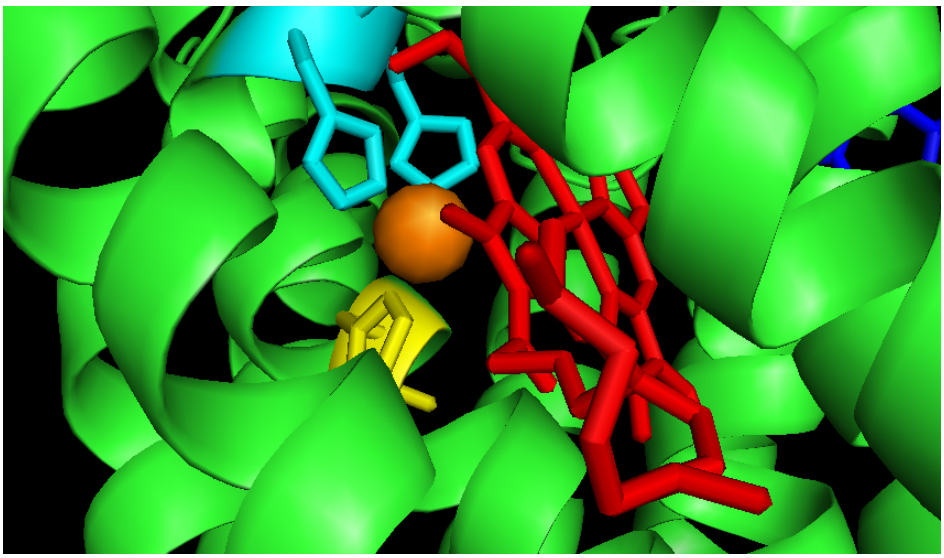

Figure 4.5: The active center of the aa_3 C*c*O of *P. denitrificans.*
Heme a_3 is shown in red, Cu_B in orange with its complexing histidines H325 and H326 in cyan and H276 in yellow. Pdb file 3HB3 was used to prepare this figure with the pymol software.

Acidic amino acid residues were introduced to potentially reverse the electrostatic properties of the active center completely, whereas basic amino acid residues were introduced to potentially maintain the electrostatic properties after losing Cu_B. Metal determination verified the absence of one copper atom per C*c*O molecule for all four mutations (H276D/E/K/R). Since Cu_A is a binuclear center and mutations were introduced in one of the Cu_B complexing histidines, the missing copper atom is most likely Cu_B. In addition, the EPR-spectra also show that Cu_A is still present since the Cu_A signal is still present and a high-spin heme signal appears, which is consistent with the loss of Cu_B. Activity measurements showed approximately 10% activity for the acidic variants and 2% for the basic variants. H276K and H276R were therefore considered as inactive. Exchanging a positive charge (Cu_B) for a

negative charge (D or E) probably results in a change in the heme a_3 position relatively to the former Cu_B position. This might also result in an impaired amino acid surrounding of heme *a*. The acidic variants showed a very low oxygen reductase activity. Considering that horse heart cytochrome *c* exhibits very low oxygen consumption activity itself, it is feasible that the acidic variants show a similar activity at heme a_3 because a real oxygen reductase activity is not expected with potentially altered distances in the active center. The remaining 10% oxygen reductase activity in variants H276K/R may be considered to be an unspecific, not oxidoreductase correlated oxygen-consuming activity at heme a_3 similar to the activity observed at cytochrome *c*. The mutation of H276 to aspartate or glutamate may be considered to be a very drastic change in the electrostatic properties around the active center. The same is true for the mutation of H276 to lysine or arginine, but the acidic variations seem to have an even greater impact. Therefore, a change in the overall fold, especially of SU I, cannot be ruled out. It was shown previously, that mutation of one amino acid is sufficient to change specific enzyme activity and structure drastically or even lead to cell death [121; 122].

Analyzing the catalase activity of these variants, a rise, or at least no change in catalase activity (k_{cat}) compared to the rec. WT C*c*O was expected but surprisingly not observed. Moreover, a 40% and 60% reduction of k_{cat} was observed with the lysine and arginine variants, respectively. Additionally, a correlation with K_M was observed, showing an increase in K_M with a decrease in k_{cat}, when comparing the lysine and arginine variants. Additional amino groups probably result in a stronger coordination of either water molecules or hydrogen peroxide molecules and, therefore, decelerate the reaction by arresting either the product or the educt. In heme dependent catalases, a histidine residue complexes hydrogen peroxide [53]. Complexing H_2O_2 by amino groups therefore seems feasible. The more intense decrease in k_{cat} by the arginine variant might, therefore, be due to the higher number of amino-groups and to sterical hindrance because of the bulkier side chain. The Cu_B complexing amino acid H276 was also replaced by aspartate and glutamate. The decrease in k_{cat} compared to the rec. WT C*c*O was even higher than it was after introducing basic residues. A decrease of 70% and 60% was measured for the aspartate and the glutamate variants respectively. The K_M value increased compared to the ATCC WT C*c*O in the same way as it did in the basic variants. This

effect was less pronounced with higher k_{cat} values. The decrease in k_{cat}, compared to the rec. WT C*c*O, was probably due to the reduction of space beause of electrostatic interactions between heme a_3 and the additional acidic amino acid residue. Increasing the length of the amino acid side chain resulted in an increase of k_{cat}. The longer glutamate side chain probably decreases the mobility of heme a_3 compared to the aspartate residue.

Acidic substitutions result in a more effective reduction of k_{cat} compared to basic amino acid residues. The reason for this might be the electrostatic attraction between an acidic side chain and heme a_3. The decrease in k_{cat} of the basic amino acid residues may be due to additional amino groups and a tighter coordination of educt and/or products. Additionally, these variants confirmed that Cu_B is not of any importance for the catalase reactivity of C*c*O because all variants showed considerable catalase activity. Therefore, the Cu_B ligands are negligible as well. A complete destruction of the active centers structure due to of the described mutations could be ruled out as the UV/vis-spectra at least showed the presence of the heme *a* moieties in the protein. A change of the water molecule-network due to mutations cannot be excluded as the reason for the observed differences.

4.2.3. Variants in Aromatic Amino Acids

Another two sets of variants carrying mutations in aromatic amino acids near the active center were constructed. The first main set consisted of variants W164F, Y167F and W164F Y167F, whereas the second set consisted of W272F, Y280F and W272F Y280F.

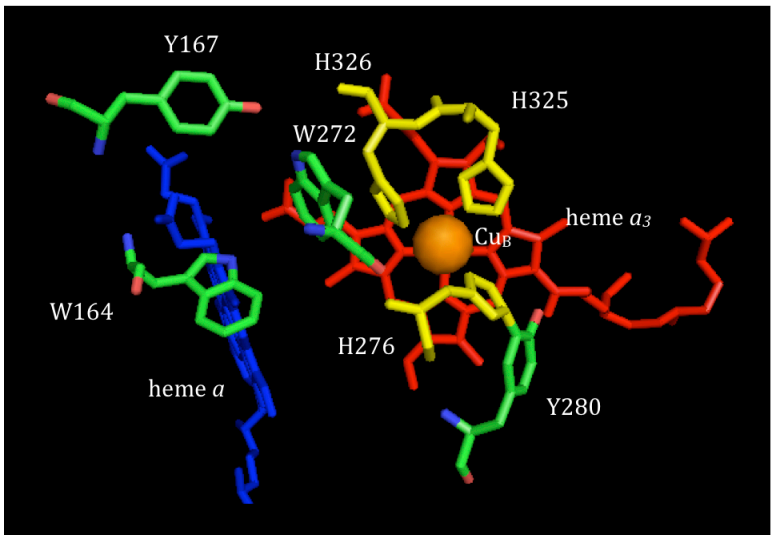

Figure 4.6: Aromatic amino acids, near the active center, that were changed via mutagenesis (green). The Cu_B (orange) complexing histidines are shown in yellow, heme *a* in blue and heme a_3 in red. The picture was prepared with pymol and pdb file 3HB3.

4.2.3.1. First Characterization of Aromatic Variants

Determination of metal content showed two iron ions present in all variants but the loss of one copper ion in variants W164F Y167F, W272F, Y280F and W272F Y280F. Since Cu_A is a binuclear center in SU II and mutations were introduced near the binuclear center in SU I, the missing copper atom is most likely Cu_B. Oxygen reductase activity was in accordance with metal content determination and showed the loss of oxygen reductase activity for all variants lacking Cu_B. The variant W164F showed approximately 10% oxygen reductase activity, which is in accordance with the literature [123]. W164 exhibits two hydrogen bonds; the first one between the backbone amide bond and a heme *a* propionate and the second one between the tryptophan nitrogen and a heme a_3 propionate [18]. Introducing the mutation W164F would result in the loss of the hydrogen bond connecting W164 and heme a_3. Nevertheless, in the unlikely event that the mutation led to a structural change, moving the backbone of W164 to a position preventing the formation of both hydrogen bonds cannot be ruled out. The loss of the hydrogen bond connecting W164 and heme a_3 might be the reason for the decrease in oxygen reductase activity. In 2009, Richter and Ludwig speculated that the radical signal at Y167 is an energetic dead end, suggesting several other amino acids forming radicals and therefore taking part in the C*c*O reaction cycle, such as W164 [38]. Changing this

amino acid to phenylalanine would render the radical formation on W164 impossible. However, this amino acid seems to be of importance for the natural reaction cycle.

Y167F shows an oxygen reductase activity of approximately 80% reaching nearly wild type activity, which is also in accordance with the literature [38]. EPR data show no Y167 radical related signal. Only a slight decrease in oxygen reductase activity leads to the assumption that the radical present in the wild type protein is of no significance for the oxygen reductase activity. The 20% of missing oxygen reductase activity might be caused by minor structural changes, leading to a small decrease in oxygen reductase activity. The crystal structure of this variant shows two prominent conformations for the mutated residue F167 (J. Koepke *et al.* unpublished results). This might lead to changes in accessibility of the active center resulting in the observed decrease of oxygen reductase activity.

4.2.3.2. Catalase Reaction Dependent Kinetics of the Variants

Comparing the k_{cat} and K_M values of all variants, W164F exhibits a k_{cat} similar to the rec. WT C*c*O but with an increased K_M. W164 forms hydrogen bonds to both heme moieties, as described. Mutating W164 to phenylalanine leads to the loss of the hydrogen bond to the heme a_3 propionate. This change could free additional product or educt complexing residues, as well as interfering with the educt uptake and/or product release, increasing the K_M. The K_M values of all other variants did not change significantly.

The decrease in k_{cat} of Y167F and W272F is very similar. Y167 and W272 are connected via a hydrogen bond. The drastic decrease of k_{cat} by 60-70% leads to the speculation that the hydrogen bond of those two amino acids is of particular importance for either the polarization/stretching of the peroxide bond or the positioning of educts and products. An alternative explanation for the similar decrease in k_{cat} could be that the position of the amino acids is important to form a short lived radical, important for the catalase reaction, which eventually relaxes on the porphyrin moiety yielding the described narrow 12 G radical signal. This suggestion is supported by the MYW motive, crucial for peroxidases near the active center [124]. This motive is not present near the described amino acids of the aa_3

C*c*O of *P. denitrificans*. Some peroxidases show an amino acid radical probably originating at that motive, which relaxes on the porphyrin moiety. A similar signal was already assigned to a porphyrin radical in bovine C*c*O [109; 110] and also looks very similar to the narrow 12 G radical signal.

Y280 is covalently linked to the copper complexing H276 [18; 24]. Mutating Y280 to phenylalanine leads to the loss of this cross-link. Therefore, H276 gains flexibility. This is probably the reason for the loss of Cu_B and for the decrease of k_{cat}. The more flexible H276 and the other two copper complexing histidines H325 and H326 are, the higher the probability for complexing water or hydrogen peroxide as these are the amino acids also known to complex the aforementioned in catalases.

The double variants show a combination of properties of the single variants supporting the assumptions made previously.

Summarizing, the loss of the hydrogen bond between heme a_3 and W164 may lead to an increase of K_M due to increased binding or accessibility of the active center for educts and/or products. The hydrogen bond between Y167 and W272 is important for either the polarization/stretching of the peroxide bond or the positioning of products and educts. Another possibility could be the formation of a very short-lived radical intermediate on either of those two amino acids, which relaxes on the heme moiety, giving rise to the narrow 12 G radical signal in EPR spectra. Altering the optimal conformation of these amino acids by destroying the hydrogen bond results in a slower relaxation and a decrease in k_{cat}. The expected EPR signal is probably magnetically coupled to the heme a_3 of the active center in the absence of Cu_B and therefore EPR silent. Additionally, the loss of the crosslink between Y280 and H276 leads to an increased flexibility of H276, H325 and H326 and, therefore, to an increased binding of water or hydrogen peroxide decreasing the k_{cat}.

4.2.3.3. EPR-Spectroscopy of Aromatic Variants

One feature shared by all variants is the appearance of an intense high-spin heme axial signal at a g-value of approximately g~6.106 (1100 G). This signal is also present in very low amounts in the ATCC WT C*c*O pointing to a small amount of protein featuring an uncoupled active center. The active center is usually magnetically coupled and therefore EPR silent [98]. This coupling is not present if

Cu_B is missing and, therefore, an additional high-spin heme signal, resulting from heme a_3, is visible. The appearance of this high-spin heme signal in variants where Cu_B is present, indicates that the magnetic coupling of the active centers is not solely dependent on the porphyrin rings and metal ions. In fact, it also involves the surrounding amino acids and the correct positioning of these amino acids. Since these surrounding amino acids are mutated in the described variants, an appearance of the high-spin heme signal seems feasible. The intensity of the signal is different in all variants but present independently of the oxidation state of the originating intermediate. This signal decreases in all variants under conditions inducing the F-intermediate in the WT C*c*O ("F-intermediate" or "F-state"), with Y280F showing the most intense decrease in signal intensity upon entering the "F-intermediate". Additionally to that, every variant shows another signal appearing or growing in intensity at g~4.477 (1500 G) upon entering the "F-state". Small amounts of this signal are also present in the F-intermediate of the ATCC WT C*c*O. The additional signal at g~4.477 (1500 G) is only present in minor amounts in the ATCC WT C*c*O but this signal is also present in the O-intermediate ruling out a dependency on hydrogen peroxide. The ATCC WT C*c*O only shows the presence of this signal in small amounts suggesting that this signal is somehow related to the normally EPR silent active center. A small amount of "not completely intact" C*c*O without the magnetic coupling of the active center would lead a minor amount of the described signal.

The decrease of the intense axial signal at g~6.106 (1100 G) upon entering the "F-intermediate" suggests a change in heme a_3. One possible reason could be, that the distance between heme a_3 and Cu_B increases upon entering the "F-intermediate". In a minor population of C*c*O, this could lead to a "recoupling" of the active center, decreasing a possible signal arising from heme a_3. Differences in signal appearance suggest two different populations of heme a_3 for the variants showing the described signal at g~ 6.106 (1100 G) with a shoulder. These two populations differ most likely in the ligation and/or orientation of heme a_3. The fact that this signal does not completely disappear is probably due to a small amount of damaged protein. A change of shape and intensity of the heme *a* rhombic EPR signal at g~2.686 and 2.316 as well as the loss of signal at g~1.562 are probably related to changes in the amino acids surrounding of heme a_3 effecting heme *a*.

All variants, except Y167F, showed the same changes in the shape of the Cu_A signal at g~2.239 upon oxidation. Additionally, the fine structure changes slightly upon entering the "F-intermediate". These data suggest minor changes in SU II harboring Cu_A, validating the theory that one mutation is capable of changing the overall structure of the protein, as discussed above. However, if any Cu_B is present and uncoupled, it might have an influence on the EPR spectra as well. The Y167 radical related signal is present in the "P-intermediate" of all variants except Y167F and W164F Y167F. The intensity increases upon oxidation in variants W164F and Y280F, but decreases in W272F and W272F Y280F. As these variants showed not more than 10% oxygen reductase activity, the Y167 radical related signal was considered negligible for the oxygen reductase activity but is further discussed in 4.4.

The narrow 12 G signal is present in the "F-intermediates" of all variants in comparable amounts originating from O_{asis} and decreases or increases upon oxidation. Nevertheless, signal intensity originating from O_{ox} clearly correlates with the k_{cat} of the catalase reaction. Only the O_{ox} state was considered here since the O_{asis} state is a mixture of different natural intermediates and, therefore, yields different intermediates of the catalase reaction cycle upon reaction with hydrogen peroxide and flash freezing.

The only variant showing the narrow 12 G radical signal at conditions inducing the P-intermediate in the WT is W272F originating from $O_{ox.}$ This observation suggests that W272F enters the "active" state described in connection to the catalase activity of the "P-intermediate" in 4.2.1, earlier than the other variants. The narrow 12 G radical signal could be assigned to a porphyrin radical, similar to the bovine C*c*O [109; 110]. Contrary to these findings, Yu *et al.* postulated recently that the narrow 12 G radical signal is related to a radical on the Y280 equivalent in *Paracoccus denitrificans* C*c*O [125]. This postulate is not in agreement with the fact that the variant Y280F shows the narrow 12 G radcial signal as well. The narrow 12 G radical signal is plausibly assigned to a porphyrin radical. Signal intensity of the narrow 12 G signal is correlated to k_{cat} of the catalase reaction.

4.2.3.4. UV/vis-Spectroscopy of Variants

Analyzing the UV/vis-spectra of the variants W272F, Y280F and W272F Y280F did not show any signals related to P- and F-intermediates originating from O_{asis}. However, the conditions inducing a P- or F-intermediate in the WT were termed "P-" or "F-intermediate" to clarify i.e. the amount of hydrogen peroxide used when discussing conditions leading to specific signals. The variants W272F and W272F Y280 only showed minor changes with five molar equivalents of hydrogen peroxide. The only signal present is a negative difference absorption signal at 605 nm varying in signal intensity. The signal in the presence of five molar equivalents of hydrogen peroxide does not change upon oxidation. The "F-intermediate" shows a similar negative signal, which, in contrast, decreases strongly in intensity upon oxidation. A slight blue-shifted signal near 575 nm, probably related to the "F-intermediate", appears in variants Y280F and W272F Y280F. This finding supports the theory that the UV/vis spectra of these artificial intermediates are not related to the catalase activity of C*c*O since all described variants show considerable catalase activity. Variants W164F, Y167F and W164F Y167F showed a slightly different behavior compared to the other three variants. W164F shows only a very low intensity negative signal originating from O_{asis}, which decreases upon oxidation but a very low intensity signal related to the F-intermediate is visible at 580 nm, which increases upon previous oxidation of the protein. Since W164F shows 10% oxygen reductase activity, the formation of a very small amount of F-intermediate is feasible. Y167F is showing 80% oxygen reductase activity and, therefore, shows the signals corresponding to the P- and F-intermediates but with a very low intensity. The F-intermediate has a signal with a shoulder at 610 nm, which decreases upon oxidation. The intermediate-related signals increase upon oxidation. W164F Y167F shows a strong intensity negative signal at 605 nm in the "F-intermediate", which drastically decreases upon oxidation. An F-intermediate related signal appears with very low intensity. Since all variants, except Y167F, are partly reduced after purification and the use of hydrogen peroxide acts as an oxidizing agent, the 605 nm negative signal is probably an artifact of the variant being oxidized by hydrogen peroxide in the "F-intermediate". This explains the drastic decrease of the negative signal upon oxidation. Nevertheless, the only variants showing significant signs of a

true F-intermediate are the variants that show at least 10% oxygen reductase activity. It is, therefore, postulated that the difference absorption spectra of the variants are not related to the catalase activity of C*c*O but to the oxygen reductase activity.

To summarize, the UV/vis-spectra are obviously not related to the catalase activity. The P-intermediate does not show considerable catalase activity and is probably not involved in the catalase reaction. Measurements using inhibitors and variants showed that neither Cu_B nor a reduced heme a_3 are involved in the catalase reaction. Complexing Cu_B with ammonia even resulted in an increase in catalase activity. Variants showed that the hydrogen bond between Y167 and W272 is probably important either for the positioning of product and/or educt, radical intermediate formation or for polarizing/stretching the peroxide bond. An increase in flexibility and number of free histidines near the active center decreases the catalase activity because of side chains complexing either water or hydrogen peroxide. We additionally showed that a porphyrin radical is involved in the catalase reaction cycle of C*c*O.

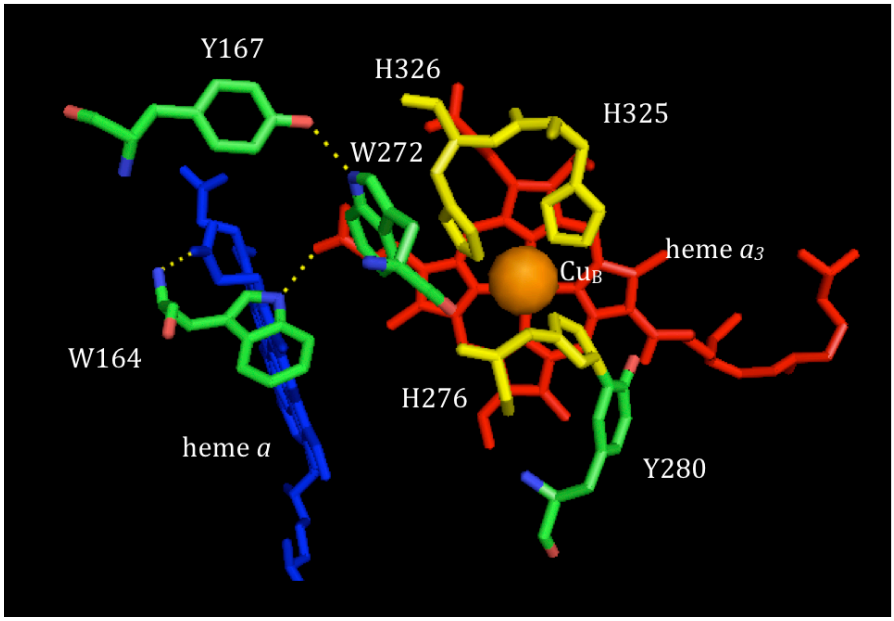

Figure 4.7: Aromatic amino acids (green) relevant to the catalase reaction mechanism near the active center.

The Cu_B (orange) complexing histidines are depicted in yellow, heme *a* in blue and heme a_3 in red. Hydrogen bonds are represented as yellow dotted lines. The picture was prepared with pymol and pdb file 3HB3.

Table 4.1: Summary of the results obtained for variants in aromatic amino acids, starting from O_{asis}. The label "unsure" points out that only a very low intensity signal is visible and the origin of this signal is not clearly assignable to the corresponding intermediate. 100% relative oxidase acitivty correspond to approximately 450 e^-/s whereas n/a stands for not available due to technical restrictions such as an oxygen reductase activity that was not measurable.

	W164F$_{asis}$	**Y167F$_{asis}$**	**W164F Y167F$_{asis}$**	**W272F$_{asis}$**	**Y280F$_{asis}$**	**W272F Y280F$_{asis}$**
P-intermediate	no	yes	no	no	no	no
F-intermediate	unsure	yes	no	no	no	no
Y167 radical	**+**	**((+))**	**((+))**	**+**	**(+)**	**-**
12 G signal	**++**	**++**	**++**	**+**	**++**	**+**
k_{cat} / min^{-1}	195.5 ± 67.5	79.1 ± 10.9	144.5 ± 14.8	50.4 ± 14.1	112.1 ± 17.8	73.5 ± 9.1
relative *Cc*O activity	12.5 ± 2.3	83.3 ± 2.2	1.0 ± 0.1	n/a	n/a	n/a

Table 4.2: Summary of the results obtained for the aromatic amino acid variants, starting from O_{ox}. The label unsure points out that only a very low intensity signal is visible and the origin of this signal is not clearly assignable to the corresponding intermediate. 100% relative oxidase acitivty correspond to approximately 450 e^-/s.

	W164F$_{ox}$	**Y167F$_{ox}$**	**W164F Y167F$_{ox}$**	**W272F$_{ox}$**	**Y280F$_{ox}$**	**W272F Y280F$_{ox}$**
P-intermediate	no	yes	no	no	no	no
F-intermediate	unsure	yes	unsure	no	unsure	no
Y167 radical	**++**	**-**	**-**	**-**	**++**	**-**
12 G signal	**++**	**(+)**	**(+)**	**(+)**	**+**	**++**

The 12 G narrow EPR signal of all variants shows comparable intensity if starting from O_{asis}, despite big differences in the k_{cat} values of the catalase reaction. The obtained EPR signals do not represent the protein in turnover but in a "frozen" condition due to the low temperature (20 K). Difference UV/vis spectra of the O_{asis} - O_{ox} intermediates show that the O_{asis} intermediate contains several other

intermediates apart from the O-intermediate. Inducing the F-intermediate by adding 500 molar equivalents of hydrogen peroxide to the asis C*c*O and flash freezing the sample, therefore, leeds to the C*c*O being in several different intermediates showing different potential radical signals. This leads to different results comparing the O_{asis} and O_{ox} states. Since the O_{ox} state represents one defined intermediate and not a mixture of intermediate, this state is compared to the kinetic data showing a correlation of the intensity of the described radical signal with the k_{cat} of the catalase reaction. Kinetic measurements are not affected by this difference, since turnover conditions lead to both O states converging into each other.

4.2.4. The Origin of the Oxygen Produced

Another open question is the origin of the oxygen produced during the catalase reaction. Catalases catalyze the disproportion of two molecules of hydrogen peroxide to two molecules of water and one molecule of oxygen (see Introduction 1.5), where the oxygen produced is generated from one single hydrogen peroxide molecule. The oxygen produced by the C*c*O catalase reaction could either be from one hydrogen peroxide molecule (similar to heme dependent catalases) or one oxygen atom from each hydrogen peroxide molecule, resulting in a mixed molecule (see figure 4.8).

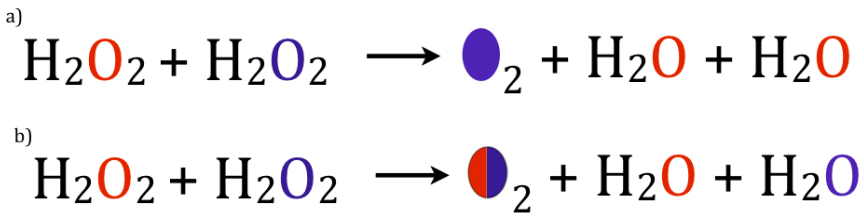

Figure 4.8: The two possible origins of the produced oxygen during the catalase reaction.
In the first possibility (a)) oxygen originates from one single hydrogen peroxide molecule, whereas b) shows the possibility of oxygen generation using one atom of each hydrogen peroxide molecule.

GCMS analysis of oxygen produced with a defined percentage of isotopically labeled hydrogen peroxide resulted in a combination of completely labeled and non-labeled oxygen molecules. The measured ratio between labeled and non-labeled oxygen

was always slightly shifted towards the non-labeled oxygen. The reason for this deviation is the transport and incubation time of the sealed vessels as well as the transport time of headspace gas with a syringe into the GCMS spectrometer. Small amounts of atmospheric oxygen shifted the ratio to non-labeled oxygen and decreased the measured amount of labeled oxygen. This technical problem is also the reason for the small amount of ^{34}O measured. We therefore postulate that the oxygen generated during the catalase reaction of C*c*O arises from one single hydrogen peroxide molecule as seen in figure 4.8 a). This is in accordance with the reaction mechanism of the human catalase published previously [53; 107].

The reaction cycle suggested by Konstantinov *et al.* is not completely in agreement with the reaction mechanism suggested in this work. Konstantinov suggested in 1992 a reaction cycle for the catalase activity of C*c*O involving the generation of superoxide [60]. Two molecules of superoxide, together with protons, are converted to oxygen and hydrogen peroxide. According to this reaction cycle, two molecules of oxygen are produced from three molecules of hydrogen peroxide. Nevertheless, in 1992, Ksenzenko *et al.* [102] calculated a superoxide concentration in the low µM range using a spin trap, trapping superoxide radicals, but added hydrogen peroxide in the low mM concentration range. The calculated concentration of superoxide and, therefore, oxygen would be in the low mM concentration range. This discrepancy was explained by the SOD activity of C*c*O. We showed that even mM concentrations of superoxide donor results only in a very low amount of oxygen being produced. Additionally, we were not able to reproduce the experiments presented in reference [60], pointing out that at least in the system used in this work, superoxide is not produced. We, therefore, consider that at least this part of their reaction cycle is not in agreement with the data presented in this work.

Summarizing the obtained data, the following mechanism for the catalase reaction is suggested: The first intermediate is very similar to the O-intermediate proposed by Michel in 1999 [49]. The bound water is released as the first hydrogen peroxide molecule enters C*c*O. The amino acid W164 is thereby probably involved in either an educt entry channel or a product release channel. The entered peroxide molecule is oriented in the right position probably by W272 and Y167. At this time, the peroxide is already bound to the heme a_3 iron. The peroxide bond is broken, one of the protons is probably bound by an unknown amino acid, presumably one of the

aromatic amino acids near the active center or one of the copper complexing histidines and further used for the generation of water. However, we cannot rule out that one of the two protons is pumped and another proton is taken up from the solvent to be passed to the OH^--ion, resulting in the formation of water. At that time, the first oxygen atom fully binds to heme a_3 forming an oxoferryl state that is EPR silent. The iron atom of heme a_3 and the porphyrin ring, forming a radical, provide the electrons needed for this first reaction. This intermediate is very similar to the F-intermediate. The second hydrogen peroxide is probably positioned via hydrogen bonds by amino acids near the active center. The protons are transferred to the oxoferryl oxygen generating water bound to heme a_3. This is probably achieved via aromatic amino acids near the active center. Oxygen is now generated from the second hydrogen peroxide molecule. With oxygen leaving the active center, the initial state is regenerated (see figure 4.9).

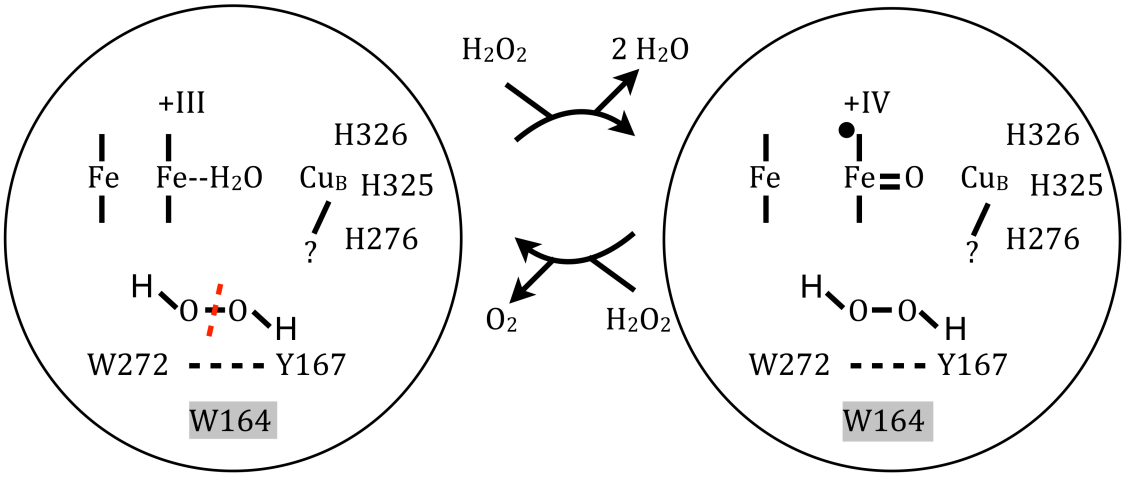

Figure 4.9: Proposed reaction cycle for the catalase reaction of C*c*O.

Starting from an O-like intermediate, the first molecule of hydrogen peroxide binds to heme a_3, releasing water from the active center. This figure shows the dynamic states during turnover. The reaction of hydrogen peroxide with heme a_3 generates another water molecule forming an oxoferryl state with a porphyrin radical. The second hydrogen peroxide donates its protons to the oxygen of the oxoferryl state, forming water. That leaves one molecule of oxygen originating from the second hydrogen peroxide. The amino acid W164 is presumably involved in either an educt entrance channel or a product release channel.

4.3. Comparison to Catalases

On a structural account, catalases and cytochrome *c* oxidases are very different, the former being globule, soluble proteins and the latter being membrane proteins [18; 44; 53; 126; 127]. Nevertheless, they share some similarities. For the comparison of catalases and C*c*O, this work focuses on A-type cytochrome *c* oxidases and on so-called "monofunctional", heme containing catalases. The first similarity present is in the active center of both enzymes, harboring a heme moiety, but the exact nature of the hemes can be different [52; 53; 70; 124; 128; 129]. The discussed C*c*Os show solely heme *A* being present in the active center, whereas the "monofunctional" catalases can be divided into small subunit catalases, possessing heme *B* and large subunit catalases, containing heme *D* [124]. One main difference between catalases and C*c*O, and probably also one of the reasons for the enormous difference in k_{cat}, is the fact that the catalase is soluble and can, therefore, be accessed by hydrophilic molecules from all sides, whereas C*c*O is a membrane protein and can only be accessed from two sides by polar, soluble molecules. Another difference is a bundle of conserved amino acid residues near the active center of catalases, providing a constant supply of hydrogen peroxide molecules. Another important bundle of amino acids is formed by a histidine and an asparagine, allowing formation of hydrogen bonds as well as the capability of accepting and donating protons [53]. The area surrounding the active center of catalases is, apart from the described hydrophilic amino acids, very hydrophobic to ensure the correct efflux of produced water and the specificity for hydrogen peroxide. Catalases additionally feature at least three different channels leading to the active center.

C*c*O also features at least three channels leading to the active center but lacks the described important amino acids. Histidine residues are in close proximity to the active center but are not in the right orientation and probably not in the right distance to serve as hydrogen peroxide "delivering" amino acid residues [18; 44].

Summarizing, the only structural similarities, a heme and aromatic amino acids are present in the active center, as well as a largely hydrophobic surrounding of the active center in both types of enzymes (see figure 4.10). However, the overall structure is very different.

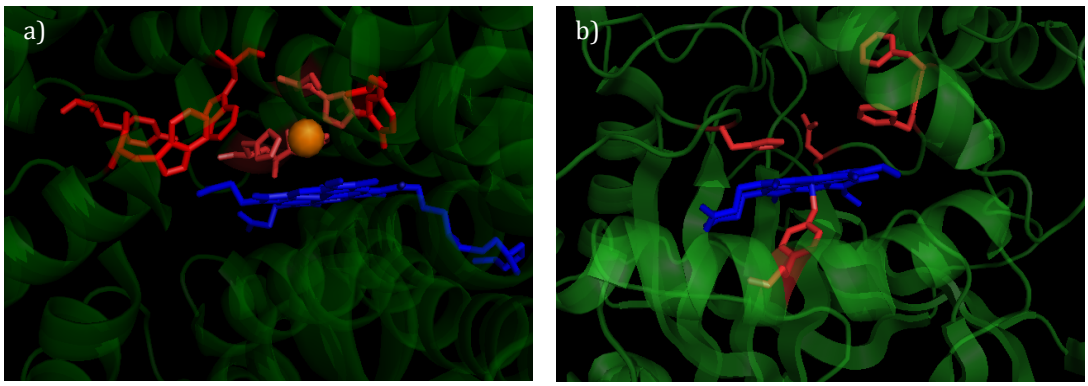

Figure 4.10: Comparison of aa_3 C*c*O (a)) and human catalase (b)).
Both enzymes feature a heme moiety as well as aromatic amino acids near the active center.

Comparing the reaction cycles of both enzymes, several similarities are present, especially in the proposed catalase activity reaction cycle of C*c*O to real catalases. One main similarity is the presence of an oxoferryl state and the absence of a reduced heme moiety during the reaction cycle. Additionally, catalases possess a porphyrin π-radical, whereas C*c*O shows the narrow 12 G radical signal, which is probably also a porphyrin radical. Oxygen evolving from both proteins originates from one hydrogen peroxide molecule [18; 49; 52; 53; 70; 71; 107; 124; 126-130]. These mechanistical similarities support the theory that structure is not necessarily correlated to function. Nevertheless, certain amino acids are important for function like the conserved histidine and asparagine in real catalases.

4.4. The Role of Tyrosine 167 in the Natural Reaction Cycle

Tyrosine 167 was postulated to be an energetic dead end in the reaction cycle of C*c*O as energetically the most stable radical [38; 123]. Analyzing the appearance of this Y167 radical in the different WT C*c*Os used in this work did show differences in signal intensity upon oxidation and between these WT C*c*Os. Anyhow, all WT C*c*Os showed similar oxygen reductase activity, suggesting that the signal intensity of this radical signal is not related to the catalytic oxygen reductase activity. Additionally, von der Hocht *et al.* showed that the purification of C*c*O and measurements at pH 7.5 and 8, respectively, results in the absence of the Y167 radical signal [97]. These measurements suggest that Y167 is not directly involved in the C*c*O reaction cycle, as stated in the literature.

Oxygen reductase activity measurements of the Y167F variant support this theory, showing at least 80% activity. In this variant, the discussed tyrosine residue was exchanged by a phenylalanine, missing the ability to form the radical. EPR data showed the absence of the Y167 radical related signal. Nevertheless, the formation of a P- and F-intermediate was possible.

This again suggests that the intensity of the different significant signals present in the difference absorption spectra recorded for the artificial intermediates are not linked to the natural oxygen reductase activity. This is supported by all WT C*c*Os used in this work showing similar catalytic activity but drastically different signal intensity of the characteristic P- and F-intermediate related signals. This suggests that at least the yield of P- and F-intermediates is not correlated with the oxygen reductase activity.

4.5. Physiological Relevance of the C*c*O Catalase Activity

The catalase activity that C*c*O exhibits, compared to real catalases, has an approximately $0.25*10^9$-fold decreased k_{cat} [63]. This side reaction, therefore, seems to be negligible. Nevertheless, taking supercomplexes of respiratory enzymes, as present for example in mitochondria of different organisms, into account, the catalase activity of C*c*O might become physiologically important [64; 131-133]. The presence of supercomplexes in bovine mitochondria was shown for example by electron microscopy, showing the presence of at least one copy of complex I, two copies of complex III and one copy of complex IV. The presence of different supercomplexes was also shown for plants [64; 132; 133]. Complexes I and III are known to produce ROS during catalytic turnover [22]. The produced ROS are mostly superpoxide radicals. However a small amount of hydrogen peroxide is still present. Superoxide radicals are known to disproportiante to hydrogen peroxide as well [134]. With complex IV exhibiting a catalase activity, there would be a membrane bound, supercomplex associated possibility to remove hydrogen peroxide right at its origin. Nevertheless, we cannot rule out that the proteins of the supercomplex are not the main producers of hydrogen peroxide. C*c*O showing a catalase activity decreases the possibility of ROS taking effect on the membrane, thiols or methionines within the supercomplex or damage DNA in close proximity

[135-138]. Since most prokaryotic membranes are not prone to “destruction” by oxidation, damage to the cell membrane becomes negligible for prokaryotes but remains a problem for eukaryotes [138; 139].

Catalases present near the supercomplex are only present in a soluble form. Considering that the supercomplex consists of membrane proteins and, therefore, ROS probably are released near the middle of the membrane, C*c*O being present as a membrane bound protein with an additional catalase feature becomes more feasible. C*c*O being present would result in the degradation of hydrogen peroxide right at its origin in the membrane, reducing the damaging effect of ROS. Hydrogen peroxide is therefore degraded, no matter if it resides in the membrane or in the cytoplasm using this combination of soluble catalases and C*c*O. Since approximately 0.4% of the consumed oxygen is accidently reduced to hydrogen peroxide [140], and already 1 µM hydrogen peroxide inhibits the growth of *E.coli*, a catalase side reaction of C*c*O seems useful [140; 141].

In addition to that, one could argue that a catalase activity being a prominent side reaction in heme containing metalloproteins, such as met-hemoglobin and C*c*O [57-59], is a relict from ancient times when oxygen started to develop on earth. The bacterium *Aquifex aeolicus* is considered as a very early organism. This bacterium is hyperthermophilic and, since oxygen solubility is temperature dependent, lives on very low oxygen concentrations (1%). Nevertheless, its genome carries several peroxidase (also degrading hydrogen peroxide but without the production of oxygen) genes but no gene coding for a catalase. Upon addition of hydrogen peroxide to the bacterium, a strong gas production is visible, typical for a catalase reaction [142]. Therefore, a strong catalase activity of the cytochrome *c* oxidase from *A. aeolicus* seems feasible and remains to be proven. A positive control of the catalase reaction would show that the reactivity towards hydrogen peroxide observed for the *P. denitrificans* C*c*O is an evolutionary artifact, protecting cells from oxidative stress. The ability of terminal oxidases to act as ROS protectants seems to have been invented several times since alternative oxidases show a ROS protecting activity in plants as well [143-146].

The strain MR3 carries a deletion in the non-expressing gene coding for SU I of C*c*O (*ctaDI*) as well as a deletion of *ORF4,* which shows a 98% identity to an *ahpD* homologue. Two different promoters control the expression of these two genes. The

alkylhydroperoxidase AhpD is part of a two protein system (AhpC and AhpD) protecting against oxidative stress. Both genes coding for these proteins are present in *P. denitrificans*. Reactive oxygen species are reacting with two cysteines present in AhpC, forming an intramolecular disulfide bond. AhpD regenerates this disulfide bond. Nevertheless, AhpD shows similar reactivity if present alone [141; 147-151]. As *ahpD* is located next to *ctaDI* together with the increase in catalase activity in the MR3 WT C*c*O, it suggests a regulatory mechanism probably dependent on the level of oxygen and/or ROS [34]. This, in turn, would mean that the regulation level of *ahpD* is coupled to the regulation of *ctaDI*. Assuming that *ctaDI* regulates the expression of *ctaDII*, this would suggest that C*c*O not only contributes to the *pmf* used for ATP-generation but also contributes actively to ROS protection. This in turn would mean that the regulation by *ctaDI* leads to small intentional changes in C*c*O biogenesis, resulting in an enhanced catalase activity. These changes do not affect the oxygen reductase activity but increase the catalase activity of C*c*O to protect from an increased level of ROS.

4.6. The Nature of the Differences between the ATCC WT C*c*O and the Recombinant WT C*c*O

The rec. WT C*c*O shows a 20-fold increase in k_{cat} of the catalase reaction compared to the ATCC WT C*c*O. After discussing the kinetics and the mechanism of the catalase reaction in detail, the origin of the difference in catalase activity, will now be discussed. The difference in catalase activity is also obvious in the UV/vis-spectra (see 4.1.1.2). Therefore, EPR data were recorded for the present, artifical O-, P- and F-intermediates to check for possible differences in the active center.

4.6.1. EPR Data of the ATCC WT C*c*O and Recombinant WT C*c*O

EPR-spectra of the P-intermediates of both wild types did not show any differences comparing O_{asis} to O_{ox}. Both wild types show a radical signal in the P-intermediate. This radical is more intense in the ATCC WT C*c*O compared to the rec. WT C*c*O, similar to the intensity of the optical P-intermediate related signals. In 2004 Budiman *et al.* [71] already described this signal and discovered that this radical is

located on the amino acid Y167. It was previously published that this radical signal is present in different artificial P-intermediates [71; 72; 110]. Van Wonderen *et al.* shows measurements lacking this signal in the P-intermediate if starting from O_{ox} (unpublished results). The environment needed for this radical signal remains questionable so far. Differences between van Wonderen *et al.* and this work are a decrease in pH value by 0.5 during purification and an increase in pH value of 1 during measurements done as well as a 1:1 molar ratio of hydrogen peroxide instead of a 1:5 molar ratio used by van Wonderen *et al*. Another difference is the freezing time during the preparation of EPR samples. Since there is no automatic setup, samples were frozen by hand and therefore may involve different time spans for the two experimentators, freezing the samples. The generation of the Y167 radical related signal, therefore, may be pH and time dependent. Since the conditions required for the formation of the Y167 radical are questionable, the intensity difference of this radical in the ATCC WT C*c*O and rec. WT C*c*O remains elusive. One possibility could be a lesser part of the protein population being trapped in an artificial electron sink in the rec. WT C*c*O. This is supported by the small percentage of radical signal present, similar to the intensity of P-intermediate related UV/vis signal present. The importance of this radical was already discussed by several groups [38; 71; 123]. Since the P-intermediate only needs small amounts of hydrogen peroxide and is, therefore, not important for the catalase activity, the Y167 radical will only be shortly discussed if present in the intermediate generated with conditions yielding the F-intermediate in the WT C*c*O.

Two other aromatic amino acids near the active center are W272 and Y280, which is cross-linked to H276. It is postulated that these amino acids might also generate a radical that is important for the function of C*c*O [123]. The small population of the Y167 radical related signal could, therefore, be a minor population of C*c*O being trapped in the thermodynamically more stable Y167 radical form instead of another aromatic amino acid [38].

The conditions generating the F-intermediate in the WT C*c*O show the most pronounced catalase activity, and a narrow 12 G signal present in both wild type C*c*Os originating from O_{asis}. This signal completely disappears upon oxidation of the ATCC WT C*c*O and remains unchanged upon oxidation of the rec. WT C*c*O. The existence of the narrow 12 G signal in the F-intermediate suggests an involvement

of this signal in the catalase reaction of C*c*O. The origin of the narrow signal was discussed in 4.2, and a porphyrin radical seems probable. The removal of the sharp radical upon oxidation of the ATCC WT C*c*O points out that the two observed O-intermediates are different from each other, at least in the ATCC WT C*c*O, and suggests either a mixture of different intermediates in O_{asis} or two different conformations of C*c*O. This is in good agreement with the difference spectra obtained from O_{asis}-O_{ox} showing a mixture of different natural intermediates being present in the O_{asis} state in both WT C*c*Os. However, the fact that the oxidation of the ATCC WT C*c*O changes, for example the intensity of the 12 G signal but does not significantly change the signal of the rec. WT, supports the theory of two different conformations in the two WT C*c*Os.

Oxidation of the rec. WT C*c*O did not change the UV/vis-spectra significantly and did not change the EPR-spectra at all. Contrary to that, both methods showed changes of the ATCC WT C*c*O upon oxidation. This result indicates the presence of a possible second conformation of the ATCC WT CcO as suggested already by Ji and co-workers and other groups [152-155]. The rec. WT C*c*O did not change upon oxidation, suggesting a higher probability for one of these two conformations. The fact that the F-intermediate of the ATCC WT C*c*O did not change significantly when starting with O_{ox} in the UV/vis-spectra, but showed the obvious change in the 12 G signal seems contrary at first. However, the UV/vis-spectra were recorded at room temperature and under turnover conditions, whereas the EPR-spectra were recorded at 20 K. The ATCC WT C*c*O was frozen immediately upon entering the F-intermediate for the EPR experiments. Possible differences could therefore be due to the optical spectra recorded under turnover conditions and the EPR spectra recorded in a “frozen” condition at 20 K.

4.6.2. Structural Reasons

DSC-data was recorded to support the theory of different conformations and small structural defects. The rec. WT C*c*O indeed showed storage and freeze-thaw cycle dependent changes in structural stability. The stability of the ATCC WT C*c*O did not change upon storage and freeze-thaw cycles. Comparing the DSC data of both wild types one day after purification and storage at -80°C including one freeze-thaw

cycle did not show any significant changes in thermal stability. The only difference visible between the two WT C*c*Os, is an approximate 2°C shift in T_M of the signal, relating to the melting and/or disassembly of SU I and II, and a shift in the detergent related signal of approximately 5°C. The slight shift in T_M of SU I and II probably results from different amounts of detergent and natural lipids present in the sample. This is supported by the change in detergent related signal. The dependence of catalytic activity on natural lipids and detergent amount was previously shown [154] and a slight shift in T_M therefore seems feasible for different lipid and detergent amounts.

Two days and two freeze-thaw cycles did not change the overall stability drastically. Contrary to that, storage for six days and three freeze-thaw cycles changed the structural stability of the rec. WT C*c*O drastically. The signal related to SU III and IV at 43°C increases and another signal with a transition midpoint temperature of 35°C appears. The new signal could be due to detached and/or partly denatured SU III and IV. Detached SU III and IV would show different transition midpoint temperatures compared to the subunits still attached, due to the missing interactions to the core subunits.

The increase in heat capacity of the 43°C signal could be related to different interactions of SU III and IV to subunits I and II. Additionally to that, the detergent related signal at 30°C shifts to 18°C with a shoulder at 22°C. This signal might support the theory of detached SU III and IV because the interactions of SU III and IV with detergent micelles would change the free detergent related transition midpoint temperature. Nevertheless, a change in transition midpoint temperature related to detergent effects could also be related to changes in detergent behavior (changes in phase behavior) related to freeze-thaw cycles, but this signal would probably appear already after two days and two freeze-thaw cycles [156].

This difference of the rec. WT C*c*O, showing a change in structural behavior, especially the proposed change in interaction of SU III and IV with the core subunits, supports the theory of two different forms or conformations of the enzyme and was previously described by Ji and co-workers [155]. Elferink et al. [154] also published the appearance of a second conformation of C*c*O upon storage at room temperature. Morin and Freire [153] showed that increasing ionic strength decreases the stability

of yeast C*c*O and speculated that an increase in ionic strength favors a second conformation of C*c*O with a decreased interaction of SU I and II.

All prior experiments postulated the existence of a second conformation with a different overall peptide arrangement or a different water network in the protein. Disturbing this fine balanced equilibrium, for example by small structural changes of the polypeptide backbone could result in a faster relaxation into one of the two different forms (see figure 4.11). Another possibility could be a relaxation of the rec. WT C*c*O into a new conformation not observable for the ATCC WT C*c*O. There is, however, no evidence for this theory yet.

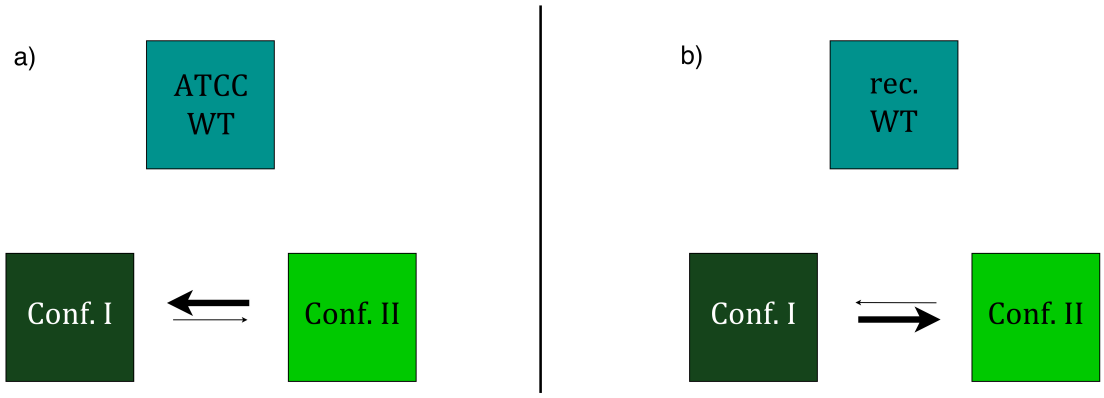

Figure 4.11: Equilibrium of two different conformations of the ATCC WT C*c*O (a) and the rec. WT C*c*O (b).

The ATCC WT C*c*O probably favors conformation I (conf I), the rec. WT C*c*O probably conformation II (conf II). The rec. WT CcO undergoes a faster transition into conformation II, whereas the ATCC WT C*c*O remains in conformation I.

The rec. WT C*c*O was constructed using a low copy number plasmid, potentially resulting in an over-production of SU I compared to the other subunits. This fact might result in small structural changes in the peptide structure, and consequently in the water network, potentially induced by a non-correct insertion of the metal co-factors. A lack of other chaperones could not be ruled out but seems unlikely, since this would probably result in major structural changes leading to an altered oxygen reductase activity. Structural changes and an altered interaction of SU I and II might result in a faster relaxation of the rec. WT C*c*O into a second conformation, similar to the ones described in the preceding paragraph. The different interaction of SU I and II in the second conformation could lead to the detachment or at least to

different interactions to subunits III and IV suggested by capillary DSC. This, in turn, might change the accessibility of the active center for hydrogen peroxide, changing the speed of the reaction. It is therefore postulated that the rec. WT C*c*O relaxes faster into a second conformation of the oxidized form due to small structural defects caused by plasmid coding of subunit I, compared to the ATCC WT C*c*O. This second conformation exhibits an increased catalase activity e.g. due to an increased accessibility of the active center for hydrogen peroxide.

A potential overproduction and, subsequently, a lack of metal inserting chaperones, due to plasmid coding, and, as a result, minor differences in metal insertion into SU I leading to a drastic change in catalase activity, are postulated.

Greiner *et al.* [99] suggested a co-translational insertion of copper and heme moieties. Consequently, the rec. WT C*c*O was supplemented with a His_6-tag to provide copper atoms complexed by the His_6-tag during assembly of SU I. Providing copper directly to the protein might increase the probability of a correct insertion of Cu_B. Metal determination of this WT C*c*O showed no irregularities concerning the redox active metal centers but an increased zinc content. This increase in zinc content is probably due to zinc ions bound to the His_6-tag of C*c*O. It was already previously shown that zinc ions are able to influence catalases, it therefore seems feasible that this might also be possible for C*c*O, increasing the catalase activity sligthly [125; 157]. Contrary to that theory, it is known that zinc ions bind to C*c*O having an inhibitory effect [117; 158]. Nevertheless, oxygen reductase activity did not show any differences; therefore binding of zinc ions to the His_6-tag is more feasible than inhibition by zinc ions. The catalase activity dependent kinetic data of the his-tagged rec. WT C*c*O showed no significant differences in catalase activity compared to the rec. WT C*c*O without His_6-tag but a slight tendency to higher K_M and k_{cat} values. This is probably due to the bound zinc ion, as discussed above. Nevertheless, the observed differences are not significant.

Crystal structures of the ATCC (2.8 Å) and rec. wild type C*c*Os (2.25 Å) are available [18; 44] but the structure of the rec. WT C*c*O was obtained by molecular replacement using the ATCC WT C*c*O data. Model bias caused by molecular replacement at the obtained resolution may prevent that small differences in structure can be observed. Differences in structure would be detectable if a very high resolution crystal structure of the rec. WT C*c*O is determined *de novo*.

Since the DSC data suggested structural reasons for the observed differences, chaperones were introduced to the same plasmid, which encodes SU I.

4.6.3. Introducing Chaperones

The rec. WT C*c*O was constructed by supplementing a deletion strain, lacking the two coding genes for SU I of aa_3 C*c*O, with a low copy-number plasmid carrying the expressed gene for this SU. A potential overproduction of SU I could, therefore, not be ruled out. A lack of chaperones caused by this potential overproduction may result in small structural differences of the rec. WT C*c*O compared to the ATCC WT C*c*O. Consequently, the gene coding for CtaG, a copper inserting chaperone [39; 99], was added and in a second experiment, the genes for CtaG and Surf1c, a heme inserting chaperone [39], was added on the same plasmid as SU I raising the level of these chaperones in the cell.

Expression of both chaperones was verified by Western blotting. Only minor, insignificant increases in oxygen reductase activity were observed. Catalase activity related kinetic parameters showed no significant differences in K_M but a decrease in k_{cat} by approximately 20% for the one-chaperone added rec. WT C*c*O and approximately 40% for the two chaperones added rec. WT C*c*O. This subsequent decrease in catalase activity supports the hypothesis of slightly misplaced metal centers, resulting in minor structural changes, obvious also in the DSC data of the rec. WT C*c*O. To further characterize this form of the rec. WT C*c*O, the yield of optical P- and F-intermediates was analyzed as well as the formation of the narrow 12 G signal, in EPR-spectroscopy.

The yield of optical P-intermediate related features in both chaperone added rec. WT C*c*Os is surprisingly even smaller than the yield of the P-intermediate in the rec. WT C*c*O without added chaperones. The F-intermediate related signal shows the same behavior originating from O_{asis}. According to the hypothesis of chaperones improving the metal insertion into SU I, the yield of both intermediates originating from O_{asis} and O_{ox} should increase compared to the rec. WT C*c*O. Additionally, the maximum absorption in both chaperone added rec. WT C*c*Os is located at 579 nm and 578 nm, suggesting the formation of a F*-intermediate similar state.

The yield of P-intermediate did not change when starting from O_{ox}. Only the one-chaperone added rec. WT C*c*O showed an increase in yield of the F-intermediate and a shift of the absorption maximum to 578 nm. The two chaperones added rec. WT C*c*O did not change intensity but shows a shift of the absorption maximum to 580 nm.

According to von der Hocht *et al.*, the only differences between the P- and F-intermediates are the Cu_B ligands [49; 97]. Since the active center for the catalase activity is heme a_3, the Cu_B moiety would be of little importance. This suggests that the difference absorption spectra are not of particular importance for the catalase activity but show only the differences in Cu_B-ligands.

The shoulder visible in all rec. WT C*c*O F-intermediates suggests the presence of a different ligand near Cu_B for a very small portion of the overall population. The very low yield of P-intermediate also suggests only a small difference comparing the O- and P-intermediate. This observation would consequently lead to the assumption that both chaperone added wild type C*c*Os need a higher hydrogen peroxide concentration to form the P- and F-intermediates. This, in turn, would lead to a higher K_M compared to the rec. WT C*c*O and ATCC WT C*c*Os. No significant differences in K_M-values were detected. It is, therefore, more likely that the influence of Cu_B and therefore the yield of P- and F-intermediates are negligible for the catalase activity.

The F-intermediate originating from O_{asis} shows a very low intensity Y167 radical related signal for the two-chaperones added rec. WT C*c*O. Originating from O_{asis} this radical is probably a very small amount of protein "trapped" in an energy sink with the Y167 radical present as previously discussed [38]. Nevertheless, this signal is not observed when starting from O_{ox} suggesting that the energy sink is not present after oxidation. Another plausible explanation is the previously discussed mixture of intermediates if originating from O_{asis} that might also lead to a small population of C*c*O yielding the Y167 radical.

The F-intermediate of both chaperone added wild type C*c*Os shows the narrow 12 G signal to be present in decreasing intensity with increasing number of chaperones. The decrease in intensity supports the theory that chaperones aid the correct incorporation of redox active metal centers.

The radical 12 G signal of both chaperone added rec. WT C*c*Os has a signal intensity that is somewhere between the signal intensity of the rec. WT C*c*O and the ATCC WT C*c*O. No clear differences are visible when comparing the one-chaperone added rec. WT C*c*O to the two-chaperones added rec. WT C*c*O. The theory that this narrow EPR radical signal is related to the catalase activity is supported by the two-chaperones added rec. WT C*c*O having a k_{cat} that is between the values seen for the rec. WT C*c*O and ATCC WT C*c*O and a signal intensity of the narrow 12 G signal that is between the intensity seen for the rec. WT C*c*O and ATCC WT C*c*O.

The height of the signal, within a certain tolerance value, is dependent on the freezing time during sample preparation. Since freezing of the EPR samples is not automated but samples are frozen manually, freezing times could vary slightly. Therefore, signal intensities that are very close to each other, such as the one-chaperone added rec. WT C*c*O and the two-chaperones added rec. WT C*c*O are difficult to measure. The tendencies of the signal heights of the chaperone added rec. WT C*c*Os being in between the rec. WT C*c*O and the ATCC WT C*c*O are nevertheless true. However, these measurements have to be repeated. The difference in signal height between the one-chaperone added rec. WT C*c*O and the two-chaperones added rec. WT C*c*O is not clearly measurable. The small difference in signal intensity discussed, could be caused by small time delays in sample preparation.

Finally, it is concluded that the addition of chaperone genes to the SU I coding plasmid in the rec. WT C*c*O led to a significant decrease in catalase activity and that the 12 G radical EPR signal intensity is related to catalase activity. It is, therefore, postulated that one main, but not the only reason for differences in the rec. WT C*c*O and the ATCC WT C*c*O is the lack of chaperones, which is caused by a potential overexpression due to plasmid coding. The small resulting structural defects, probably in metal insertion, could lead to slight changes in protein structure and as a consequence thereof small defects in the water network of aa_3 C*c*O. These differences might lead to minor changes in the accessibility of the active center of C*c*O for hydrogen peroxide or in the accessibility of the product exit channel leading to an increased catalase activity. Despite the homologous recombinant expression of the rec. WT C*c*O, a different lipid composition of the ATCC WT C*c*O and the rec. WT C*c*O could not be ruled out leading to different accessibilities of the active center

of C*c*O for hydrogen peroxide [159]. This would lead to different k_{cat} values as observed. However, this possibility seems improbable because, in both cases, the same organism was used for the production of protein.

Table 4.3: Correlation of the narrow 12 G EPR signal with the k_{cat} of the catalase reaction starting from O_{ox}

100% relative oxidase acitivty correspond to approximately 450 e^-/s. Chap 1 and Chap 2 stand for the rec. WT C*c*O with one or two additional chaperones respectively.

	ATCC WT C*c*O$_{ox}$	**rec. WT C*c*O$_{ox}$**	**Chap 1$_{ox}$**	**Chap 2$_{ox}$**
12 G signal	**-**	**+**	**(+)**	**(+)**
k_{cat} / min^{-1}	9.6 ± 2.0	200.4 ± 32.6	166.8 ± 32.6	118.6 ± 19.6
relative C*c*O activity	100.0 ± 10.9	100.0 ± 12.8	114.0 ± 8.0	118.0 ± 5.9

Comparing the obtained k_{cat} values of the catalase reaction with the signal intensity of the narrow 12 G radical EPR signal starting from O_{ox}, a clear correlation is visible. The described EPR signal was therefore considered as functionally important for the catalase activity.

4.6.4. The MR3 Wild Type

The MR3 wild type [34] can be considered to be an intermediate step between the ATCC WT and the rec. WT, possessing a deletion of the non-expressed gene of SU I and a deletion of *ORF4*. The expressed gene for SU I is still located on the chromosome, therefore no plasmids were added. This results in no overexpression and no changes in sequence (see figure 4.12).

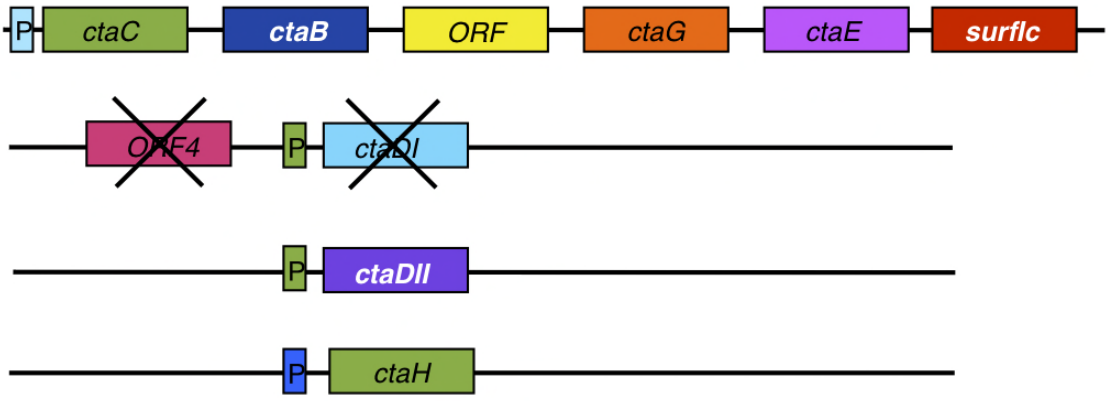

Figure 4.12: Genetic arrangement in the MR3 WT.
Promoters are denoted with P. Genes are given in italics with their respective gene product in brackets: *ctaC* (SU II), *ctaB* (farnesyltransferase), *ctaG* (chaperone for copper insertion), *ctaE* (SU III), *surf1c* (chaperone for heme insertion), *ctaDI* (SU I, non-expressed), *ctaDII* (SU I, expressed), *ctaH* (SU IV), *ORF4* (hypothetical Alkylhydroperoxidase).

Therefore, the same results as shown for the ATCC WT C*c*O were expected for the MR3 WT C*c*O. Indeed, the oxygen reductase activity shows no differences compared to the ATCC and the rec. WT C*c*O. Contrary to that, the k_{cat} of the catalase reaction increases by a factor of 18 compared to the ATCC WT C*c*O and nearly reaches the rec. WT C*c*O level. The K_M value shows a slight increase, suggesting a slightly stronger binding of the educt and/or product. This difference was not expected, and so the UV/vis-spectra and EPR-spectra were recorded and compared to the ATCC and rec. WT C*c*O.

The P-intermediates originating from O_{asis} and O_{ox} show slight shifts in maximum difference absorption to 612 nm and 611 nm, respectively. The levels are reduced compared to the ATCC WT C*c*O caused by an increased catalase activity. The increased catalase activity decomposes the small amount of hydrogen peroxide added to induce the P-intermediate. That results in a decrease of signal intensity of the P-intermediate.

The F-intermediate of the MR3 WT C*c*O is very similar to the F-intermediate of the ATCC WT C*c*O and the rec. WT C*c*O. The difference absorption maximum shifts from 580 nm to 579 nm when starting from O_{ox}, also decreasing the shoulder present in O_{asis} at approximately 610 nm. The huge excess of hydrogen peroxide results in similar spectra for the rec. WT C*c*O, ATCC WT C*c*O and MR3 WT C*c*O. The small

shoulder suggests small amounts of protein present with a different ligand at Cu_B. Nevertheless, this observation does not contradict to the hypothesis that the optical spectra are not related to the actual catalase mechanism.

The EPR spectrum of the F-intermediate originating from O_{asis} shows a very intense 12 G radical signal which is strongly reduced upon prior oxidation of the protein. This behavior was already observed for the ATCC WT C*c*O, whereas the rec. WT C*c*O did not show any difference in signal intensity of the 12 G signal upon oxidation. Summarizing the results of the MR3 WT C*c*O, similarities with the rec. WT C*c*O are present in the catalase reaction and the 12 G signal intensity, whereas the reduction of the 12 G signal upon prior oxidation is similar to the ATCC WT C*c*O. This observation suggests another reason, next to missing chaperones, for the obvious differences of the MR3 WT C*c*O and the ATCC WT C*c*O.

Since only the non-expressed genes for SU I and *ORF4* were deleted, it was looked for the possible gene product of *ORF4* and a 93% sequence identity to alkylhydroperoxidases was found. Hydroperoxidases are ubiquitous housekeeping proteins that combine a catalase and peroxidase activity [124]. Koshkin *et al*. described the kinetics of the alkylhydroperoxidase AhpD of *Mycobacterium tuberculosis* in 2003 [149]. AhpD exhibits alone or in combination with AhpC a hydrogen peroxide decomposing activity. Both genes coding for these proteins are also present in *P. denitrificans*. This system of two enzymes provides protection against oxidative stress. One main feature of all C*c*O wild types, apart from the ATCC WT C*c*O is the deletion of this *ORF4*. A lack of the gene product of *ORF4* causing oxidative stress and therefore damaging the rec. WT C*c*O, leading to an increase in catalase acitivty is not ruled out. Nevertheless, the ATCC WT C*c*O and the rec. WT C*c*O are not showing any differences in oxygen reduction activity, which strongly suggests, that oxidative damage is not the reason for an increase in catalase activity of the rec. WT C*c*O.

Discussing the data obtained from the MR3 WT C*c*O, the existence of either an RNA regulation by the non-expressing gene *ctaDI* or a regulation mechanism related to *ORF4* that is not yet known, is postulated. Nevertheless, it is striking that the deletion of one open reading frame, probably coding for a protein that is an ROS protectant, increases the antioxidative features of a second protein having the non-expressing gene for the main catalytic subunit of this protein in close proximity,

even if controlled by different promoters. A regulating mechanism, involving *ORF4* seems plausible. It cannot be ruled out that *ctaDI* and/or *ORF4* feature a regulation mechanism important for the equilibrium of the two different conformations of C*c*O. This would lead to the assumption that the catalase activity of C*c*O is somehow controllable. The high similarity of the MR3 WT C*c*O in the catalase reaction to the rec. WT C*c*O supports the theory of a second conformation. The MR3 WT C*c*O would, therefore, be preferred in the conformation with increased catalase activity, due to the missing regulation by *ctaDI* and/or *ORF4.* The observed reduction in the 12 G EPR signal shows that the radical associated with this signal is either not necessarily important for the catalase activity or magnetically coupled to the active center upon oxidation in the ATCC WT C*c*O. A magnetic coupling upon prior oxidation suggests a change in distance between the radical and the remaining parts of the active center upon prior oxidation. This structural change is not occuring in the rec. WT C*c*O but small defects in metal insertion into the rec. WT C*c*O would also lead to possible differences in the magnetic coupling, affecting the 12 G radical EPR signal. Oxidation of the ATCC and MR3 WT C*c*O therefore leads to changes, not possible in the rec. WT C*c*O, because of changes in the positioning of the active center.

Summarizing, the difference between the ATCC WT C*c*O and the rec. WT C*c*O is caused by a combination of a lack of chaperones, due to plasmid coding of SU I and results in small structural changes in the water network and amino acid side chain orientation. Additionally, a possible regulation mechanism involving *ctaDI* and *ORF4* is not present in the rec. WT C*c*O and seems to be at least part of the reason for the observed differences.

5. Summary

5.1. Summary

Cytochrome *c* oxidase (C*c*O) is part of the respiratory chain and catalyzes the reduction of oxygen to water. In addition to using electrons and protons from opposite sides of the membrane, C*c*O uses the Gibbs free energy of the reduction of oxygen to water to pump protons across the cell membrane of prokaryotes or across the inner mitochondrial membrane of eukaryotes. The electrochemical gradient formed is used by the F_0F_1-ATP synthase to generate ATP from ADP and inorganic phosphate [6; 7].

The active center of C*c*O contains a Cu_B-ion and heme a_3. Variants of the aa_3 C*c*O were previously used, for example, to characterize the different channels leading to the active center. These variants were constructed using a deletion strain of *P. denitrificans* (Δ*ctaDI*, Δ*ctaDII,* Δ*ORF4,* Δ*ccoN*) deficient in subunit I (SU I) of aa_3 C*c*O. This deletion strain was complemented with the gene expressing SU I, including the mutation, on a low copy number plasmid [18; 42; 44]. The variants were compared to the ATCC WT C*c*O, but consistently variants should be compared to the supplemented deletion strain, namely the rec. WT C*c*O, containing the same genetic background as the variants. This has initially been done by Angerer [72] showing differences for the catalase side reaction. Metallo-proteins containing the same metal ion (i.e. an iron atom) can catalyze different reactions and the specificity of the catalyzed reaction is controlled by the amino acid environment. This fact leads to the conclusion that side reactions of metalloproteins are very likely. The existence of side reactions of metallo-proteins have been shown by several groups [29; 55-59; 160; 161].

A-type C*c*Os, for example, show a peroxidase activity [59] and a catalase activity [58]. Konstantinov and co-workers already extensively investigated this catalase activity [60-62; 101; 103]. Nevertheless, this catalase activity was not yet characterized for the *P. denitrificans* C*c*O. Furthermore, there is still some debate about reaction mechanisms for the catalase reactions catalyzed by C*c*O [61; 103; 115]. Consequently, this work focused on two points:

- The catalase activity of the aa_3 C*c*O of *P. denitrificans* was investigatd in a detailed way for the first time. A 20-fold increase in k_{cat} for the rec. WT C*c*O was found, compared to the ATCC WT C*c*O. Since the rec. WT is complemented with a low copy-number plasmid, an overproduction of the plasmid encoded SU I is expected. This overproduction could lead to a lack of metal co-factor inserting chaperones, which in turn could lead to small structural changes due to false insertion of the metal centers. DSC measurements were carried out to analyze the rec. WT C*c*O and the ATCC WT C*c*O and it was found that the rec. WT C*c*O loses stability upon three-freeze-thaw cycles and storage for six days at -80°C, whereas the ATCC WT C*c*O showed no effect.

  One might assume that the catalase activity of C*c*O is a side reaction of partly denatured rec. WT C*c*O. Therefore, freshly prepared rec. WT C*c*O was subjected to freeze-thaw cycles, a decrease of the catalase and oxygen reductase activity were observed. Heating C*c*O even led to the loss of catalase activity. These results show that the catalase activity is associated with the C*c*O and not with an unspecific reaction of partly accessible heme due to denatured protein.

  The lack of chaperones might be the reason for the increase in catalase activity. Therefore, the rec. WT C*c*O was complemented by cloning the genes for the metal inserting chaperones CtaG and Surf1c on the same plasmid, which encodes SU I [39; 99; 162-164]. One construct carried *ctaG* next to *ctaDII*, whereas the other construct carried both, *ctaG* and *surf1c* additionally to *ctaDII*. The addition of chaperones leads to an up to two-fold decrease in k_{cat} of the catalase activity compared to the rec. WT C*c*O. This observation shows that structural changes are involved but not the only reason for the differences between the ATCC WT C*c*O and the rec. WT C*c*O.

  EPR spectroscopy showed a narrow radical signal in the F-intermediate. The intensity of this signal was high in the rec. WT C*c*O, low in the ATCC WT C*c*O and decreased upon addition of chaperones compared to the rec. WT C*c*O, supporting the assumption that part of the difference between the ATCC WT C*c*O and rec. WT C*c*O originates from a lack of metal inserting chaperones.

  The MR3 WT is an intermediate between the ATCC WT and rec. WT having a deletion of the non-expressed gene for SU I, *ctaDI*, and the alkylhydroperoxidase coded by *ORF4* [34; 147-151]. This intermediate WT C*c*O shows an increased k_{cat}

despite any plasmid coding. Since only these two genes are deleted, a regulatory mechanism of either one of these two genes or both genes is considered to be feasible.

Several groups [100; 153; 155] already observed a second conformation of C*c*O with differences especially in contact of SU I and II. These speculations fit very well to the data obtained by DSC, suggesting a higher probability for the rec. WT C*c*O staying in one conformation. At the same time, the ATCC WT C*c*O shows a higher probability for the "first" conformation, whereas the rec. WT C*c*O shows a higher probability for the "second" conformation.

Considering the results for the MR3 WT C*c*O, a combination of the assumed lack of gene regulation by *ctaDI* and/or *ORF4* and small defects in the orientation of the amino acid chain and/or water network of C*c*O may lead to a faster transition of the rec. WT C*c*O into the second conformation with altered subunit contact. This change might lead to an improved accessibility of heme a_3 for hydrogen peroxide, increasing the k_{cat} of the catalase activity. One could argue that the genes *ctaDI* and *ORF4* are responsible for a regulation of the catalase activity of C*c*O *in vivo.* Such a regulation would imply the possibility to increase the catalase activity of C*c*O under specific, unknown circumstances.

- Different inhibitors and variants were used to investigate the catalase activity of *P. denitrificans* aa_3 C*c*O to identify a potential mechanism for this side reaction. Cyanide and azide fully inhibited the catalase reaction of aa_3 C*c*O suggesting a heme moiety as active center. The use of carbon monoxide did not show any inhibiting effect, speaking for the absence of a reduced heme (Fe^{2+}) in the catalase activity reaction cycle. Orii and Okunuki first described the binding of hydrazine to C*c*O and von der Hocht *et al.* showed the binding of ammonia to Cu_B. The influence of ammonia on the catalase activity was analyzed and showed a substantial increase of activity at high pH. Additionally to the described measurements, the variants H276D/E/K/R were investigated and showed the loss of Cu_B. Ammonia complexing Cu_B shows an increase of catalase activity and variants lacking Cu_B still have a considerable catalase activity. This observation demonstrates that Cu_B is dispensable for the catalase activity of C*c*O.

Since the P-intermediate differs from the F-intermediate only in the nature of the fourth Cu_B ligand, conclusions drawn from the optical spectra of the artificial intermediates are negligible.

EPR-spectra recorded of the rec. WT C*c*O and ATCC WT C*c*O showed a narrow EPR radical signal with a width of 12 G in the catalase reaction. A porphyrin radical could be assigned to this signal by comparing it to similar signals [109; 110]. The influence on the catalase reaction of aromatic amino acids near the active center was checked by constructing several variants. We found that the exact positioning of W164, combined with the hydrogen bond to heme a_3, is probably crucial for the accessibility of the active center. The hydrogen bond connecting W272 and Y167 is essential, either for the positioning of the amino acids or for the polarization/orientation of the hydrogen peroxide molecule. Mutating either of these amino acids results in a comparable decrease in k_{cat}. W272 and Y167 are, therefore, important for the catalase activity. Changing Y280 to phenylalanine probably results in an increased flexibility of H276, which, in WT C*c*O, is cross-linked to Y280 [18; 44]. This change, in turn, results in the loss of Cu_B and an increase in flexibility of the remaining two copper-complexing histidines. Since histidines are capable of liganding water and hydrogen peroxide, the k_{cat} decreases probably due to the three more flexible histidines presumably complexing educt and/or product.

The oxygen produced during the catalase reaction was analyzed by gas chromatography-mass spectrometry using a reactant mixture of $H_2{}^{16}O_2$ and $H_2{}^{18}O_2$. With this mixture it could be shown that the evolving oxygen originates from one single hydrogen peroxide molecule.

The following mechanism for the catalase reaction seems feasible:

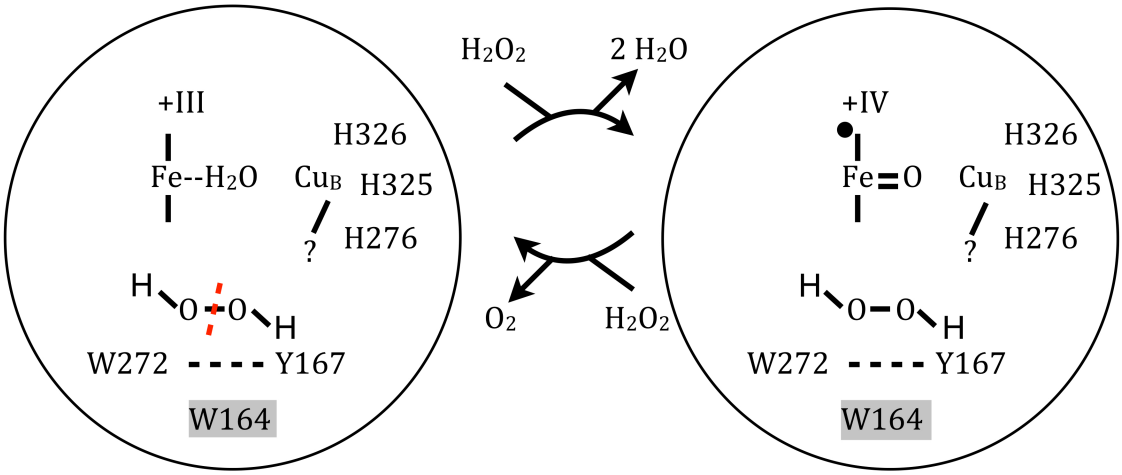

Figure 5.1: Proposed catalase mechanism of the aa_3 C*c*O.
The first hydrogen peroxide molecule leads to the release of the water bound to heme a_3 and induces the formation of another water molecule and an oxoferryl state. The second hydrogen peroxide molecule reacts to oxygen. The protons of this hydrogen peroxide molecule may be used to form water with the oxoferryl oxygen. The amino acid W164 is presumably involved in either an entrance channel or a product release channel.

Comparing the turnover numbers of the aa_3 C*c*O of *P. denitrificans* to the turnover number of catalases, one could argue about the physiological importance of this side reaction. Considering the formation of supercomplexes in mitochondria, containing one copy of Complex I, two copies of Complex III and one copy of Complex IV, the physiological importance becomes obvious. Since complex I and III are known to produce ROS, a protein with an inherent catalase activity seems to be useful to destroy produced hydrogen peroxide right at its origin [22; 64; 65; 131-133]. Even if soluble catalases were present on both sides of, for example, the inner mitochondrial membrane, C*c*O featuring a catalase activity would be useful for the degradation of hydrogen peroxide, which is generated inside the membrane, yielding a high local concentration. Soluble catalases cannot degrade hydrogen peroxide present inside the membrane. The catalase activity of C*c*O would protect the organism and prevent, for example, the oxidation of lipids, which is detrimental for the organism.

In conclusion, this work shows two possible explanations for the difference in the ATCC WT C*c*O and rec. WT C*c*O and, additionally, shows a reaction cycle and

highlights the important amino acids of the catalase reaction of C*c*O. A physiological relevance could be assigned to the side reaction, shown by C*c*O.

Future work should focus on the analysis of the potential overproduction of the plasmid coded gene *ctaDII*. Analysis of transcription levels for *ctaDII* and quantitative analysis of the produced amount of SU I of C*c*O might lead to the determination of the level of potential overproduction of SU I.

These measurements show that previously published experiments concerning side reactions of C*c*O obtained with a recombinant system have to be considered with caution.

5.2. Zusammenfassung

Die aa_3 Cytochrom *c* Oxidase (C*c*O) des Bodenbakteriums *Paracoccus denitrificans* (*P. denitrificans*) ist eine der terminalen Oxidasen der Atmungskette [131; 165; 166]. Aufgrund des hohen Verwandtschaftsgrades zur C*c*O aus der eukaryontischen, mitochondrialen Atmungskette wird die aa_3 C*c*O aus *P. denitrificans* als Modellprotein verwendet [34-37].

C*c*Os katalysieren die vier-Elektronen Reduktion von molekularem Sauerstoff zu Wasser. Die Reduktion von Sauerstoff ist an das Pumpen von vier Protonen pro reduziertem Sauerstoffmolekül über die Zellmembran der Bakterien oder die innere Mitochondrienmembran von Eukaryonten gekoppelt. Die Reduktion von Sauerstoff zu Wasser, durch Elektronen von der äußeren Membranseite, verbraucht vier weitere Protonen aus dem Cytoplasma (bei Prokaryonten) oder aus der mitochondrialen Matrix (bei Eukaryonten). Durch diesen Pumpvorgang in Verbindung mit der Reduktion von Sauerstoff zu Wasser wird die chemische Energie der Reaktion in einem elektrochemischen Protonengradienten über der Membran gespeichert [49; 167-169]. Dieser elektrochemische Gradient wird durch die F_0F_1-ATP-Synthase zur Synthese von Adenosin-5'-Triphosphat (ATP) aus ADP und anorganischem Phosphat genutzt [6; 7].

Die Reduktion von Sauerstoff zu Wasser wird im aktiven Zentrum der C*c*O, welches Häm a_3 und Cu_B enthält, katalysiert. Elektronen werden vom reduzierten Cytochrom *c* über zwei weitere redox-aktive Metallzentren, Cu_A in Untereinheit (UE) II und Häm *a* in UE I, auf das aktive Zentrum bestehend aus Häm a_3 und Cu_B in UE I übertragen [18; 44].

Die C*c*O ist ein Metalloprotein. Metalloproteine besitzen Metallzentren, die an der Katalyse beteiligt sind, dabei können verschiedene Reaktionen durch dieselben Metalle katalysiert werden. Die Selektivität der enzymatisch katalysierten Reaktion wird hierbei durch die Aminosäue-Umgebung des Proteins bestimmt. Es ist daher nicht ungewöhnlich, dass Metalloproteine Nebenreaktionen katalysieren, wie z.B. eine Katalase oder Peroxidase Reaktion, bei Enzymen, die Häme besitzen. Diese Nebenreaktionen wurden für die C*c*O bereits 1963 im Fall der Katalase und 1982 im Fall der Peroxidase Reaktion beobachtet [29; 55-59; 160; 161].

Die Katalasereaktion der aa_3 C*c*O aus *P. denitrificans* wurde ausführlich an verschiedenen Varianten untersucht. Dafür wurde aus einem Deletionsstamm (Δ*ctaDI*, Δ*ctaDII,* Δ*ORF4,* Δ*ccoN*) ein rekombinanter Wildtyp (rek. WT) konstruiert. Hierfür wurde der Deletionsstamm mit einem das Gen *ctaDII* tragendem Plasmid ergänzt. *ctaDII* codiert für die erste Untereinheit der aa_3 C*c*O [34]. Diese rek. WT C*c*O wurde mit der natürlich vorkommendem ATCC WT C*c*O (American Type Culture Collection Wildtyp) verglichen. Es wurden keine signifikanten Unterschiede in der C*c*O-Aktivität, der Anzahl der Untereinheiten, dem Vorhandensein aller Metallzentren und der UV/vis-Spektren gefunden, allerdings wies die Katalase Aktivität der rek. WT C*c*O einen 20 fach erhöhten k_{cat} im Vergleich zur ATCC WT C*c*O auf. Daher wurden folgende Punkte untersucht:

- Zuerst wurde der Unterschied zwischen der rek. WT C*c*O und der ATCC WT C*c*O charakterisiert. Die Ausbeute der durch Wasserstoffperoxid induzierten künstlichen katalytischen Intermediate der ATCC WT C*c*O und rek. WT C*c*O wurde mittels UV/vis Spektroskopie gemessen und verglichen. Die deutlich geringere Ausbeute an P-Intermediat der rek. WT C*c*O unterstützt die Befunde der beschriebenen kinetischen Messungen.
  Die Insertion der redox-aktiven Metallzentren in UE I erfolgt co-translational durch die Chaperone Surf1c (Häm-Insertion) und CtaG (Kupfer-Insertion) [39; 99; 162-164]. Die Untereinheit (UE) I der C*c*O ist im rek. WT auf einem Plasmid kodiert. Auch unter Verwendung eines low-copy-Plasmids kommt es potentiell im geringen Maße zu einer Überproduktion dieser Untereinheit. Dies wiederum kann zu einem Mangel an Chaperonen führen. Ein Mangel an Chaperonen könnte zu leichten Änderungen in der Position der Metallzentren bzw. der umgebenden Aminosäuren führen, was ebenfalls die Wassnetzwerke innerhalb des Proteins verändern kann. Diese Hypothese, dass leichte strukturelle Unterschiede und eine geringere Stabilität der rek. WT C*c*O die Ursache für die Unterschiede zwischen der rek. WT C*c*O und der ATCC WT C*c*O sind, konnte mittels Kalorimetrie (DSC) verifiziert werden. DSC-Messungen der ATCC WT C*c*O und der rek. WT C*c*O unterschieden sich direkt nach der Aufreinigung nicht signifikant. Wurde die rek. WT C*c*O allerdings 6 Tage bei -80°C gelagert und drei Einfrier-Auftau-Zyklen

unterzogen, war eine deutliche Abnahme der strukturellen Integrität erkennbar. Die ATCC WT C*c*O zeigte keine Veränderungen unabhängig von Lagerungszeit und Einfrier-Auftau-Zyklen.

Um die vorgeschlagene Hypothese weiter zu prüfen wurde entweder das Gen *ctaG* (Chaperon für den Kupfer-Einbau) oder *surf1c* (Chaperon für den Häm-Einbau) zusammen mit *ctaG* auf dasselbe Plasmid kloniert, welches das Gen für die UE I trägt. Auch für diese neuen Wildtypen wurden die kinetischen Parameter der Katalase Reaktion der C*c*O bestimmt. Es stellte sich heraus, dass mit zunehmender Anzahl der Chaperon-Gene, der k_{cat} um bis zu 50% gegenüber der rek. WT C*c*O reduziert werden kann.

Es wurde ein weiterer Wildtyp (MR3 WT) verwendet, der ein Zwischenstadium zwischen dem ATCC WT und dem rek. WT darstellt. Dieser Wildtyp weist eine Deletion des nicht-exprimierten Gens für die UE I, *ctaDI*, und der Alkylhydroperoxidase, kodiert durch *ORF4,* auf [34; 147-151]. Die C*c*O des MR3 WT zeigt eine gegenüber der ATCC WT C*c*O um den Faktor 18 höheren k_{cat} der Katalasereaktion.

Alle C*c*O kodierenden Gene sind allerdings auf dem Chromosom vorhanden und nicht auf einem Plasmid. Da dieser Wildtyp ausschließlich eine Deletion von *ctaDI* und des Gens für eine Alkylhydroperoxidase zeigt, kann ein regulatorischer Mechanismus eines dieser beiden Gene oder beider Gene postuliert werden.

Verschiedene Arbeitsgruppen zeigten bereits 1991, dass C*c*O unter definierten Umständen eine zweite Konformation einnimmt. Die Untereinheiten I und II weisen in dieser Konformation z.b. weniger starke Interaktionen auf [100; 153; 155].

Zusammenfassend ist eine Kombination aus Mangel an Chaperonen zusammen mit einer Regulation der Expression der ersten Untereinheit durch die Gene *ctaDI* und/oder *ORF4* ein wahrscheinliches Szenario für den Unterschied zwischen der rek. WT C*c*O und der ATCC WT C*c*O. Die fehlende Genregulation, zusammen mit dem Mangel an Chaperonen führt wahrscheinlich zu kleineren strukturellen Änderungen in der Orientierung der Aminosäureseitenketten und dadurch zu einem veränderten Wassernetzwerk. Es ist anzunehmen, dass die rek. WT C*c*O dadurch

schneller in die beschriebene zweite Konformation mit veränderten Interaktionen der Untereinheiten relaxiert. Dies könnte zu einer veränderten Zugänglichkeit des Häm a_3 und einer veränderten Orientierung und Polarisation der Bindung von Wasserstoffperoxid und dadurch zu einer erhöhten Katalaseaktivität führen.

Eine *in vivo* Regulation der *ctaDII* Expression durch *ctaDI* und *ORF4* kann nicht ausgeschlossen werden und könnte eine Möglichkeit sein, die Katalaseaktivität der C*c*O unter bisher unbekannten Umständen gewollt zu erhöhen, z.B. bei hohen Wasserstoffperoxid-Konzentrationen.

- Weiterhin wurde im Rahmen dieser Arbeit der der Katalasereaktion zugrunde liegende Reaktionsmechanismus untersucht. Hierfür wurden zuerst verschiedene Inhibitoren der C*c*O eingesetzt und deren Einfluss auf die Katalaseaktivität der aa_3 C*c*O aus *P. denitrificans* untersucht. Zyanid und Azid führten zu einer nahezu vollständigen Inhibierung der Katalaseaktivität. Dies lässt den Schluss zu, dass das aktive Zentrum der Katalasereaktion eine Häm-Gruppe ist. Da CO keinen inhibierenden Effekt zeigte, konnte ausgeschlossen werden, dass ein reduziertes Häm (Fe^{2+}) Teil eines Intermediates ist. Orii und Okunuki haben 1963 als erste die Bindung von Hydrazin an C*c*O beschrieben. Von der Hocht *et al.* zeigten dann in 2011 die Bindung von Ammoniak an Cu_B. Daher wurde der Einfluss von Ammoniak auf die Katalaseaktivität untersucht um eine Beteiligung von Cu_B zu zeigen oder auszuschließen. Ein Anstieg der Geschwindigkeit der Katalasereaktion auf das etwa 2 fache konnte bei hohen pH-Werten beobachtet werden [58; 97].

  Zusätzlich dazu wurden die Varianten H276D/E/K/R untersucht, welche kein Cu_B mehr enthalten. Da alle Varianten und die WT C*c*O, bei welchem Cu_B durch Ammoniak komplexiert ist, eine erhebliche Katalaseaktivität zeigen, kann geschlossen werden, dass Cu_B für die Katalasereaktion nicht notwendig ist. Weiterhin kann daraus geschlossen werden, dass die UV/vis-Spektren der P- und F-Intermediate, die künstlich durch Zugabe von Wasserstoffperoxid hergestellt worden sind, nebensächlich für die Katalase

Reaktion sind, da diese in keiner Korrelation zu den verschiedenen k_{cat}-Werten der einzelnen WT C*c*Os und der Varianten stehen.

EPR-Spektren der rek. und ATCC WT C*c*O zeigten ein sehr schmales Signal mit einer Breite von 12 G. Dieses Signal konnte einem Porphyrin Radikal zugeordnet werden, wie es auch aus dem Reaktionsmechanismus der Katalasen bekannt ist [70; 109; 110].

Um den Einfluss von aromatischen Aminosäuren in umittelbarer Nähe des aktiven Zentrums weiter zu untersuchen, wurden verschiedene Varianten konstruiert und deren kinetischen Parameter, sowie EPR-Spektren gemessen. Dabei konnten folgende Thesen aufgestellt werden:

Die exakte Position der Aminosäure W164 in Kombination mit der Wasserstoffbrückenbindung zum Häm a_3 ist wahrscheinlich für die Zugänglichkeit des aktiven Zentrums wichtig.

Die Wasserstoffbrückenbindung [18; 44] zwischen W272 und Y167 ist essentiell, entweder für die Positionierung der Aminosäuren oder um das Wasserstoffperoxid zu positionieren und/oder zu polarisieren. Wird eine dieser Aminosäuren mutiert, kommt es in beiden Fällen zu ähnlichen Abnahmen in der Katalase Aktivität. Weiterhin könnten Mutationen einer der beiden Aminosäuren die Zugänglichkeit des aktiven Zentrums für Wasserstoffperoxid verändern.

Wird die Aminosäure Y280 verändert, so nimmt, wahrscheinlich, die Flexibilität von H276 zu, welches kovalent an Y280 gebunden ist. Diese erhöhte Flexibilität wiederum sorgt für den Verlust von Cu_B, wodurch die verbleibenden zwei Kupfer-Ionen komplexierenden Aminosäuren zusammen mit H276 in der Lage sind entweder das Produkt und/oder das Edukt der Katalase Reaktion zu komplexieren. Dadurch verringert sich der k_{cat} der Katalase Reaktion.

Der Sauerstoff, der während der Katalase Reaktion entsteht, kann entweder das Produkt eines einzigen Wasserstoffperoxidmoleküls sein, oder aber es könnte eine Mischung von je einem Sauerstoffatom aus beiden Wasserperoxidmolekülen sein. Diese Frage wurde durch Gaschromatographie-Massenspektrometrie-Experimenten mit einer Edukt-Mischung aus $H_2{}^{16}O_2$ und $H_2{}^{18}O_2$ beantwortet. Es konnte gezeigt werden,

dass der entstehende Sauerstoff aus einem Molekül Wasserstoffperoxid generiert wird. Zusammenfassed kann folgender Mechanismus postuliert werden:

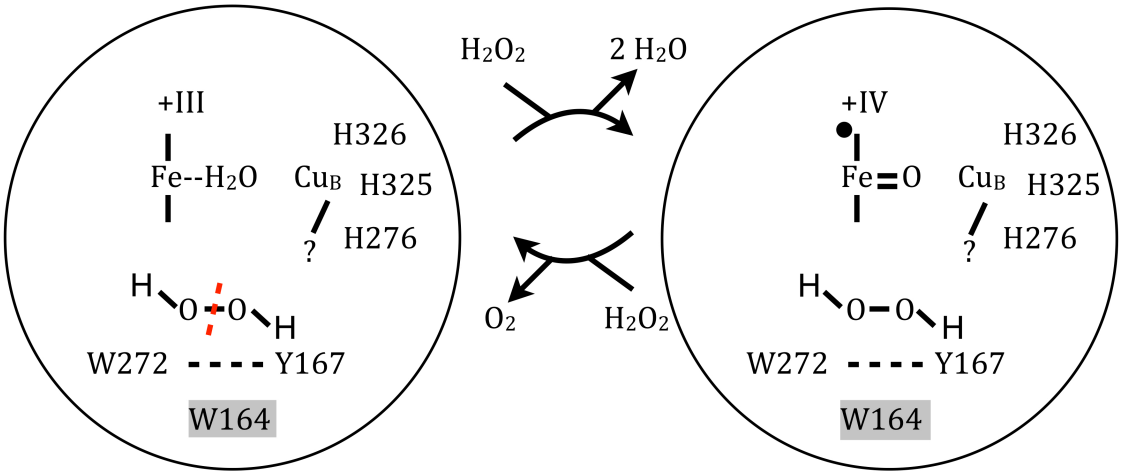

Figure 5.2: Wahrscheinlicher Katalase Mechanismus der aa_3 C*c*O.
Das erste Wasserstoffperoxidmolekül führt zur Freisetzung des gebundenen Wassers und reagiert zu einem weiteren Wassermolekül und einem Oxoferrylzustand. Das zweite Molekül reagiert zu molekularem Sauerstoff. Die Protonen reagieren mit dem Oxoferryl Sauerstoff zu Wasser.

Werden die Reaktionsgeschwindigkeiten der Katalase Aktivität der aa_3 C*c*O aus *P. denitrificans* mit der Reaktionsgeschwindigkeit der Katalase [63] verglichen, so ist eine physiologische Bedeutung dieser Reaktion fraglich. Bedenkt man nun aber das Vorkommen der C*c*O in Superkomplexen, die zwei Kopien Komplex I, eine Kopie Komplex III und eine Kopie Komplex IV enthalten, so wird die physiologische Relevanz dieser Reaktion offensichtlicher. Es konnte bereits sowohl für Komplex I als auch für Komplex III gezeigt werden, dass beide Komplexe reaktive Sauerstoff Spezies generieren [22; 64; 65; 131-133]. Daher könnte eine C*c*O, die in der Lage ist, Wasserstoffperoxid direkt im Superkomplex abzubauen sinnvoll sein. Weiterhin können klassische Katalasen nur auf den gegenüberliegenden Seiten der Membran, also im Falle von *P. denitrificans* im Periplasma und Cytoplasma, vorkommen, nicht jedoch innerhalb der Membran. Ein membrangebundenes Protein mit Katalase Aktivität würde daher den Organismus vor Wasserstoffperoxid in der Membran schützen und Effekte, wie z.B. die Oxidation von Lipiden, vermindern.

Zusammenfassend ist zu sagen, dass der Unterschied zwischen der rek. WT C*c*O und der ATCC WT C*c*O auf eine Kombination eines Chaperonmangels und einer fehlenden, wahrscheinlichen Regulation durch *ctaDI* und/oder *ORF4* zurückzuführen ist. Weiterhin konnte im Rahmen dieser Arbeit ein Reaktionsmechanismus für die Katalase Aktivität der aa_3 C*c*O aus *P. denitirifcans* postuliert werden. Es konnte ebenfalls über eine physiologische Relevanz dieser Nebenreaktion spekuliert werden.

6. References

[1] D. L. Nelson and M. M. Cox (1982). Lehninger, Principles of Biochemistry, Worth Publishers.

[2] T. Kenakin (1997), Differences between natural and recombinant G protein-coupled receptor systems with varying receptor/G protein stoichiometry, *Trends Pharmacol Sci*, **18**, 456-464.

[3] S. Butenas, J. Krudysz-Amblo and K. G. Mann (2010), Posttranslational modifications and activity of natural and recombinant tissue factor, *Thromb Res*, **125 Suppl 1**, S26-28.

[4] O. A. Neumüller (1979). Römpps Chemie-Lexikon. Stuttgart, Frankh.

[5] P. Mitchell (1961), Coupling of phosphorylation to electron and hydrogen transfer by a chemi-osmotic type of mechanism, *Nature*, **191**, 144-148.

[6] C. von Ballmoos, A. Wiedenmann and P. Dimroth (2009), Essentials for ATP synthesis by F1F0 ATP synthases, *Annu Rev Biochem*, **78**, 649-672.

[7] D. Okuno, R. Iino and H. Noji (2011), Rotation and structure of FoF1-ATP synthase, *J Biochem*, **149**, 655-664.

[8] Y. Hatefi and D. L. Stiggal (1976). Metal-Containing Flavoprotein Dehydrogenases. New York, Academic Press.

[9] Y. Hatefi (1985), The mitochondrial electron transport and oxidative phosphorylation system, *Annu Rev Biochem*, **54**, 1015-1069.

[10] J. F. Turrens (1997), Superoxide production by the mitochondrial respiratory chain, *Biosci Rep*, **17**, 3-8.

[11] U. Brandt (2006), Energy converting NADH:quinone oxidoreductase (complex I), *Annu Rev Biochem*, **75**, 69-92.

[12] L. A. Sazanov and P. Hinchliffe (2006), Structure of the hydrophilic domain of respiratory complex I from Thermus thermophilus, *Science*, **311**, 1430-1436.

[13] Y. Hatefi, A. G. Haavik and D. E. Griffiths (1961), Reconstitution of the electron transport system. I. Preparation and properties of the interacting enzyme complexes, *Biochem Biophys Res Commun*, **4**, 441-446.

[14] O. Warburg (1924), Über Eisen, den sauerstoffübertragenden Bestandteil des Atmungsfermentes., *Biochemische Zeitschrift*, 16.

[15] M. Saraste (1990), Structural features of cytochrome oxidase, *Q Rev Biophys*, **23**, 331-366.

[16] G. T. Babcock and M. Wikstrom (1992), Oxygen activation and the conservation of energy in cell respiration, *Nature*, **356**, 301-309.

[17] M. W. Calhoun, J. W. Thomas and R. B. Gennis (1994), The cytochrome oxidase superfamily of redox-driven proton pumps, *Trends Biochem Sci*, **19**, 325-330.

[18] S. Iwata, C. Ostermeier, B. Ludwig and H. Michel (1995), Structure at 2.8 A resolution of cytochrome c oxidase from Paracoccus denitrificans, *Nature*, **376**, 660-669.

[19] F. Malatesta, G. Antonini, P. Sarti and M. Brunori (1995), Structure and function of a molecular machine: cytochrome c oxidase, *Biophys Chem*, **54**, 1-33.

[20] S. Ferguson-Miller and G. T. Babcock (1996), Heme/Copper Terminal Oxidases, *Chem Rev*, **96**, 2889-2908.

[21] C. Ostermeier, S. Iwata and H. Michel (1996), Cytochrome c oxidase, *Curr Opin Struct Biol*, **6**, 460-466.

[22] M. D. Brand (2010), The sites and topology of mitochondrial superoxide production, *Exp Gerontol*, **45**, 466-472.

[23] J. W. de Gier, M. Lubben, W. N. Reijnders, C. A. Tipker, D. J. Slotboom, R. J. van Spanning, A. H. Stouthamer and J. van der Oost (1994), The terminal oxidases of Paracoccus denitrificans, *Mol Microbiol*, **13**, 183-196.

[24] T. Tsukihara, H. Aoyama, E. Yamashita, T. Tomizaki, H. Yamaguchi, K. Shinzawa-Itoh, R. Nakashima, R. Yaono and S. Yoshikawa (1996), The whole structure of the 13-subunit oxidized cytochrome c oxidase at 2.8 A, *Science*, **272**, 1136-1144.

[25] S. Buschmann, E. Warkentin, H. Xie, J. D. Langer, U. Ermler and H. Michel (2010), The structure of cbb3 cytochrome oxidase provides insights into proton pumping, *Science*, **329**, 327-330.

[26] T. Tiefenbrunn, W. Liu, Y. Chen, V. Katritch, C. D. Stout, J. A. Fee and V. Cherezov (2011), High resolution structure of the ba3 cytochrome c oxidase from Thermus thermophilus in a lipidic environment, *PLoS One*, **6**, e22348.

[27] G. Buse, T. Soulimane, M. Dewor, H. E. Meyer and M. Bluggel (1999), Evidence for a copper-coordinated histidine-tyrosine cross-link in the active site of cytochrome oxidase, *Protein Sci*, **8**, 985-990.

[28] D. A. Berthold, M. E. Andersson and P. Nordlund (2000), New insight into the structure and function of the alternative oxidase, *Biochim Biophys Acta*, **1460**, 241-254.

[29] M. S. Albury, C. Elliott and A. L. Moore (2009), Towards a structural elucidation of the alternative oxidase in plants, *Physiol Plant*, **137**, 316-327.

[30] V. B. Borisov, R. B. Gennis, J. Hemp and M. I. Verkhovsky (2011), The cytochrome bd respiratory oxygen reductases, *Biochim Biophys Acta*, **1807**, 1398-1413.

[31] F. L. Sousa, R. J. Alves, M. A. Ribeiro, J. B. Pereira-Leal, M. Teixeira and M. M. Pereira (2012), The superfamily of heme-copper oxygen reductases: types and evolutionary considerations, *Biochim Biophys Acta*, **1817**, 629-637.

[32] J. van der Oost, A. P. de Boer, J. W. de Gier, W. G. Zumft, A. H. Stouthamer and R. J. van Spanning (1994), The heme-copper oxidase family consists of three distinct types of terminal oxidases and is related to nitric oxide reductase, *FEMS Microbiol Lett*, **121**, 1-9.

[33] B. Ludwig (1992), Terminal oxidases in Paracoccus denitrificans, *Biochim Biophys Acta*, **1101**, 195-197.

[34] M. Raitio, J. M. Pispa, T. Metso and M. Saraste (1990), Are there isoenzymes of cytochrome c oxidase in Paracoccus denitrificans?, *FEBS Lett*, **261**, 431-435.

[35] M. Raitio, T. Jalli and M. Saraste (1987), Isolation and analysis of the genes for cytochrome c oxidase in Paracoccus denitrificans, *Embo J*, **6**, 2825-2833.

[36] P. Steinrucke, G. C. Steffens, G. Panskus, G. Buse and B. Ludwig (1987), Subunit II of cytochrome c oxidase from Paracoccus denitrificans. DNA sequence, gene expression and the protein, *Eur J Biochem*, **167**, 431-439.

[37] J. Cao, J. Shapleigh, R. Gennis, A. Revzin and S. Ferguson-Miller (1991), The gene encoding cytochrome c oxidase subunit II from Rhodobacter sphaeroides; comparison of the deduced amino acid sequence with sequences of corresponding peptides from other species, *Gene*, **101**, 133-137.

[38] O. M. Richter and B. Ludwig (2009), Electron transfer and energy transduction in the terminal part of the respiratory chain - lessons from bacterial model systems, *Biochim Biophys Acta*, **1787**, 626-634.

[39] F. A. Bundschuh, K. Hoffmeier and B. Ludwig (2008), Two variants of the assembly factor Surf1 target specific terminal oxidases in Paracoccus denitrificans, *Biochim Biophys Acta*, **1777**, 1336-1343.

[40] H. Witt and B. Ludwig (1997), Isolation, analysis, and deletion of the gene coding for subunit IV of cytochrome c oxidase in Paracoccus denitrificans, *J Biol Chem*, **272**, 5514-5517.

[41] C. Kulajta, J. O. Thumfart, S. Haid, F. Daldal and H. G. Koch (2006), Multi-step assembly pathway of the cbb3-type cytochrome c oxidase complex, *J Mol Biol*, **355**, 989-1004.

[42] U. Pfitzner, A. Odenwald, T. Ostermann, L. Weingard, B. Ludwig and O. M. Richter (1998), Cytochrome c oxidase (heme aa3) from Paracoccus denitrificans: analysis of mutations in putative proton channels of subunit I, *J Bioenerg Biomembr*, **30**, 89-97.

[43] L. O. Essen, A. Harrenga, C. Ostermeier and H. Michel (2003), 1.3 A X-ray structure of an antibody Fv fragment used for induced membrane-protein crystallization, *Acta Crystallogr D Biol Crystallogr*, **59**, 677-687.

[44] J. Koepke, E. Olkhova, H. Angerer, H. Muller, G. Peng and H. Michel (2009), High resolution crystal structure of Paracoccus denitrificans cytochrome c oxidase: new insights into the active site and the proton transfer pathways, *Biochim Biophys Acta*, **1787**, 635-645.

[45] V. Sharma, M. Wikstrom and V. R. Kaila (2012), Dynamic water networks in cytochrome cbb(3) oxidase, *Biochim Biophys Acta*, **1817**, 726-734.

[46] M. Wikstrom (1981), Energy-dependent reversal of the cytochrome oxidase reaction, *Proc Natl Acad Sci U S A*, **78**, 4051-4054.

[47] T. Ogura and T. Kitagawa (2004), Resonance Raman characterization of the P intermediate in the reaction of bovine cytochrome c oxidase, *Biochim Biophys Acta*, **1655**, 290-297.

[48] M. Wikstrom (1989), Identification of the electron transfers in cytochrome oxidase that are coupled to proton-pumping, *Nature*, **338**, 776-778.

[49] H. Michel (1999), Cytochrome c oxidase: catalytic cycle and mechanisms of proton pumping--a discussion, *Biochemistry*, **38**, 15129-15140.

[50] R. Mitchell and P. R. Rich (1994), Proton uptake by cytochrome c oxidase on reduction and on ligand binding, *Biochim Biophys Acta*, **1186**, 19-26.

[51] T. Yonetani and T. Asakura (1968), Studies on cytochrome c peroxidase. XII. Crystalline synthetic enzymes containing unnatural heme prosthetic groups, *J Biol Chem*, **243**, 4715-4721.

[52] A. Deisseroth and A. L. Dounce (1970), Catalase: Physical and chemical properties, mechanism of catalysis, and physiological role, *Physiol Rev*, **50**, 319-375.

[53] C. D. Putnam, A. S. Arvai, Y. Bourne and J. A. Tainer (2000), Active and inhibited human catalase structures: ligand and NADPH binding and catalytic mechanism, *J Mol Biol*, **296**, 295-309.

[54] V. S. Jasion, J. A. Polanco, Y. T. Meharenna, H. Li and T. L. Poulos (2011), Crystal structure of Leishmania major peroxidase and characterization of the compound i tryptophan radical, *J Biol Chem*, **286**, 24608-24615.

[55] K. Dalziel and J. R. O'Brien (1954), Spectrophotometric studies of the reaction of methaemoglobin with hydrogen peroxide. 1. The formation of methaemoglobin-hydrogen peroxide, *Biochem J*, **56**, 648-659.

[56] X. J. Zhao, V. Sampath and W. S. Caughey (1995), Cytochrome c oxidase catalysis of the reduction of nitric oxide to nitrous oxide, *Biochem Biophys Res Commun*, **212**, 1054-1060.

[57] L. Paco, A. Galarneau, J. Drone, F. Fajula, C. Bailly, S. Pulvin and D. Thomas (2009), Catalase-like activity of bovine met-hemoglobin: interaction with the pseudo-catalytic peroxidation of anthracene traces in aqueous medium, *Biotechnol J*, **4**, 1460-1470.

[58] Y. Orii and K. Okunuki (1963), Studies on Cytochrome A. X. Effect of Hydrogen Peroxide on Absorption Spectra of Cytochrome A, *J Biochem*, **54**, 207-213.

[59] Y. Orii (1982), The cytochrome c peroxidase activity of cytochrome oxidase, *J Biol Chem*, **257**, 9246-9248.

[60] A. A. Konstantinov, N. Capitanio, T. V. Vygodina and S. Papa (1992), pH changes associated with cytochrome c oxidase reaction with H2O2. Protonation state of the peroxy and oxoferryl intermediates, *FEBS Lett*, **312**, 71-74.

[61] A. A. Konstantinov, T. Vygodina, N. Capitanio and S. Papa (1998), Ferrocyanide-peroxidase activity of cytochrome c oxidase, *Biochim Biophys Acta*, **1363**, 11-23.

[62] I. A. Bolshakov, T. V. Vygodina, R. Gennis, A. A. Karyakin and A. A. Konstantinov (2010), Catalase activity of cytochrome C oxidase assayed with hydrogen peroxide-sensitive electrode microsensor, *Biochemistry (Mosc)*, **75**, 1352-1360.

[63] G. Adam, P. Läuger and G. Stark (1977). Physikalische Chemie und Biophysik, Springer Verlag.

[64] T. Althoff, D. J. Mills, J. L. Popot and W. Kuhlbrandt (2011), Arrangement of electron transport chain components in bovine mitochondrial supercomplex I1III2IV1, *Embo J*, **30**, 4652-4664.

[65] G. Lenaz and M. L. Genova (2009), Structural and functional organization of the mitochondrial respiratory chain: a dynamic super-assembly, *Int J Biochem Cell Biol*, **41**, 1750-1772.

[66] R. W. Gracy, J. M. Talent, Y. Kong and C. C. Conrad (1999), Reactive oxygen species: the unavoidable environmental insult?, *Mutat Res*, **428**, 17-22.

[67] A. L. Tappel (1970), Biological antioxidant protection against lipid peroxidation damage, *Am J Clin Nutr*, **23**, 1137-1139.

[68] H. Kappus and H. Sies (1981), Toxic drug effects associated with oxygen metabolism: redox cycling and lipid peroxidation, *Experientia*, **37**, 1233-1241.

[69] T. Yonetani and T. Asakura (1968), Studies on cytochrome c peroxidase. XI. A crystalline enzyme reconstituted from apoenzyme and manganese protoporphyrin IX, *J Biol Chem*, **243**, 3996-3998.

[70] I. Fita and M. G. Rossmann (1985), The active center of catalase, *J Mol Biol*, **185**, 21-37.

[71] K. Budiman, A. Kannt, S. Lyubenova, O. M. Richter, B. Ludwig, H. Michel and F. MacMillan (2004), Tyrosine 167: the origin of the radical species observed in the reaction of cytochrome c oxidase with hydrogen peroxide in Paracoccus denitrificans, *Biochemistry*, **43**, 11709-11716.

[72] H. Angerer (2008). Functional and Structural Studies on the Atmungsferment Cytochrome *c* Oxidase from *Paracoccus denitrificans*. Fachbereich 14. Frankfurt am Main, Johann Wolfgang Goethe-Universität. **Dr. phil. nat.**

[73] G. Kleymann, C. Ostermeier, K. Heitmann, W. Haase and H. Michel (1995), Use of antibody fragments (Fv) in immunocytochemistry, *J Histochem Cytochem*, **43**, 607-614.

[74] D. Hanahan (1983), Studies on transformation of Escherichia coli with plasmids, *J Mol Biol*, **166**, 557-580.

[75] M. G. Marinus, M. Carraway, A. Z. Frey, L. Brown and J. A. Arraj (1983), Insertion mutations in the dam gene of Escherichia coli K-12, *Mol Gen Genet*, **192**, 288-289.

[76] J. Grodberg and J. J. Dunn (1988), ompT encodes the Escherichia coli outer membrane protease that cleaves T7 RNA polymerase during purification, *J Bacteriol*, **170**, 1245-1253.

[77] J. Sambrook and D. W. Russell (2001). Molecular Cloning: ALaboratory Manual, Cold Spring Harbor Laboratory Press.

[78] F. Sanger, S. Nicklen and A. R. Coulson (1977), DNA sequencing with chain-terminating inhibitors, *Proc Natl Acad Sci U S A*, **74**, 5463-5467.

[79] E. Gerhus, P. Steinrucke and B. Ludwig (1990), Paracoccus denitrificans cytochrome c1 gene replacement mutants, *J Bacteriol*, **172**, 2392-2400.

[80] G. Bertani (1951), Studies on lysogenesis. I. The mode of phage liberation by lysogenic Escherichia coli, *J Bacteriol*, **62**, 293-300.

[81] B. Ludwig (1986), Cytochrome c oxidase from Paracoccus denitrificans, *Methods Enzymol*, **126**, 153-159.

[82] M. Fabian and G. Palmer (1995), The interaction of cytochrome oxidase with hydrogen peroxide: the relationship of compounds P and F, *Biochemistry*, **34**, 13802-13810.

[83] J. J. Sedmak and S. E. Grossberg (1977), A rapid, sensitive, and versatile assay for protein using Coomassie brilliant blue G250, *Anal Biochem*, **79**, 544-552.

[84] P. K. Smith, R. I. Krohn, G. T. Hermanson, A. K. Mallia, F. H. Gartner, M. D. Provenzano, E. K. Fujimoto, N. M. Goeke, B. J. Olson and D. C. Klenk (1985), Measurement of protein using bicinchoninic acid, *Anal Biochem*, **150**, 76-85.

[85] E. Garman (1999), Leaving no element of doubt: analysis of proteins using microPIXE, *Structure*, **7**, R291-299.

[86] E. F. Garman and G. W. Grime (2005), Elemental analysis of proteins by microPIXE, *Prog Biophys Mol Biol*, **89**, 173-205.

[87] M. Lubben and K. Morand (1994), Novel prenylated hemes as cofactors of cytochrome oxidases. Archaea have modified hemes A and O, *J Biol Chem*, **269**, 21473-21479.

[88] A. E. Frazier and D. R. Thorburn (2012), Biochemical analyses of the electron transport chain complexes by spectrophotometry, *Methods Mol Biol*, **837**, 49-62.

[89] J. N. Lin and H. K. Kao (1998), Effect of oxidative stress caused by hydrogen peroxide on senescence of rice leaves, *Bot. Bull. Acad. Sin.*, 5.

[90] N. Ramsing and J. Gundersen Seawater and Gases, Unisense.

[91] G. Alberta. "Human Metabolome Database." from http://hmdb.ca/metabolites/HMDB06901.

[92] L. Michaelis and M. L. Menten (1913), Die Kinetik der Invertinwirkung, *Biochem. Z.*, 37.

[93] H. Lineweaver and D. Burk (1934), The Determination of Enzyme Dissociation Constants, *Journal of the American Chemical Society*, **3**, 9.

[94] E. Antonini, M. Brunori, A. Colosimo, C. Greenwood and M. T. Wilson (1977), Oxygen "pulsed" cytochrome c oxidase: functional properties and catalytic relevance, *Proc Natl Acad Sci U S A*, **74**, 3128-3132.

[95] J. K. Reichardt and Q. H. Gibson (1983), Turnover of cytochrome c oxidase from Paracoccus denitrificans, *J Biol Chem*, **258**, 1504-1507.

[96] S. E. Brand, S. Rajagukguk, K. Ganesan, L. Geren, M. Fabian, D. Han, R. B. Gennis, B. Durham and F. Millett (2007), A new ruthenium complex to study single-electron reduction of the pulsed O(H) state of detergent-solubilized cytochrome oxidase, *Biochemistry*, **46**, 14610-14618.

[97] I. von der Hocht, J. H. van Wonderen, F. Hilbers, H. Angerer, F. Macmillan and H. Michel (2011), Interconversions of P and F intermediates of cytochrome c oxidase from Paracoccus denitrificans, *Proc Natl Acad Sci U S A*, **108**, 3964-3969.

[98] C. R. Hartzell and H. Beinert (1974), Components of cytochrome c oxidase detectable by EPR spectroscopy, *Biochim Biophys Acta*, **368**, 318-338.

[99] P. Greiner, A. Hannappel, C. Werner and B. Ludwig (2008), Biogenesis of cytochrome c oxidase--in vitro approaches to study cofactor insertion into a bacterial subunit I, *Biochim Biophys Acta*, **1777**, 904-911.

[100] T. Haltia, N. Semo, J. L. Arrondo, F. M. Goni and E. Freire (1994), Thermodynamic and structural stability of cytochrome c oxidase from Paracoccus denitrificans, *Biochemistry*, **33**, 9731-9740.

[101] T. V. Vygodina and A. A. Konstantinov (1988), H2O2-induced conversion of cytochrome c oxidase peroxy complex to oxoferryl state, *Ann N Y Acad Sci*, **550**, 124-138.

[102] M. Ksenzenko, T. V. Vygodina, V. Berka, E. K. Ruuge and A. A. Konstantinov (1992), Cytochrome oxidase-catalyzed superoxide generation from hydrogen peroxide, *FEBS Lett*, **297**, 63-66.

[103] A. A. Konstantinov (1998), Cytochrome c oxidase as a proton-pumping peroxidase: reaction cycle and electrogenic mechanism, *J Bioenerg Biomembr*, **30**, 121-130.

[104] K. U. Ingold, T. Paul and M. J. Young (1997), Invention of the first azo compound to serve as a superoxide thermal source under physiological conditions: Concept, synthesis, and chemical properties., *J Am Chem Soc*, 2.

[105] M. Fabian, W. W. Wong, R. B. Gennis and G. Palmer (1999), Mass spectrometric determination of dioxygen bond splitting in the "peroxy"

intermediate of cytochrome c oxidase, *Proc Natl Acad Sci U S A*, **96**, 13114-13117.

[106] S. Junemann, P. Heathcote and P. R. Rich (2000), The reactions of hydrogen peroxide with bovine cytochrome c oxidase, *Biochim Biophys Acta*, **1456**, 56-66.

[107] R. C. Jarnagin and J. H. Wang (1958), Investigation of the Catalytic Mechanism of Catalase and Other Ferric Compounds with Doubly O-labeled Hydrogen Peroxide, *J Am Chem Soc*, **4**, 2.

[108] J. Vlasits, C. Jakopitsch, M. Schwanninger, P. Holubar and C. Obinger (2007), Hydrogen peroxide oxidation by catalase-peroxidase follows a non-scrambling mechanism, *FEBS Lett*, **581**, 320-324.

[109] S. E. Rigby, S. Junemann, P. R. Rich and P. Heathcote (2000), Reaction of bovine cytochrome c oxidase with hydrogen peroxide produces a tryptophan cation radical and a porphyrin cation radical, *Biochemistry*, **39**, 5921-5928.

[110] P. R. Rich, S. E. Rigby and P. Heathcote (2002), Radicals associated with the catalytic intermediates of bovine cytochrome c oxidase, *Biochim Biophys Acta*, **1554**, 137-146.

[111] D. M. Mitchell, J. R. Fetter, D. A. Mills, P. Adelroth, M. A. Pressler, Y. Kim, R. Aasa, P. Brzezinski, B. G. Malmstrom, J. O. Alben, G. T. Babcock, S. Ferguson-Miller and R. B. Gennis (1996), Site-directed mutagenesis of residues lining a putative proton transfer pathway in cytochrome c oxidase from Rhodobacter sphaeroides, *Biochemistry*, **35**, 13089-13093.

[112] V. Drosou, F. Malatesta and B. Ludwig (2002), Mutations in the docking site for cytochrome c on the Paracoccus heme aa3 oxidase. Electron entry and kinetic phases of the reaction, *Eur J Biochem*, **269**, 2980-2988.

[113] C. Ostermeier, A. Harrenga, U. Ermler and H. Michel (1997), Structure at 2.7 A resolution of the Paracoccus denitrificans two-subunit cytochrome c oxidase complexed with an antibody FV fragment, *Proc Natl Acad Sci U S A*, **94**, 10547-10553.

[114] J. M. Wrigglesworth (1984), Formation and reduction of a 'peroxy' intermediate of cytochrome c oxidase by hydrogen peroxide, *Biochem J*, **217**, 715-719.

[115] M. Wikstrom (2012), Active site intermediates in the reduction of O(2) by cytochrome oxidase, and their derivatives, *Biochim Biophys Acta*, **1817**, 468-475.

[116] T. V. Vygodina, C. Pecoraro, D. Mitchell, R. Gennis and A. A. Konstantinov (1998), Mechanism of inhibition of electron transfer by amino acid

replacement K362M in a proton channel of Rhodobacter sphaeroides cytochrome c oxidase, *Biochemistry*, **37**, 3053-3061.

[117] T. V. Vygodina, W. Zakirzianova and A. A. Konstantinov (2008), Inhibition of membrane-bound cytochrome c oxidase by zinc ions: high-affinity Zn2+-binding site at the P-side of the membrane, *FEBS Lett*, **582**, 4158-4162.

[118] H. J. H. Fenton (1894), Oxidation of tartaric acid in presence of iron, *J. Chem. Soc. Trans.*, **65**, 13.

[119] Q. H. Gibson, G. Palmer and D. C. Wharton (1965), The Binding of Carbon Monoxide by Cytochrome C Oxidase and the Ratio of the Cytochromes a and A3, *J Biol Chem*, **240**, 915-920.

[120] P. Hellwig, A. Bohm, U. Pfitzner, W. Mantele and B. Ludwig (2008), Spectroscopic study on the communication between a heme a3 propionate, Asp399 and the binuclear center of cytochrome c oxidase from Paracoccus denitrificans, *Biochim Biophys Acta*, **1777**, 220-226.

[121] A. Elmgren, R. Mollicone, M. Costache, C. Borjeson, R. Oriol, J. Harrington and G. Larson (1997), Significance of individual point mutations, T202C and C314T, in the human Lewis (FUT3) gene for expression of Lewis antigens by the human alpha(1,3/1,4)-fucosyltransferase, Fuc-TIII, *J Biol Chem*, **272**, 21994-21998.

[122] V. V. Petrov (2010), Point mutations in Pma1 H+-ATPase of Saccharomyces cerevisiae: influence on its expression and activity, *Biochemistry (Mosc)*, **75**, 1055-1063.

[123] F. MacMillan, K. Budiman, H. Angerer and H. Michel (2006), The role of tryptophan 272 in the Paracoccus denitrificans cytochrome c oxidase, *FEBS Lett*, **580**, 1345-1349.

[124] M. Zamocky, P. G. Furtmuller and C. Obinger (2008), Evolution of catalases from bacteria to humans, *Antioxid Redox Signal*, **10**, 1527-1548.

[125] M. A. Yu, T. Egawa, K. Shinzawa-Itoh, S. Yoshikawa, V. Guallar, S. R. Yeh, D. L. Rousseau and G. J. Gerfen (2012), Two tyrosyl radicals stabilize high oxidation states in cytochrome C oxidase for efficient energy conservation and proton translocation, *Journal of the American Chemical Society*, **134**, 4753-4761.

[126] M. R. Murthy, T. J. Reid, 3rd, A. Sicignano, N. Tanaka and M. G. Rossmann (1981), Structure of beef liver catalase, *J Mol Biol*, **152**, 465-499.

[127] J. Bravo, M. J. Mate, T. Schneider, J. Switala, K. Wilson, P. C. Loewen and I. Fita (1999), Structure of catalase HPII from Escherichia coli at 1.9 A resolution, *Proteins*, **34**, 155-166.

[128] M. Azizov Iu, G. I. Likhtenshtein and A. P. Purmal (1972), [Binuclear structure of the active center of catalase], *Biokhimiia*, **37**, 620-628.

[129] P. Chelikani, I. Fita and P. C. Loewen (2004), Diversity of structures and properties among catalases, *Cell Mol Life Sci*, **61**, 192-208.

[130] P. Chelikani, X. Carpena, I. Fita and P. C. Loewen (2003), An electrical potential in the access channel of catalases enhances catalysis, *J Biol Chem*, **278**, 31290-31296.

[131] A. Stroh, O. Anderka, K. Pfeiffer, T. Yagi, M. Finel, B. Ludwig and H. Schagger (2004), Assembly of respiratory complexes I, III, and IV into NADH oxidase supercomplex stabilizes complex I in Paracoccus denitrificans, *J Biol Chem*, **279**, 5000-5007.

[132] N. V. Dudkina, R. Kouril, K. Peters, H. P. Braun and E. J. Boekema (2010), Structure and function of mitochondrial supercomplexes, *Biochim Biophys Acta*, **1797**, 664-670.

[133] S. J. Ramirez-Aguilar, M. Keuthe, M. Rocha, V. V. Fedyaev, K. Kramp, K. J. Gupta, A. G. Rasmusson, W. X. Schulze and J. T. van Dongen (2011), The composition of plant mitochondrial supercomplexes changes with oxygen availability, *J Biol Chem*, **286**, 43045-43053.

[134] B. H. Bielski, Allen, A. O. (1977), Mechanism of the Disproportionation of Superoxide Radicals, *The Journal of Physical Chemistry*, **81**, 3.

[135] D. H. Flint, J. F. Tuminello and M. H. Emptage (1993), The inactivation of Fe-S cluster containing hydro-lyases by superoxide, *J Biol Chem*, **268**, 22369-22376.

[136] C. C. Winterbourn and D. Metodiewa (1999), Reactivity of biologically important thiol compounds with superoxide and hydrogen peroxide, *Free Radic Biol Med*, **27**, 322-328.

[137] P. Rai, T. D. Cole, D. E. Wemmer and S. Linn (2001), Localization of Fe(2+) at an RTGR sequence within a DNA duplex explains preferential cleavage by Fe(2+) and H2O2, *J Mol Biol*, **312**, 1089-1101.

[138] J. A. Imlay (2003), Pathways of oxidative damage, *Annu Rev Microbiol*, **57**, 395-418.

[139] B. H. Bielski, R. L. Arudi and M. W. Sutherland (1983), A study of the reactivity of HO2/O2- with unsaturated fatty acids, *J Biol Chem*, **258**, 4759-4761.

[140] L. C. Seaver and J. A. Imlay (2001), Hydrogen peroxide fluxes and compartmentalization inside growing Escherichia coli, *J Bacteriol*, **183**, 7182-7189.

[141] L. C. Seaver and J. A. Imlay (2001), Alkyl hydroperoxide reductase is the primary scavenger of endogenous hydrogen peroxide in Escherichia coli, *J Bacteriol*, **183**, 7173-7181.

[142] G. Deckert, P. V. Warren, T. Gaasterland, W. G. Young, A. L. Lenox, D. E. Graham, R. Overbeek, M. A. Snead, M. Keller, M. Aujay, R. Huber, R. A. Feldman, J. M. Short, G. J. Olsen and R. V. Swanson (1998), The complete genome of the hyperthermophilic bacterium Aquifex aeolicus, *Nature*, **392**, 353-358.

[143] A. L. Umbach, F. Fiorani and J. N. Siedow (2005), Characterization of transformed Arabidopsis with altered alternative oxidase levels and analysis of effects on reactive oxygen species in tissue, *Plant Physiol*, **139**, 1806-1820.

[144] T. Magnani, F. M. Soriani, V. P. Martins, A. M. Nascimento, V. G. Tudella, C. Curti and S. A. Uyemura (2007), Cloning and functional expression of the mitochondrial alternative oxidase of Aspergillus fumigatus and its induction by oxidative stress, *FEMS Microbiol Lett*, **271**, 230-238.

[145] Q. Li, Z. Bai, A. O'Donnell, L. M. Harvey, P. A. Hoskisson and B. McNeil (2011), Oxidative stress in fungal fermentation processes: the roles of alternative respiration, *Biotechnol Lett*, **33**, 457-467.

[146] V. P. Martins, T. M. Dinamarco, F. M. Soriani, V. G. Tudella, S. C. Oliveira, G. H. Goldman, C. Curti and S. A. Uyemura (2011), Involvement of an alternative oxidase in oxidative stress and mycelium-to-yeast differentiation in Paracoccidioides brasiliensis, *Eukaryot Cell*, **10**, 237-248.

[147] D. R. Sherman, K. Mdluli, M. J. Hickey, C. E. Barry, 3rd and C. K. Stover (1999), AhpC, oxidative stress and drug resistance in Mycobacterium tuberculosis, *Biofactors*, **10**, 211-217.

[148] P. J. Hillas, F. S. del Alba, J. Oyarzabal, A. Wilks and P. R. Ortiz De Montellano (2000), The AhpC and AhpD antioxidant defense system of Mycobacterium tuberculosis, *J Biol Chem*, **275**, 18801-18809.

[149] A. Koshkin, C. M. Nunn, S. Djordjevic and P. R. Ortiz de Montellano (2003), The mechanism of Mycobacterium tuberculosis alkylhydroperoxidase AhpD as defined by mutagenesis, crystallography, and kinetics, *J Biol Chem*, **278**, 29502-29508.

[150] A. Koshkin, G. M. Knudsen and P. R. Ortiz De Montellano (2004), Intermolecular interactions in the AhpC/AhpD antioxidant defense system of Mycobacterium tuberculosis, *Arch Biochem Biophys*, **427**, 41-47.

[151] A. Koshkin, X. T. Zhou, C. N. Kraus, J. M. Brenner, P. Bandyopadhyay, I. D. Kuntz, C. E. Barry, 3rd and P. R. Ortiz de Montellano (2004), Inhibition of

Mycobacterium tuberculosis AhpD, an element of the peroxiredoxin defense against oxidative stress, *Antimicrob Agents Chemother*, **48**, 2424-2430.

[152] P. E. Morin, D. Diggs and E. Freire (1990), Thermal stability of membrane-reconstituted yeast cytochrome c oxidase, *Biochemistry*, **29**, 781-788.

[153] P. E. Morin and E. Freire (1991), Direct calorimetric analysis of the enzymatic activity of yeast cytochrome c oxidase, *Biochemistry*, **30**, 8494-8500.

[154] M. G. Elferink, T. Bosma, J. S. Lolkema, M. Gleiszner, A. J. Driessen and W. N. Konings (1995), Thermostability of respiratory terminal oxidases in the lipid environment, *Biochim Biophys Acta*, **1230**, 31-37.

[155] H. Ji, T. K. Das, A. Puustinen, M. Wikstrom, S. R. Yeh and D. L. Rousseau (2010), Modulation of the active site conformation by site-directed mutagenesis in cytochrome c oxidase from Paracoccus denitrificans, *J Inorg Biochem*, **104**, 318-323.

[156] Anatrace Detergents and their Uses in Membrane Protein Science. Anatrace.

[157] W. Hilgenberg, T. Rausch and H. Lüken (1981), The Effect of Light and Zinc on Catalase Activity during the Development of *Phycomyces blakesleeanus* Bgff., *Biochem. Physiol. Pflanzen*, 6.

[158] S. S. Kuznetsova, N. V. Azarkina, T. V. Vygodina, S. A. Siletsky and A. A. Konstantinov (2005), Zinc ions as cytochrome C oxidase inhibitors: two sites of action, *Biochemistry (Mosc)*, **70**, 128-136.

[159] K. Shinzawa-Itoh, H. Aoyama, K. Muramoto, H. Terada, T. Kurauchi, Y. Tadehara, A. Yamasaki, T. Sugimura, S. Kurono, K. Tsujimoto, T. Mizushima, E. Yamashita, T. Tsukihara and S. Yoshikawa (2007), Structures and physiological roles of 13 integral lipids of bovine heart cytochrome c oxidase, *Embo J*, **26**, 1713-1725.

[160] E. Forte, A. Urbani, M. Saraste, P. Sarti, M. Brunori and A. Giuffre (2001), The cytochrome cbb3 from Pseudomonas stutzeri displays nitric oxide reductase activity, *Eur J Biochem*, **268**, 6486-6491.

[161] H. J. Lee, R. B. Gennis and P. Adelroth (2011), Entrance of the proton pathway in cbb3-type heme-copper oxidases, *Proc Natl Acad Sci U S A*, **108**, 17661-17666.

[162] F. A. Bundschuh, A. Hannappel, O. Anderka and B. Ludwig (2009), Surf1, associated with Leigh syndrome in humans, is a heme-binding protein in bacterial oxidase biogenesis, *J Biol Chem*, **284**, 25735-25741.

[163] A. Hannappel, F. A. Bundschuh and B. Ludwig (2011), Role of Surf1 in heme recruitment for bacterial COX biogenesis, *Biochim Biophys Acta*.

[164] A. Hannappel, F. A. Bundschuh and B. Ludwig (2011), Characterization of heme-binding properties of Paracoccus denitrificans Surf1 proteins, *Febs J*, **278**, 1769-1778.

[165] L. Hederstedt (2002), Succinate:quinone oxidoreductase in the bacteria Paracoccus denitrificans and Bacillus subtilis, *Biochim Biophys Acta*, **1553**, 74-83.

[166] T. Kleinschroth, M. Castellani, C. H. Trinh, N. Morgner, B. Brutschy, B. Ludwig and C. Hunte (2011), X-ray structure of the dimeric cytochrome bc(1) complex from the soil bacterium Paracoccus denitrificans at 2.7-A resolution, *Biochim Biophys Acta*, **1807**, 1606-1615.

[167] M. Wikstrom (2000), Proton translocation by cytochrome c oxidase: a rejoinder to recent criticism, *Biochemistry*, **39**, 3515-3519.

[168] D. Bloch, I. Belevich, A. Jasaitis, C. Ribacka, A. Puustinen, M. I. Verkhovsky and M. Wikstrom (2004), The catalytic cycle of cytochrome c oxidase is not the sum of its two halves, *Proc Natl Acad Sci U S A*, **101**, 529-533.

[169] D. M. Popovic and A. A. Stuchebrukhov (2004), Proton pumping mechanism and catalytic cycle of cytochrome c oxidase: Coulomb pump model with kinetic gating, *FEBS Lett*, **566**, 126-130.

.

7. Appendix

7.1. DNA-Sequence of pFH21

DNA-Sequence of pFH21 including *ctaDII*, *ctaG* and *surf1c* under the control of the *ctaC*-Promoter.

```
     1  ctcgggccgt ctcttgggct tgatcggcct tcttgcgcat ctcacgcgct
cctgcggcgg cctgtagggc aggctcatac ccctgccgaa ccgcttttgt cagccggtcg
gccacggctt ccggcgtctc aacgcgcttt gagattccca gcttttcggc caatccctgc
ggtgcatagg cgcgtggctc gaccgcttgc
        gagcccggca gagaacccga actagccgga agaacgcgta gagtgcgcga
ggacgccgcc ggacatcccg tccgagtatg gggacggctt ggcgaaaaca gtcggccagc
cggtgccgaa ggccgcagag ttgcgcgaaa ctctaagggt cgaaaagccg gttagggacg
ccacgtatcc gcgcaccgag ctggcgaacg

<.....................................................................
.....................................Mob.............................
.....................................................................
.....<
        d  r  a  t  e  q  a  q  d  a  k  k  r  m  e  r  a  g  a  a
a  q  l  a  p  e  y  g  q  r  v  a  k  t  l  r  d  a  v  a  e  p
t  e  v  r  k  s  i  g  l  k  e  a  l  g  q  p  a  y  a  r  p  e
v  a  q

   201  gggctgatgg tgacgtggcc cactggtggc cgctccaggg cctcgtagaa
cgcctgaatg cgcgtgtgac gtgccttgct gccctcgatg ccccgttgca gccctagatc
ggccacagcg gccgcaaacg tggtctggtc gcgggtcatc tgcgctttgt tgccgatgaa
ctccttggcc gacagcctgc cgtcctgcgt
        cccgactacc actgcaccgg gtgaccaccg gcgaggtccc ggagcatctt
gcggacttac gcgcacactg cacggaacga cgggagctac ggggcaacgt cgggatctag
ccggtgtcgc cggcgtttgc accagaccag cgcccagtag acgcgaaaca acggctactt
gaggaaccgg ctgtcggacg gcaggacgca

<.....................................................................
.....................................Mob.............................
.....................................................................
.....<
         p  s  i  t  v  h  g  v  p  p  r  e  l  a  e  y  f  a  q
i  r  t  h  r  a  k  s  g  e  i  g  r  q  l  g  l  d  a  v  a  a
a  f  t  t  q  d  r  t  m  q  a  k  n  g  i  f  e  k  a  s  l  r
g  d  q  t

   401  cagcggcacc acgaacgcgg tcatgtgcgg gctggtttcg tcacggtgga
tgctggccgt cacgatgcga tccgccccgt acttgtccgc cagccacttg tgcgccttct
cgaagaacgc cgcctgctgt tcttggctgg ccgacttcca ccattccggg ctggccgtca
tgacgtactc gaccgccaac acagcgtcct
        gtcgccgtgg tgcttgcgcc agtacacgcc cgaccaaagc agtgccacct
acgaccggca gtgctacgct aggcggggca tgaacaggcg gtcggtgaac acgcggaaga
gcttcttgcg gcggacgaca agaaccgacc ggctgaaggt ggtaaggccc gaccggcagt
actgcatgag ctggcggttg tgtcgcagga

<.....................................................................
```

```
.....................................Mob.................................
.....................................................................
.....<
          l  p  v   v  f  a   t  m  h  p   s  t  e   d  r  h   i  s  a
t   v  i  r   d  a  g   y  k  d  a   l  w  k   h  a  k   e  f  f  a   a
q  q   e  q  s   a  s  k  w   w  e  p   s  a  t   m  v  y  e   v  a  l
v  a  d

   601  tgcgccgctt ctctggcagc aactcgcgca gtcggcccat cgcttcatcg
gtgctgctgg ccgcccagtg ctcgttctct ggcgtcctgc tggcgtcagc gttgggcgtc
tcgcgctcgc ggtaggcgtg cttgagactg gccgccacgt tgcccatttt cgccagcttc
ttgcatcgca tgatcgcgta tgccgccatg
        acgcggcgaa gagaccgtcg ttgagcgcgt cagccgggta gcgaagtagc
cacgacgacc ggcgggtcac gagcaagaga ccgcaggacg accgcagtcg caacccgcag
agcgcgagcg ccatccgcac gaactctgac cggcggtgca acgggtaaaa gcggtcgaag
aacgtagcgt actagcgcat acggcggtac

<.....................................................................
.....................................Mob.............................
.....................................................................
.....<
        k  r  r  k   e  p  l   l  e  r   l  r  g  m   a  e  d   t  s  s
a  a  w  h   e  n  e   p  t  r   s  a  d  a   n  p  t   e  r  e   r  y
a  h   k  l  s   a  a  v   n  g  m  k   a  l  k   k  c  r   m  i  a  y
a  a  m

   801  cctgcccctc ccttttggtg tccaaccggc tcgacggggg cagcgcaagg
cggtgcctcc ggcgggccac tcaatgcttg agtatactca ctagactttg cttcgcaaag
tcgtgaccgc ctacggcggc tgcggcgccc tacgggcttg ctctccgggc ttcgccctgc
gcggtcgctg cgctcccttg ccagcccgtg
        ggacggggag ggaaaaccac aggttggccg agctgccccc gtcgcgttcc
gccacggagg ccgcccggtg agttacgaac tcatatgagt gatctgaaac gaagcgtttc
agcactggcg gatgccgccg acgccgcggg atgcccgaac gagaggcccg aagcgggacg
cgccagcgac gcgagggaac ggtcgggcac

<.....................................................................
.....................................Mob.............................
.....................................................................
.....<
          g  a  g   g  k  q  h   g  v  p   e  v  p   a  a  c  p   p  a
e   p  p  g   s  l  a  q   t  y  e   s  s  k   a  e  c  l   r  s  r   r
r  r   s  r  r  g   v  p  k   s  e  p   s  r  g  a   r  d  s   r  e  r
a  l  g  h

  1001  gatatgtgga cgatggccgc gagcggccac cggctggctc gcttcgctcg
gcccgtggac aaccctgctg gacaagctga tggacaggct gcgcctgccc acgagcttga
ccacagggat tgcccaccgg ctacccagcc ttcgaccaca tacccaccgg ctccaactgc
gcggcctgcg gccttgcccc atcaattttt
        ctatacacct gctaccggcg ctcgccggtg gccgaccgag cgaagcgagc
cgggcacctg ttgggacgac ctgttcgact acctgtccga cgcggacggg tgctcgaact
ggtgtcccta acgggtggcc gatgggtcgg aagctggtgt atgggtggcc gaggttgacg
cgccggacgc cggaacgggg tagttaaaaa

<.....................................................................
.................................Mob.................................
.....................................................................<<
          i  h  p   r  h  g   r  a  a  v   p  q  s   a  e  s   p  g  h
v   v  r  s   s  l  s   i  s  l  s   r  r  g   v  l  k   v  v  p  i   a
w  r   s  g  l   r  r  g  c   v  w  r   s  w  s   r  p  r  r   g  q  g
m
```

```
  1201  ttaattttct ctggggaaaa gcctccggcc tgcggcctgc gcgcttcgct
tgccggttgg acaccaagtg gaaggcgggt caaggctcgc gcagcgaccg cgcagcggct
tggccttgac gcgcctggaa cgacccaagc ctatgcgagt gggggcagtc gaaggcgaag
cccgcccgcc tgccccccga gcctcacggc
        aattaaaaga gacccctttt cggaggccgg acgccggacg cgcgaagcga
acggccaacc tgtggttcac cttccgccca gttccgagcg cgtcgctggc gcgtcgccga
accggaactg cgcggacctt gctgggttcg gatacgctca cccccgtcag cttccgcttc
gggcgggcgg acgggggget cggagtgccg

  1401  ggcgagtgcg ggggttccaa gggggcagcg ccaccttggg caaggccgaa
ggccgcgcag tcgatcaaca agccccggag gggccacttt ttgccggagg gggagccgcg
ccgaaggcgt gggggaaccc cgcaggggtg cccttctttg ggcaccaaag aactagatat
agggcgaaat gcgaaagact taaaaatcaa
        ccgctcacgc ccccaaggtt cccccgtcgc ggtggaaccc gttccggctt
ccggcgcgtc agctagttgt tcggggcctc cccggtgaaa aacggcctcc ccctcggcgc
ggcttccgca ccccccttggg gcgtccccac gggaagaaac ccgtggtttc ttgatctata
tcccgcttta cgctttctga atttttagtt

  1601  caacttaaaa aaggggggta cgcaacagct cattgcggca ccccccgcaa
tagctcattg cgtaggttaa agaaaatctg taattgactg ccacttttac gcaacgcata
attgttgtcg cgctgccgaa aagttgcagc tgattgcgca tggtgccgca accgtgcggc
accctaccgc atggagataa gcatggccac
        gttgaatttt ttccccccat gcgttgtcga gtaacgccgt ggggggcgtt
atcgagtaac gcatccaatt tcttttagac attaactgac ggtgaaaatg cgttgcgtat
taacaacagc gcgacggctt ttcaacgtcg actaacgcgt accacggcgt tggcacgccg
tgggatggcg tacctctatt cgtaccggtg

>>.......Rep........>

m  e  i  s  m  a

  1801  gcagtccaga gaaatcggca ttcaagccaa gaacaagccc ggtcactggg
tgcaaacgga acgcaaagcg catgaggcgt gggccgggct tattgcgagg aaacccacgg
cggcaatgct gctgcatcac ctcgtggcgc agatgggcca ccagaacgcc gtggtggtca
gccagaagac actttccaag ctcatcggac
        cgtcaggtct ctttagccgt aagttcggtt cttgttcggg ccagtgaccc
acgtttgcct tgcgtttcgc gtactccgca cccggcccga ataacgctcc tttgggtgcc
gccgttacga cgacgtagtg gagcaccgcg tctacccggt ggtcttgcgg caccaccagt
cggtcttctg tgaaaggttc gagtagcctg

>.....................................................................
.....................................Rep..............................
.....................................................................
.....>
        t  q  s  r  e  i  g  i  q  a  k  n  k  p  g  h  w  v  q  t
e  r  k  a  h  e  a  w  a  g  l  i  a  r  k  p  t  a  a  m  l  l
h  h  l  v  a  q  m  g  h  q  n  a  v  v  v  s  q  k  t  l  s  k
l  i  g

  2001  gttctttgcg gacggtccaa tacgcagtca aggacttggt ggccgagcgc
tggatctccg tcgtgaagct caacggcccc ggcaccgtgt cggcctacgt ggtcaatgac
cgcgtggcgt ggggccagcc ccgcgaccag ttgcgcctgt cggtgttcag tgccgccgtg
gtggttgatc acgacgacca ggacgaatcg
        caagaaacgc ctgccaggtt atgcgtcagt tcctgaacca ccggctcgcg
acctagaggc agcacttcga gttgccgggg ccgtggcaca gccggatgca ccagttactg
gcgcaccgca ccccggtcgg ggcgctggtc aacgcggaca gccacaagtc acggcggcac
caccaactag tgctgctggt cctgcttagc

>.....................................................................
.....................................Rep..............................
.....................................................................
```

```
.....>
         r  s  l   r  t  v  q   y  a  v   k  d  l   v  a  e  r   w  i
s   v  v  k   l  n  g  p   g  t  v   s  a  y   v  v  n  d   r  v  a   w
g  q   p  r  d  q   l  r  l   s  v  f   s  a  a  v   v  v  d   h  d  d
q  d  e  s

  2201  ctgttggggc atggcgacct gcgccgcatc ccgaccctgt atccgggcga
gcagcaacta ccgaccggcc ccggcgagga gccgcccagc cagcccggca ttccgggcat
ggaaccagac ctgccagcct tgaccgaaac ggaggaatgg gaacggcgcg ggcagcagcg
cctgccgatg cccgatgagc cgtgttttct
        gacaaccccg taccgctgga cgcggcgtag ggctgggaca taggcccgct
cgtcgttgat ggctggccgg ggccgctcct cggcgggtcg gtcgggccgt aaggcccgta
ccttggtctg gacggtcgga actggctttg cctccttacc cttgccgcgc ccgtcgtcgc
ggacggctac gggctactcg gcacaaaaga

>.....................................................................
.....................................Rep.............................
.....................................................................
.....>
         l  l  g   h  g  d   l  r  r  i   p  t  l   y  p  g   e  q  q
l   p  t  g   p  g  e   e  p  p  s   q  p  g   i  p  g   m  e  p  d   l
p  a   l  t  e   t  e  e  w   e  r  r   g  q  q   r  l  p  m   p  d  e
p  c  f

  2401  ggacgatggc gagccgttgg agccgccgac acgggtcacg ctgccgcgcc
ggtagcactt gggttgcgca gcaacccgta agtgcgctgt tccagactat cggctgtagc
cgcctcgccg ccctatacct tgtctgcctc cccgcgttgc gtcgcggtgc atggagccgg
gccacctcga cctgaatgga agccagcttt
        cctgctaccg ctcggcaacc tcggcggctg tgcccagtgc gacggcgcgg
ccatcgtgaa cccaacgcgt cgttgggcat tcacgcgaca aggtctgata gccgacatcg
gcggagcggc gggatatgga acagacggag gggcgcaacg cagcgccacg tacctcggcc
cggtggagct ggacttacct tcggtcgaaa
        >..........................Rep..........................>>
        l  d  d  g   e  p  l   e  p  p   t  r  v  t   l  p  r   r  -

  2601  atgcttgtaa accgttttgt gaaaaaattt ttaaaataaa aaaggggacc
tctagggtcc ccaattaatt agtaatataa tctattaaag gtcattcaaa aggtcatcca
ccggatcaat tcccctgctc gcgcaggctg ggtgccaagc tctcgggtaa catcaaggcc
cgatccttgg agcccttgcc ctcccgcacg
        tacgaacatt tggcaaaaca ctttttttaaa aattttattt tttcccctgg
agatcccagg ggttaattaa tcattatatt agataatttc cagtaagttt tccagtaggt
ggcctagtta aggggacgag cgcgtccgac ccacggttcg agagcccatt gtagttccgg
gctaggaacc tcgggaacgg gagggcgtgc

  2801  atgatcgtgc cgtgatcgaa atccagatcc ttgacccgca gttgcaaacc
ctcactgatc cgcatgcccg ttccatacag aagctgggcg aacaaacgat gctcgccttc
cagaaaaccg aggatgcgaa ccacttcatc cggggtcagc accaccggca agcgccgcga
cggccgaggt cttccgatct cctgaagcca
        tactagcacg gcactagctt taggtctagg aactgggcgt caacgtttgg
gagtgactag gcgtacgggc aaggtatgtc ttcgacccgc ttgtttgcta cgagcggaag
gtcttttggc tcctacgctt ggtgaagtag gccccagtcg tggtggccgt tcgcggcgct
gccggctcca gaaggctaga ggacttcggt

  3001  gggcagatcc gtgcacagca ccttgccgta gaagaacagc aaggccgcca
atgcctgacg atgcgtggag accgaaacct tgcgctcgtt cgccagccag gacagaaatg
cctcgacttc gctgctgccc aaggttgccg ggtgacgcac accgtggaaa cggatgaagg
cacgaaccca gtggacataa gcctgttcgg
        cccgtctagg cacgtgtcgt ggaacggcat cttcttgtcg ttccggcggt
tacggactgc tacgcacctc tggctttgga acgcgagcaa gcggtcggtc ctgtctttac
ggagctgaag cgacgacggg ttccaacggc ccactgcgtg tggcaccttt gcctacttcc
gtgcttgggt cacctgtatt cggacaagcc
```

```
  3201  ttcgtaagct gtaatgcaag tagcgtatgc gctcacgcaa ctggtccaga
accttgaccg aacgcagcgg tggtaacggc gcagtggcgg ttttcatggc ttgttatgac
tgttttttttg gggtacagtc tatgcctcgg gcatccaagc agcaagcgcg ttacgccgtg
ggtcgatgtt tgatgttatg gagcagcaac
        aagcattcga cattacgttc atcgcatacg cgagtgcgtt gaccaggtct
tggaactggc ttgcgtcgcc accattgccg cgtcaccgcc aaaagtaccg aacaatactg
acaaaaaaac cccatgtcag atacggagcc cgtaggttcg tcgttcgcgc aatgcggcac
ccagctacaa actacaatac ctcgtcgttg

>>.....
.....Sm.....
.....>
                                        m   r  s  r   n  w  s  r   t  l
t   e  r  s   g  g  n  g   a  v  a   v  f  m   a  c  y  d   c  f  f   g
v  q   s  m  p  r   a  s  k   q  q  a   r  y  a  v   g  r  c   l  m  l
w  s   s  n

  3401  gatgttacgc agcagggcag tcgccctaaa acaaagttaa acatcatgag
ggaagcggtg atcgccgaag tatcgactca actatcagag gtagttggcg tcatcgagcg
ccatctcgaa ccgacgttgc tggccgtaca tttgtacggc tccgcagtgg atggcggcct
gaagccacac agtgatattg atttgctggt
        ctacaatgcg tcgtcccgtc agcgggattt tgtttcaatt tgtagtactc
ccttcgccac tagcggcttc atagctgagt tgatagtctc catcaaccgc agtagctcgc
ggtagagctt ggctgcaacg accggcatgt aaacatgccg aggcgtcacc taccgccgga
cttcggtgtg tcactataac taaacgacca

>.....
.....Sm.....
.....
.....>
          d  v  t   q  q  g   s  r  p  k   t  k  l   n  i  m   r  e  a
v   i  a  e   v  s  t   q  l  s  e   v  v  g   v  i  e   r  h  l  e   p
t  l   l  a  v   h  l  y  g   s  a  v   d  g  g   l  k  p  h   s  d  i
d  l  l

  3601  tacggtgacc gtaaggcttg atgaaacaac gcggcgagct ttgatcaacg
acctttgga aacttcggct tcccctggag agagcgagat tctccgcgct gtagaagtca
ccattgttgt gcacgacgac atcattccgt ggcgttatcc agctaagcgc gaactgcaat
ttggagaatg gcagcgcaat gacattcttg
        atgccactgg cattccgaac tactttgttg cgccgctcga aactagttgc
tggaaaacct ttgaagccga aggggacctc tctcgctcta agaggcgcga catcttcagt
ggtaacaaca cgtgctgctg tagtaaggca ccgcaatagg tcgattcgcg cttgacgtta
aacctcttac cgtcgcgtta ctgtaagaac

>.....
.....Sm.....
.....
.....>
       v  t  v  t   v  r  l   d  e  t   t  r  r  a   l  i  n   d  l  l
e  t  s  a   s  p  g   e  s  e   i  l  r  a   v  e  v   t  i  v   v  h
d  d   i  i  p   w  r  y   p  a  k  r   e  l  q   f  g  e   w  q  r  n
d  i  l

  3801  caggtatctt cgagccagcc acgatcgaca ttgatctggc tatcttgctg
acaaaagcaa gagaacatag cgttgccttg gtaggtccag cggcggagga actctttgat
ccggttcctg aacaggatct atttgaggcg ctaaatgaaa ccttaacgct atggaactcg
ccgcccgact gggctggcga tgagcgaaat
        gtccatagaa gctcggtcgg tgctagctgt aactagaccg atagaacgac
tgttttcgtt ctcttgtatc gcaacggaac catccaggtc gccgcctcct tgagaaacta
ggccaaggac ttgtcctaga taaactccgc gatttacttt ggaattgcga taccttgagc
```

```
ggcgggctga cccgaccgct actcgcttta

>.....................................................................
.....................................Sm.................................
.....................................................................
.....>
         a  g  i   f  e  p  a   t  i  d   i  d  l   a  i  l  l   t  k
a   r  e  h   s  v  a  l   v  g  p   a  a  e   e  l  f  d   p  v  p   e
q  d   l  f  e  a   l  n  e   t  l  t   l  w  n  s   p  p  d   w  a  g
d  e  r  n

  4001  gtagtgctta cgttgtcccg catttggtac agcgcagtaa ccggcaaaat
cgcgccgaag gatgtcgctg ccgactgggc aatggagcgc ctgccggccc agtatcagcc
cgtcatactt gaagctagac aggcttatct tggacaagaa gaagatcgct tggcctcgcg
cgcagatcag ttggaagaat ttgtccacta
        catcacgaat gcaacagggc gtaaaccatg tcgcgtcatt ggccgtttta
gcgcggcttc ctacagcgac ggctgacccg ttacctcgcg gacggccggg tcatagtcgg
gcagtatgaa cttcgatctg tccgaataga acctgttctt cttctagcga accggagcgc
gcgtctagtc aaccttctta aacaggtgat

>.....................................................................
.....................................Sm.................................
.....................................................................
.....>
          v  v  l   t  l  s   r  i  w  y   s  a  v   t  g  k   i  a  p
k   d  v  a   a  d  w   a  m  e  r   l  p  a   q  y  q   p  v  i  l   e
a  r   q  a  y   l  g  q  e   e  d  r   l  a  s   r  a  d  q   l  e  e
f  v  h

  4201  cgtgaaaggc gagatcacca aggtagtcgg caaataatgt ctaacaattc
gttcaagccg acgccgcttc gcggcgcggc ttaactcaag cgttagatgc actaagcaca
taattgctca cagccaaact atcaggtcaa gtctgctttt attattttta agcgtgcata
ataagcccta cacaaattgg gagatatatc
        gcactttccg ctctagtggt tccatcagcc gtttattaca gattgttaag
caagttcggc tgcggcgaag cgccgcgccg aattgagttc gcaatctacg tgattcgtgt
attaacgagt gtcggtttga tagtccagtt cagacgaaaa taataaaaat tcgcacgtat
tattcgggat gtgtttaacc ctctatatag
        >..................Sm.................>>
        y  v  k  g   e  i  t   k  v  v   g  k  -

  4401  atgaaaggct ggctttttct tgttatcgca atagttggcg aagtaatcgc
aacatccgca ttaaaatcta gcgagggctt tactaagctg atccggtgga tgacctttg
aatgaccttt aatagattat attactaatt aattggggac cctagaggtc ccctttttta
ttttaaaaat tttttcacaa aacggtttac
        tactttccga ccgaaaaaga acaatagcgt tatcaaccgc ttcattagcg
ttgtaggcgt aattttagat cgctcccgaa atgattcgac taggccacct actggaaaac
ttactggaaa ttatctaata taatgattaa ttaacccctg ggatctccag gggaaaaaat
aaaatttta aaaaagtgtt ttgccaaatg

  4601  aagcataaag ctggcggcac ctcgctaacg gattcaccgt ttttatcagg
ctctgggagg cagaataaat gatcatatcg tcaattatta cctccacggg gagagcctga
gcaaactggc ctcaggcatt tgagaagcac acggtcacac tgcttccggt agtcaataaa
ccggtaaacc agcaatagac ataagcggct
        ttcgtatttc gaccgccgtg gagcgattgc ctaagtggca aaaatagtcc
gagaccctcc gtcttattta ctagtatagc agttaataat ggaggtgccc ctctcggact
cgtttgaccg gagtccgtaa actcttcgtg tgccagtgtg acgaaggcca tcagttattt
ggccatttgg tcgttatctg tattcgccga

  4801  atttaacgac cctgccctga accgacgacc gggtcgaatt tgctttcgaa
tttctgccat tcatccgctt attatcactt attcaggcgt agcaccaggc gtttaagggc
accaataact gccttaaaaa aattacgccc cgccctgcca ctcatcgcag tcggcctatt
```

```
ggttaaaaaa tgagctgatt taacaaaaat
        taaattgctg ggacgggact tggctgctgg cccagcttaa acgaaagctt
aaagacggta agtaggcgaa taatagtgaa taagtccgca tcgtggtccg caaattcccg
tggttattga cggaattttt ttaatgcggg gcgggacggt gagtagcgtc agccggataa
ccaatttttt actcgactaa attgttttta

  5001  ttaacgcgaa ttttaacaaa atattaacgc ttacaatttc cattcgccat
tcaggctgcg caactgttgg gaagggcgat cggtgcgggc ctcttcgcta ttacgccagc
tggcgaaagg gggatgtgct gcaaggcgat taagttgggt aacgccaggg ttttcccagt
cacgacgttg taaaacgacg gccagtgagc
        aattgcgctt aaaattgttt tataattgcg aatgttaaag gtaagcggta
agtccgacgc gttgacaacc cttcccgcta gccacgcccg gagaagcgat aatgcggtcg
accgctttcc ccctacacga cgttccgcta attcaaccca ttgcggtccc aaaagggtca
gtgctgcaac attttgctgc cggtcactcg

                                                          XbaI
                                                        -+-----
                                              SacI      ScaI
                                             -----+    ---+--
  5201  gcgcgtaata cgactcacta tagggcgaat tggagctcat cagtactcta
gaattgccgc tgcctgatac gccagatcag cgccactgtc atccctgccc aaaccgcagc
gatcatgaac cattgcgcgg catagctcag gtggttgttc ggaatgccct cgaccgcgac
cgggatcggc cgcaccccct gcgcatcgcc
        cgcgcattat gctgagtgat atcccgctta acctcgagta gtcatgagat
cttaacggcg acggactatg cggtctagtc gcggtgacag tagggacggg tttggcgtcg
ctagtacttg gtaacgcgcc gtatcgagtc caccaacaag ccttacggga gctggcgctg
gccctagccg gcgtgggggа cgcgtagcgg

<<.....
.....Surf1c.....
.....<
                                                        -   f  q
r   q  r  i   r  w  i  l   a  v  t   m  g  a   w  v  a  a   i  m  f   w
q   a  a  y   s  l  h  n   n  p  i   g  e  v   a  v  p  i   p  r  v   g
q   a  d  g

  5401  ccgcacctcg gccgccacga ccagcaccgg ctcggtcccc agctgcgcgg
ccatggcggg cacgtcgcgg gcgaaccaga cattctcggt caggttgggc tcgggcgtgg
cgctgccctt ttcgtcgggc cagtgcaggt tgcccgccac ctccagccgc accggcgggc
gcggggcacg cttgtggtcc tgatcgacga
        ggcgtggagc cggcggtgct ggtcgtggcc gagccagggg tcgacgcgcc
ggtaccgccc gtgcagcgcc cgcttggtct gtaagagcca gtccaacccg agcccgcacc
gcgacgggaa aagcagcccg gtcacgtcca acgggcggtg gaggtcggcg tggccgcccg
cgccccgtgc gaacaccagg actagctgct

<.....
.....Surf1c.....
.....
.....<
          r  v  e   a  a  v   v  l  v  p   e  t  g   l  q  a   a  m  a
p   v  d  r   a  f  w   v  n  e  t   l  n  p   e  p  t   a  s  g  k   e
d   p  w  h   l  n  g   a  v  e  l   r  v  p   p  r  p   a  r  k  h   d
q   d  v

  5601  agccccgatc cagcaggatc ctgcgcccgt catcggtgac gaaacccgag
acgacctgat agccgccgcc cgcctcgcgc gtgcccgaca gcacgtcgat ctcctgaccc
gtggtctggc ccgaaaccag caccggcatg tatttcatcg acggattcac cgccgccggc
aggggcacgg gccggccctc gatcctttgc
        tcggggctag gtcgtcctag gacgcgggca gtagccactg ctttgggctc
tgctggacta tcggcggcgg gcggagcgcg cacgggctgt cgtgcagcta gaggactggg
caccagaccg ggctttggtc gtggccgtac ataaagtagc tgcctaagtg gcggcggccg
```

```
tccccgtgcc cggccgggag ctaggaaacg

<.....................................................................
.....................................Surf1c..........................
.....................................................................
.....<
       f  g  r  d  l  l  i  r  r  g  d  d  t  v  f  g  s  v  v  q
y  g  g  g  a  e  r  t  g  s  l  v  d  i  e  q  g  t  t  q  g  s
v  l  v  p  m  y  k  m  s  p  n  v  a  a  p  l  p  v  p  r  g  e
i  r  q


ScaI

---+--
  5801  tgaatctggg cgatcagccc ttctttccag tccagccgct gaagctgcca
catgcccagc gaaatcagga tggcgcagcc caccacaccg acgatcagcg ggaacaggta
acggcgcatc gaaatggccc tcctagtact tcagtttacg gtcggttccg ttttcgcgtc
cagcgccgcc tgtttgggcg cgggcggatc
        acttagaccc gctagtcggg aagaaaggtc aggtcggcga cttcgacggt
gtacgggtcg ctttagtcct accgcgtcgg gtggtgtggc tgctagtcgc ccttgtccat
tgccgcgtag ctttaccggg aggatcatga agtcaaatgc cagccaaggc aaaagcgcag
gtcgcggcgg acaaacccgc gcccgcctag

<.....................................................Surf1c...
.....................................................<<
        q  i  q  a  i  l  g  e  k  w  d  l  r  q  l  q  w  m  g
l  s  i  l  i  a  c  g  v  v  g  v  i  l  p  f  l  y  r  r  m

<<.........................ctaG.............................<

-  n  v  t  p  e  t  k  a  d  l  a  a  q  k  p  a  p  p  d

  6001  ggtccgatgg aaggtatagg acagggtgat gtcgcggatg cgaccggcgt
cgcggtcgtt caccagatcg gcatcgacga agaagctgac cggcatctcg acccgctccc
ccggctgcag ggtctgctcg gtaaagcaga agcattcaat cttgttgaag aaatagccgg
ccgcatcggg cgccacgtta tagctcgccg
        ccaggctacc ttccatatcc tgtcccacta cagcgcctac gctggccgca
gcgccagcaa gtggtctagc cgtagctgct tcttcgactg gccgtagagc tgggcgaggg
ggccgacgtc ccagacgagc catttcgtct tcgtaagtta gaacaacttc tttatcggcc
ggcgtagccc gcggtgcaat atcgagcggc

<.....................................................................
.....................................ctaG.............................
.....................................................................
.....<
        t  r  h  f  t  y  s  l  t  i  d  r  i  r  g  a  d  r  d
n  v  l  d  a  d  v  f  f  s  v  p  m  e  v  r  e  g  p  q  l  t
q  e  t  f  c  f  c  e  i  k  n  f  f  y  g  a  a  d  p  a  v  n
y  s  a

  6201  tgccggtcac cggctcgtcg gtgttgttga tcgcctcgta gaaggcgatg
gcgttctcgc cgatcttcag ctccatctcg cgctgcatcg ggcggaaggt ccagccgaga
ttgctgtccg cattggcgtc gaagcgcacc cggatctttt cgtccagcac cgtgtccgac
gcggcctcgg ccacgttggt ggtgccggca
        acggccagtg gccgagcagc cacaacaact agcggagcat cttccgctac
cgcaagagcg gctagaagtc gaggtagagc gcgacgtagc ccgccttcca ggtcggctct
aacgacaggc gtaaccgcag cttcgcgtgg gcctagaaaa gcaggtcgtg gcacaggctg
cgccggagcc ggtgcaacca ccacggccgt

<.....................................................................
```

```
.....................................ctaG.................................
.....................................................................
.....<
       t  g  t  v  p  e  d  t  n  n  i  a  e  y  f  a  i  a  n  e
g  i  k  l  e  m  e  r  q  m  p  r  f  t  w  g  l  n  s  d  a  n
a  d  f  r  v  r  i  k  e  d  l  v  t  d  s  a  a  e  a  v  n  t
t  g  a


SacI

-----+
  6401  aagccggtta ccttgcagaa ccaggaatag aacggcaccg ccgcccagct
gagcgcaccc atcagcacca cgacgccggc cagcatggcc acggtgcggg tgttcgacct
tggcttcccg ccgctcattg gttcgcccct cctgagctca tcaatgcgcg tgtgcgcgat
cccagtcctc gcgcttgggc agggtctcga
       ttcggccaat ggaacgtctt ggtccttatc ttgccgtggc ggcgggtcga
ctcgcgtggg tagtcgtggt gctgcggccg gtcgtaccgg tgccacgccc acaagctgga
accgaagggc ggcgagtaac caagcgggga ggactcgagt agttacgcgc acacgcgcta
gggtcaggag cgcgaacccg tcccagagct

<.....................................................................cta
G.....................................................................<<
       f  g  t  v  k  c  f  w  s  y  f  p  v  a  a  w  s  l  a
g  m  l  v  v  v  g  a  l  m  a  v  t  r  t  n  s  r  p  k  g  g
s  m

<<.....................ctaDII.....................<

-  h  a  h  a  r  d  w  d  e  r  k  p  l  t  e

  6601  aggtatgctc gggcggcggc gagggcaggg tccattccag cgtgtcggca
tgctcgttcc agtagttcgg cacgttcacg cgcttgccgg cgaagagcgt gtagaacacg
atgccgatga agaacaggaa ggacgcgaag gagatatagg cgccgatcga cgagatgttg
ttccaatagg cgaactcgac cggatagtcg
       tccatacgag cccgccgccg ctcccgtccc aggtaaggtc gcacagccgt
acgagcaagg tcatcaagcc gtgcaagtgc gcgaacggcc gcttctcgca catcttgtgc
tacggctact tcttgtcctt cctgcgcttc ctctatatcc gcggctagct gctctacaac
aaggttatcc gcttgagctg gcctatcagc

<.....................................................................
.....................................ctaDII.............................
.....................................................................
.....<
       f  t  h  e  p  p  p  s  p  l  t  w  e  l  t  d  a  h  e  n
w  y  n  p  v  n  v  r  k  g  a  f  l  t  y  f  v  i  g  i  f  f
l  f  s  a  f  s  i  y  a  g  i  s  s  i  n  n  w  y  a  f  e  v
p  y  d

  6801  atatagcgcc gcggcatgcc ctggcggccc aggaagtgct gcgggaagaa
gatcaggttc gagccgatga acatcatcca gaaatgcagc tggcccgccc attccgggta
ttgccggccc gacatcttgc cgatccagta atagaccccg gcgaagatgc cgaacaccgc
gcccagcgac atcacgtagt ggaagtgggc
       tatatcgcgg cgccgtacgg gaccgccggg tccttcacga cgcccttctt
ctagtccaag ctcggctact tgtagtaggt ctttacgtcg accgggcggg taaggcccat
aacggccggg ctgtagaacg gctaggtcat tatctggggc cgcttctacg gcttgtggcg
cgggtcgctg tagtgcatca ccttcacccg

<.....................................................................
.....................................ctaDII.............................
.....................................................................
```

```
.....<
        i  y  r   r  p  m  g   q  r  g   l  f  h   q  p  f  f   i  l
n   s  g  i   f  m  m  w   f  h  l   q  g  a   w  e  p  y   q  r  g   s
m  k   g  i  w  y   y  v  g   a  f  i   g  f  v  a   g  l  s   m  v  y
h  f  h  a

  7001  cacgacgtaa taggtgtcgt gatagacccg gtccagcggc gcctggctca
gcaccacgcc ggtcacgccg ccgacggtga acaggaacag gaagccgaag gcccagagca
tcggcgtctt gaactcgatg ctgccgcccc acatggtcgc gatccacgag aagaccttga
tgccggtggg caccgcgatg gtcatggtcg
        gtgctgcatt atccacagca ctatctgggc caggtcgccg cggaccgagt
cgtggtgcgg ccagtgcggc ggctgccact tgtccttgtc cttcggcttc cgggtctcgt
agccgcagaa cttgagctac gacggcgggg tgtaccagcg ctaggtgctc ttctggaact
acggccaccc gtggcgctac cagtaccagc

<.....................................................................
.....................................ctaDII..........................
.....................................................................
.....<
         v  v  y   y  t  d   h  y  v  r   d  l  p   a  q  s   l  v  v
g   t  v  g   g  v  t   f  l  f  l   f  g  f   a  w  l   m  p  t  k   f
e  i   s  g  g   w  m  t  a   i  w  s   f  v  k   i  g  t  p   v  a  i
t  m  t

  7201  ccagcatgaa ataggcctgc tgggtcagcg acatgccggc cgtgtacatg
tggtgcgccc agacgacgaa gcccaggatg ccgatcgccg ccatggccag caccatcggc
aggtagccga agatcggctt cttggcgaag gtcgagatga cgtggctgat gatgccgaag
cccggcagga tgatgatata gacctcggga
        ggtcgtactt tatccggacg acccagtcgc tgtacggccg gcacatgtac
accacgcggg tctgctgctt cgggtcctac ggctagcggc ggtaccggtc gtggtagccg
tccatcggct tctagccgaa gaaccgcttc cagctctact gcaccgacta ctacggcttc
gggccgtcct actactatat ctggagccct

<.....................................................................
.....................................ctaDII..........................
.....................................................................
.....<
        a  l  m  f   y  a  q   q  t  l   s  m  g  a   t  y  m   h  h  a
w  v  v  f   g  l  i   g  i  a   a  m  a  l   v  m  p   l  y  g   f  i
p  k   k  a  f   t  s  i   v  h  s  i   i  g  f   g  p  l   i  i  i  y
v  e  p

  7401  tggccgaaga accacaggat gtgctggtaa agcaccgggt cgccgccgcc
ggccggatcg aagaactgcg tgccgaagtt gcggtccatc agcagcatgg tgatcgcgcc
cgccagaacc ggcagcgaca gcaggatcag ccaggcggtg atgaagaccg accaggcaaa
cagcggcacc ttgaacagcg tcatgcccgg
        accggcttct tggtgtccta cacgaccatt tcgtggccca gcggcggcgg
ccggcctagc ttcttgacgc acggcttcaa cgccaggtag tcgtcgtacc actagcgcgg
gcggtcttgg ccgtcgctgt cgtcctagtc ggtccgccac tacttctggc tggtccgttt
gtcgccgtgg aacttgtcgc agtacgggcc

<.....................................................................
.....................................ctaDII..........................
.....................................................................
.....<
        h  g  f   f  w  l  i   h  q  y   l  v  p   d  g  g  g   a  p
d   f  f  q   t  g  f  n   r  d  m   l  l  m   t  i  a  g   a  l  v   p
l  s   l  l  i  l   w  a  t   i  f  v   s  w  a  f   l  p  v   k  f  l
t  m  g  p

  7601  tgcgcgcatg ttgaggaagg tggtgatgat gttgatcgcg cccaggatcg
```

```
acgaggcacc cgagacgtgg acggcaaaga tcgccaggtc catggaatag cccgcctcgg
tggtcgagag cggcgggtag agcacccagc cgacgcccga acccatctgg tcgttgccgc
ccggcgccag cagcgaggcg acgcccaggg
        acgcgcgtac aactccttcc accactacta caactagcgc gggtcctagc
tgctccgtgg gctctgcacc tgccgtttct agcggtccag gtaccttatc gggcggagcc
accagctctc gccgcccatc tcgtgggtcg gctgcgggct tgggtagacc agcaacggcg
ggccgcggtc gtcgctccgc tgcgggtccc

<.....
.....ctaDII.....
.....
.....<
         a  r  m   n  l  f   t  t  i  i   n  i  a   g  l  i   s  s  a
g   s  v  h   v  a  f   i  a  l  d   m  s  y   g  a  e   t  t  s  l   p
p  y   l  v  w   g  v  g  s   g  m  q   d  n  g   g  p  a  l   l  s  a
v  g  l

  7801  ccacgccgca gacatacatc cagtaggaga ggttgttcag ccgcgggaag
gccatgtccg gggcgccgat atgcagcggc atgaaatagt tgccgaaacc gccgaacagt
gccgggatca cgacgaagaa catcatgagc acgccgtggt aggtgatcat gacgttccac
aggtgtccgt tcggggtgca ttccgccgag
        ggtgcggcgt ctgtatgtag gtcatcctct ccaacaagtc ggcgcccttc
cggtacaggc cccgcggcta tacgtcgccg tactttatca acggctttgg cggcttgtca
cggccctagt gctgcttctt gtagtactcg tgcggcacca tccactagta ctgcaaggtg
tccacaggca agccccacgt aaggcggctc

<.....
.....ctaDII.....
.....
.....<
        a  v  g  c   v  y  m   w  y  s   l  n  n  l   r  p  f   a  m  d
p  a  g  i   h  l  p   m  f  y   n  g  f  g   g  f  l   a  p  i   v  v
f  f   m  m  l   v  g  h   y  t  i  m   v  n  w   l  h  g   n  p  t  c
e  a  s

  8001  gcgtcggcga tgagacgcgc gccttccagg cacatgtatt gcacgcccgg
atgctgcagt tccatccgca tatagacggt gaagcatacc gagatcaggc cgacgatgcc
ggccgtgaac aggtaaagga taccgatatc cttgtggttt gttgacatga accagcgggt
gaagaacccg cgggtgtcat gatggtcacc
        cgcagccgct actctgcgcg cggaaggtcc gtgtacataa cgtgcgggcc
tacgacgtca aggtaggcgt atatctgcca cttcgtatgg ctctagtccg gctgctacgg
ccggcacttg tccatttcct atggctatag gaacaccaaa caactgtact tggtcgccca
cttcttgggc gcccacagta ctaccagtgg

<.....
.....ctaDII.....
.....
.....<
         a  d  a   i  l  r  a   g  e  l   c  m  y   q  v  g  p   h  q
l   e  m  r   m  y  v  t   f  c  v   s  i  l   g  v  i  g   a  t  f   l
y  l   i  g  i  d   k  h  n   t  s  m   f  w  r  t   f  f  g   r  t  d
h  h  d  g


XbaI

-+----
  8201  gtggccgtga acggctgcgt ctgccatgcg tggactccct agacatgcgg
ctggccggcg caaaggccga cggactcgcc tgtttctaga actagaggat cccctgaggc
cgccggcatt cggtcctgca ccagaaccat atcttacccc ggcgggcaag ccatacctat
cgacttcttg tcaaaaaagc cctaggcggg
```

```
        caccggcact tgccgacgca gacggtacgc acctgaggga tctgtacgcc
gaccggccgc gtttccggct gcctgagcgg acaaagatct tgatctccta ggggactccg
gcggccgtaa gccaggacgt ggtcttggta tagaatgggg ccgcccgttc ggtatggata
gctgaagaac agtttttttcg ggatccgccc
                              start
        <.........ctaDII.........<<
          h  g  h   v  a  a   d  a  m

  8401  gcttcatgac aaggaccggt tccatgacag acgcttcgtt ttcacccttc
cggacgcatc tcgatcagga ccgcgcgctc actcctgcgc gacgccctgg ccggcgcgga
tgacggcgaa cttttcctgg aacgctcccg ttccgaggcg ctggtcttcg acgacggccg
gctgcgcacc gcaagctatg atgccgagca
        cgaagtactg ttcctggcca aggtactgtc tgcgaagcaa aagtgggaag
gcctgcgtag agctagtcct ggcgcgcgag tgaggacgcg ctgcgggacc ggccgcgcct
actgccgctt gaaaaggacc ttgcgagggc aaggctccgc gaccagaagc tgctgccggc
cgacgcgtgg cgttcgatac tacggctcgt

  8601  gggcttcggc ctgcgtgccg tgcgggacga agctagctta tcgataccgt
cgacctcgag ggggggcccg gtacccagct tttgttccct ttagtgaggg ttaattgcgc
gcttggcgta atcatggtca tagctgtttc ctgtgtgaaa ttgttatccg ctcacaattc
cacacaacat acgagccgga agcataaagt
        cccgaagccg gacgcacggc acgccctgct tcgatcgaat agctatggca
gctggagctc ccccccgggc catgggtcga aaacaaggga aatcactccc aattaacgcg
cgaaccgcat tagtaccagt atcgacaaag gacacacttt aacaataggc gagtgttaag
gtgtgttgta tgctcggcct tcgtatttca

  8801  gtaaagcctg gggtgcctaa tgagtgagct aactcacatt aattgcgttg
cgctcactgc ccgctttcca gtcgggaaac ctgtcgtgcc agctgcatta atgaatcggc
caacgcgcgg ggagaggcgg tttgcgtatt gggcgcatgc ataaaaactg ttgtaattca
ttaagcattc tgccgacatg gaagccatca
        catttcggac cccacggatt actcactcga ttgagtgtaa ttaacgcaac
gcgagtgacg ggcgaaaggt cagccctttg gacagcacgg tcgacgtaat tacttagccg
gttgcgcgcc cctctccgcc aaacgcataa cccgcgtacg tatttttgac aacattaagt
aattcgtaag acggctgtac cttcggtagt

<<.....................................................Cam.............
.....................................<

-  h  i  p  w  r  a  p  l  p  p  k  r  i  p  r  m  c  l  f  q  q
l  e  n  l  m  r  g  v  h  f  g  d

  9001  caaacggcat gatgaacctg aatcgccagc ggcatcagca ccttgtcgcc
ttgcgtataa tatttgccca tggtgaaaac gggggcgaag aagttgtcca tattggccac
gtttaaatca aaactggtga aactcaccca gggattggct gagacgaaaa acatattctc
aataaaccct ttagggaaat aggccaggtt
        gtttgccgta ctacttggac ttagcggtcg ccgtagtcgt ggaacagcgg
aacgcatatt ataaacgggt accacttttg cccccgcttc ttcaacaggt ataaccggtg
caaatttagt tttgaccact ttgagtgggt ccctaaccga ctctgctttt tgtataagag
ttatttggga aatcccttta tccggtccaa

<.....................................................................
.....................................Cam..............................
.....................................................................
.....<
         c  v  a   h  h  v  q   i  a  l   p  m  l   v  k  d  g   q  t
y  y  k  g   m  t  f  v   p  a  f   f  n  d   m  n  a  v   n  l  d   f
s  t   f  s  v  w   p  n  a   s  v  f   f  m  n  e   i  f  g   k  p  f
y  a  l  n

  9201  ttcaccgtaa cacgccacat cttgcgaata tatgtgtaga aactgccgga
aatcgtcgtg gtattcactc cagagcgatg aaaacgtttc agtttgctca tggaaaacgg
```

```
tgtaacaagg gtgaacacta tcccatatca ccagctcacc gtctttcatt gccatacgga
attccggatg agcattcatc aggcgggcaa
        aagtggcatt gtgcggtgta gaacgcttat atacacatct ttgacggcct
ttagcagcac cataagtgag gtctcgctac ttttgcaaag tcaaacgagt acctttgcc
acattgttcc cacttgtgat agggtatagt ggtcgagtgg cagaaagtaa cggtatgcct
taaggcctac tcgtaagtag tccgcccgtt

<.....................................................................
.....................................Cam..............................
.....................................................................
.....<
         e  g  y  c  a  v  d  q  s  y  i  h  l  f  q  r  f  d  d
h  y  e  s  w  l  s  s  f  t  e  t  q  e  h  f  v  t  y  c  p  h
v  s  d  w  i  v  l  e  g  d  k  m  a  m  r  f  e  p  h  a  n  m
l  r  a

  9401  gaatgtgaat aaaggccgga taaaacttgt gcttattttt ctttacggtc
tttaaaaagg ccgtaatatc cagctgaacg gtctggttat aggtacattg agcaactgac
tgaaatgcct caaaatgttc tttacgatgc cattgggata tatcaacggt ggtatatcca
gtgatttttt tctccatttt agcttcctta
        cttacactta tttccggcct attttgaaca cgaataaaaa gaaatgccag
aaatttttcc ggcattatag gtcgacttgc cagaccaata tccatgtaac tcgttgactg
actttacgga gttttacaag aaatgctacg gtaaccctat atagttgcca ccatataggt
cactaaaaaa agaggtaaaa tcgaaggaat

<.....................................................................
.............................Cam.....................................
.....................................................<<
        l  i  h  i  f  a  p  y  f  k  h  k  n  k  k  v  t  k  l  f
a  t  i  d  l  q  v  t  q  n  y  t  c  q  a  v  s  q  f  a  e  f
h  e  k  r  h  w  q  s  i  d  v  t  t  y  g  t  i  k  k  e  m

  9601  gctcctgaaa atctcgataa ctcaaaaaat acgcccggta gtgatcttat
ttcattatgg tgaaagttgg aacctcttac gtgccgatca acgtctcatt ttcgccaaaa
gttggcccag ggcttcccgg tatcaacagg gacaccagga tttatttatt ctgcgaagtg
atcttccgtc acaggtattt attcgaagac
        cgaggacttt tagagctatt gagtttttta tgcgggccat cactagaata
aagtaatacc actttcaacc ttggagaatg cacggctagt tgcagagtaa aagcggtttt
caaccgggtc ccgaagggcc atagttgtcc ctgtggtcct aaataaataa gacgcttcac
tagaaggcag tgtccataaa taagcttctg

  9801  gaaagggcct cgtgatacgc ctatttttat aggttaatgt catgataata
atggtttctt agacgtcagg tggcactttt cggggaaatg tgcgcgcccg cgttcctgct
ggcgctgggc ctgtttctgg cgctggactt cccgctgttc cgtcagcagc ttttcgccca
cggccttgat gatcgcggcg gccttggcct
        ctttcccgga gcactatgcg gataaaaata tccaattaca gtactattat
taccaaagaa tctgcagtcc accgtgaaaa gccccctttac acgcgcgggc gcaaggacga
ccgcgacccg gacaaagacc gcgacctgaa gggcgacaag gcagtcgtcg aaaagcgggt
gccggaacta ctagcgccgc cggaaccgga

<<....................................................................
.................Mob.................................................
.................................<
                                                  -  s  l  l  p  k
k  s  t  l  h  c  k  e  p  f  h  a  r  g  r  e  q  q  r  q  a  q
k  q  r  q  v  e  r  q  e  t  l  l  k  e  g  v  a  k  i  i  a  a
a  k  a

 10001  gcatatcccg attcaacggc cccagggcgt ccagaacggg cttcaggcgc
tcccgaaggt
        cgtatagggc taagttgccg gggtcccgca ggtcttgccc gaagtccgcg
```

```
agggcttcca

<.............................Mob.............................<
        q  m  d  r   n  l  p   g  l  a   d  l  v  p   k  l  r   e  r  l
```

7.2. Plasmid Maps

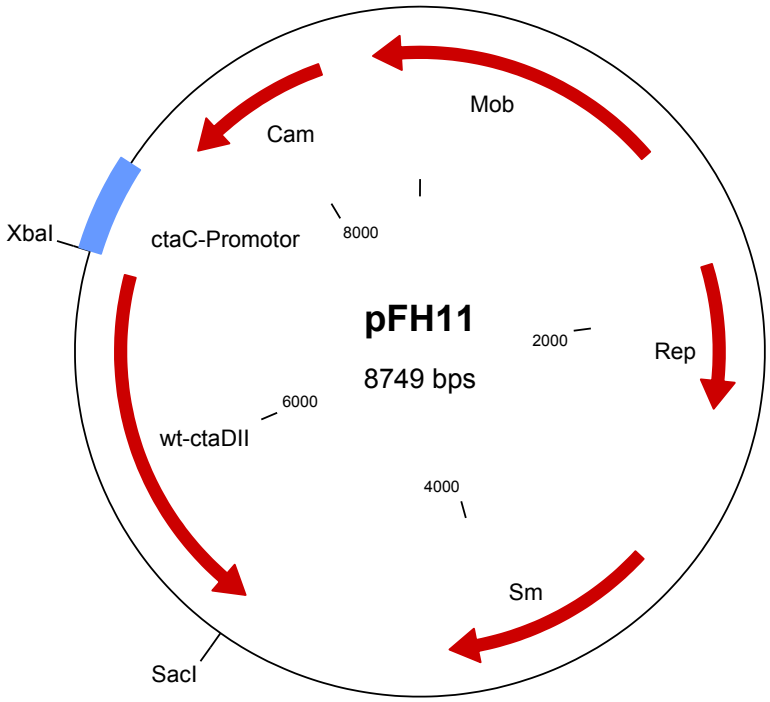

Figure 7.1: Plasmid Map of pFH11 containing *ctaDII.*

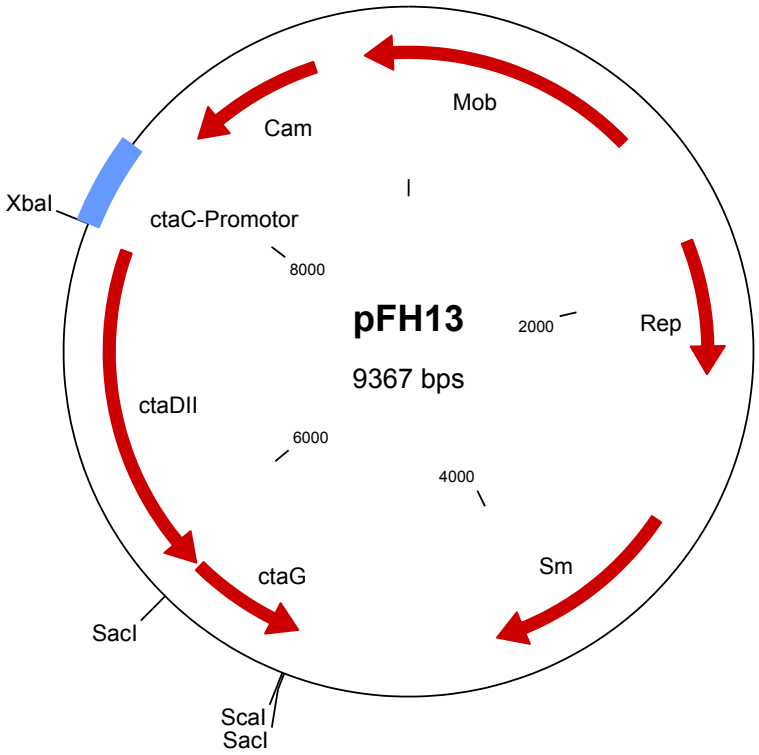

Figure 7.2: Plasmid Map of pFH13 containing *ctaDII* and *ctaG.*

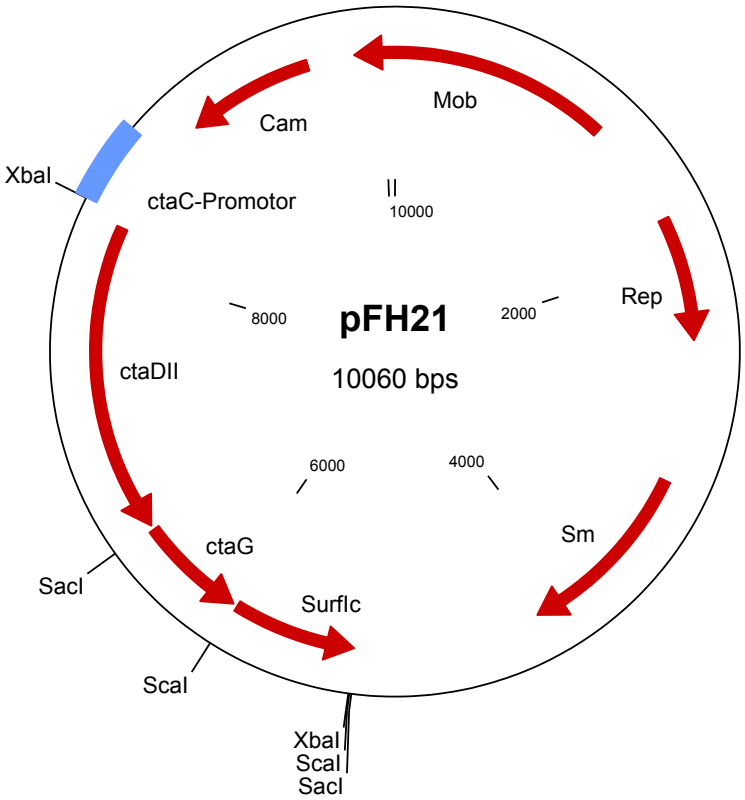

Figure 7.3: Plasmid Map of pFH21 containing *ctaDII*, *ctaG* and *surf1c*.

7.3. Software

Bruker XEpr

Unisense Sensor Trace Basic

Microsoft Word (for Mac)

Microsoft Excel (for Mac)

Origin 6-8

Clone Manager 9

TidasDAQ

User Interface Software for Lambda 35 (Perkin Elmer) and Cary 100 Scan (Varian)

Unicorn 5.11

MacPymol

EndNote X4

Several Programs such as Gel Documentation Software related to the described Hardware

8. List of Publications

8.1. Publications

Thesis related:

Von der Hocht, I., van Wonderen, J. H., Hilbers, F., MacMillan, F. and Michel, H.: "*Interconversions of P and F intermediates of cytochrome c oxidase from Paracoccus denitrificans*", PNAS, 2011, 108, 10, 3964-3969

Hilbers, F., von der Hocht, I., Ludwig, B. and Michel, H.: "*True wild type and recombinant wild type cytochrome c oxidase from Paracoccus denitrificans show a 20-fold difference in their catalase activity*", BBA, 2012, 1827, 319-327

Not Thesis related:

Sielaff, H., Rennekamp, H., Waechter, A., Xie, H., Hilbers, F., Feldbauer, K., Dunn, S.D., Engelbrecht, S., and Junge, W.: *„Domain compliance and elastic power transmission in rotary F_oF_1- ATPase"*, PNAS, 2008, 105, 46, 17760-17765

Fiedler, **A.**, Rehdorf, J., Hilbers, F., Jordan, L., Stribl, C. and Benecke, M.: *"Detection of Semen (Human and Boar) and Saliva on Fabrics by a Very High Powered UV-/VIS-Light Source"*, The Open Forensic Science Journal, 2008,1, 12-15

Hilbers, F., Junge, W. and Sielaff, H.: *" The torque of rotary F-ATPase can unfold subunit gamma to generate a swivel joint if rotor and stator are cross-linked*", PloS One, 2013, accepted

8.2. Posters and oral Presentations

17th EBEC, Freiburg, Germany, 15th – 20th September 2012 (poster presented)

Centre for Molecular and Structural Biochemistry, Early Years Researchers' Colloquium, Norwich, UK, 7th October 2011 (Oral presentation: Hydrogen Peroxide decomposition by aa_3 Cytochrome *c* Oxidase from *Paracoccus denitrificans*)

GBM Molecular Life Sciences, Frankfurt, Germany, 25th - 28th September 2011 (poster presented)

GRC Bioenergetics, Andover, NH, USA, 26th - 1st June/July 2011 (poster presented)

16th EBEC, Warsaw, Poland, 17th - 21st July 2010 (poster presented)

15th EBEC, Dublin, Ireland, 19th - 24th July 2008 (poster presented)

Danksagung

Im Folgenden möchte ich mich bei allen Personen bedanken, die mir bei dieser Arbeit halfen und zur Seite standen:

Prof. Dr. Dr. h. c. Hartmut Michel, der mir die Möglichkeit gab diese Arbeit in seiner Abteilung anzufertigen und Ergebnisse mit mit kritisch diskutierte.

Prof. Dr. Bernd Ludwig, der sich bereit erklärte als universitärer Betreuer zu fungieren und sich viel Zeit für die Diskussion von Ergebnissen nahm.

Dr. Iris von der Hocht, für die unermüdliche Hilfsbereitschaft, sei es Korrektur lesen, diskutieren oder Kaffe / Biergespräche.

Hao Xie, für die zahlreichen (wissenschaftlichen) Diskussionen, die Unterhaltung auf fast allen Dienstreisen, viele Hindernissläufe und Biere, Wasserpistolenschlachten, Hubschrauberausflüge und Essen bei KFC.

Martin Kohlstädt, für unzählige (Wasserpistolen)Schlachten, fürs Kaffee und Wasser holen, sowie einige Bierabende.

Hannelore Müller, die mir in allen Laborfragen mit Rat und Tat zur Seite stand, mich durch meinen ersten Marathon begleitet hat und immer eingesprungen ist, wenn jemand benötigt wurde.

Suzan Rührer für viele Senseopads und Diskussionen.

Cornelia Münke, die mir ebenfalls während meiner Laborzeit mehr als hilfreich zur Seite stand.

Prof. Bode und Wolfram Lorenzen für die Zusammenarbeit während der GC-MS-Messungen.

Dr. Fraser MacMillan, Dr. Jesscia van Wonderen und Morgan Bye für die EPR-Messungen, Diskussionen und Ausflüge in die Innenstadt von Norwich. Im speziellen Dr. Jessica van Wonderen ebenfalls für das extreme schnelle Korrektur lesen.

Dr. Julian Langer und Imke Wüllenweber für die MS-Messungen.

Der Kaffeetruppe MMB für die netten Pausen.

Allen Mitgliedern der Abteilung MMB für die tolle Arbeitsatmosphäre.

Carolin Gloger und Matthias Seemann-Gloger, für die Hilfe bei allen Umzügen, unzählige (Grill)Abende, den Kaffee und die vielen Unternehmungen, Festivals, Spaß und Heiterkeit.

Sven Reuschel und Sina Weghorst für die Besuche, Hilfe beim Umzug und Zerstreuung in der Heimat.

Eintracht Frankfurt Rugby und im speziellen Marko Deichmann und Thomas Nöth, für die sportlichen und sozialen Herausforderungen und den Zusammenhalt im Team, sowie die Organisation der kleinen und großen Dinge des Vereinslebens.

Dr. Hendrik Sielaff, Dr. Jürgen Clausen und Henning Rennekamp für die AGOT-Schlachten, Wochenenden voller Brettspiele und für die jährliche Tour zur Spiel.

Wera Ulferts, die immer hinter mir stand und ohne die das alles nicht funktioniert hätte.

Meinen Eltern und meinem Bruder für die jederzeit bedingungslose Unterstützung.